

Dissertation zur Erlangung des Doktorgrades  
der Fakultät für Chemie und Pharmazie  
der Ludwig-Maximilians-Universität München

# Design and Synthesis of Ligands for the FK506- Binding Proteins and the Serotonin Transporter

---

**Ranganath Gopalakrishnan**

aus

Ahmedabad, India

2012

## Erklärung

Diese Dissertation wurde im Sinne von § 7 der Promotionsordnung vom 28. November 2011 von Herrn Prof. Dr. Turck betreut.

### EidessTattliche Versicherung

Diese Dissertation wurde eigenständig und ohne unerlaubte Hilfe erarbeitet.

München, am ..06/02/2012..

.....

(Ranganath Gopalakrishnan)

Dissertation eingereicht am ...06/02/2012..

1. Gutachter: Prof. Dr. C. Turck

2. Gutachter: Prof. Dr. R. Beckmann

Mündliche Prüfung am 29/03/2012

## Acknowledgements

First and foremost I want to thank my advisor Dr. Felix Hausch. It has been an honor to work with him. He has taught me, both consciously and unconsciously, how good medicinal chemistry has to be carried out; I appreciate his contributions and sincerely thank him for providing such a great working atmosphere in the lab. I would also like to thank my doctoral supervisor Prof. Turck, the thesis committee for reviewing this thesis and Prof. Holsboer for the financial support.

The members of the Hausch group have contributed immensely to my personal and professional time at MPI. The group has been a source of friendship as well as collaboration. I am especially grateful to Dr. Christian Kozany and Bastiaan Hoogeland for testing my compounds in the FKBP project. I am indebted to Dr. Serena Cuboni for establishing the SERT uptake assay. I appreciate the inputs and discussions with Yansong Wang and Steffen Gaali. I also like to extend my thanks to all the others in the Hausch group for the nice time we had together in the lab and in private. I am thankful to the Lead Discovery Center (Dortmund) for the discussion and the inputs they have given at various points of the thesis. I would like to show my gratitude to Dr. Andreas Bracher (MPI Biochemistry) for solving the co-crystal structures of my compounds with FKBP51. My time at the Max Planck Institute of Psychiatry was made enjoyable in large part due to the many friends that became a part of my life. I would like to thank Roshan and Anupam for the nice lunch and coffee sessions with the provocative discussions that we have had together.

I would like to thank Carola Hetzel for helping me in the administrative and other associated problems. Her doors had been always open whenever I needed assistance.

I am grateful for time spent with my friends here in Munich especially Nagarjuna, Kirti, Venkatesh, Anoop, Rochelle, Gurumoorthy, Jeeva, Krishna, Jyoti, Aarathi, Sham, Shravan, Dinesh and rest of the Indian group who were involved in 4 seasons of MPI Cricket, fun, food and various other parties.

I would like to especially thank Juhi Sardana for her support in the good and the bad times.

Last but not the least; I would like to thank my family for all their love and encouragement. I pay my gratitude for my loving, supportive, encouraging parents who have raised me and supported me in all my endeavors.

## Abstract

The aim of this cumulative thesis was to develop new chemical tools to investigate proteins involved in depression. The thesis has been divided in two parts with the first major part aimed at generating the first synthetic ligands for FKBP51 and FKBP52. FKBP51 and FKBP52 are co-chaperons of steroid hormone receptor-HSP90 complexes. FKBP51 has been implicated in various mood affective disorders. The second part of my thesis is aimed at the synthesis of chemical tools to study the targets of clinically used antidepressants.

**Part 1:** The FK506-binding proteins 51 and 52 are co-chaperons that modulate the signal transduction of the glucocorticoid receptor. Single nucleotide polymorphisms in the gene encoding FKBP51 have been associated with a variety of psychiatric disorders. FK506 and rapamycin are two macrocyclic natural products, which unselectively bind to these proteins with nanomolar affinity. A structural alignment of FKBP51 and 52 revealed a structural divergence at the 80s loop which is a major functional determinant for the effect on steroid hormone receptors. Hence the ligand-80s loop interaction is likely to be functionally important and further offers the possibility to discriminate between FKBP homologs. Taking a simplified FK506 analog as a chemical starting point we followed two different approaches to target the 80s loop of FKBP51 and FKBP52.

In the first approach the tert-pentyl group in the synthetic lead compound was replaced with cyclohexyl derivatives that resembled the pyranose group in the natural product FK506. A detailed SAR was established which indicated that FKBP5s are tolerant towards changes in the stereochemistry of the cyclohexyl (pyranose) substituents. In the second approach we envisaged to bio-isosterically replace the  $\alpha$ -ketoamide moiety by a sulfonamide. For a rapid and efficient derivatization of a focused sulfonamide library I established a solid phase strategy which has led to the identification of 2 series of ligands with submicromolar affinity. Co-crystal structures of representative FKBP ligands of both series confirmed the hypothesized binding mode. The best substructures identified in both approaches were subsequently integrated into bi/polycyclic scaffolds with reduced conformational flexibility. The sulfonamide substructures turned out to be highly active in this context.

**Part 2:** Tricyclic antidepressants (TCA) have an extremely broad pharmacology that is still not completely understood. To explore the mechanism of antidepressants in more detail we envisioned a photo-labeling approach to better define the TCA-binding proteome.

Towards this goal, I synthesized the imipramine analogs Azidopramine and Azidobupramine which retained the drug-like properties of the parent tricyclic antidepressants and the strong inhibitory activity of the human serotonin transporter. Both compounds were photoreactive while Azidobupramine contained an additional acetylene tag for click chemistry.

Importantly, these probes are amenable to integral transmembrane proteins which comprise all currently known antidepressant targets. These probes could enable the activity based-profiling of known antidepressant targets in endogenous tissues as well as the structural fine-mapping of the binding sites in these proteins.

## Contents

<b>1. Medicinal chemistry approach to identify new ligands for FKBP51 and FKBP52 .....</b>	<b>1</b>
<b>1.1 Introduction .....</b>	<b>2</b>
1.1.1 FK506-Binding protein (FKBP) family .....	2
1.1.2 Domain Structure of FKBP5 .....	3
1.1.3 Immunosuppressive FKBP Ligands .....	3
1.1.4 Non-Immunosuppressive FKBP Ligands .....	4
1.1.4.1 Neuroimmunophilin Ligands .....	4
1.1.4.2 Rotamase Ligands.....	8
1.1.4.3 Microbial inhibitors. ....	11
1.1.5 Interaction of FKBP51 and FKBP52 with the Hsp90 machinery and its role in GR maturation and gene transcription .....	12
1.1.6 Biological roles of FKBP51 and FKBP52 .....	13
1.1.6.1 Stress related disorders.....	13
1.1.6.2 Cancer etiology.....	15
1.1.6.3 Other Biological Implications .....	15
1.1.7 Structural Differences between FKBP51 and FKBP52 FK1 domain .....	15
1.1.7.1 Comparison of FKBP51 and 52 structures with PPLase inhibitors.....	17
<b>1.2 Manuscripts and Patents.....</b>	<b>19</b>
1.2.1 The Chemical Biology of Immunophilin Ligands (Manuscript-1) .....	20
1.2.2 Aim of Manuscripts 2 and 3 .....	46
1.2.2.1 Evaluation of Synthetic FK506 Analogs as Ligands for FKBP51 and FKBP52 (Manuscript-2).....	47
1.2.2.1.1 Discussion (Manuscript-2).....	105
1.2.2.2 Exploration of Pipecolate Sulfonamides as Binders of the FK506-Binding Proteins 51 and 52 (Manuscript 3).....	107
1.2.2.2.1 Discussion (Manuscript 3).....	157
1.2.3 Design of Ligand Efficiency by Conformation Control (Manuscript 4).....	160

1.2.3.1.1	Background .....	161
1.2.3.1.2	Result and Discussion.....	162
1.2.3.1.3	Experimental section.....	164
<b>2.</b>	<b>Synthesis of novel photoactivable Tricyclic antidepressant analogs .....</b>	<b>167</b>
<b>2.1</b>	<b>Introduction .....</b>	<b>168</b>
2.1.1	Depression.....	168
2.1.2	Monoamine Hypothesis .....	168
2.1.3	Monoamine transporter inhibitors as antidepressants .....	169
2.1.4	SAR studies of TCA class of drugs .....	170
<b>2.2</b>	<b>Aim of the work (Manuscript-5) .....</b>	<b>173</b>
<b>2.3</b>	<b>Discussion.....</b>	<b>187</b>
<b>3.</b>	<b>Summary .....</b>	<b>188</b>
<b>4.</b>	<b>Materials .....</b>	<b>189</b>
4.1	Solvents, reagents and salts .....	189
4.2	Chemicals .....	191
<b>5.</b>	<b>Personal Future Outlook.....</b>	<b>196</b>
<b>6.</b>	<b>Curriculum Vitae .....</b>	<b>197</b>
<b>7.</b>	<b>References .....</b>	<b>199</b>

**1. Medicinal chemistry approach to identify new ligands  
for FKBP51 and FKBP52**

## 1.1 Introduction

### 1.1.1 FK506-Binding protein (FKBP) family

The immunosuppressive drugs FK506, Rapamycin and Cyclosporin A bind to a highly conserved class of protein family referred to as immunophilins, which exhibit peptidyl prolyl cis/trans isomerase (PPIase) activity<sup>1-3</sup>. The immunophilin family consists of the FKBP family of proteins which binds to FK506 or Rapamycin and the cyclophilin family which bind cyclosporin A.

**Table 1**<sup>3-6</sup>

No.	Protein	Cellular compartment where found
1	FKBP12	Cytosolic
2	FKBP12.6	Cytosolic
3	FKBP 13	Endoplasmatic reticulum
4	FKBP 15	Endoplasmatic reticulum
5	FKBP 22	Endoplasmatic reticulum
6	FKBP 24	Endoplasmatic reticulum
7	FKBP 25	Nuclear/ cytosolic
8	FKBP 36	Nuclear
9	FKBP 38	Cytoplasmic
10	FKBP 51	Cytoplasmic
11	FKBP 52	Cytoplasmic
12	FKBP 60	Endoplasmatic reticulum
13	FKBP 65	Endoplasmatic reticulum
14	FKBP 133	Nuclear

The mammalian FKBP family can be classified based on their molecular weight or the cellular compartments where they are found. In humans the FKBP family consists of FKBP12, FKBP12.6, FKBP 13, FKBP15, FKBP22, FKBP24, FKBP25, FKBP36, FKBP38, FKBP51, FKBP52, FKBP60, FKBP65 and FKBP133 (numbers indicate their molecular weight)<sup>3-5,7,8</sup> most of which bind to FK506 and exhibit PPIase activity. FKBP38 doesn't have an intrinsic PPIase activity but the PPIase activity of this domain is stimulated by  $\text{Ca}^{2+}/\text{CaM}$ <sup>9,10</sup>. Within the

FKBP family FKBP12, FKBP12.6, FKBP38, FKBP51 and FKBP52 are the most studied and explored members. All the available FKBP structures are largely analogous<sup>3,4</sup>.

These PPIases are distributed in three major cellular compartments (cytosolic, endoplasmatic reticulum, nuclear) and control a number of cellular processes. Human and microbial FKBP have also been shown to exhibit chaperone activity independent of their PPIase activity e.g. FKBP52, PpFKBP35 etc (**Table 1**).

### 1.1.2 Domain Structure of FKBP

Sequence alignment and structural data across the human FKBP family suggest that the amino acid residues which form the PPIase active site and the FK506 binding site remain conserved. The domain to which the prototypical natural products bind is termed as the FK1 binding domain which also has the peptidyl-prolyl *cis-trans* isomerase (PPIase) activity. PPIase (also known as rotamase activity) is a function that catalyzes the conversion of peptidyl-prolyl bonds from *trans*- to *cis*-proline or vice versa, which often is a rate-limiting step in protein folding<sup>11</sup>. The smaller FKBP like FKBP12 and FKBP12.6 contain only one domain. Larger FKBP can contain a second FKBP-like domain which is often devoid of the PPIase activity and is termed as the FK2 domain. Larger FKBP like FKBP51 and FKBP52 contain a FK2 domain which has higher similarity to FKBP38. FKBP60 and FKBP65 contain up to four PPIase domains. The next accompanying domain in FKBP51 and FKBP52 is the tetratricopeptide repeat domain or the TPR domain. TPR domains often mediate binding to the Hsp90 machinery.

### 1.1.3 Immunosuppressive FKBP Ligands

The prototypical ligands of the FKBP family are FK506 (**1**) and Rapamycin (**2**) (**Fig. 1**). These natural products have immunosuppressive activity and are used in the clinic for the suppression of immune responses after organ transplantation to prevent allograft rejection.

FK506 (Tacrolimus) **1** was first isolated and characterized from *Streptomyces tsukubaensis* which gave the nomenclature to its protein targets, the family of FK506-binding proteins (FKBP). FK506 consist of two domains, first a FKBP binding domain and second an effector domain which mediates the immunosuppressive activity. The FKBP-FK506 complex binds and allosterically inhibits the secondary target calcineurin to which the effector domain binds and thus induces its immunosuppressive effect<sup>12</sup>. FKBP12 is the major player that mediates the immunosuppressive action of FK506<sup>13,14</sup>.

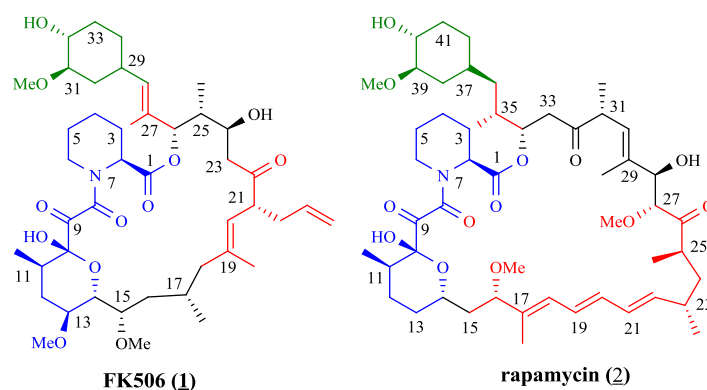


**Figure 1 Structures of the immunosuppressive natural product ligands.** Blue: immunophilin-binding domain (FKBP for FK506 and Rapamycin); red: effector domain (calcineurin for FK506, FRB domain of mTOR for Rapamycin); green: binds to both FKBP and CaN/mTOR<sup>15</sup>.

The second natural binder of FKBP, Rapamycin (Sirolimus) **2**, was isolated from *Streptomyces hygroscopicus*. The immunosuppressive activity of this compound is exhibited via a different ternary partner, the serine-threonine protein kinase mammalian target of Rapamycin (mTOR). mTOR inhibition has been shown to block various signaling pathways that control protein translation which play a crucial role in cell cycle progression<sup>16-18</sup>.

A series of immunosuppressive Rapamycin and FK506 analogs are presently used in the clinic or in various phases of clinical trials as these natural products have been shown to be effective in various disorders like breast cancer, melanoma and advanced renal cell carcinoma, metastatic soft-tissue sarcomas etc<sup>15</sup>.

## 1.1.4 Non-Immunosuppressive FKBP Ligands

### 1.1.4.1 Neuroimmunophilin Ligands

Apart from their immunosuppressive activity Rapamycin and FK506 were also shown to have additional neuroprotective and neurotrophic effects. Studies have shown that the natural products partially mediate these effects via the calcineurin or mTOR dependent pathway<sup>19,20</sup>. In any case the immunosuppressive effects of FK506 and Rapamycin limit the chronic use of these agents for neurological indications. Contrasting studies have shown that some neurological effects are partially independent of the calcineurin or mTOR inhibition which stimulated intense efforts across the pharmaceutical industry to identify and develop non-immunosuppressive immunophilin ligands<sup>6,21,22</sup>.

The medicinal chemistry campaigns undertaken by the pharmaceutical industry resulted in identification of many FKBP ligands without immunosuppressive activity (**Fig. 2 and 3**). Several of these compounds were shown to be neuroprotective or neuroregenerative<sup>15,22,23</sup>. Apart from these primary cellular effects these compounds were also shown to have effects in animal models of diabetic neuropathy<sup>24</sup>, traumatic brain injury<sup>25</sup>, Parkinson's disease<sup>26-28</sup>, cerebral ischemia<sup>29,30</sup>, as well as in various models of physical neuronal injury<sup>15,22,24,31</sup>.

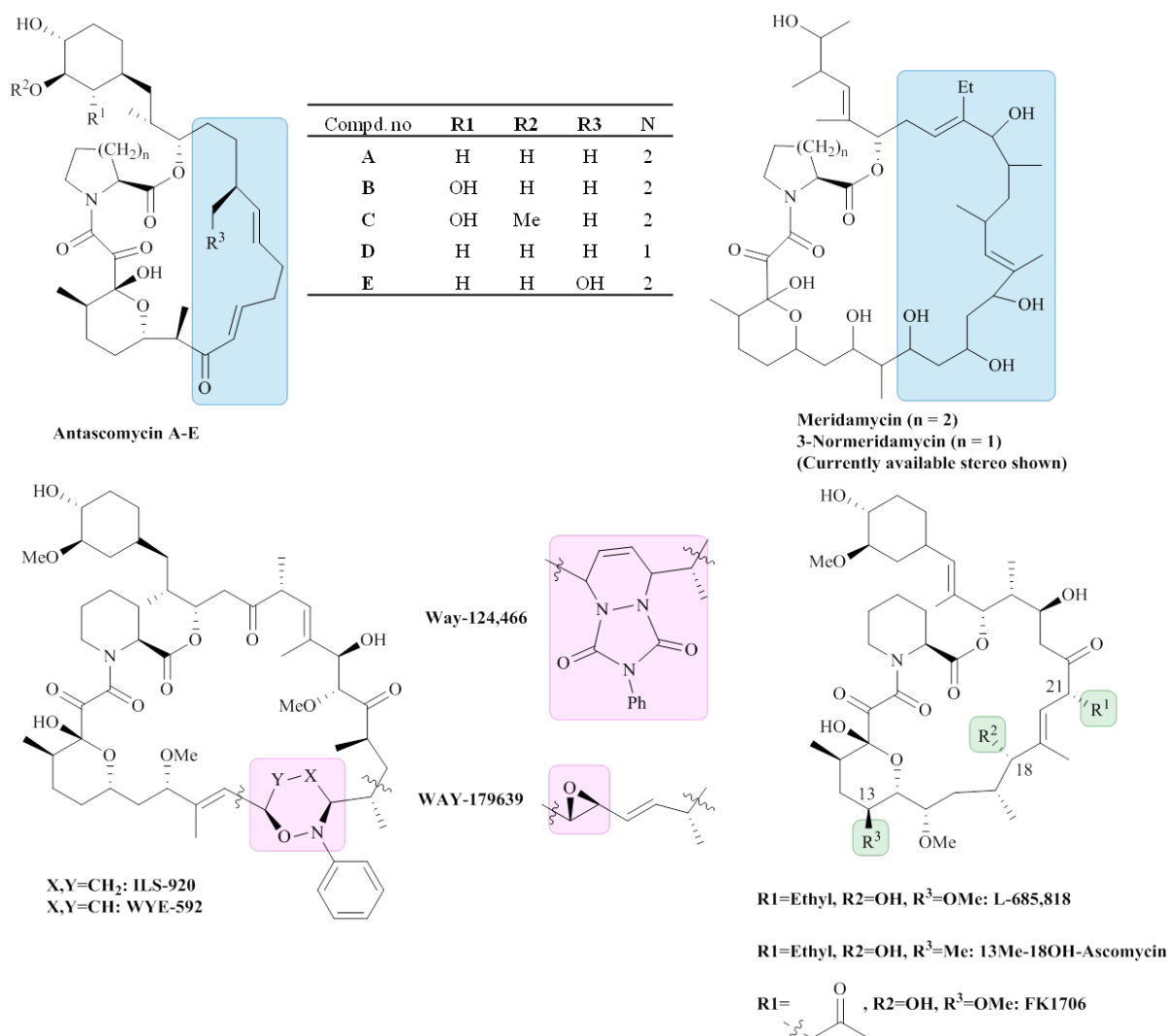


**Figure 2: Natural product-derived non-immunosuppressive FKBP ligands.** Modifications compared to FK506 or Rapamycin are shaded<sup>15</sup>.

The non-immunosuppressive FKBP ligands differed from the immunosuppressive counterparts in two different ways. In the semi- or bio-synthetic analogs the substituents at the effector region were altered which resulted in complete loss of binding to calcineurin/ mTOR (e.g., FK1706, meridamycin, normeridamycin, ILS920, Way-124466, Wye-592, L685-818, shown in

**Fig. 2).** The developed synthetic ligands mimicked the dicarbonyl pipercolyl moiety of the natural products and were devoid of the effector region substituents which bind to calcineurin or mTOR (e.g., V-10,367, JNJ460/GM284, GPI1046, GPI1485 in **Fig. 3** or compound **3** shown in **Fig. 4**).

Clinical trials of some of the above mentioned compounds suggested that FKBP blockade seems to be well tolerated in humans as no toxic side effects have been reported at doses which might result in complete saturation of intracellular FKBP pools (in blood)<sup>32</sup>.

Nearly all of the biochemical studies reported have been carried out for FKBP12. Most of the reported synthetic FKBP ligands are based on the dicarbonyl pipercolyl/prolyl-scaffold which is derived from the natural products FK506 or Rapamycin (**Fig. 1**). GPI1046 was one of the first small molecule analogs of FK506 which was designed to preserve the FKBP binding part. It was originally reported to be a potent inhibitor of FKBP12 but these findings have been contradicted by a number of groups<sup>15,33</sup>.

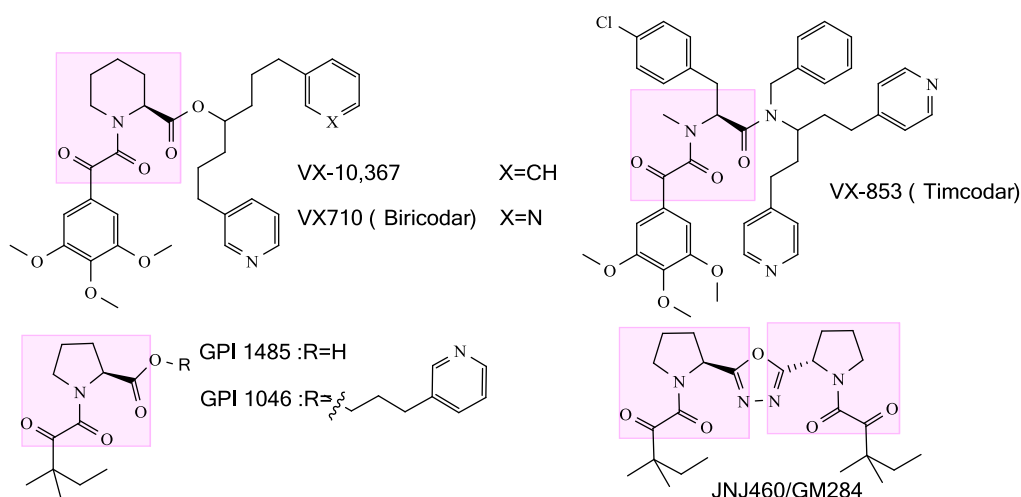


**Figure 3: Synthetic FKBP ligands.** The dicarbonyl pipercolyl moiety derived from the central core of FK506 or Rapamycin or equivalent groups are shaded<sup>15</sup>.

There are also discrepancies on the effect of GPI1046 regarding its neurotrophic/neuroprotective effects<sup>34,35</sup>. Other GPI1046 analogs (e.g., compound **3**<sup>36</sup> or JNJ460/GM284<sup>37</sup>) have also been reported for their biological effects and FKBP12 inhibition. In addition JNJ460/GM284 has also been reported to have submicromolar FKBP52 inhibition<sup>37</sup>. GPI1046 is believed to be a pro-drug and metabolizes in the body to release GPI1485. GPI1485 has been

shown to be devoid of PPIase activity<sup>38</sup> and has failed to show efficacy in clinical trials for Parkinson's disease/ erectile dysfunction after nerve injury<sup>39</sup>.

V-10,367 and Biricodar are the most potent synthetic FKBP12 ligand reported to date<sup>40,41</sup>. V-10,367 has been tested in a number of cellular and animal models for neuroprotection or neuroregeneration. A very close analog Biricodar (VX-710) was reported to retain very high potency for FKBP12 in a PPIase assay ( $K_d=3.7\text{nM}$ )<sup>41</sup> and inhibit the P-glycoprotein (*MDR1*) with  $0.75\mu\text{M}$ <sup>42</sup>. Biricodar has also been investigated in several clinical trials as a chemosensitizing agent<sup>43</sup>, however, without any beneficial clinical effects.

Apart from GPI1046 and Biricodar, Timcodar is the third FK506 analog to have entered clinical trials. The natural products FK506 and Rapamycin apart from inhibiting FKBP are also known to be inhibitors of P-glycoprotein 1, a major drug efflux transporter<sup>44</sup>. Similar to Biricodar, Timcodar (VX-853, **Fig. 3**) has also been shown to be a potent inhibitor of P-gp<sup>142</sup>. P-gp inhibition could be a partial contributor to the observed neurological effects of Timcodar and analogs thereof (e.g., V13-661 and V-13670) since these compounds have been shown to lack FKBP binding but retain P-gp inhibition<sup>15</sup>.

All though these FKBP analogs have reached the clinics their selectivity profile is not yet known. The only FKBP protein for which selective binders have been identified and reported in literature is hFKBP38. The Cycloheximide analog DM-CHX (**Fig. 4**) has been shown to selective bind FKBP38 ( $K_d=85\text{nM}$ ) and showed >200-fold selectivity against several other FKBP homologs<sup>30</sup>. A co-crystal structure of a close analog (Cycloheximide N-ethylethanoate) was solved in complex with an FKBP-like protein from *Burkholderia pseudomallei* revealing a totally novel FKBP-ligand interaction pattern<sup>45</sup>. In contrast to its precursor Cycloheximide, DM-CHX is devoid of inhibition of protein translation.

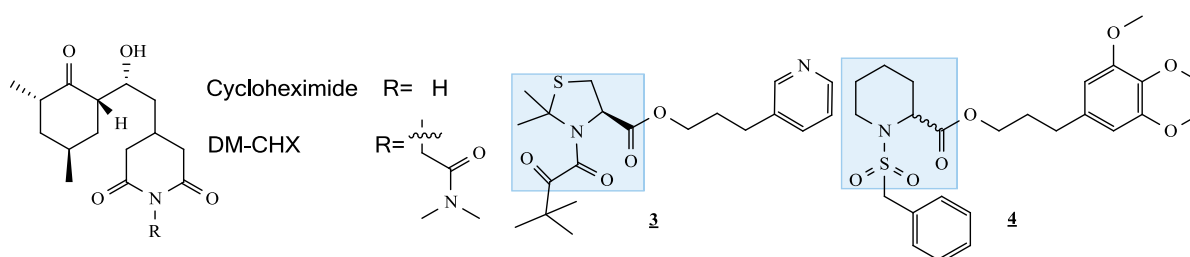


**Figure 4: Synthetic FKBP ligands.** The dicarbonyl pipercolyl moiety derived from the central core of FK506 or Rapamycin or equivalent groups are shaded<sup>15</sup>.

### 1.1.4.2 Rotamase Ligands

Most of the rotamase (PPIase) ligands have been developed for the prototypical FKBP12 ligand binding pocket. The basic pharmacophore that is required for FKBP binding is depicted in **Fig. 5**<sup>46</sup>.

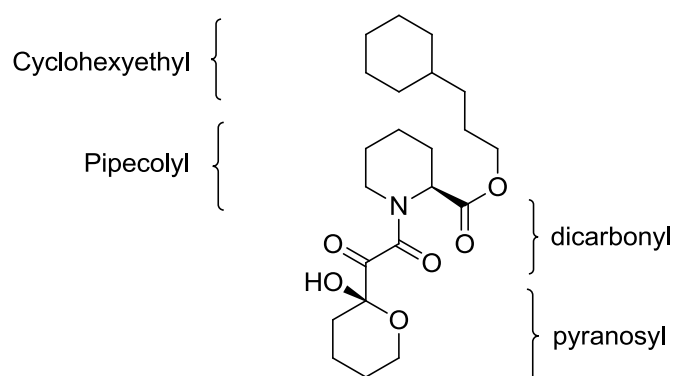


**Figure 5:** The minimal binding domain that is required for compounds to bind to FKBP12.

Many of the novel FKBP ligands that have been described in literature have the above basic pharmacophore conserved in one form or the other. A detailed structure activity relationship (SAR) around each of the minimal binding domain is surveyed below.

#### a) Pipecolate core.

The pipecolate core that is present in FK506 and Rapamycin sits in the pipecolate binding pocket which is formed by Val<sup>55</sup>, Phe<sup>46</sup> and the Asp<sup>37</sup> in FKBP12 and the indole ring of Trp-59 which forms the floor of the FKBP12 binding pocket<sup>47,48</sup>. The first compounds had the pipecolate core conserved<sup>47</sup>. In GPI1046 (**Fig. 3**) the six membered pipecolate core was replaced by a proline. The next generation of compounds were the rigidified analogs by Agouron/ Pfizer, where the relatively open binding pocket of FKBP12 had been taken into advantage<sup>49</sup>. In these compound a substituent at the axial position at C<sup>6</sup> of the pipecolate core was introduced and further cyclized with the C<sup>1</sup> carbonyl to yield a [3.3.1] aza amide core (**6**) or a polycyclic scaffold **7** (**Fig. 6**) These polycyclic analogs were shown to be useful cores for binding to FKBP12.

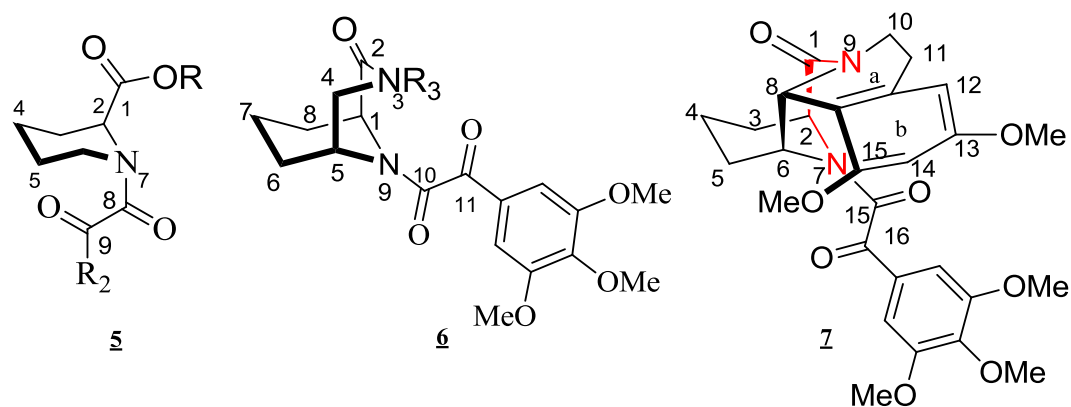


**Figure 6:** General structures of various pipercolate core analogs identified for FKBP12.

b) Pyranose group.

The pyranose moiety present in the natural products FK506 and Rapamycin have been substituted by many different analogs. Holt *et al.* made a series of compounds and showed that the oxygen on the pyranose group is not required for activity (**Table. 2**, e.g., compounds 10-12)<sup>46</sup>. The pyranose group was further completely substituted by tert-pentyl group to give compounds with better binding affinity. This tert-pentyl group was subsequently adopted in many of the reported FKBP12 compounds.

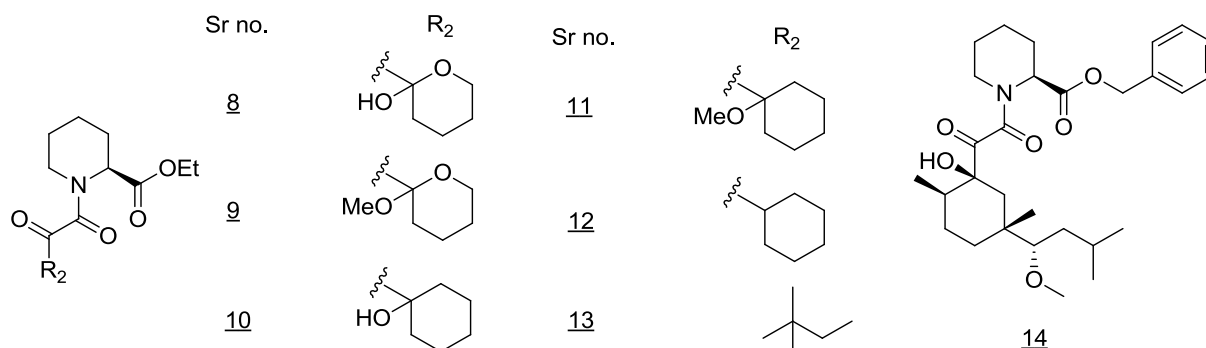


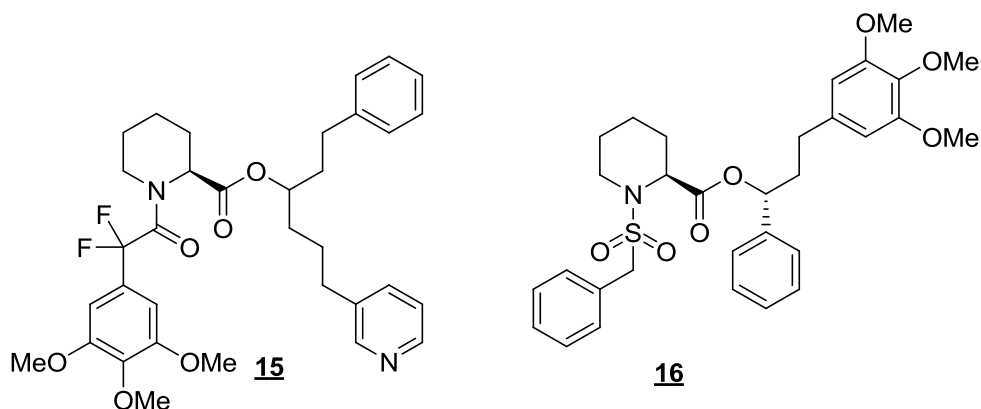
**Table 2** Pyranose group substituents<sup>50-52</sup>.

Tatlock *et al.* replaced the pyranose moiety with the (*R*)-(-)-Carvone moiety followed by a derivatization of the C-15 position which resulted in compound **14** exhibiting remarkable affinity for FKBP12. The reason for its high affinity could be due to a hydrophobic collapse caused by the additional alkyl side chain which causes better FKBP12 binding<sup>53</sup>.

c) Dicarboxyl group.

The electrophilicity of the  $\alpha$ -ketoamide moiety present in most of the non-immunosuppressive FK506 analogs is an undesired reactive liability that could result in metabolic instability or potential toxicity. The amide carbonyl was shown to be important for activity as it is involved

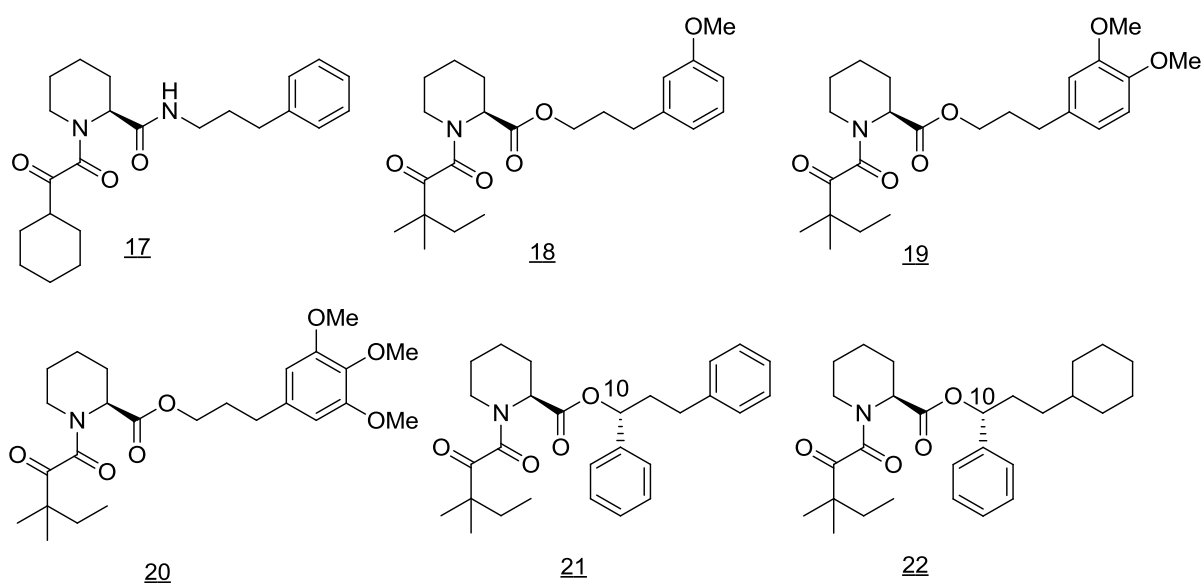
in hydrogen bonding with the Tyr82 of FKBP12. Reduction of the ketone to alcohol<sup>46</sup> or substitution by a di-fluoride **15**<sup>54</sup> did not result in a detrimental change in activity. Bioisosteric replacement of the dicarbonyl group with a sulfonamide (**16**) resulted in compounds having equivalent affinity compared to the ketoamides<sup>55,56</sup>.



**Figure 7:** Compounds where the diketo moiety has been replaced by other substituents.

d) Cyclohexylethyl substituent (Top group)

The pipercolate C<sup>1</sup> ester was also replaced by an amide (**17**) which completely abolished binding to FKBP12<sup>46,57</sup>. Introduction of substituents around the phenyl group (**18-20**) resulted in compounds having better binding affinity.



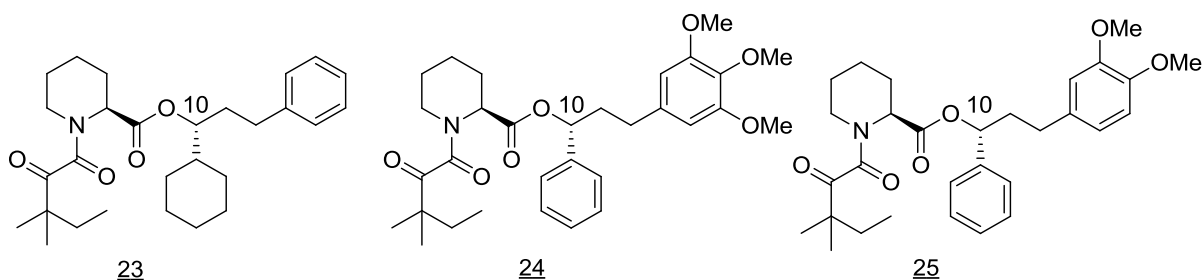


**Figure 8:** Top group modifications of the non-immunosuppressive FKBP12 ligands.

Substitution at the carbinol centre (C10) with phenyl or cyclohexyl groups led to a 10-20 fold increase in activity compared to that of **18-20**. The stereochemistry at the new chiral centre is of importance<sup>46</sup>. R enantiomer is 20-40 fold more active than S enantiomer. Compound **25** with two substituents and phenyl substitution at carbinol centre had the best activity in this series of compound synthesized<sup>46</sup>.

#### 1.1.4.3 Microbial inhibitors.

Apart from the human FKBP, FKBP isoforms have also been identified in various parasites and microorganisms which have been suggested as potential anti-infective targets<sup>58</sup>. The most widely studied microbial FKBP homolog is the Mip (macrophage infectivity potentiator) protein which is present in human pathogens like *Legionella pneumophila*, the causing agent of Legionnaire's disease, or *Trypanosoma cruzi*, the pathogen causing Chagas disease. *L. pneumophila* Mip and the Mip from *T. cruzi* were shown to facilitate infectivity and invasion in host tissues in a PPIase dependent and FK506-sensitive manner<sup>59,60</sup>. Oz *et al.* further showed that the non-immunosuppressive analog L-685,818 (**Fig. 2**) was active in an animal model of *T. cruzi* infection<sup>61</sup> since the immunosuppressive activity of FK506 would confound the study of the role microbial FKBP on pathogenicity of microorganisms and parasites. The NMR structure of *L. pneumophila* Mip in complex with Rapamycin was solved by Ceymann *et al.*<sup>62</sup> which gave an insight into the binding mode of these compounds in the microbial FKBP. A structure based design approach was carried out by Juli *et al.* where they designed a series of pipercolate-containing sulfonamides as surrogates of Rapamycin. Exemplary compound **4** (**Fig. 4**) inhibited the microbial FKBP with an IC<sub>50</sub> of 6μM compared to 0.2μM for human FKBP12. However, compound **4** was inactive in an assay for macrophage-like cell infection whereas Rapamycin as control was active<sup>63</sup>.

A NMR structure of N-ethyl-CHX (**Fig. 4**) with Mip from *Burkholderia pseudomallei* revealed a highly unexpected dynamic rearrangement of the active site that has never been observed in

any of the FKBP co-crystal structures before<sup>45</sup>. The N-ethyl-CHX analog inhibited the PPIase activity of *Burkholderia pseudomallei* Mip with a  $K_i=6.5\mu\text{M}$ .

### 1.1.5 Interaction of FKBP51 and FKBP52 with the Hsp90 machinery and its role in GR maturation and gene transcription

The steroid hormone receptors (SHRs), especially the glucocorticoid receptor (GR), reside in the cytosol and migrate to the nucleus upon activation. Other are nuclear in both forms, i.e., in the presence or absence of the ligand (e.g. progesterone receptor)<sup>64</sup>. Before the newly synthesized SHRs become receptive to the ligand / hormone they must undergo a heat shock protein (Hsp) assisted maturation process (**Fig. 9**). The first step includes the binding of Hsp70 and Hsp40 to the GR. The second step includes the binding of SHRs to Hsp90 which occurs in the presence of Hsp70 and Hsp organizing protein (Hop), which binds the chaperones by virtue of two separate tetratricopeptide repeat (TPR) domains<sup>65</sup>.

A stabilization protein (p23) further stabilizes the Hsp90-SHR complex in its ATP bound form to form the intermediate complex<sup>66</sup>. Binding of ATP reduces the affinity of Hsp90 for Hop, which results in the dissociation of Hop and Hsp70 followed by the simultaneous recruitment of other TPR proteins, Cyp40, FKBP51, FKBP52 or PP5, to form the oligomeric SHR-Hsp90 mature complex. The mature complex, depending on the co-chaperone it contains, maintains the SHR in a structural conformation that is either highly (FKBP52) or weakly (FKBP51) responsive to hormone binding<sup>67-69</sup>. This antagonistic effect of FKBP51 and FKBP52 towards the GR has been attributed to differences in the 80s loop of the FK1 domain in these two proteins<sup>70</sup>. The FKBP5s compete for binding to the SHR-HSP90 complex to form the mature complex and, as a result, over-expression of FKBP51 will decrease the receptor regulation by FKBP52<sup>67</sup>. After hormone binding the hormone-receptor complex translocates to the nucleus where it binds to hormone response elements and regulates gene transcription<sup>71</sup>.

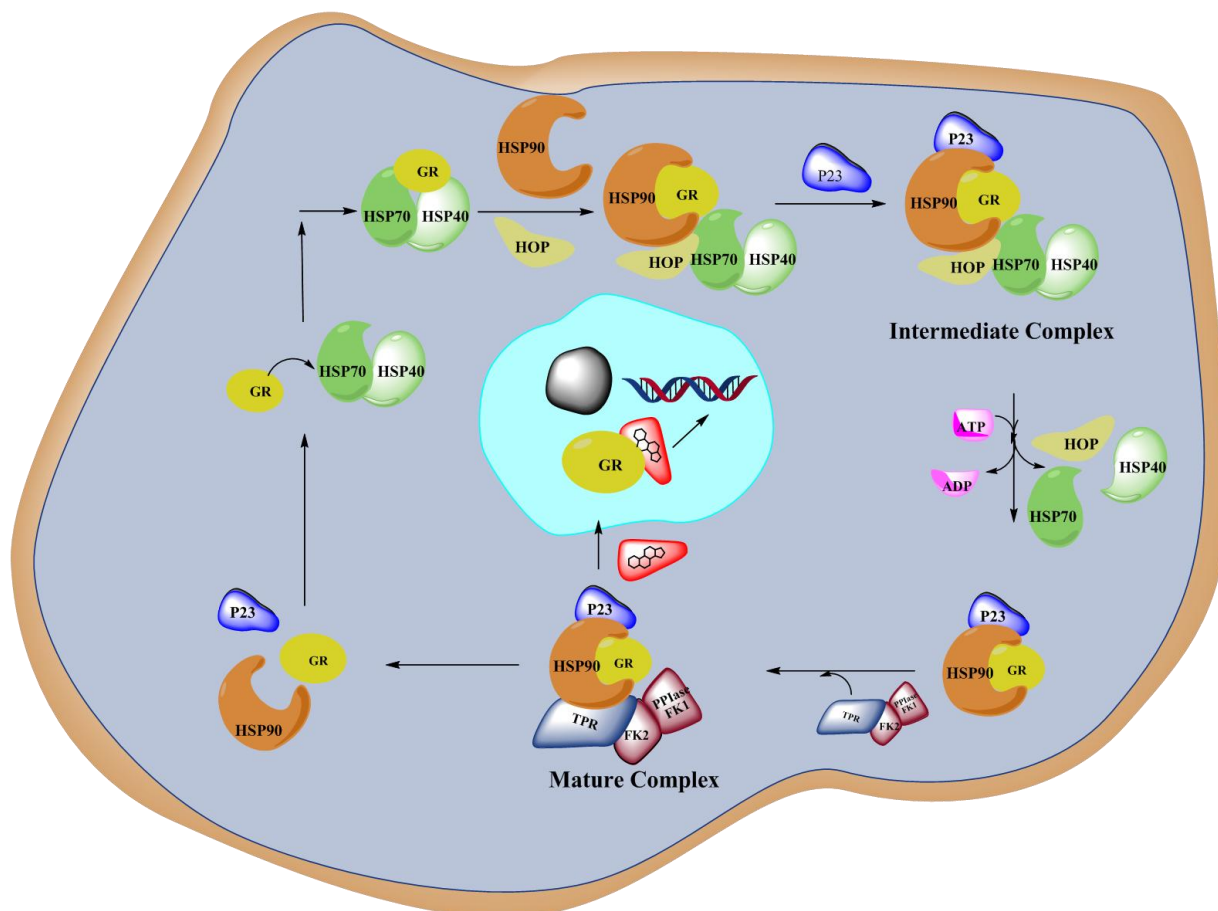


**Figure 9:** Schematic representations of the steroid hormone receptor maturation process and hormone binding regulated by FKBP5s.

## 1.1.6 Biological roles of FKBP51 and FKBP52

### 1.1.6.1 Stress related disorders

Chronic and acute stress coping behavior in humans is controlled by a stress hormone system, the hypothalamus-pituitary-adrenal (HPA) axis. An imbalance in this system is thought to underlie the risk and course of diseases like post-traumatic stress disorder (PTSD), major depression, anxiety disorder and bipolar depression<sup>72,73</sup>. The HPA axis is a complex hormone cascade mechanism comprising the hypothalamus which secretes the corticotrophin-releasing hormone (CRH) after external stress stimuli. Upon stimulation by CRH the pituitary gland triggers the synthesis and secretion of the adrenocorticotrophic hormone (ACTH) which in turn acts on the adrenal cortex and results in the secretion of glucocorticoid hormones (especially cortisol) which act on various tissues (**Fig. 10**). A critical feature of the HPA axis is the negative feedback inhibition exerted by cortisol via the GR which keeps the stress reaction in balance. During stress related disease conditions the basal set point of the HPA axis hormones

and the reactivity of the HPA axis is altered which is interpreted as the body's inability to adequately cope and terminate the stress response, resulting in an increased risk of disease development<sup>73</sup>. The opposing functions of FKBP51 and FKBP52 on GR<sup>67,68</sup>, along with human genetic studies have identified FKBP51 as a candidate associated with major depression<sup>74</sup>. Several studies have shown a correlation between FKBP51 genetic polymorphisms and antidepressant response<sup>74-77</sup>. FKBP51 polymorphisms have also been linked with suicidal tendency<sup>78-81</sup>, peri-traumatic dissociation<sup>82</sup>, psychosocial stress coping<sup>83</sup>, and PTSD<sup>84</sup>. FKBP51 polymorphisms have also been shown to modify the effects of early life trauma in PTSD<sup>84,85</sup> and depression<sup>86</sup>.

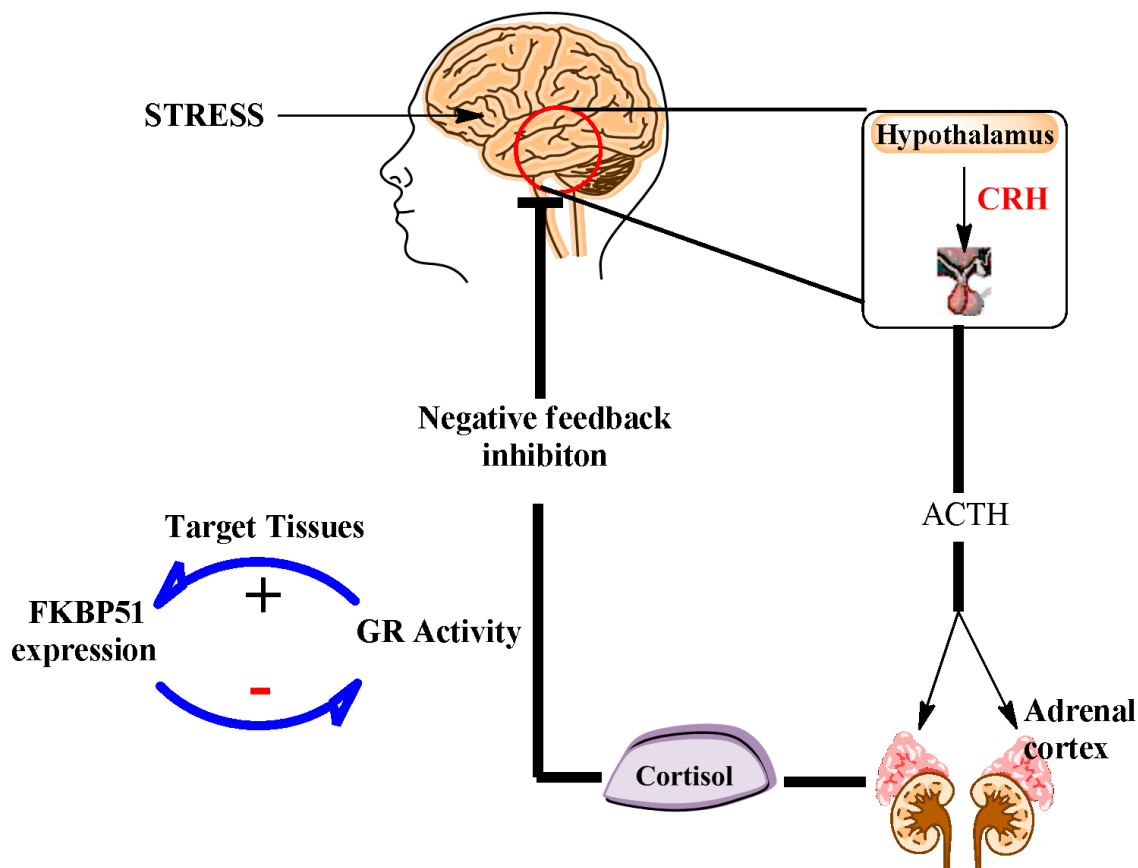


**Figure 10:** Schematic representation of role of FKBP51 in the HPA axis and regulation of the HPA axis during external stress.

The role of FKBP51 in stress coping behavior has very recently been firmly shown in several independent animal model studies<sup>87-90</sup>. These findings strongly supported FKBP51 as novel therapeutic target for psychiatric disorders. Unfortunately neither FK506 nor Rapamycin can be used as tools to further dissect the role of FKBP51 and FKBP52 as they have nearly equipotent affinities for all FKBP. Hence, selective FKBP inhibitors are required to better understand the underlying biology of these larger FKBP with respect to psychiatric disorders.

### 1.1.6.2 Cancer etiology

FKBP51 and FKBP52 have been recently implicated in a variety of cancers<sup>91,92</sup>. Both proteins have been identified to be regulated in a number of cancers. FKBP51 was found to be up-regulated in prostatic hyperplasia and in prostate cancer cells<sup>93</sup>. In addition, the FK506-binding ability of FKBP51 has been identified as a positive regulator of androgen receptor and androgen-dependent cell growth in prostate cancer cells<sup>94,95</sup>. The effect of FKBP51 on GR has been suggested to suppress proliferation in colorectal adenocarcinomas<sup>96</sup>. A recent study has outlined the role of FKBP51 in melanocyte malignancy<sup>97</sup>. Apoptosis induced by irradiation was seen in cells with silenced FKBP51, while control cells showed autophagy. This study showed that inhibition of apoptosis in control cells involved FKBP51-dependent activation of NF- $\kappa$ B upon irradiation<sup>97</sup>. In a pancreatic cell line Pei et al. identified FKBP51 as a scaffolding protein to enhance the dephosphorylation of the cell growth regulator Akt by the phosphatase PHLPP<sup>98</sup>. FKBP51 has been shown to be up-or down-regulated depending on the cell and cancer sub-type and activation or inhibition of FKBP51 can ultimately produce a beneficial effect to treat proliferating cancer cells. Thus, these opposing effects of FKBP51 have to be fine-tuned and taken into consideration before developing a FKBP51-based cancer therapy.

### 1.1.6.3 Other Biological Implications

**Neurite Outgrowth:** FKBP52 and FKBP51 have also been found to have antagonistic effects on neurite outgrowth. In N2a cells FKBP52 was shown to increase neurite outgrowth while FKBP51 was shown to shunt neurite outgrowth<sup>99</sup>.

**Immune system:** FKBP51 has also been discovered to play a role in immune related disease and inflammation. In patients suffering from rheumatoid arthritis FKBP51 is found to be expressed in bone marrow cells<sup>100</sup>. During the treatment therapy of chronic obstructive pulmonary disease in patients FKBP51 expression is seen to be increased in sputum cells<sup>101</sup>.

### 1.1.7 Structural Differences between FKBP51 and FKBP52 FK1 domain

A three dimensional alignment of several crystal forms of the FK506-binding domain of FKBP51 (305R)<sup>102</sup> and FKBP52 (1P5Q)<sup>103</sup>, to be published) revealed that the largest structural divergence between the two proteins are found at the adjacent 40s and the 80s loop (residues 71-76 and 118-122 for FKBP51, respectively) (**Fig. 11**). In the 40s loop of FKBP51 Asp<sup>74</sup> and Glu<sup>75</sup> is replaced by Lys<sup>74</sup> and Asp<sup>75</sup> in FKBP52. The Glu<sup>75</sup> in FKBP51 is about 2Å closer to the PPIase active site than Asp<sup>75</sup> in FKBP52. The tip of the 80s loop in these proteins also has structural divergences which basically comprises of Leu<sup>119</sup> (FKBP51) and Pro<sup>119</sup> (FKBP52).

The Leu<sup>119</sup>-Pro<sup>120</sup> peptide bond is always found in *cis* conformation in all known FKBP51 structures while the Pro<sup>119</sup>-Pro<sup>120</sup> bond has been suggested to be present either in a *cis* or a *trans* conformations. Cellular studies have shown the residue at position 119 to be a major functional determinant for the diverging effects of FKBP51 and FKBP52 on the steroid hormone receptor<sup>70</sup>.

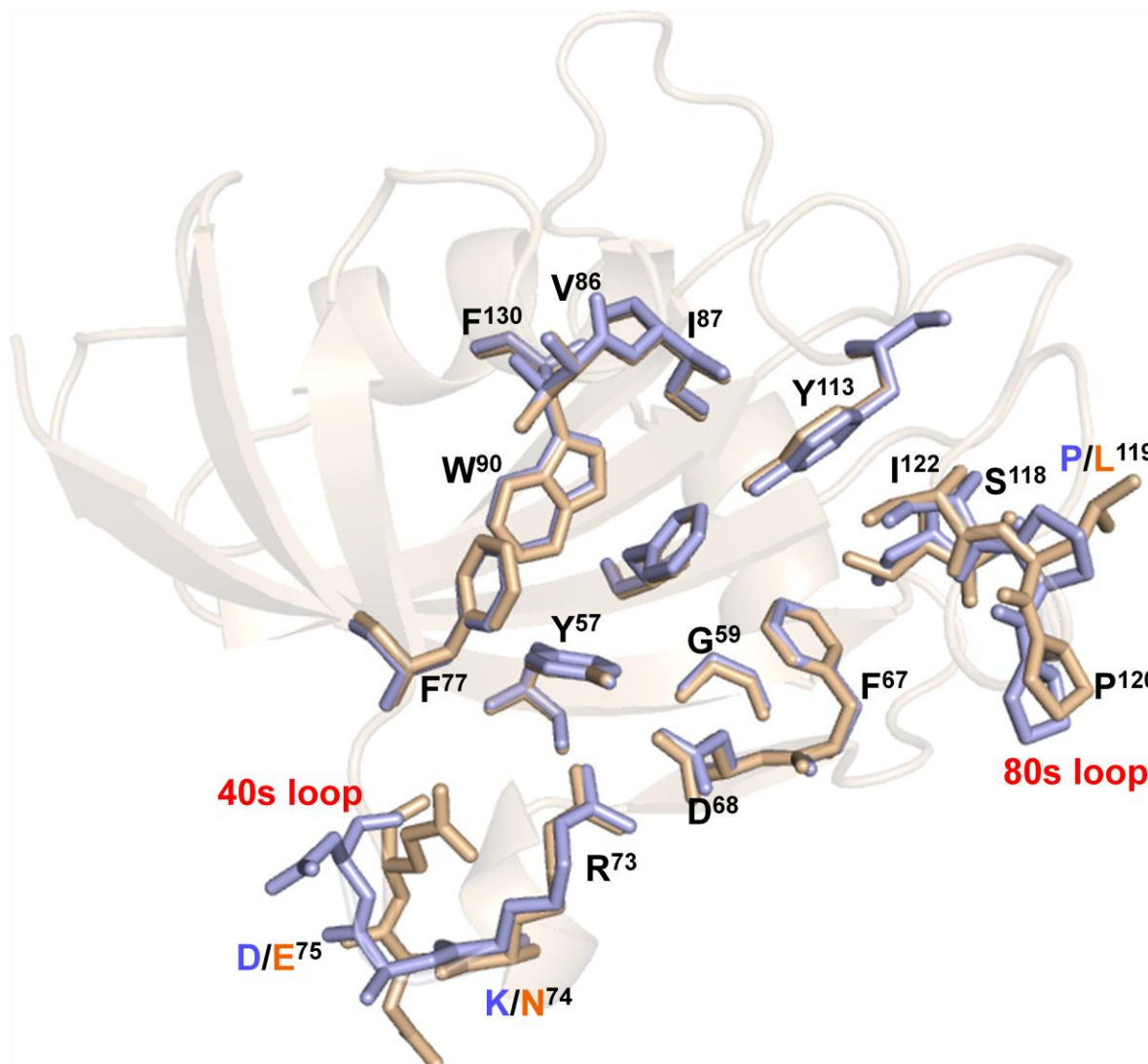


**Figure 11:** Overlay and cartoon representation of the crystal structure of the FK506-binding domains of FKBP51 (305R) shaded in light brown and FKBP52 (unpublished) shaded in light blue. The amino acid residues forming the FK506-binding pocket, the 40s and the 80s loop are shown in stick representation. The structural differences between the two proteins are indicated, the amino acid residue indicated in dark brown corresponds to FKBP51 and amino-acid residue in dark blue corresponds to FKBP52.

### 1.1.7.1 Comparison of FKBP51 and 52 structures with PPIase inhibitors

The core interactions of FK506 are well conserved in the co-crystal structures of FKBP51 (305R) and FKBP52 (unpublished). The pipercolate core of FK506 sits atop the indole ring of Trp<sup>90</sup>, which forms the bottom of the binding pocket. The C<sup>1</sup>-carbonyl has a tight hydrogen bond contact to the backbone amide of Ile<sup>87</sup>, which is also seen in the co-crystal structures of FKBP12. The C<sup>8</sup>-carbonyl is involved in a hydrogen bond with Tyr<sup>113</sup>. Tyr<sup>113</sup> in FKBP51 approaches the C<sup>1</sup>-carbonyl at an angle of 107° with respect to the carbonyl plane and below van der Waals distance of 3.17 Å which is consistent with an attractive dipolar interaction<sup>102,104</sup>. In FKBP52 this attractive dipolar interaction is less pronounced with the Tyr<sup>113</sup> approaching the C<sup>1</sup> carbonyl at an angle of 104.5° and larger distances of 3.36 Å to 3.48 Å. In both the FK506 co-crystal structures the exocyclic hydroxyl group at C<sup>10</sup> engages in a hydrogen bond with the side chain of Asp<sup>68</sup>. The pyranose group of FK506 (**1**) approaches the 80s loop in both the structures and the C<sup>11</sup> methyl group fills the hydrophobic pocket formed by Ile<sup>122</sup>, Tyr<sup>113</sup> and Phe<sup>67</sup> (**Fig. 9a, 9c and 9d**). The C<sup>9</sup>-keto oxygen in both the structures occupies a cavity which is formed by the ε-hydrogens of Tyr<sup>57</sup>, Phe<sup>67</sup> and Phe<sup>130</sup>.

The crystal structures of FKBP51 and FKBP52 with FK506 (**1**) and compound **26**<sup>105</sup> adopt a very similar binding topology (unpublished). In compound **26** (**Fig. 12b**) most of the above described interactions with FKBP51 and FKBP52 are well conserved as seen in the FK506 structures. The C<sup>9</sup>-keto oxygen in **26** occupies a similar position to the keto group of FK506. Owing to the absence of corresponding hydroxyl group in **26** the hydrogen bond with Asp<sup>68</sup> is no longer observed. The tert-pentyl group sits in the same pocket that is occupied by the pyranose group in the FK506 co-crystal structure. The dimethoxyphenyl ring A sits in the cradle that is created by residues Gly<sup>84</sup> – Ile<sup>87</sup> and Tyr<sup>113</sup>. Ring B stacks on the edge of Phe<sup>77</sup>. In FKBP51 the carboxyl group engages in electrostatically enhanced hydrogen bonds with Lys<sup>109</sup> and Arg<sup>31</sup> of a neighboring FKBP51 molecule in the crystal.

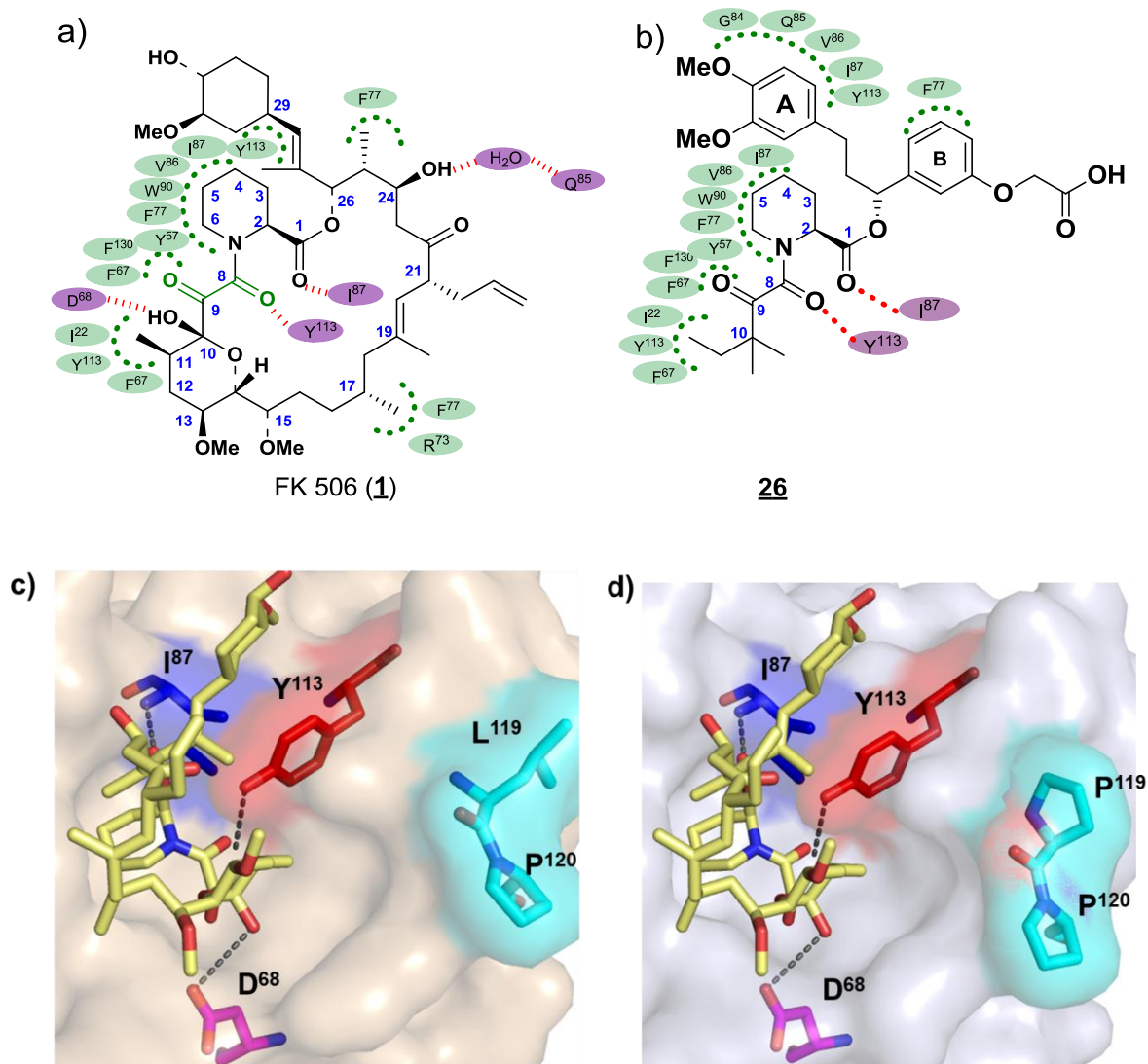


**Figure 12:** Natural and synthetic FKBP ligands (a) Structure of FK506 (**1**), (b) prototypic synthetic ligand of FKBP51 **26** which is devoid of immunosuppressive activity (hydrophobic contacts with FKBP51 are indicated in green, hydrogen bonds formed are dotted in pink and atom numbering of both ligands are shown in blue), (c) binding mode of FK506 (**1**) in complex with the FK1 domain of FKBP51(305R)<sup>102</sup>, (d) binding mode of FK506 (**1**) in complex with the FKBP52 FK1 domain (unpublished). The conserved H-bonds between O<sup>1</sup>-**1** and HN-Ile<sup>87</sup> (blue), O<sup>8</sup>-**1** and HO-Tyr<sup>113</sup> (red) and HO<sup>10</sup>-**1** and O-Asp<sup>68</sup> (magenta) dotted in black. Leu<sup>119</sup> and Pro<sup>120</sup> at the top of the 80s loop in FKBP51 and Pro<sup>119</sup> and Pro<sup>120</sup> at the top of the 80s loop in FKBP52 are colored in cyan in both the structures.

Based on these observations it was hypothesized that optimization of interaction with the 80s loop of the protein has the highest probability of achieving selectivity and functional relevance within the two large FKBP5s.

## **1.2 Manuscripts and Patents**

- 1. The Chemical Biology of Immunophilin Ligands (Manuscript-1)**
- 2. Evaluation of Synthetic FK506 analogs as Ligands for FKBP51 and FKBP52 (Manuscript-2)**
- 3. Exploration of Pipecolate Sulfonamides as Binders of the FK506-Binding Proteins 51 and 52 (Manuscript-3)**
- 4. Design of Ligand efficiency by conformation control (Manuscript-4)**

### 1.2.1 The Chemical Biology of Immunophilin Ligands (Manuscript-1)

The immunophilin ligands Cyclosporin A, FK506 and Rapamycin are known and used in the clinic for their immunosuppressive properties. Pharmaceutical companies have over the years invested on many medicinal chemistry campaigns to develop drugs based on these immunosuppressive natural products. The immunosuppressive and the non-immunosuppressive analogs have been clinically used or investigated in various types of cancers, coronary angioplasty, dermatology, hepatitis C infections, and neuroprotection. The immunophilins have further been found to play a role in various conditions which has led to increased interest in novel immunophilin ligands. Furthermore, the immunophilin ligands have been used as sophisticated tools in chemical biology for the understanding of various cellular functions and mechanisms. The progress in the above areas in the last five years has been reviewed in the underlying manuscript. Part of this review has been implemented in the introduction section of this thesis.

My main contribution to this review where sections **3.3** FKBP51 and FKBP52, **3.4** Microbial FKBP5s and their role in anti parasitic action, **3.5** Non-immunosuppressive cyclosporin analogs, **3.6** Non-peptidic cyclophilin inhibitors.

➤ **The Chemical Biology of Immunophilin Ligands.**

S. Gaali, **R. Gopalakrishnan**, Y. Wang, C. Kozany and F. Hausch\*.

Current Medicinal Chemistry, 2011, 18, 5355-5379.

Copyright permission granted by Bentham Science Publishers

## The Chemical Biology of Immunophilin Ligands

S. Gaali, R. Gopalakrishnan, Y. Wang, C. Kozany and F. Hausch\*

Max Planck Institute of Psychiatry, Kraepelinstr. 2, 80804 Munich, Germany

**Abstract:** The immunophilin ligands cyclosporin A, FK506 and rapamycin are best known for their immunosuppressive properties and their clinical use in transplantation medicine. These compounds or their analogs are also clinically used or investigated in various types of cancer, coronary angioplasty, dermatology, hepatitis C infections, and neuroprotection. Furthermore, the role of immunophilins in various pathologies is increasingly being recognized, supporting the preclinical drug development for novel immunophilin targets. Finally, immunophilin ligands are widely used as sophisticated tools in chemical biology. This review shows the progress on three major areas made in the last five years. An update of the immunosuppressive ligands and their clinical applications is discussed in the first part of the review, followed by a discussion about the emerging immunophilin targets and their respective ligands. The final section gives a detailed assessment of immunophilin ligand-based tools.

**Keywords:** FK506, rapamycin, cyclosporin, immunosuppressant, chemical dimerizers.

### 1. INTRODUCTION

The characterization of the molecular mechanism of action of the natural products cyclosporin A (CsA), FK506 and rapamycin in the early 1990s constitutes one of the finest examples in the discipline of chemical biology. The elucidation of chemically induced protein-protein dimerization as the underlying principle of the immunosuppressive action of these compounds continues to fascinate and inspire generations of scientists.

CsA, FK506 and rapamycin are truly remarkable molecules. First, they bind with very high affinity to their cognate immunophilin partners, called cyclophilins (Cyp) for CsA and FK506-binding proteins (FKBP), for FK506 and rapamycin. The binding to immunophilins usually inhibits their common enzymatic activity, the catalysis of the isomerization around a peptidyl-prolyl bond. In some cases the active sites of immunophilins are also involved in non-catalytic protein-protein interactions that are blocked by immunophilin ligands, possibly giving rise to novel therapeutic options.

Second, and most remarkably, the natural product ligands CsA, FK506 and rapamycin impart a gain-of-function on their immunophilin partners thereby endowing them with the ability to form ternary complexes with the phosphatase calcineurin (for CsA and FK506) or with the kinase mTOR (mammalian Target Of Rapamycin). The possibility to rapidly dimerize appropriately tagged proteins within living cells has inspired numerous sophisticated chemical approaches to address biological questions.

Third, the ternary interaction partners calcineurin and mTOR are key nodes in signal transduction pathways that are essential - amongst others - for immune responses. The inhibition of the latter proteins accounts for the potent immunomodulative activities of CsA, FK506 or rapamycin. This property has transformed the practice of transplantation medicine. Finally, the structural complexity of these natural immunophilin ligands continues to inspire organic chemists to devise total syntheses for these natural products with ever-increasing sophistication.

This review focuses on recent advances in the use of immunophilin ligands in basic as well as translational life sciences. In the first part, we provide a brief overview of the immunosuppressive immunophilin ligands and natural or synthetic analogs thereof. In more detail we discuss the established or emerging clinical applications of rapamycin analogs beyond the immune system and the recent findings on the mechanism of action of rapamycin. The second part covers non-immunosuppressive immunophilin analogs, starting with their historically prominent

role in neurobiology. We then extend to immunophilin homologs (beyond the prototypical FKBP12 and CypA) that have been postulated to be involved in these and other novel possible clinical indications. We then provide an update of the recently published non-immunosuppressive immunophilin ligands. For a summary on the wealth of synthetic approaches to immunophilin ligands before 2005 the reader is referred to comprehensive prior reviews [1, 2]. Likewise, ligands for parvulins, the third major family of prolyl-peptidyl isomerases, have been covered extensively elsewhere [3]. In the last two sections we present the assay systems that are available to characterize immunophilins and recently developed methods where immunophilin ligands (mostly for FKBP12) play a key role in chemically addressing or controlling proteins in living cells or even higher organisms.

### 2. IMMUNOSUPPRESSIVE IMMUNOPHILIN LIGANDS

The prototypic ligands of immunophilins are the immunosuppressants cyclosporin A (CsA), FK506 and rapamycin (Fig. 1). All three compounds are used in the clinic for immunosuppression after organ transplantation to prevent allograft rejection.

Cyclosporin A (CsA, the active ingredient of Sandimmune®, Fig. 1) was first isolated in 1976 from *Trichoderma polysporum* and was the first macrolide with immunosuppressive properties to be discovered. It is a cyclic undecapeptide that binds to the class of cyclophilins (Cyp) [4]. The Cyp-CsA complex forms a ternary complex with the phosphatase calcineurin (CN). In this heterocomplex calcineurin is unable to dephosphorylate its substrate nuclear factor of activated T-cells (NF-AT) which is required for T-cell activation and IL-2 expression [5].

FK506 (Tacrolimus, the active ingredient of Prograf®, Fig. 1) was isolated from *Streptomyces tsukubaensis* and gave the name to its protein targets, the family of FK506-binding proteins (FKBP). FK506 consists of a FKBP-binding domain and an effector domain that conveys the immunosuppressive activity (Fig. 1). Like Cyp-CsA, the FKBP-FK506 complex binds to and allosterically inhibits the common secondary target calcineurin and thereby induces the same immunosuppressive effect [5]. The main FKBP that mediates the immunosuppressive action of FK506 is thought to be FKBP12, with minor contributions of FKBP12.6 and FKBP51 [6, 7].

Rapamycin (Sirolimus, the active ingredient of Rapamune®, Fig. 1) was isolated from *Streptomyces hygroscopicus* in the mid-1970s. It also binds to FKBP but exhibits its immunosuppressive activity via a different mechanism. The FKBP-rapamycin complex differs from FK506 in its ternary partner, the serine-threonine protein kinase mammalian target of rapamycin (mTOR). The allosteric inhibition of the latter results in the blockade of various downstream signaling pathways that control translation of proteins crucial for cell cycle progression [8-10]. mTOR resides

\*Address correspondence to this author at the Max Planck Institute of Psychiatry, Kraepelinstr. 2, 80804 Munich, Germany; Tel: +49(89)30622640; Fax: +49(89)30622610; E-mail: hausch@mpipsykl.mpg.de

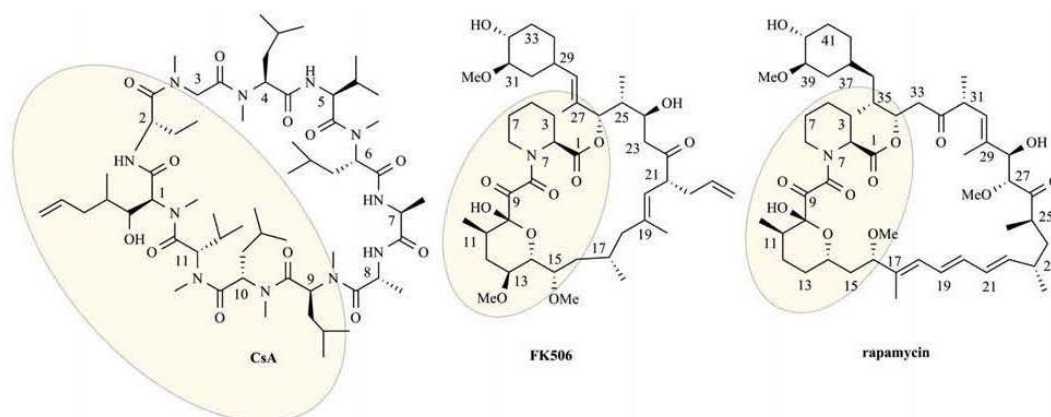


Fig. (1). Highlighted: immunophilin-binding domain (Cyp for CsA, FKBP for FK506 and rapamycin); Aminoacids 3-7 of CsA, Atoms 19-22 and 27-33 of FK506: calcineurin-binding domain; Atoms 15-27 and 34-46 of Rapamycin: mTOR Binding Domain.

endogenously in two multiprotein heterocomplexes, called mTORC1 and mTORC2. The phosphorylation of the mTORC1 substrate S6K has consistently been shown to be highly rapamycin-sensitive. However, the phosphorylation of the second well established mTORC1 substrate 4E-BP1 was recently shown by several groups to be partially rapamycin-resistant, probably in a cell-context dependent manner [11, 12]. This could contribute to the rapamycin-resistance that has been observed for several cancer cell lines. On the other hand, the partial inhibition of only mTORC1 might contribute to the effectiveness on the immune system and the rather benign side effect profile of rapamycin as it was shown to be much more effective on normal lymphocytes than active-site mTOR inhibitors [13]. The selective inhibition by rapamycin of only some mTORC1 phosphorylation sites was attributed to the allosteric nature of the inhibition by the FKBP12-rapamycin complex. The differentiated inhibitory activity of rapamycin – compared to mTORC1 knockdown or mTOR active site inhibitors – seems to be a more general phenomenon as it was also shown for certain phosphorylation sites in the recently identified mTORC1 substrate Grb10 [10] and for the mTORC1-controlled autophagy pathway [14].

The second mTORC2 complex, an activating kinase of Akt/PKB, is thought to be largely rapamycin-resistant upon acute treatment. However, mTORC2 was shown to be sensitive to long-term rapamycin treatment in susceptible cell lines. This was explained by the inhibition of the assembly of novel mTORC2 complexes from *de novo* synthesized mTOR protein [15, 16].

The action of rapamycin is usually discussed and investigated in the context of FKBP12 as the relevant co-inhibitory partner although there is little experimental evidence for this exclusive role. Recently, rapamycin and the analog WAY-179639 (Fig. 5) were shown to bind and inhibit mTOR directly at high concentrations in an FKBP-independent manner [17]. Importantly, the FKBP-independent inhibition by rapamycin was effective on mTOR downstream targets that were previously thought to be rapamycin-resistant in an FKBP-context.

The molecular details of mTOR signaling and rapamycin action in the immune system have emerged to be complex and are still not fully understood. It is now clear that rapamycin should be rather considered an immunomodulator as it was shown to have various and sometimes even activating effects on several cell types of the adaptive as well as on the innate immune system [18-21]. For example, rapamycin was shown to enhance proinflammatory responses in myeloid dendritic cells and in macrophages and it

facilitated the generation of long-lived CD8<sup>+</sup> memory cells [22, 23]. Of particular importance might be the finding that rapamycin can actually facilitate the maturation and expansion of regulatory T cells thereby possibly enhancing allograft tolerance. This could be used for the tailored *ex vivo* expansion of Treg cells in cell-based immunotherapies [24]. In summary, the functional profile of rapamycin in the immune system is complex and could contribute to the effectiveness and tolerability of this molecule in organ transplantations.

Chronic rapamycin treatment has recently been shown to enhance the life span in mice [25, 26]. Rapamycin had previously been shown to induce longevity in a number of invertebrate animal models. Mechanistically, the life span prolonging activity of rapamycin was interpreted as a pharmacological mimic of cellular starvation, reminiscent of caloric restriction which is a well established protocol to promote longevity. This is consistent with the well-known role of mTOR as a coordinator of cellular energy status and nutrient availability [27]. Importantly, in addition to life span extension rapamycin might also improve the quality of life in the elderly as rapamycin was shown to improve the cognitive and behavioral deficits in several animal models of neurodegeneration like Huntington's, Parkinson's and Alzheimer's disease [28-32]. Rapamycin is known to induce autophagy *via* mTOR inhibition and it was shown that this may enhance the clearance of protein aggregates in animal models of Huntington's and Alzheimer's disease [28, 29, 31]. In animal models of Parkinson's disease rapamycin was shown to protect from L-DOPA induced mTOR-mediated side effects or *via* modulation of 4E-BP1-mediated translation. Intriguingly, the allosteric inhibition of only the mTORC1 complex but not the mTORC2 complex by rapamycin was found to be crucial for the protective effects of rapamycin as the active-site competitive mTOR inhibitor Torin1 contrarily induced neuronal death [30, 32].

As mTOR acts on various downstream targets like S6Kinase and 4E-binding protein that promote cell growth and proliferation rapamycin and its analogues were also developed as anti-cancer drugs. A major limitation of rapamycin is its poor solubility. Nevertheless, there are several ongoing clinical test phases for evaluation of rapamycin as a single agent or in combination therapy mainly in tumors with hyperactive PI3K/Akt signaling, e.g., where the expression of the tumor suppressor PTEN is reduced. Abraxis BioScience developed Nab<sup>TM</sup>-Rapamycin (ABI-009) which is bound to albumin to utilize the tumors' attraction to albumin which delivers higher concentrations of the drug to where it is needed [33]. A clinical test phase I is still ongoing (NCT00635284).

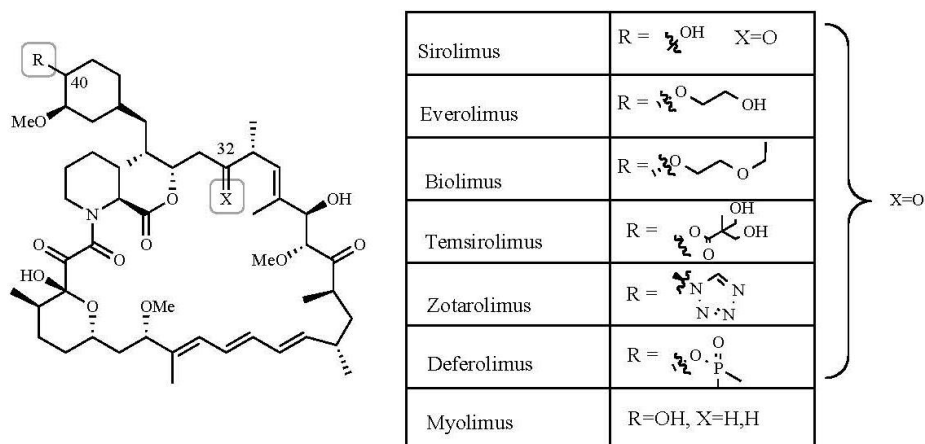


Fig. (2). Clinically used rapamycin analogs.

To improve the aqueous solubility of rapamycin several analogs or prodrugs were developed that all carry a hydrophilic group at the C-40 position of rapamycin (Fig. 2). Temsirolimus (CCI-779, the active ingredient of Torisel®) is a dihydroxyester of rapamycin obtained by lipase-catalyzed esterification of the C-40 hydroxyl group [34]. It displays better aqueous solubility and showed effects in clinical trials of a wide variety of cancer subtypes such as breast cancer, melanoma and advanced renal cell carcinoma. Temsirolimus was approved in 2007 for treatment of advanced kidney cancer by the FDA. Everolimus (RAD001, the active ingredient of Afinitor®, Zortress/Certican®, Promus® and Xience®) is used for preventing allograft rejection of adult kidney transplant recipients and for patients with advanced kidney cancer after failure of either sunitinib or sorafenib and was approved by the FDA in 2009 and 2010, respectively. Everolimus also shows strong effects in a number of other tumors like neuroendocrine tumors, breast cancer, advanced hepatocellular carcinoma or advanced gastric cancer where numerous clinical test phases in stage II or III are ongoing. Everolimus has become a major economical success reaching sales of 1.9 billion dollar worldwide in 2009. Ridaforolimus (Deferolimus, AP23573, MK-8669, Fig. 2), the C40-dimethylphosphinate derivative of rapamycin, has succeeded in clinical test phase III in January 2011 for treating patients with metastatic soft-tissue sarcomas.

Besides immunosuppression and oncology, the third major indication for rapamycin analogs is coronary angioplasty [35, 36].

Here, they are used in drug-eluting stents where they suppress the restenosis of vessel stents by proliferating smooth muscle cells that depend on the mTOR pathway. Zotarolimus (ABT-578, Fig. 2), the C40-tetrazole [37], was approved in 2008 by the FDA and is used as a coronary smooth muscle cell proliferation inhibitor for drug eluting coronary stents. Biolimus (Umirolimus, Biolimus A9), the C40-ethoxyethyl derivative of rapamycin is also clinically used for this indication. Myolimus (SAR-943) is the 32-desoxyderivative of rapamycin that was reported to have improved metabolic stability [38, 39]. It is clinically investigated for use in drug-eluting coronary stents [<http://elixirmedical.com/products/drug-eluting-stent-system?myolimus>].

Ascomycin (FK-520, FR-900520, Immunomycin, L-683590, Fig. 3) was isolated from *Streptomyces hygroscopicus* and differs from FK506 only at position 21 where the allyl group is exchanged by ethyl. Ascomycin also shows strong immunosuppressant effects [40]. The more lipophilic C33-chlorine analog pimecrolimus (SDZ ASM 981, Elidel®, Fig. 3) is clinically used as a topical immunosuppressant for treating skin diseases [41].

Sanglifehrin A is a member of a class of macrolides isolated from the actinomycete strain *Streptomyces* A92-308110 which binds potently to cyclophilins. It also exhibits immunosuppressant activity, although less potently than CsA. The spiro lactam moiety of sanglifehrin A was shown to be dispensable for cyclophilin

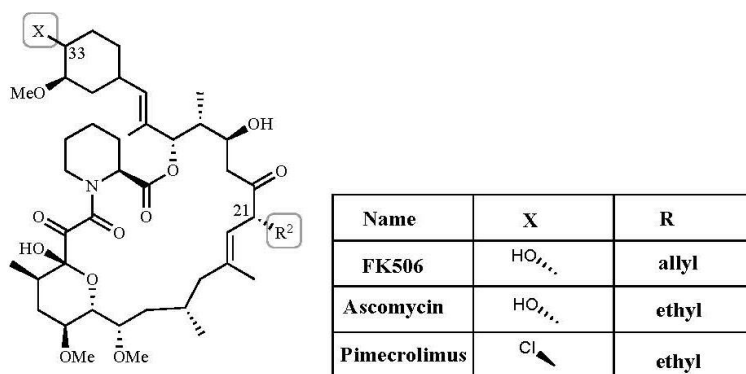


Fig. (3). Clinically used FK506 analogs.

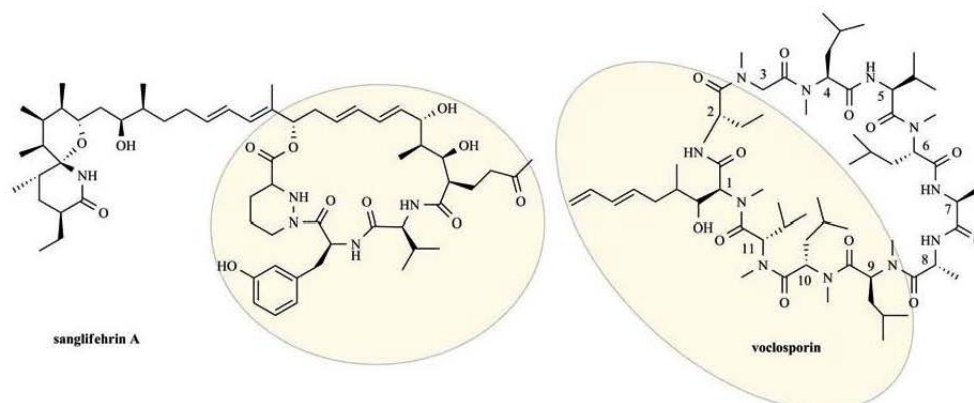


Fig. (4). Highlighted: cyclophilin-binding domain; Aminoacids 3-7 of voclosporin: calcineurin-binding domain; Effector Domain of Sanglifehrin A is unknown.

binding but necessary for immunosuppressive properties [42, 43]. The Cyp-sanglifehrin A complex is not binding or inhibiting calcineurin nor mTOR indicating a different mechanism of action compared to the before mentioned immunophilin ligands. The relevant target(s) of sanglifehrin A remain to be established. Recently, sanglifehrin A was shown to suppress the expression of numerous cytokines as well as the migration of dendritic cells. Importantly, this effect was insensitive to an excess of CsA or a non-immunosuppressive CsA analog, indicating that cyclophilin binding is likely not required for the immunosuppressive effect of sanglifehrin A [44].

E-ISA247 (voclosporin) is a semisynthetic analog of cyclosporin A, where the non-canonical amino acid 4-[(E)-2-butenyl]-4,N-dimethyl-L-threonine (MeBmt) in position 1 was replaced by 4-[(E)-2,4-pentadienyl]-4,N-dimethyl-L-threonine (E-MePmt). The affinity of E-ISA247 for CypA was found to be comparable to CsA (13-15nM) while the Z-isomer (Z-ISA247) bound slightly weaker (60nM). The molecular binding mode of the CypA/E-ISA247 complex was determined to be conserved. The additional terminal methylene group in E-ISA247 was designed to improve the interaction with calcineurin in the ternary complex with CypA. In turn E-ISA247 was found to have higher immunosuppressive activity than CsA. E-ISA247 is being investigated in two phase III trials for psoriasis and in two phase II/III trials for non-infectious uveitis [45].

Total syntheses have been developed for most of the natural product immunophilin ligands. Their structural complexity, however, still challenges the capabilities of modern organic chemistry and these molecules continue to be synthetic targets for improved synthetic methodologies [46, 47]. More recently, the gene clusters coding for the biosynthesis of several immunophilin-binding natural products have been elucidated [48-51]. This has enabled biotechnological approaches for genetically engineered analogs of these very complex natural products.

### 3. NON-IMMUNOSUPPRESSIVE IMMUNOPHILIN LIGANDS

#### 3.1. Neuroimmunophilin Ligands

In the early 1990s FK506, rapamycin and CsA were shown to have additional neuroprotective and neurotrophic effects. These effects can partially be explained by the classical (i.e., immunosuppressive) activity, i.e., *via* calcineurin as it was recently unambiguously shown that the direct inhibition of calcineurin can protect neurons [52]. In contrast, rapamycin was recently found to

block mTOR-dependent axon regeneration explaining some of the earlier reported discrepancies for the neuroprotective actions of rapamycin [53]. In any case, the suppression of immune responses that comes along with FK506, CsA or rapamycin would severely limit the chronic use of these agents for neurological indications. Therefore, the finding that the neuroprotective and neurotrophic effects were partially independent of calcineurin or mTOR inhibition in several experimental paradigms stimulated intense efforts across the pharmaceutical industry for the identification of non-immunosuppressive immunophilin ligands [2, 54, 55].

Several non-immunosuppressive FKBP ligands (Fig. 5 and 6) were shown to be neuroprotective [56] or to increase neurite outgrowth in a variety of neuronal cell systems [54, 57-67]. In addition, non-immunosuppressive immunophilin ligands were active in animal models of diabetic neuropathy [68], traumatic brain injury [69], cerebral ischemia [57, 70], Parkinson's disease [58, 59, 71], as well as various types of physical neuronal injury [54, 60-62, 68, 72].

The non-immunosuppressive FKBP ligands are either semi- or biosynthetic analogs of FK506 or rapamycin where the effector domain was abolished (e.g., FK1706, meridamycin, normeridamycin, ILS920, Way-124466, Wye-592, L685-818, shown in Fig. 5) or small synthetic molecules that mimic the dicarbonyl pipercolyl moiety of the natural products (e.g., V-10,367, JNJ460/GM284, GPII406, GPII485, compound **1**, shown in Fig. 6). FK1706 is a semi-synthetic non-immunosuppressive derivative of FK506 obtained by Wacker oxidation of the allyl-group at C21 [279]. The pharmacokinetic parameters of FK1706 were recently investigated in a small phase I clinical trial [74]. Pharmacokinetic measurements showed that at the doses used the intracellular FKBP pools (in blood) were likely saturated. The fact that no drug-induced discontinuations were reported over the two-week time period indicate that FKBP blockade seems to be tolerated in humans for extended periods of time.

L-685,818 is a semi-synthetic non-immunosuppressive analog of ascomycin obtained by allylic selenium oxidation [75]. The related 13-Me-18-OH FK520 is the selenium oxidation product of a biosynthetic analog of ascomycin obtained from a genetically engineered *S. hygroscopicus* strain [60]. Its affinity to FKBP12 (0.2nM) and to FKBP52 (86nM) is identical to FK506. L-685,818 and 13-Me-18-OH FK520 were active in a rat sciatic nerve crush model [54, 60].

WYE-592, ILS-920 and WAY-124,466 (Fig. 5) are semi-synthetic derivatives of rapamycin that were modified at the triene

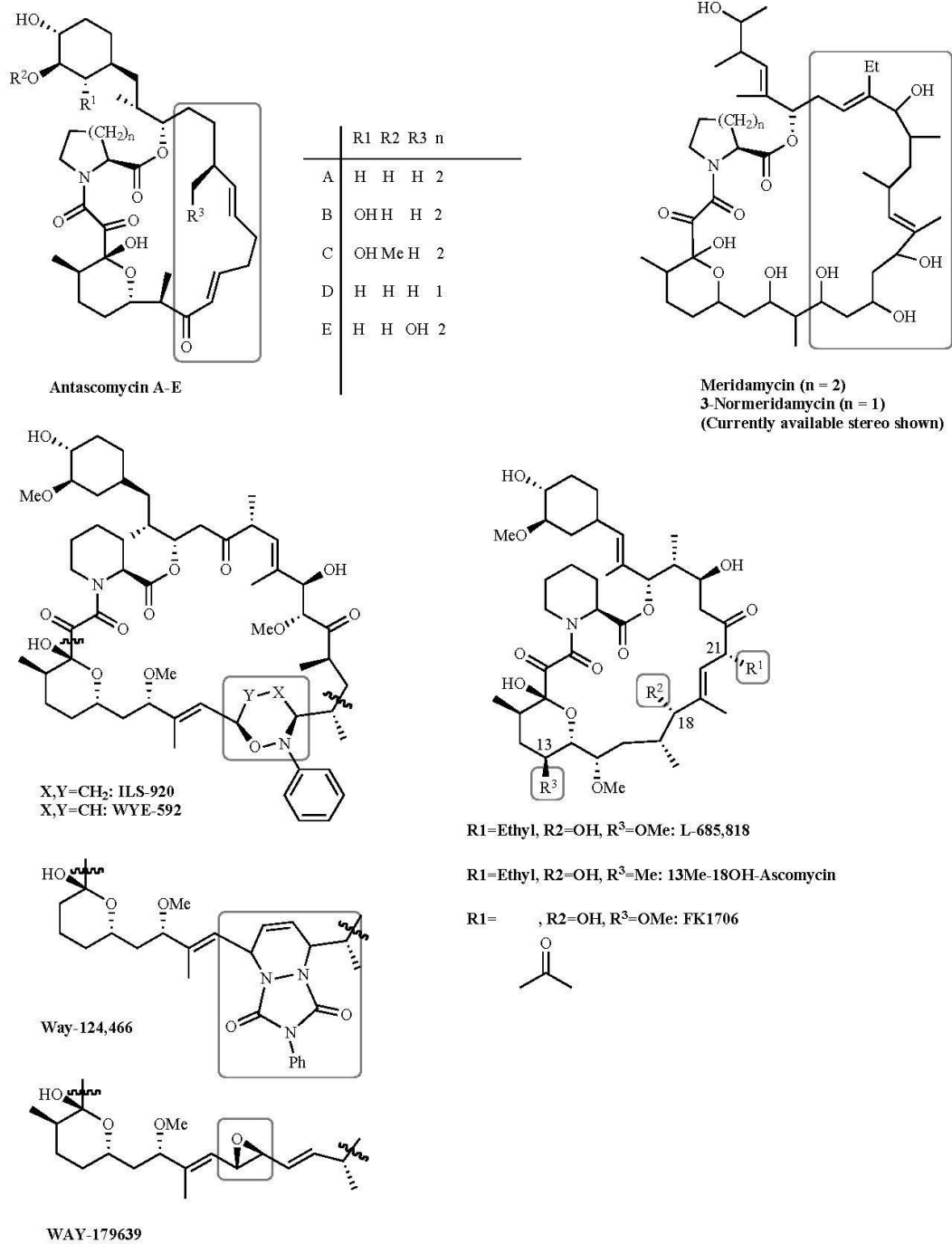
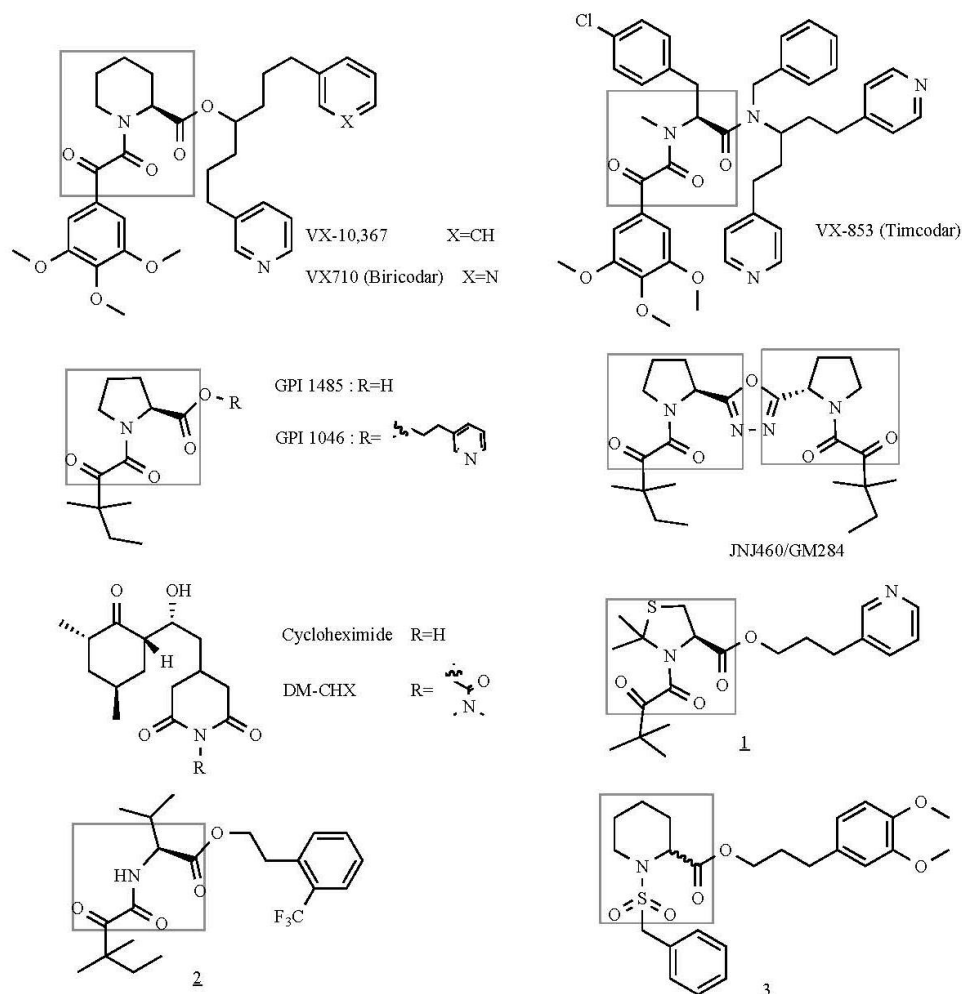


Fig. (5). Natural product-derived non-immunosuppressive FKBP ligands. Modifications compared to FK506 or rapamycin are shaded.

moiety by a Diels-Alder reaction to impair mTOR binding [57, 76]. WYE-592 and WAY-124,466 were active in a neurite outgrowth assay [54, 57]. ILS-920 showed neurotrophic activity in a rodent model for ischemic stroke and recently a phase I clinical trial for this compound was completed (clinicaltrials.gov: NCT00827190).

Meridamycin and 3-normeridamycin (Fig. 5), isolated from *Streptomyces* strains, and the antascomycins (Fig. 5), isolated from a strain of *Micromonospora*, are structurally similar to FK506 and rapamycin in the FKBP-binding part but differ in the effector region. Likewise, they potently bind FKBP12 but lack



**Fig. (6).** Synthetic FKBP ligands. The dicarbonyl pipercolyl moiety derived from the central core of FK506 or rapamycin or equivalent groups are shaded.

immunosuppressive effects. Meridamycin and 3-normeridamycin showed activity in neuronal cell-based assays [58, 59].

Most reported synthetic FKBP ligands are based on the dicarbonyl pipercolyl/prolyl-scaffold derived from the natural products FK506 or rapamycin (Fig. 6). V-10,367 is the most potent synthetic FKBP12 ligand reported to date ( $K_d=0.5\text{nM}$ ) [77]. It has been tested in a number of cellular and animal models for neuroprotection or neuroregeneration. A very close analog of V-10,367, bircodan (VX-710), was reported to retain very high potency for FKBP12 in a PPIase assay ( $K_d=3.7\text{nM}$ ) [78] and to bind the P-glycoprotein (*MDR1*) with  $0.75\mu\text{M}$  [79]. Bircodan was investigated in several clinical trials as a chemosensitizing agent where it was generally well tolerated but showed only very weak efficacy in enhancing the performance of chemotherapeutics against various cancers [80]. In these trials steady state serum levels of  $10\mu\text{M}$  bircodan were achieved suggesting that a prolonged blockade of FKBP is tolerated in humans.

GPI1046 is a typical small molecule analog of FK506 designed to preserve the FKBP-binding part of FK506. It has been extensively reported to promote a variety of neurotrophic/neuroprotective effects, sometimes with extreme potencies,

although there were also contrary reports [81, 82]. Neurotrophic/neuroprotective activities have also been reported for GPI1046 analogs (e.g., compound **1** [83] or JNJ460/GM284 [62]). GPI1046 was originally reported to be a potent FKBP12 inhibitor but this has been challenged by a number of groups [57, 82, 84-86, own unpublished results]. While GPI1046 is inactive for at least two FKBP homologs (FKBP51 and FKBP52, own unpublished results), JNJ460/GM284 was reported as a submicromolar FKBP52 inhibitor that should be metabolically more stable as the labile ester linkage of GPI1046 was removed [62]. GPI1046 is likely at least partially a prodrug, releasing GPI1485 after *in vivo* ester hydrolysis [55]. GPI1485 was tested in two phase II clinical trials for Parkinson's disease and for erectile dysfunction after nerve injury where it failed to show efficacy [88]. GPI1485 was reported to be inactive in a PPIase assay [278], the profile for other FKBP or other targets is unknown. In light of these uncertainties any conclusions regarding the implication of FKBP in experiments with GPI1046 should be interpreted very cautiously.

While most of the early studies focused on the prototypical FKBP12 it is now clear that at least some of the effects of FK506 analogs must be mediated by additional targets. These conclusions

were reached by studying primary neurons from FKBP12-deficient mice [89] as well as by using various FK506 analogs that do not bind to FKBP12, e.g., compounds like timcodar and V-13,661 or V-13,670 that are presumably analogs of timcodar (Fig. 6) [61, 71, 90]. The selectivity profile of these compounds for other FKBP family members is, unfortunately, unknown. Timcodar was reported to be active and equipotent to V-10,367 in two animal models for peripheral nerve diseases (pyridoxine-induced large fiber sensory neuropathy and streptozotocin-induced diabetic neuropathy) [90]. Timcodar was tested in two prospective double-blind placebo-controlled proof-of-concept study for enhancement of cutaneous nerve regeneration and for regenerative sprouting of epidermal nerve fibers where it was shown to be safe but ineffective for the clinical end points [91, 92]. Vertex advanced timcodar in a phase II clinical study for diabetic neuropathy in 1998 but results of this trial have not been disclosed.

In addition to FKBP12 several other FKBP homologs have been put forward as relevant targets of neuroimmunophilin ligands. For FKBP38 the cycloheximide analog DM-CHX (Fig. 6) was developed that potently bound human FKBP38 ( $K_d=85\text{nM}$ ) and showed >200-fold selectivity against several other FKBP homologs [70]. As such, DM-CHX is the most selective FKBP-ligand publicly disclosed. Recently, the structure of a close analog (cycloheximide N-ethylethanoate) was solved in complex with an FKBP-like protein from *Burkholderia pseudomallei* revealing a totally novel FKBP-ligand interaction pattern [93]. It will be interesting to see if FKBP38 adopts a similar conformation in complex with DM-CHX. Of note, cycloheximide is best known for its potent inhibition of protein translation and as such of little use to study FKBP biology in cellular systems. It is therefore important that DM-CHX is devoid of the protein synthesis inhibition associated with the parent cycloheximide. DM-CHX was active in an animal model of focal cerebral ischemia.

A number of studies have suggested the large FKBP52 as a possible neuroimmunophilin target candidate [57, 62, 89, 94, 95]. Most studies assigned an anti-neurotrophic function to FKBP52 based on FKBP52 overexpression, FKBP52 knockdown or anti-FKBP52 antibody treatment. However, in N2a cells FKBP52 was found to increase neurite outgrowth while for the closely related FKBP51 the opposite effect was observed in these cells [95]. Mechanistically, a number of hypotheses have been suggested to explain any anti-neurotrophic effects of FKBP52, including the actions on steroid hormone receptors and on calcium channels (discussed further below). The Beaulieu lab showed that FKBP52 can bind to the microtubule-associated protein tau [96]. Recombinant FKBP52 also inhibits the tau-induced polymerization of purified tubulin although this was not reproduced in a whole cell lysate system [97]. The effect of FKBP-ligands was not tested and since it was reported earlier that the FK506-binding domain of FKBP52 was dispensable for the microtubule-disassembling activity [98] it is unclear how to integrate these findings into a mechanism for neuroimmunophilin ligands. The closely related FKBP51 was also shown to bind tau and  $\alpha$ -tubulin *in vitro* [97, 98]. The Dickey lab showed that FKBP51 can stabilize tau possibly by reducing tau ubiquitinylation. In their system FKBP51 enhanced microtubule formation in a PPlase-activity dependent manner although no direct pharmacological inhibition studies were performed. Given the partially diverging findings, the physiological and pharmacological relevance of the role of the large FKBP51 and microtubule dynamics needs to be further defined in animal models and in studies with inhibitors.

While it is clear that FKBP ligands can have neuroprotective or neurotrophic activities in appropriate settings the field has been plagued by inconsistencies and conflicting results possibly caused by differences in the neuronal systems, animal models or ligands used. Importantly, the molecular mechanisms underlying the neuroprotective/neurotrophic activities of immunophilin ligands or

the relevant targets are still a matter of substantial debate [55], and a number of hypotheses have been put forward. FKBP12 is known to bind the TGF $\beta$  type 1 receptor, and FKBP ligands were shown to enhance TGF $\beta$ R1 signaling [62]. Interestingly, this is one of the examples of a direct protein-FKBP interaction that utilizes the FK506-binding site but does not seem to involve peptidyl-prolyl isomerization [99]. The Ras/Raf/MAPK pathway was shown to be involved in the enhancement of neurite outgrowth by FKBP ligands [67]. This can be explained by the recently described enhancement of Ras depalmitoylation/inactivation by FKBP12 [100]. The aggregation of  $\alpha$ -synuclein was shown to be enhanced by FKBP12 and other FKBP5s in an FK506-sensitive manner [87, 101, 102]. This could contribute to the effects observed in animal models of Parkinson's disease. To identify the targets of the non-immunosuppressive rapamycin analogs WYE-592 and ILS-920 (Fig. 5) a proteomic analysis of pull-down experiments identified FKBP52 as a preferred interaction partner. Compared to the parent compound rapamycin these two derivatives seem to have further acquired the additional property to bind the CACNB1 subunit of L-type voltage-gated calcium channel leading to a diminished  $\text{Ca}^{2+}$  ion conductance [57].

The regulation of  $\text{Ca}^{2+}$  signaling is a recurring but still insufficiently defined theme in FKBP biology. FKBP12 and 12.6 have long been known for their FK506-sensitive association with the ryanodine or  $\text{IP}_3$  receptors which release  $\text{Ca}^{2+}$  from the endoplasmic reticulum or from the sarcoplasmic reticulum in muscle cells. FK506 and rapamycin were reported to weakly inhibit the sarco-endoplasmic reticulum  $\text{Ca}^{2+}$  ATPase (SERCA) which transports  $\text{Ca}^{2+}$  from the cytosol into intracellular  $\text{Ca}^{2+}$  stores [103-105]. However, these results have been challenged [103, 106]. In any case, the concentrations of FK506 or rapamycin that were necessary for SERCA inhibition were very high and are difficult to be reconciled with the potencies usually observed for neurotrophic effects. The action of GPII046 was also reported to deplete sarco-endoplasmic  $\text{Ca}^{2+}$  stores but the underlying molecular mechanism was not elucidated [107].

FKBP12 and FKBP52 were both shown to interact with numerous transient receptor potential receptor channels (TRP-C) in an FK506-sensitive manner [94, 108-110]. FKBP52 reduced the channel conductance of TRPL and TRPV5 while it enhanced it for TRPC1. The effects on TRP channel conductance were sensitive to PPlase-inactivating mutations in FKBP52 and proline mutations in the TRP channel. TRPC1 is known to mediate axon guidance and Shim *et al.* could show that this was modulated by FKBP52 whereas a PPlase-inactive mutant displayed a dominant-negative phenotype [94].

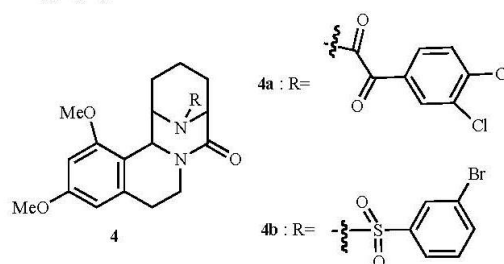


Fig. (7). Constrained polycyclic FKBP ligands.

The three natural products CsA, FK506 and rapamycin as well as several of their derivatives are all inhibitors of the P-glycoprotein 1, a major drug efflux transporter [111]. In fact, three non-immunosuppressive derivatives of CsA and FK506 have been developed as specific P-gp 1 inhibitors, e.g., valsopodar (PSC-833,

Fig. 9), biricodar (VX-710, a close analog of VX-10,367) and timcodar (VX-853, Fig. 6). The direct binding of FK506 analogs to P-gp 1 was proven by photocrosslinking experiments using a radioactively labeled, photoreactive analog of biricodar [79]. The fact that timcodar and presumably close relatives thereof (e.g., V13-661 and V-13670) lack FKBP binding but retain P-gp inhibition [90] suggests that P-gp inhibition could contribute to some of the observed neurotrophic/neuroprotective effects as has been discussed in the patent literature [2].

### 3.2. Novel FKBP Ligands

Compared to the activities before 2005 relatively few efforts for discovery of novel synthetic FKBP ligands have been described in the last six years. This is likely due to inconsistencies and uncertainties regarding the relevant target(s) and due to the disappointing results from the clinical trials for GPI1485 and timcodar. It should be noted that while effective in animal models for neurological disorders both compounds do not target human FKBP12 and may not target FKBP51 at all.

Most medicinal chemistry efforts have targeted the prototypical FKBP12. Pfizer elaborated on earlier work [112] to investigate the polycyclic scaffold **4** as a preferred FKBP binding motif [113]. They made use of the relatively open FKBP12 binding site to introduce a substituent at the axial position at C<sup>6</sup> of the pipercolate that constitutes the core of FK506 and rapamycin and is found in most FKBP ligands. The C<sup>6</sup>-substituent was further cyclized with the C<sup>1</sup>-carbonyl to yield a very rigid [3.3.1] aza-amide core where the C<sup>1</sup>-carbonyl is preoriented for productive H-bond interaction with Ile<sup>56</sup> of FKBP12. Hudack *et al.* further installed a tetrahydroisoquinoline moiety *via* acyl iminium chemistry. Systematic elaboration of the structure activity relationship identified the oxygen at C<sup>1</sup> as being essential whereas ketoamides, sulfonamides, sulfamides, ureas and  $\alpha,\alpha$ -difluoro amides were tolerated as substituents at N<sup>7</sup>. The best compounds were compounds **4a** and **4b** with 34nM and 54nM affinity for FKBP12, respectively. A follow-up methodology paper by the Pfizer group described the optimized library synthesis of sulfamide ligands for FKBP12 but no biological data were presented [114].

Based on computer modeling, Zhao *et al.* designed and synthesized a series of non-cyclic derivatives of GPI-1046 exemplified by compound **2** (Fig. 6) [63]. They proposed that these compounds could adopt an energetically favored binding mode analogous to GPI-1046 when bound to FKBP12. Six out of eleven test compounds were effective in a cellular neurite outgrowth assay but no binding data for FKBP12 were presented.

FKBP12 has been the seminal example for a structure-based screening approach of small organic fragments using nuclear magnetic resonance spectroscopy [115]. Following this tradition, Röhrig *et al.* linked two fragments previously known to bind to two adjacent sites on the FKBP12 surface with different linker

structures and evaluated them using an NMR-based method previously developed by the authors [116]. The best compound **5** (Fig. 8) had an affinity for FKBP12 of 80nM determined in a fluorescence quenching assay, similar to previously described conjugates [115].

NMR was also applied by Stebbins *et al.* to screen a small library of fragments or natural products for novel FKBP12 binders [117]. Several hits with micromolar affinity were identified and confirmed by isothermal calorimetry. Exploration of hit **6a** (Fig. 8) led to compound **6b** with an estimated affinity of 0.2 $\mu$ M as determined by NMR titration. Compounds **6a** and **6b** were active in a neurite outgrowth assay. The affinity of fragment **6a** was confirmed by an independent group by isothermal calorimetry, surface plasmon resonance and a mass spectroscopy-based assay [118].

### 3.3. FKBP51 and FKBP52

In addition to FKBP12 the two large human FKBP51 and FKBP52 have recently received considerable attention. These large FKBP homologs are cochaperones that are best known for the regulation of steroid hormone receptors in association with the heat shock protein 90 (Hsp90) [119]. Interestingly, in spite of their high degree of homology FKBP51 and FKBP52 regulate the glucocorticoid receptor in opposing directions, with FKBP51 being an inhibitory and FKBP52 being a stimulatory factor. Knockout mice revealed an essential role of FKBP52 for a correct sex steroid hormone-dependent development [120]. The importance of the inhibitory FKBP51 on organismic steroid homeostasis is supported by primate species that naturally overexpress a hyper-inhibitory version of FKBP51 [119]. Intriguingly, FKBP51 and FKBP52 might also share a mutually redundant but essential function as the double knockout of both proteins was reported to be embryonic lethal [121]. The nature of this synthetic lethality remains to be elucidated.

The expression of FKBP51 is consistently induced by stress and by numerous steroids [122-124]. Numerous human genetic studies have indicated a role of FKBP51 in the pathogenesis of stress-related psychiatric disorders [125, 126]. Mechanistically, FKBP51 is thought to reduce the responsiveness of the glucocorticoid receptor to the hormone cortisol that is secreted in response to stressful situations. Knockdown of FKBP51 in the amygdala was shown to reduce an anxiety-like behavior in the elevated plus maze test, but only after a prior stress challenge [122]. Similar results were observed with constitutive FKBP51-knockout mice [127, 128].

In addition to affective disorders FKBP51 has also emerged as a potential target for various types of cancer [129, 130]. FKBP51 has been repeatedly been shown to be upregulated in many cancer cell lines including prostate cancer. Recently, the Paschal and the Sanchez groups independently showed that FKBP51 unexpectedly

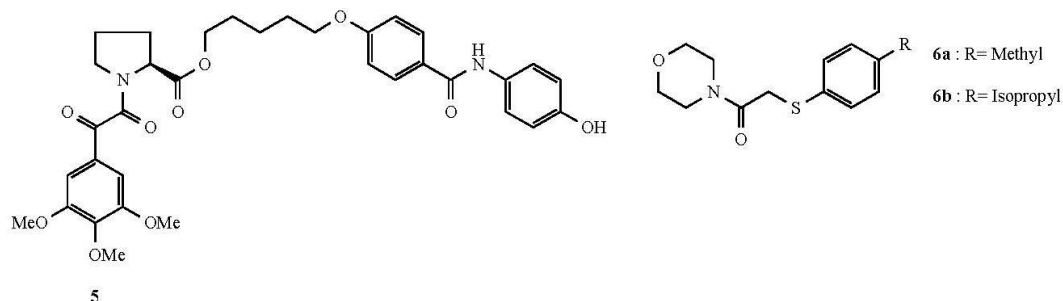


Fig. (8). FKBP ligands discovered by NMR screening approaches.

enhanced androgen receptor signaling in various prostate cancer cells [131, 132] possibly leading to a vicious fast forward feedback loop. Importantly, the stimulating effect of FKBP51 on the androgen receptor was found to be sensitive to FK506. Whether these intriguing findings extend to the situation *in vivo* or to the clinically more important androgen-independent prostate cancer subtypes remains to be established.

Romano *et al.* showed that silencing of FKBP51 sensitizes malignant melanoma cells to radiation in cell culture and in a xenograft model [133]. The authors showed that FKBP51 silencing abolished irradiation-induced NF- $\kappa$ B activation which had previously been shown to depend on FKBP51 [134]. The role of FKBP51 in cancers is, however, complex and likely cell-type dependent. In a pancreatic cell line FKBP51 silencing was shown to enhance chemoresistance. In the search for an underlying mechanism Pei *et al.* identified FKBP51 as an adaptor protein to enhance the dephosphorylation of Akt, a kinase frequently deregulated in cancer, by the phosphatase PHLPP [135]. Whether FKBP51 functions as a tumor suppressor remains to be investigated and recent data from the Romano lab indicate that this does not seem to be the general case [277].

The effects of FKBP51 and FKBP52 on steroid hormone receptors were both demonstrated to be independent of peptidyl-prolyl-isomerase activity. However, the effects of both proteins were shown to be sensitive to FKBP ligands like FK506 or rapamycin indicating that the FK506-binding site is important for steroid hormone receptor regulation [136-138]. However, the effects of FKBP ligands on steroid hormone receptors in cellular assays are confounded by the P-glycoprotein inhibition typically exerted by these compounds since it was shown that the intracellular (i.e., active concentration) of steroid hormones is modulated by P-gp [139, 140]. The cellular characterization of FKBP51 and FKBP52 is further complicated by the antagonistic role of these close homologs on steroid hormone signaling stressing the need for subtype-selective inhibitors. Towards this goal a series of high-resolution structures of the FK506-binding domain of FKBP51 was recently published [141]. This showed the expected high structural similarity of the active site that was previously observed within the FKBP family. But it also indicated divergences in the loop regions that might be a starting point for achieving subtype selectivity. So far only one small synthetic ligand, SLF (also known as AP1497, Fig. 14c), has been described for FKBP51 in addition to FK506 and rapamycin [142].

### 3.4 Microbial FKBP5s and their Role in Antiparasitic Action

Several FKBP isoforms have been identified in various pathogenic microorganisms and parasites and were suggested as potential anti-infective targets [143]. The most widely studied microbial FKBP homolog is the Mip (macrophage infectivity potentiator) protein which is present in human pathogens like *Legionella pneumophila*, the causing agent of Legionnaire's disease, or *Trypanosoma cruzi*, the pathogen causing Chagas disease. *L. pneumophila* Mip was shown to facilitate intracellular survival and infectivity in an animal model in a PPIase-dependent manner [144]. Likewise, the Mip from *T. cruzi* enhanced HeLa cell invasion by this species in an FK506-sensitive manner [145]. However, immunosuppression by FK506 would be counterproductive for the study or treatment of pathogens and Oz *et al.* showed that the nonimmunosuppressive analog L-685,818 (Fig. 5) but not FK506 itself was active in an animal model of *T. cruzi* infection [146].

Ceymann *et al.* solved the NMR structures of *L. pneumophila* Mip in complex with rapamycin [147]. Building on this structure Juli *et al.* rationally designed a series of pipercolate-containing sulfonamides [148]. The best compound **3** (Fig. 6) inhibited *L. pneumophila* Mip with an IC<sub>50</sub> of 6  $\mu$ M compared to 0.2  $\mu$ M for human FKBP12. However, compound **3** was inactive in an assay

for macrophage-like cell infection whereas rapamycin as control was active.

Recently, an ultra-high resolution structure of Mip from *Burkholderia pseudomallei* as well as an NMR structure in complex with the DM-CHX analog cycloheximide N-ethylethanoate was solved. This compound inhibited the PPIase activity with a K<sub>i</sub>=6.5  $\mu$ M. Most importantly, the NMR structure revealed a highly unexpected dynamic rearrangement of the active site that is distinct from all co-crystal structures obtained with FK506-derived inhibitors so far [149].

The other intensively characterized microbial immunophilin is FKBP35 from *Plasmodium falciparum*, the causing agent of malaria [143]. A related PvFKBP35 was found in *P. vivax* while *T. gondii* has a dual immunophilin, i.e., a protein having both a FKBP domain and a Cyp domain. FK506 and rapamycin are known to inhibit the growth of the above parasites in culture [143]. Monaghan *et al.* showed that non-immunosuppressive 18-hydroxy derivatives of ascocymycin (e.g., L-685,818, Fig. 5) dose-dependently inhibited the growth of *Plasmodium falciparum* in culture [150]. In this context it should be kept in mind that while L-685,818 does not inhibit calcineurin in complex with human FKBP12, it does so in complex with yeast FKBP12 [151]. It is therefore possible that L-685,818 retains the ability to form trimeric complexes with PfFKBP35 and PfcCaN which in turn could mediate the observed growth inhibition. Kumar *et al.* used affinity chromatography to show that PfFKBP35 is the predominant immunophilin in *P. falciparum* that binds to ascocymycin (the only detectable protein in their pull-down experiment) [152]. In contrast, Monaghan *et al.* used a series of ascocymycin analogs that did not bind the PfFKBP35 active site to show that they still inhibited *P. falciparum* growth [150]. This might suggest that while PfFKBP35 is the most abundant FK506-binding protein in *P. falciparum* other less abundant proteins might be more relevant for the growth-inhibiting effects. Further pharmacological studies with genetically engineered *P. falciparum* strains might be necessary to clarify the role of PfFKBP35.

### 3.5 Non-Immunosuppressive Cyclosporin Analogs

Several viruses have been shown to rely on cyclophilins as essential host factors for their replication cycle and/or for infectivity. Viral interaction partners of cyclophilins are for example the p24 capsid protein expressed by the human immunodeficiency virus-1 and the hepatitis C virus non-structural proteins NS2, NS5A and NS5B.

Several studies have shown cyclophilin ligands to reduce HCV-specific RNA replication *in vitro* and *in vivo*. Importantly, this effect was independent of calcineurin inhibition by CsA leading to the development of the non-immunosuppressive analogs Debio-025, NIM-811 and SCY-635 that are currently clinically evaluated for HCV indication. To abrogate the binding to calcineurin, these derivatives were designed to contain modifications in position 3 and 4 of CsA which were known to be critical for calcineurin engagement (Fig. 9). The branched or more bulky residues at position 4 (e.g., the Val-4 side chain of Debio-025) are thought to sterically block the interaction with the hydrophobic pocket of CaN. In addition these modifications increase the affinity for CypA [153, 154]. Antiviral efficacy was also shown for sanglifelin A and analogs thereof [43, 155-157].

Mechanistically, a consensus emerged for CypA as the major physiological anti-HCV target of cyclophilin ligands, with minor possible contributions of CypB, Cyp E, Cyp H and Cyp40 [43, 156]. Recently, a novel CsA-binding protein called CAHL was identified that formed complexes with NSSB and CypB, the latter interaction being sensitive to CsA [158].

A recurring problem in antiviral therapies is the rapid emergence of drug-resistant strains due to the high mutation rate of

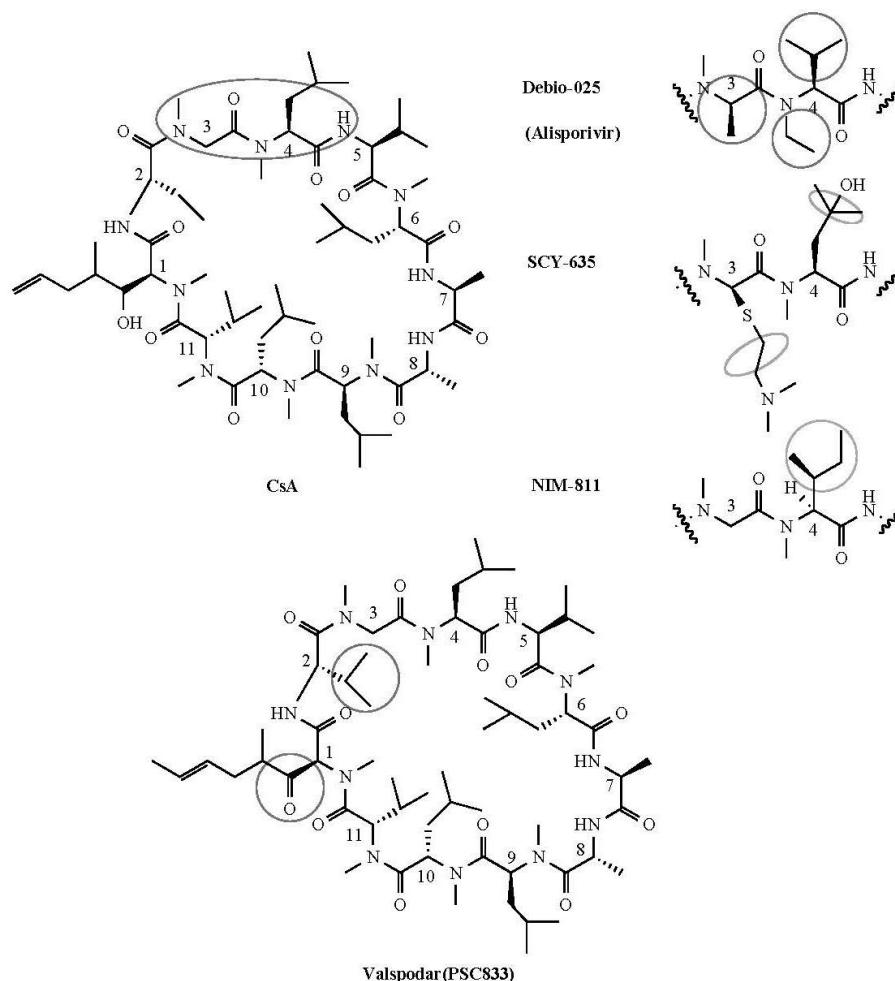


Fig. (9). Non-immunosuppressive cyclosporin analogs that have been investigated in clinical trials.

the viruses. Recent studies revealed a high barrier to resistance during Debio-025 treatment, indicating that the acquisition of independence from a host factor is a rather rare event. Importantly, no cross-resistance was observed for NIM811 or Debio-025 in combination with the current standard anti-viral therapies (pegylated interferon and ribavirin) or with new HCV-specific treatments like polymerase inhibitors or recently approved HCV protease inhibitors. Instead, additive or even synergistic antiviral activities were observed [159].

For all three CsA analogs impressive antiviral effects were observed during clinical studies which have been extensively reviewed elsewhere [160, 161]. The most prominent adverse effect seems to be hyperbilirubinemia. Alisporivir (Debio-025) is the most advanced candidate which has recently entered a phase III clinical trial (ClinicalTrials.gov Identifier: NCT01318694).

Cyclosporin A is a well established inhibitor of the P-glycoprotein 1 (P-gp 1, also called MDR-1 or ABCB1), one of the major cellular efflux pumps thought to contribute to drug resistance during chemotherapy. Valspodar (PSC833, the active agent of Amdray<sup>®</sup>, Fig. 9) was designed as a non-immunosuppressive cyclosporin D analog that has improved inhibition activity for the

P-glycoprotein (10nM) and specificity vs. several other human efflux transporters [162]. The oxidation of the hydroxyl group of the Bmt group in position 1 and the replacement of 2-aminobutyric acids in position 2 by valine abolish the affinity for most human cyclophilins [43]. Valspodar was evaluated in four phase III clinical trials in combination treatments for cancer, mostly acute myeloid leukemia. These did not show a clinical benefit compared to established chemotherapeutics used alone but rather indicated additional toxicity leading to a stop of the further clinical evaluation of PSC833.

CsA as well as three non-immunosuppressive analogs were reported to inhibit the sarco-endoplasmatic reticulum  $Ca^{2+}$  ATPase (SERCA) pump, with SERCA2b being the primary target. While the potency of CsA was found to be modest ( $>5\mu M$ ), NIM811 and sanglifehrin A inhibited SERCA2b at 100nM and 50nM concentrations, respectively [103, 106]. The direct relevant binding sites and the physiological relevance of these activities remain to be established.

Cyclophilin A is usually an intracellular protein. However, after oxidative stress or inflammatory stimuli it can be released into the extracellular space, possibly *via* a vesicular pathway [163].

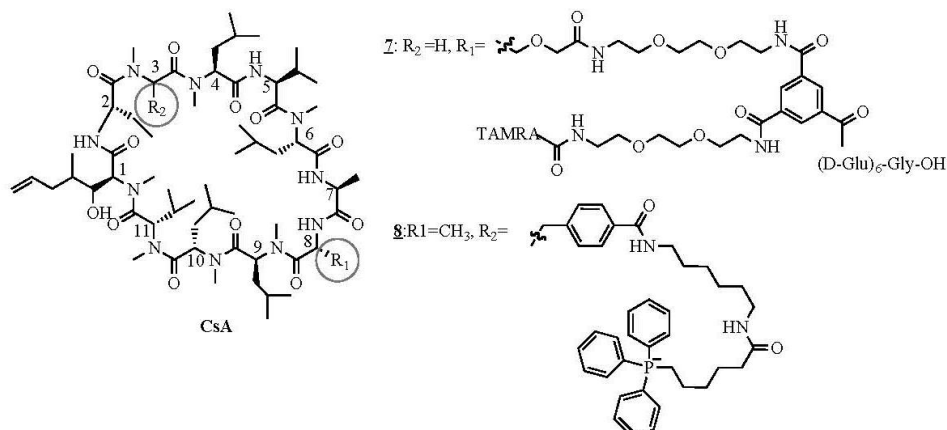


Fig. (10). Cyclosporin A analogs designed to control intra- or extracellular localization.

Extracellularly it acts as a chemoattractant by binding to the cell surface receptor CD147 (also called EMMPRIN) on leukocytes to recruit them into inflamed tissues. NIM811 completely blocked neutrophil migration in response to CypA *in vitro* and it significantly reduced the infiltration of neutrophils into LPS-challenged lung tissue *in vivo* [164]. To selectively address the extracellular pool of cyclophilins, Fischer and coworkers synthesized cell-impermeable CsA derivatives [165]. Based on earlier work [166] a highly charged oligo-glutamate tag was introduced at position 8 of [D-Ser<sup>8</sup>]-CsA (compound **7**, Fig. 10). In addition a TAMRA dye was added to track the cellular location of **7**. As expected, this compound was incapable to penetrate cells which also abrogated the immunosuppressive properties of the conjugated [D-Ser<sup>8</sup>]-CsA. However, the cell-impermeable CsA derivative still inhibited CypA-induced T cell chemotaxis. Furthermore, **7** was also active in an animal model of allergic lung inflammation after nasal application [167]. This approach could thus allow a highly focused targeting of the extracellular cyclophilins in the lung thereby substantially improving the therapeutic index of cyclophilin inhibitors for this indication.

Cyclophilin D, encoded by the *Ppif* gene, is located at the inner mitochondrial membrane where it facilitates the opening of the mitochondrial permeability transition pore (PTP). The latter plays a key role in cell death and has been implicated in a variety of diseases. Studies with CsA, sangliferrin A or non-immunosuppressive analogs thereof in combination with *Ppif*<sup>-/-</sup> transgenic mice have validated CypD as a target in animal models for heart or brain ischemia-reperfusion, collagen VI-related disorders, Alzheimer's disease, diabetes, and bipolar disorder [73, 168, 169].

A first clinical support for the concept of CypD inhibition was provided in two small trials of patients with myocardial infarction [170] or collagen VI myopathies [171]. It should be noted that the doses of CsA used in these studies were rather low leaving some uncertainties whether immunosuppressive (i.e., calcineurin inhibition) or non-immunosuppressive (i.e., CypD inhibition) is primarily responsible for the observed effects. Recently, a phase II/III clinical trial with cyclosporin was initiated by the European brain injury consortium for traumatic brain injury (press release www.neurovive.com).

It should be noted that the CD147-CypA system discussed above has recently been shown to also contribute to reperfusion injury after myocardial ischemia [172]. It is therefore possible that some of the effects observed with CsA analogs in animal models of myocardial ischemia might be due to the blockade of the CD147-CypA engagement.

The structures of CypA and CypD were shown to be very similar [173] indicating that the development of subtype-specific Cyp-inhibitors is likely challenging. In order to preferentially target CypD in cells, Malouitre *et al.* introduced a triphenylphosphonium moiety at the 3-position of CsA (compound **8** in Fig. 10) [174]. This modification abrogated calcineurin binding. The lipophilic cationic TTP<sup>+</sup> group was intended to enrich the conjugate in the negatively polarized inner membrane of mitochondria where CypD is located. Subsequent cellular assays suggested a preferential inhibition of mitochondrial CypD compared to cytosolic CypA.

### 3.6. Non-Peptidic Cyclophilin Inhibitors

Numerous groups explored novel cyclophilin inhibitors unrelated to the archetypical CsA scaffold. Towards this end a variety of *in silico* screening methods were applied based on the available crystal structures.

Guichou *et al.* defined two hydrophobic pockets that harbor the CsA residues MeVal11 and Abu2 in the CsA/CypA cocrystal structure. In addition, a hydrogen bond acceptor corresponding to the carbonyl of MeBmt1 was defined as a key interaction [175]. Based on this pharmacophore they analyzed a database containing 296,387 commercially available compounds for potential CypA binders. Among the identified *in silico* hits compound **9** (Fig. 11) was reported to inhibit CypA PPIase activity with an IC<sub>50</sub> of 0.32 μM although this could not be replicated in a competitive fluorescence polarization assay (own unpublished observations) [176]. Numerous analogs of this hit were prepared with reported inhibitory activities up to 14nM. **9** was shown to block the cell infection competence of HIV-1 virions.

Jiang and coworkers described quinoxaline derivatives as possible lead structures to inhibit cyclophilin D [177, 178]. The best compound **10** bound CypD with an affinity of 2μM as determined by surface plasmon resonance and confirmed by tryptophan quenching and PPIase assays. This compound also inhibited Ca<sup>2+</sup>-dependent mitochondrial swelling and showed a ten-fold selectivity for CypD vs. CypA.

Jiang and colleagues also employed high-throughput *in silico* docking to identify potential CypA ligands resulting in compounds like **11** (Fig. 11) with a reported IC<sub>50</sub>=5μM in a PPIase assay [179]. In a subsequent study these authors merged the identified sulfanilamide moiety with the 2,3-di(furan-2-yl)quinoxaline scaffold identified earlier (e.g., in compound 10) resulting in compounds like **12** with a reported PPIase-inhibitory activity of 1μM [180]. In both studies the binding observed by surface

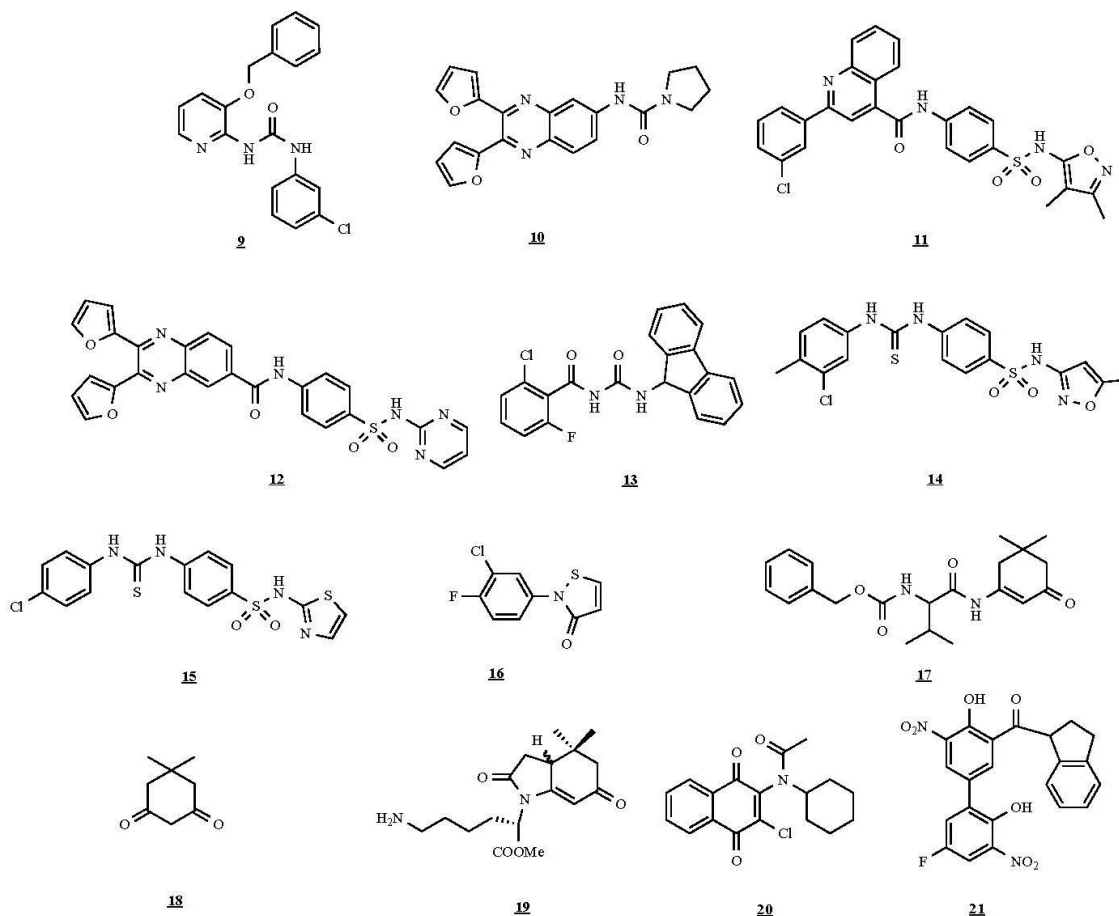


**Fig. (11).** Non-peptidic cyclophilin inhibitors.

plasmon resonance were substantially weaker than the data from the PPIase assays leaving some uncertainties regarding the true affinities.

Ni *et al.* used a computational *de novo* design approach based on the CypA/sanglifehrin cocystal. This led to a series of acylureas exemplified by compound **13**, which was reported to inhibit the PPIase activity of CypA with a remarkable  $IC_{50}$  of 1.5nM [181].

Yang and coworkers designed dual inhibitors for CypA and for the HIV-1 capsid protein based on a thiourea motif [182]. Compound **14** was described to inhibit CypA PPIase activity with an  $IC_{50}$  of 0.65 $\mu$ M while the affinity determined in a tryptophan fluorescence quenching assay was 56 $\mu$ M. The compound was shown to reduce the assembly rate of the capsid protein and to display anti-Simian immunodeficiency virus activity. Control experiments confirmed that compound **14** was inactive at the HIV1 protease or HIV1 integrase. Further modification around compound **14** resulted in compound **15** which inhibits CypA PPIase activity with an  $IC_{50}$  of 0.13  $\mu$ M and having equivalent antiviral activity [183].

Mori *et al.* recently identified compound **16** in a medium throughput screening for the PPIase Pin1. Surprisingly, this substance also inhibited CypA with an  $IC_{50}$  of 14 $\mu$ M while it was inactive for FKBP12 [184].

Walkinshaw and colleagues used the LIDEAUS docking algorithm to search the Maybridge chemical database consisting of 50,000 different compounds [185]. Dimedone **18** was identified as a weakly binding fragment which was confirmed by X-ray cocystallography. Based on the observed binding mode analogs like compound **17** were synthesized that inhibited CypA with 28 $\mu$ M. The affinity was confirmed by surface plasmon resonance and tryptophan quenching experiments, and the molecular binding mode was confirmed by X-ray cocystallography. Based on these results the Walkinshaw and Turner groups went on to design constrained dimedone analogs like compound **19** with an  $IC_{50}$  of 8.6 $\mu$ M in a PPIase assay and a  $K_d$  of 16 $\mu$ M as determined in a tryptophan quenching assay [186]. When applied to *C. elegans* **19** caused a phenotype characterized by reduced fecundity and growth.

Dearmond *et al.* used a mass spectrometry based H/D exchange technology to identify CypA ligands [187]. Among the multiple hits compound **20** was estimated by the MS assay to have an affinity of 2 $\mu$ M. This substance was shown to inhibit the PPIase activity of CypA in a single dose assay.

Dugave and coworkers used the special properties of oxorhenium complexes for a combinatorial self-assembly approach to generate novel CypA ligands [188]. A small library of fragments was derivatized with an oxorhenium precursor and reacted with a small library of thiol-containing building blocks. The resulting

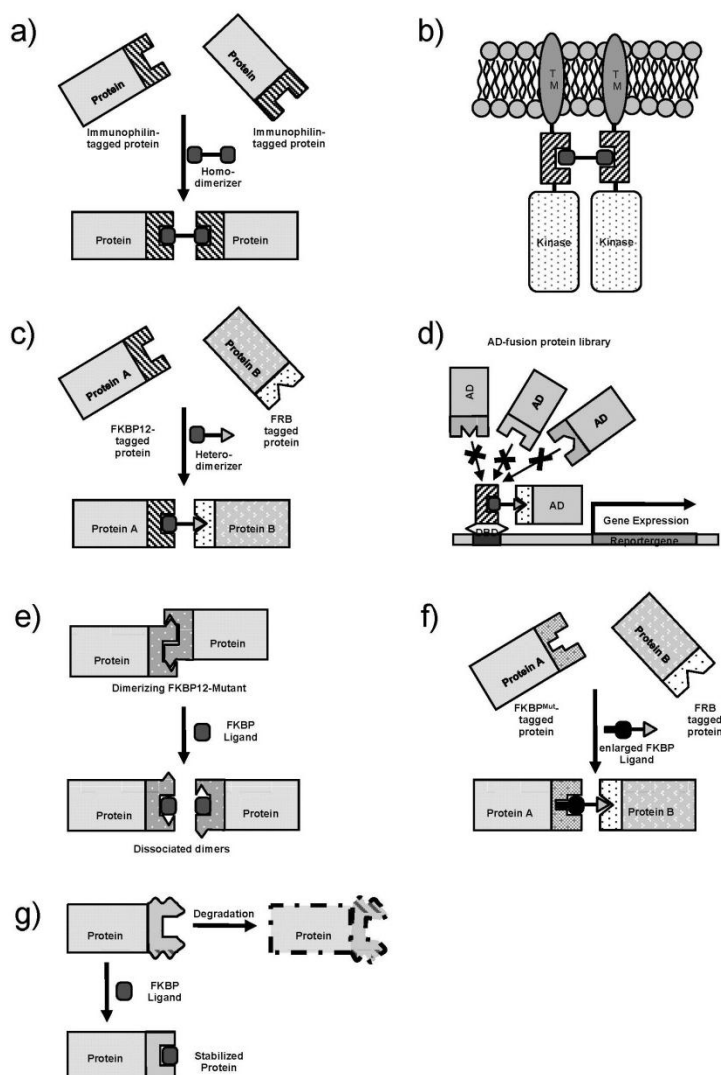


**Fig. (12). Principles and applications of chemical dimerizers.**

a) Principle of chemical homodimerization. The protein of interest is fused to a dimerizable protein tag like FKBP12 (shaded). The dimerization is triggered by the addition of a symmetrical chemical dimerizer (squares) like AP1510 to induce a trimeric complex. b) Example of homodimerization used to mimic receptor tyrosine kinase activation. A receptor tyrosine kinase domain is fused to an immunophilin binding tag (shaded) and a membrane localization sequence (TM). The addition of a homodimerizer induces autophosphorylation of the kinase domains and activates downstream signaling. c) Principle of heterodimerization. One protein of interest is fused to an immunophilin binding tag (e.g., FKBP12), the other is fused to an orthogonal recognition domain (e.g., FRB for rapamycin). The dimerization is triggered by the addition of an unsymmetrical chemical dimerizer (square + triangle) like rapamycin to induce a trimeric complex. d) The yeast three hybrid system as an application of heterodimerization. An immunophilin binding domain like FKBP12 (shaded) is fused to a DNA binding domain (DBD) from a transcription factor. An immunophilin ligand (square) like rapamycin or FK506 is conjugated to a chemical compound of interest (triangle). A library of proteins (grey dotted) is fused to the activation domain of a transcription factor (AD). *Via* trimerization only those fusion proteins that are able to bind the chemical compound of interest are recruited to the DNA and induce transcription and detectable expression of a reporter gene. e) Principle of reverse dimerization. The FKBP12 (F36M) mutant (white dotted) was shown to inherently dimerize. Tagging of proteins of interest with this mutant leads to their constitutive dimerization. These homodimers can be disrupted by the addition of an immunophilin binding compound, e.g. FK506 (square). f) Principle of the 'bump and hole' strategy in the application of chemical dimerizers. To gain specificity for the protein of interest over endogenous proteins, the dimerizing agent is modified by a bulky group (bump) that abolishes binding to endogenous proteins (e.g., native FKBP). The corresponding binding tag is modified by a mutation able to accommodate the bumped ligand (e.g., FKBP12F36V, shaded + dotted). g) Example of chemically controlled protein stability. A protein of interest is fused to an immunophilin mutant (e.g., FKBP12L106P, shaded) that is inherently unstable and imparts constitutive cellular degradation on the fusion protein in the absence of a ligand. Upon addition of an FKBP ligand (e.g., Shield-1, square) the FKBP domain is stabilized and the fusion protein accumulates.

complexes were stable towards purification and were tested for CypA binding. The best substances like II-8i had an  $IC_{50}$  of 11  $\mu$ M in a tryptophan quenching assay. The authors then extended this approach in a dynamic setting where the rhenium-mediated self-assembly was carried out with mixtures of building blocks in the presence of CypA (also called Cyp18). The best compounds were reported to quench tryptophan fluorescence and to inhibit PPIase activity of CypA with  $IC_{50}$ = 0.3  $\mu$ M [189].

Daum *et al.* discovered aryl 1-indanylketoones as a preferred binding motif for CypA [190]. This motif was thought to mimic the twisted amide structure of the putative transition state of the PPIase reaction. Building on previous work they found compound **21** (Fig. 11) to inhibit the PPIase activity of CypA with an  $IC_{50}$ = 0.5  $\mu$ M which was confirmed by isothermal calorimetry and competitive fluorescence polarization. Importantly, compound **21** exhibited excellent specificity vs. numerous other human Cyp paralogs, e.g., the closely related CypB. It also was specific vs. FKBP12, albeit not vs. Pin1 the enzyme it was originally developed for.

#### 4. IMMUNOPHILIN ASSAYS

The classical assay for immunophilins is the peptidyl-prolyl isomerase (PPIase) assay that measures the catalytic activity of these enzymes to accelerate the cis-trans isomerization of amide bonds preceding a proline [191]. However, this assay is rather labor-intensive, requires the use of water-free reagents and has to be run at low temperatures within a very short time window. Using specialized equipment this assay was recently adapted to a high-throughput screening format [192].

The second commonly used assay is a tryptophan fluorescence titration assay. Many immunophilins contain a (single) tryptophan residue close to the active site (e.g., Trp59 for FKBP12 or Trp121 for CypA). Upon binding of ligands these tryptophan residues are getting buried or displaced which reduces (for FKBP) or enhances (for Cyps) their intrinsic fluorescence [193, 194]. While readily adopted in most laboratories, this assay has a rather low sensitivity and is often confounded by the intrinsic spectroscopic activity of test substances.

Radioactive assays with excellent sensitivity, high robustness and moderate to high throughput have been established [84, 195] but the radioactively labeled [3H]-FK506 is no longer commercially available.

The method of choice currently seems to be fluorescence polarization assays and a number of fluorescent tracers have been developed, e.g., FL-SLF (Fig. 14e) [142, 176, 190, 196]. These assays have been miniaturized and adapted to medium or high throughput formats. Fluorescence chemical denaturation is a label-free assay format that has recently been applied to FKBP12 in a 96-well format [197].

Classical biophysical methods like surface plasmon resonance or isothermal calorimetry have been used to confirm the affinities of novel putative FKBP ligands. In several cases this revealed substantial discrepancies in the measured affinities, depending on different assay formats applied. Not surprisingly, immunophilins have been used as model systems in proof-of-concept experiments for novel assay technologies like mass spectrometry-based screenings [118, 198]. FKBP12 has been the seminal example for an NMR-based fragment screening [115], a technology that continues to be improved [116, 117]. Finally, cellular assays for the detection of FKBP12 ligands have been developed, usually based on the disruption of a readout that depends on the chemically induced dimerization [199].

#### 5. IMMUNOPHILIN LIGANDS AS CHEMICAL BIOLOGICAL TOOLS

In the last two decades immunophilin ligands received increasing attention as tools for various applications in chemical

biology. These applications often draw on overlapping molecular mechanisms and we try here to dissect their function as tools for chemical dimerization, including three hybrid applications and conditional intracellular protein localization, or as tools to chemically tag proteins inside living cells, including approaches to regulate protein or compound stability [200, 201].

#### 5.1. Chemical Dimerizers

The most widespread application of immunophilin ligand tools is their use as chemically induced dimerizer (CID), allowing the fast conditional formation of protein complexes inside living cells. CID is based on the intrinsic property of the natural compounds FK506, rapamycin and cyclosporin A to bind two different protein targets at the same time. Therefore these compounds are often referred to as heterodimerizers. FK506 and rapamycin bind to FKBP proteins and to calcineurin (for FK506) or to the FRB domain of mTOR (for rapamycin). CsA binds simultaneously cyclophilins and calcineurin. For artificial CID and rapamycin as chemical dimerizer, pairs of proteins of interest are expressed in cells as fusion with FKBP12 and with FRB, respectively (Fig. 12c). Alternatively, fusions of FKBP12 and CaN for the application with FK506 as dimerizer were used [202, 203]. Upon addition of the cell-permeable chemical dimerizers, the classical trimeric complexes are formed (i.e., FKBP12-Rap-FRB in the case of rapamycin) bringing the two fused proteins into close spatial proximity.

While all three classes of natural immunophilin ligands can be employed for CID applications rapamycin-based technologies and methods using synthetic FKBP ligands have by far received most attention [204-208]. Rapamycin has the advantage to form a very tight trimeric complex ( $K_D$ =12nM) between two very small well-folding fusion domains (FKBP12=12kDa, FRB=11kDa) in a highly ordered fashion [196]. The latter is due to the very low affinity of rapamycin to the FRB domain alone ( $K_D$ =26  $\mu$ M), 10,000-fold lower than the binding of rapamycin to FKBP12 ( $K_D$ =0.2nM). In practice, the Rap-FRB species that in principle could interfere with the ternary complex formation in excess of rapamycin can therefore be neglected. This is important since the concentration of rapamycin in living systems is difficult to control.

A major problem in the use of the natural immunophilin ligands as tools in cellular systems is their inherent immunosuppressive activity, mediated by the inhibition of calcineurin (in the case of FK506 and CsA) or of mTOR (in the case of rapamycin). This can severely confound the intended biological experiments. For rapamycin this problem was solved by the synthesis of rapamycin derivatives like C16-(R)-methallyl rapamycin (C16-MaRap, Fig. 13) [209] or the slightly more active isomer C20-(R)-methallyl rapamycin [210]. The triene moiety and position C16 in particular is a preferred part in rapamycin since it can easily be derivatized with a number of nucleophiles [211]. These modifications disrupt the interaction with the wildtype FRB and abolish the binding to (and therefore the inhibition of) endogenous mTOR. To still allow for dimerization with the desired protein fusion constructs compensating mutations were introduced in the fused FRB-domain (called FRB\* harboring K2095P, T2098L, and W2101F). These allowed for binding of the "bumped" rapamycin analog and for ternary complex formation. Later improved versions like AP21967 and iRap (Fig. 13) were developed that were reported to display better pharmacokinetic parameters (solubility, stability, cell permeability) [212, 213] and allowed *in vivo* applications [214-217]. AP21967, originally developed by Ariad Pharmaceuticals, is now commercially available from Clontech [Clontech: Ligands for Chemically Induced Dimerization / [http://www.clontech.com/products/detail.asp?product\\_id=237800&tabno=2](http://www.clontech.com/products/detail.asp?product_id=237800&tabno=2)]. A conceptually similar approach was also described for a "bumped" FK506 and calcineurin mutants [218].

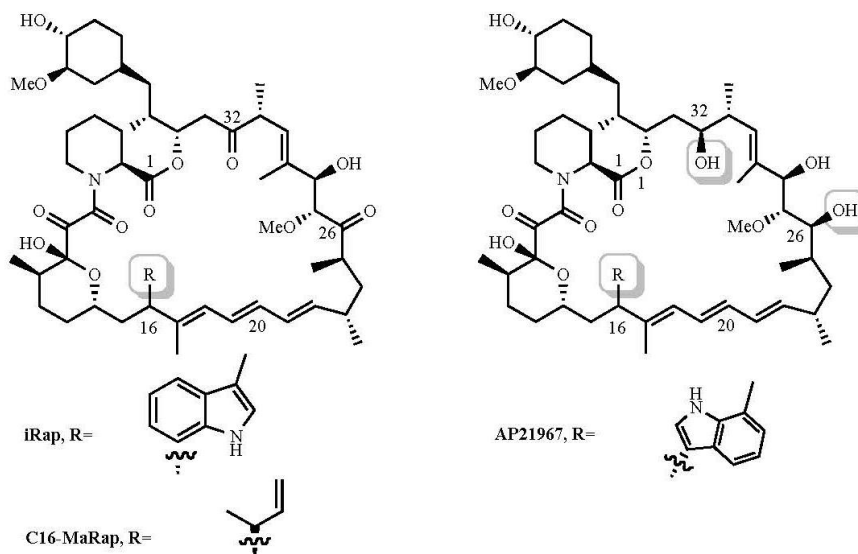


Fig. (13). Rapamycin-based non-immunosuppressive heterodimerizers

In the special case where two identical proteins are desired to be dimerized (e.g., conditional homodimerization of receptor tyrosine kinases constructs, Fig. 12b) the dimerizing problem was solved by the development of symmetric dimerizers (Fig. 12a). The first generation of this type of dimerizers was based on FK506 and CsA [219-221] but were soon replaced by smaller synthetic bivalent FKBP ligands like AP1510 (Fig. 14a) [222]. A major drawback of these compounds is their high affinity to the abundant endogenous FKBP proteins which leads to stochastic mixtures of homo- and heterodimers between overexpressed FKBP-fusion proteins and endogenous FKBP. This problem was again circumvented by the so-called „bump-hole“ approach (Fig. 12f). Based on a FKBP12-ligand cocystal structure the C9 carbonyl of AP1510 was replaced by an ethyl group which would sterically clash with the F36 of FKBP12 [223, 224]. A compensatory F36V mutation was introduced in FKBP12 fusion proteins to accommodate the ethyl-“bump” in compounds like AP20187 (Fig. 14b) [225]. The use of these bumped chemical dimerizers greatly enhanced the specificity for the dimerization of appropriately tagged proteins and significantly reduced unproductive binding to endogenous proteins. The most frequently used bumped homodimerizers for bumped FKBP12 mutants is AP20187 which is commercially available from Clontech [Clontech: Ligands for Chemically Induced Dimerization /[http://www.clontech.com/products/detail.asp?product\\_id=237800&tabno=2](http://www.clontech.com/products/detail.asp?product_id=237800&tabno=2)].

It should be noted that rapamycin-based dimerizers like AP21967 still bind to endogenous FKBP12 and therefore likely also induce trimeric FKBP12<sup>trd</sup>/Rap\*/FRB\*-fusion protein complexes. The functional consequences of this remain to be established. For CsA the orthogonal „bump-hole“ pair Melle11CsA and hCyp(S99T, F113A, C115M) was generated that is devoid of binding to the endogenous cyclophilins [226, 227].

The biological applications of dimerizers are very broad. In a classical approach, CIDs are used in the (homo-) dimerization or oligomerization (if more than one FKBP-tag is added) and activation of membrane receptors like the T-cell receptor or membrane tyrosine kinases (TCR:[219], Erythropoietin receptor: [275], PDGF-B-R / Insulin receptor:[228], epithelial Growth factor receptors / hepatocyte growth factor receptor / thrombopoietin receptor:[229]).

Another frequent application is the induced activation of apoptosis, which can be achieved by the dimerization of the FAS receptor or the dimerization of various caspases (Fas: [221], [222] / Procaspase1,8: [228] / Caspase 8: [230], [231], [232] / Caspase9: [276] / Procaspase2: [233]).

An *in vivo* application of CID-induced apoptosis is the mouse model for the study of peritoneal adhesions using macrophage Fas-induced apoptosis (MAFIA-mouse model). These mice carry a transgene for the expression of a membrane targeted FKBP12-Fas fusion protein under the control of the *c-fms* promoter, which directs the specific expression in macrophages. Injection of the molecular dimerizer AP20187 leads to the apoptotic depletion of macrophages and peritoneal adhesion formation in these transgenic mice [234, 235].

Another widely used application of CIDs is the chemical regulation of transcription. In analogy to yeast two-hybrid systems, transcription factors can be split in a DNA binding domain and a transactivation domain. The transcription factor can be activated by its reconstitution, which in turn is induced by the addition of a chemical dimerizer. Often used combinations are the DNA binding domain ZFHD1 (Zinc finger homeodomain1) and VP16 as transcriptional activator or the Gal4 DNA binding domain together with the Gal4 activation domain, each fused to FKBP12 and FRB respectively and dimerized *via* rapamycin [204, 236]. In combination with AAV vector systems as vehicle this method allows tissue-specific inducible expression in mice or the potential use for gene therapy, as for example shown by the rapamycin-inducible expression of human growth hormone [237] or erythropoietin [205] in mice after intramuscular gene transfer.

A modification of the inducible transcription system is the yeast three-hybrid approach (Fig. 12d). Originally, this method was first used to identify protein binding partners of chemical compounds. In the initial application, dexamethasone was conjugated to FK506 [238]. Correspondingly, a DNA-binding domain was fused to the hormone-binding domain of the glucocorticoid receptor, which recruited the dexamethasone-FK506 conjugate to the DNA. Screening of a cDNA library fused to a transcriptional activator domain yielded FKBP12 as an interaction partner of the dexamethasone-FK506 conjugate. Later, the three-hybrid system

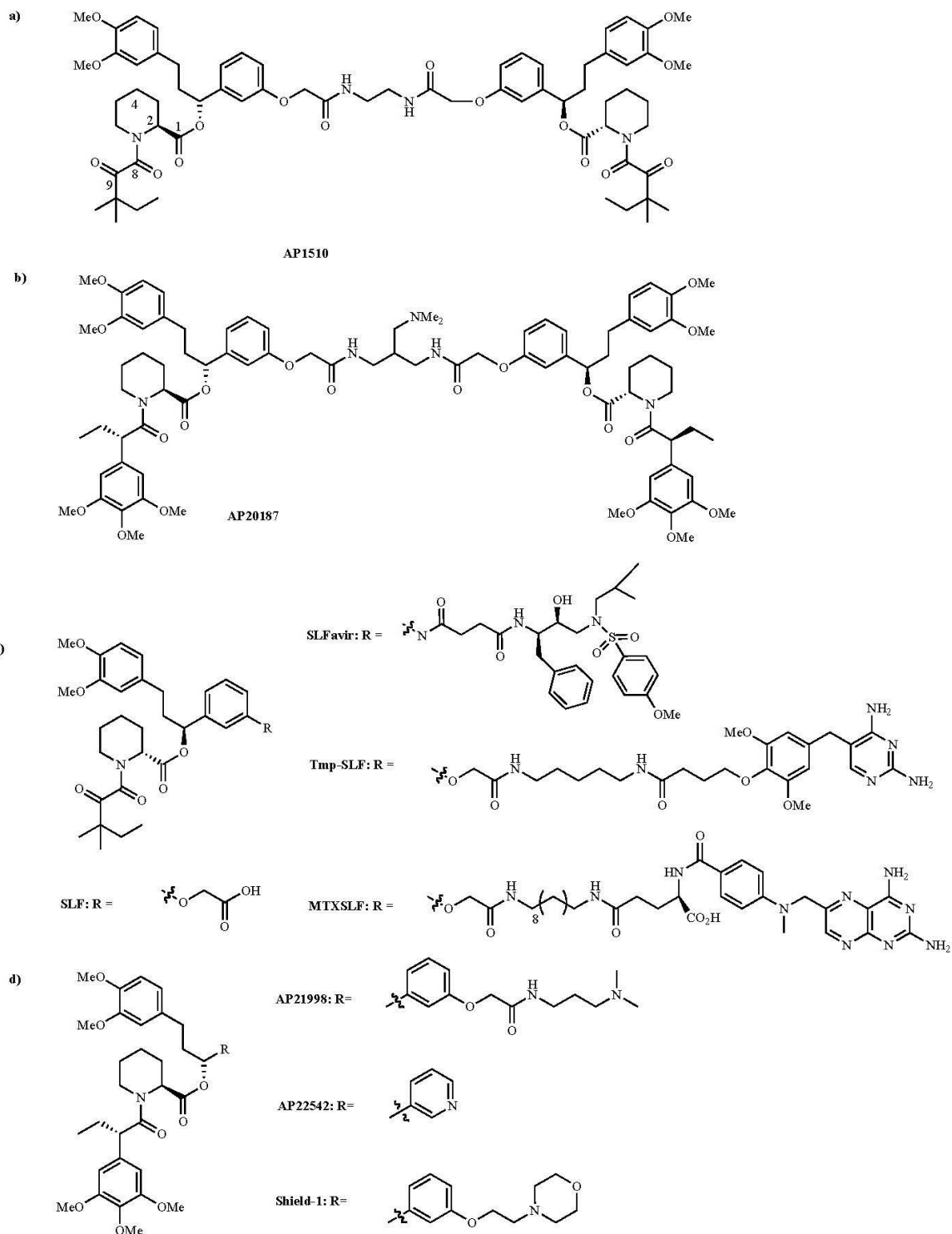


(Fig. 12). Contd.....

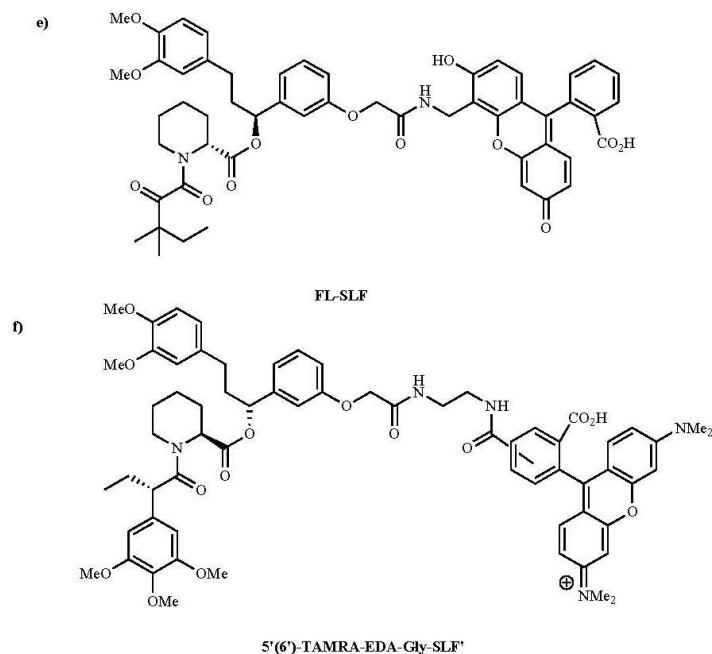


**Fig. (14).** Synthetic FKBP ligands and orthogonal selective (“bumped”) C9-ethyl derivatives. a),b) Chemical homodimerizers. c) Synthetic FKBP ligand (SLF, also known as AP1497) and exemplary conjugates thereof: SLFavir= amprenavir conjugate displaying enhanced half life; Tmp-SLF= trimethoprim conjugate for heterodimerization with bacterial dihydrofolate reductase; MTXSLF= methotrexate conjugate for preferential inhibition of *P. falciparum* dihydrofolate reductase in the absence of human FKBP12. d) Disruptors for reverse chemical dimerization or stabilizers for FKBP mutants. e),f) Fluorescent FKBP tracers.

was adapted to mammalian cell systems, for example to screen for FRB mutants binding to rapamycin derivatives [209] or to bacterial systems, e.g., using FK506-methotrexate conjugates which isolate dihydrofolate reductase as binder [239]. The orthogonal methotrexate-dihydrofolate reductase system represents a general alternative for heterodimerization, e.g., when combined with synthetic FKBP ligands like Tmb-SLF (Fig. 14c) [240].

Similar to the reconstitution of split transcriptional activators, also other proteins like enzymes may be inactivated by splitting into two pieces and reactivated by chemically induced dimerization as for example shown for the activation of a split CRE recombinase [241] or the tobacco etch virus (TEV) protease [242].

Another field where chemically induced dimerization is widely used is the conditional transport or localization of proteins or vesicles. The most popular use in this area is the inducible recruitment of signaling proteins to the plasma membrane. For this purpose, one partner of the dimerizing system is usually expressed as a myristoylated version or as a fusion with a membrane anchor. The other partner is then transferred to the membrane by dimerization. Examples for this application are the membrane recruitment of the guanine nucleotide exchange factor SOS [243], the ZAP70 kinase [244] or the AKT2 kinase [245]. By the use of suitable anchoring proteins, complementarily tagged proteins may also be targeted to the endoplasmic reticulum, Golgi or organelles like mitochondria [208]. For example, this allows displacing proteins from their endogenous site of action to a different cellular localization, where it is not functional, a method called “knocksideways” approach. As an example, this method was used for the redirection of the adaptor protein AP1 from clathrin-coated vesicles to the mitochondrial membrane [207]. Similar experiments

were reported where nuclear localization (NLS) or nuclear export signals were chemically recruited to regulate nuclear trafficking [246-248]. The transport of synaptic vesicles can also be influenced by the inducible dimerization of presynaptic proteins like VAMP2 / synaptobrevin and synaptophysin [215]. The suppression of the synaptic vesicular trafficking in transgenic mice by these MISTs (molecules for inactivation of synaptic transmission) could be linked to deficits in learning and rotarod behavior.

Last, but not least, dimerizers can be used to control posttranslational modifications like intein splicing, sumoylation or ubiquitylation. The chemical dimerizer-induced split intein fusion is able to activate trans-splicing of the fused exteins. This method was used to inducibly reconstitute an autoregulated protein kinase [249, 250]. For the induced sumoylation of proteins essentially two methods have been reported. Zhu *et al.* showed that a FKBP-tagged SUMO can be added to a FRB-tagged target protein by addition of rapamycin [251]. This way they studied the biological effects of sumoylation of RanGap1. An alternative method is the UBC9/substrate dimerization-dependent sumoylation (USDDS) [252]. This approach uses the recruiting of the sumo ligating enzyme UBC9 to a target protein by chemical dimerizers.

Immunophilin ligands were also used to conditionally disrupt constitutive dimers in a method called reverse dimerization (Fig. 12e) [253]. In this method a mutated FKBP12<sup>F36M</sup> protein is used which has the intrinsic ability to dimerize without addition of a chemical inducer. Upon addition of a ligand selective for the FKBP mutant (e.g., AP21998, Fig. 14d) the contact points are blocked and the FKBP12<sup>F36M</sup> dimers are disrupted. This technique was applied by Rivera *et al.* [254] to chemically induce the secretion of human growth hormone and insulin constructs that had been trapped in the

ER by aggregation of the fused FKBP12<sup>F36M</sup>. The secretion of the hormones could be induced by adding compound AP21998 or AP22542 which dissolved the aggregate.

### 5.2. Immunophilin Ligands to Control Protein Stability

A rather new field for immunophilin ligands, partly overlapping with their use as molecular dimerizers, is the regulation of protein stability. In one method a proteasomal subunit was fused to the yeast FKBP12 homolog while the target protein was tagged with the FRB subunit [255]. The rapamycin-induced recruitment of the proteasome to the target protein seems to be sufficient to induce the degradation of the target protein.

Similar to the split intein method described above, a split inducible ubiquitin method can be used to target proteins for degradation [256]. In this method, called split ubiquitin for the rescue of function (SURF), the protein of interest is fused to a tag derived from the C-terminal domain of ubiquitin followed in frame by FRB and/or a degron (a signal targeting the protein to proteasomal degradation). Per default, this protein fusion construct will therefore be constitutively degraded. By addition of rapamycin this construct can dimerize with a second construct harboring the N-terminal domain of ubiquitin fused to FKBP12 which induces the reconstitution of functional ubiquitin. This in turn leads to the release of the target protein from the degron by an ubiquitin-specific protease and thereby to its rescue from degradation. This technology was recently extended by the incorporation of a mutated FKBP12 tag that functioned as the degron [257].

Stankunas *et al.* observed that a triple mutation of FRB\* (FRB K2095P, T2098L, and W2101F) reported by Liberles *et al.* imparted protein instability to the proteins it was fused to, which in turn got degraded [209, 210]. Importantly, the fusion protein could be protected by the addition of C20-(R)-methallyl rapamycin which bound to and stabilized the fused FRB\* tag. This approach was further extended recently by the optimization of FRB mutants [258].

The Wandless group developed a method to control protein stability with immunophilin ligands that do not depend on dimerization anymore. This approach is based on the inherent instability of FKBP12 mutants like L106P, which act as

destabilizing domains when fused to other proteins (Fig. 12g) [259]. L106P was shown to be the most efficient destabilizing mutant and is most frequently used, either as single mutation or in FKBP12 F36V/L106P double mutants. A modified SLF ligand, called Shield-1 (Fig. 14d), can be used to stabilize the FKBP12 mutants. In further studies this method evolved by the development of improved ligands like Shield-2 [260] or by the discovery of more efficient FKBP degradation tags [261-263]. The FKBP12<sup>L106P</sup> mutant represents a “ligand-on” system where the target fusion protein is continuously degraded in the absence of the ligand. The latest trend seems to be the development of a “ligand-off” system where the addition of an FKBP ligand exposes unfolded portions of a mutant FKBP12 fusion construct thereby inducing the degradation of the fused protein [264].

Protein degradation can also be induced with appropriately functionalized immunophilin ligands. An approach called fluorophore-assisted laser inactivation (FALI) uses a fluorescein-labeled FKBP ligand (FL-SLF<sup>+</sup>) to target FKBP12<sup>F36V</sup>-tagged proteins inside cells. Using a laser, the fluorophore-bound target proteins can be rapidly inactivated in a spatially defined manner by the local generation of reactive oxygen species [265]. In an alternative method chemically induced ubiquitylation is used to target proteins for proteasomal degradation. This method is based on the recruitment of an E3-ubiquitin ligase to a protein target *via* PROteolysis TArgeting Chimeric moleculeS (PROTACS). This was achieved by conjugating an FKBP ligand to a peptidic E3-ubiquitin recognition sequence. As a proof-of-principle, the ligand-induced ubiquitin ligase-dependent degradation of a GFP-FKBP12<sup>F36V</sup> fusion protein was shown [266].

In addition to dimerization and protein (de)stabilization the exquisite recognition properties of immunophilin ligands have been employed in a number of other chemical biology applications. Recently, three groups have reported caged versions of rapamycin (Fig. 15) where rapamycin is linked to a photocleavable moiety that interferes with cell permeability, with binding to a FKBP12 mutant or with binding to the FRB domain. Photodeprotection restores the binding of rapamycin to its target, like the inhibition of mTORC1 by rapamycin [267], the recruitment of the small GTPase RAC to the plasma membrane [268] or the activation of inactive FKBP-fused focal adhesion kinase (Fak) by binding to rapamycin [269].

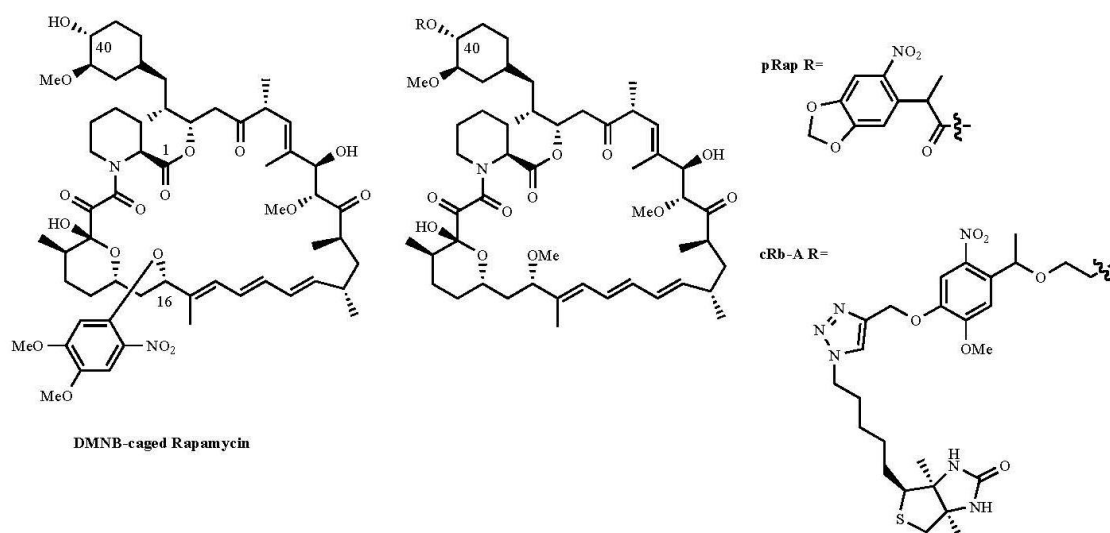


Fig. (15). Photocaged rapamycin derivatives.

The main advantage of caged rapamycin derivatives is the excellent spatial and temporal control of activation that can be achieved with light.

Marinec *et al.* expanded on previous observations that the binding of FK506 or rapamycin to endogenous FKBP proteins shelters these natural products from oxidation and degradation by cytochrome P450. They postulated that other pharmacologically active compounds might also show an elongated activity when attached to immunophilin ligands. As a proof-of-concept the HIV-protease inhibitor amprenavir was conjugated to SLF (SLFavir, Fig. 14c), which increased the half-life of the conjugate in mice [270]. Importantly, the amprenavir-SLF conjugate retained its inhibitory activity against HIV protease.

The Wandless group employed FKBP ligand conjugates to control the activity of the attached methotrexate in a cell type-dependent manner. The linker in the MTXSLF conjugate (Fig. 14c) was designed to preclude simultaneous binding to FKBP5 and dihydrofolate reductase. Complexation of the conjugate with FKBP12 was shown to reduce the inhibitory activity of the attached methotrexate. In human cells MTXSLF is trapped by the high concentrations of the high-affinity human FKBP12. This effect is much smaller in *Plasmodium falciparum* cells, consistent with the weaker affinity of pFKBP35 for MTXSLF [271, 272].

Fluorescent FKBP ligands can be used for live cell imaging of proteins tagged with the FKBP\* domain. Recently, a group by Invitrogen showed that 5'-(6')-TAMRA-EDA-Gly-SLF\* (Fig. 14f) is cell-permeable, non-toxic, displays an excellent signal-to-noise ratio and is compatible with several other commonly used fluorescent protein tags [273].

## 6. CONCLUSION

Immunophilin ligands have had – and continue to have – an enormous impact on human health and on basic life sciences alike. Whenever biological problems can be addressed by recombinantly overexpressed fusion proteins, immunophilin fusion variants offer an additional layer of chemical control. Often the use of immunophilin ligands imparts excellent temporal control (rapid and reversible) or they bring in novel functionalities unavailable through natural protein fusions.

As the biological role of human immunophilins is becoming clearer, several members of the endogenous FKBP or Cyp families are emerging as potential therapeutic targets. So far, semisynthetic analogs of CsA, FK506 and rapamycin have been by far the most successful immunophilin ligand derivatives. It is notable that, despite the importance of the immunophilins, there is a striking paucity of published results from high throughput screening campaigns, the traditional ligand generation engine of the pharmaceutical industry. The rational design approach has been more successful, with a number of synthetic ligands described for FKBP12. Most of them retain the pipecolate binding motif derived from FK506 or rapamycin. There are comparatively few reported examples of *de novo* generated immunophilin ligands that are truly structurally unrelated to FK506 or rapamycin. Those novel scaffolds have yet to show their broader biological applications.

Many studies that pharmacologically probe immunophilins still employ the prototypical immunosuppressants FK506, CsA or rapamycin, likely because they are commercially available. The interpretation of the effects observed with these compounds is however complicated by the concomitant inhibition of calcineurin and mTOR which likely occurs at lower concentrations than those required to block the immunophilin binding sites. As outlined in this review numerous non-immunosuppressive analogs are now known which are devoid of this confounding activity.

So far most studies focused on the prototypical FKBP12 or CypA. In the few cases where the affinity for other immunophilins

have been investigated most reported immunophilin ligands tended to be rather unselective within the FKBP or Cyp family. This is likely attributable to the very high degree of structural homology observed in the active site of immunophilins. For the Cyp family addressing a more diverse second binding pocket adjacent to the CsA-binding site was proposed as a strategy to achieve selectivity [274]. The need for subtype-selective inhibitors is particularly prominent in the field of neuroimmunophilins where it has been impossible so far to clearly define the contributions of individual FKBP homologs to the observed neuroprotective or neurotrophic effects. Progress in this direction is eagerly awaited.

## ACKNOWLEDGEMENT

We thank Prof. Holsboer for continuous financial support.

## REFERENCES

- Wang, X. J.; Eitzkorn, F. A., Peptidyl-prolyl isomerase inhibitors. *Biopolymers* **2006**, *84* (2), 125-46.
- Babine, R. E.; Villafranca, J. E.; Gold, B. G., FKBP immunophilin patents for neurological disorders. *Expert Opin Ther. Patents* **2005**, *15* (5), 555-573.
- Lu, K. P.; Zhou, X. Z., The prolyl isomerase PIN1: a pivotal new twist in phosphorylation signalling and disease. *Nat Rev Mol Cell Biol* **2007**, *8* (11), 904-16.
- Liu, J.; Farmer, J. D., Jr.; Lane, W. S.; Friedman, J.; Weissman, I.; Schreiber, S. L., Calcineurin is a common target of cyclophilin-cyclosporin A and FKBP-FK506 complexes. *Cell* **1991**, *66* (4), 807-15.
- Crabtree, G. R.; Schreiber, S. L., SnapShot: Ca<sup>2+</sup>/calcineurin-NFAT signaling. *Cell* **2009**, *138* (1), 210, 210 e1.
- Xu, X.; Su, B.; Barndt, R. J.; Chen, H.; Xin, H.; Yan, G.; Chen, L.; Cheng, D.; Heitman, J.; Zhuang, Y.; Fleischer, S.; Shou, W., FKBP12 is the only FK506 binding protein mediating T-cell inhibition by the immunosuppressant FK506. *Transplantation* **2002**, *73* (11), 1835-8.
- Weiward, M.; Edlich, F.; Kilka, S.; Erdmann, F.; Jarczowski, F.; Dorn, M.; Mouty, M. C.; Fischer, G., Comparative analysis of calcineurin inhibition by complexes of immunosuppressive drugs with human FK506 binding proteins. *Biochemistry* **2006**, *45* (51), 15776-84.
- Soulard, A.; Hall, M. N., SnapShot: mTOR signaling. *Cell* **2007**, *129* (2), 434.
- Laplane, M.; Sabatini, D. M., An emerging role of mTOR in lipid biosynthesis. *Curr Biol* **2009**, *19* (22), R1046-52.
- Zoncu, R.; Efeyan, A.; Sabatini, D. M., mTOR: from growth signal integration to cancer, diabetes and ageing. *Nat Rev Mol Cell Biol* **2011**, *12* (1), 21-35.
- Dowling, R. J. O.; Topisirovic, I.; Fonseca, B. D.; Sonenberg, N., Dissecting the role of mTOR: Lessons from mTOR inhibitors. *Biochimica et Biophysica Acta (BBA) - Proteins & Proteomics* **2010**, *1804* (3), 433-439.
- Choo, A. Y.; Blenis, J., Not all substrates are treated equally: implications for mTOR, rapamycin-resistance and cancer therapy. *Cell Cycle* **2009**, *8* (4), 567-72.
- Janes, M. R.; Limon, J. J.; So, L.; Chen, J.; Lim, R. J.; Chavez, M. A.; Vu, C.; Lilly, M. B.; Mallya, S.; Ong, S. T.; Konopleva, M.; Martin, M. B.; Ren, P.; Liu, Y.; Rommel, C.; Fruman, D. A., Effective and selective targeting of leukemia cells using a TORC1/2 kinase inhibitor. *Nat Med* **2010**, *16* (2), 205-13.
- Nyfelner, B.; Bergman, P.; Triantafellow, E.; Wilson, C. J.; Zhu, Y.; Radetich, B.; Finan, P. M.; Klionsky, D. J.; Murphy, L. O., Relieving autophagy and 4EBP1 from rapamycin resistance. *Mol Cell Biol* **2011**.
- Zeng, Z.; Sarbassov, D. D.; Samudio, I. J.; Yee, K. W.; Munsell, M. F.; Ellen Jackson, C.; Giles, F. J.; Sabatini, D. M.; Andreeff, M.; Konopleva, M., Rapamycin derivatives reduce mTORC2 signaling and inhibit AKT activation in AML. *Blood* **2007**, *109* (8), 3509-12.
- Sarbassov, D. D.; Ali, S. M.; Sengupta, S.; Sheen, J. H.; Hsu, P. P.; Bagley, A. F.; Markhard, A. L.; Sabatini, D. M., Prolonged rapamycin treatment inhibits mTORC2 assembly and Akt/PKB. *Mol Cell* **2006**, *22* (2), 159-68.
- Shor, B.; Zhang, W.-G.; Toral-Barza, L.; Lucas, J.; Abraham, R. T.; Gibbons, J. J.; Yu, K., A New Pharmacologic Action of CCI-779 Involves FKBP12-Independent Inhibition of mTOR Kinase Activity and Profound Repression of Global Protein Synthesis. *Cancer Research* **2008**, *68* (8), 2934-2943.
- Powell, J. D.; Delgoffe, G. M., The Mammalian Target of Rapamycin: Linking T Cell Differentiation, Function, and Metabolism. *Immunity* **2010**, *33* (3), 301-311.
- Janes, M. R.; Fruman, D. A., Immune regulation by rapamycin: moving beyond T cells. *Sci Signal* **2009**, *2* (67), pe25.
- Saemann, M. D.; Haidinger, M.; Hecking, M.; Hörl, W. H.; Weichhart, T., The Multifunctional Role of mTOR in Innate Immunity: Implications for Transplant Immunity. *American Journal of Transplantation* **2009**, *9* (12), 2655-2661.

- [21] Thomson, A. W.; Turnquist, H. R.; Raimondi, G., Immunoregulatory functions of mTOR inhibition. *Nat Rev Immunol* **2009**, *9* (5), 324-37.
- [22] Araki, K.; Youngblood, B.; Ahmed, R., The role of mTOR in memory CD8 T-cell differentiation. *Immunol Rev* **2010**, *235* (1), 234-43.
- [23] Peter, C.; Waldmann, H.; Cobbold, S. P., mTOR signalling and metabolic regulation of T cell differentiation. *Curr Opin Immunol* **2010**, *22* (5), 655-61.
- [24] Tresoldi, E.; Dell'Albani, I.; Stabilini, A.; Jofra, T.; Valle, A.; Gagliani, N.; Bondanza, A.; Roncarolo, M. G.; Battaglia, M., Stability of human rapamycin-expanded CD4<sup>+</sup>CD25<sup>+</sup> T regulatory cells. *Haematologica* **2011**, haematol.2011.041483.
- [25] Harrison, D. E.; Strong, R.; Sharp, Z. D.; Nelson, J. F.; Astle, C. M.; Flurkey, K.; Nadon, N. L.; Wilkinson, J. E.; Frenkel, K.; Carter, C. S.; Pahor, M.; Javors, M. A.; Fernandez, E.; Miller, R. A., Rapamycin fed late in life extends lifespan in genetically heterogeneous mice. *Nature* **2009**, *460* (7253), 392-5.
- [26] Chen, C.; Liu, Y.; Liu, Y.; Zheng, P., mTOR regulation and therapeutic rejuvenation of aging hematopoietic stem cells. *Sci Signal* **2009**, *2* (98), ra75.
- [27] Kaerlein, M.; Kennedy, B. K., Hot topics in aging research: protein translation and TOR signaling. *Aging Cell* **2010**, *10* (2), 185-90.
- [28] Ravikumar, B.; Vacher, C.; Berger, Z.; Davies, J. E.; Luo, S.; Oroz, L. G.; Scaravilli, F.; Easton, D. F.; Duden, R.; O'Kane, C. J.; Rubinsztein, D. C., Inhibition of mTOR induces autophagy and reduces toxicity of polyglutamine expansions in fly and mouse models of Huntington disease. *Nat Genet* **2004**, *36* (6), 585-95.
- [29] Caccamo, A.; Majumder, S.; Richardson, A.; Strong, R.; Oddo, S., Molecular interplay between mammalian target of rapamycin (mTOR), amyloid-beta, and Tau: effects on cognitive impairments. *J Biol Chem* **2010**, *285* (17), 13107-20.
- [30] Malagelada, C.; Jin, Z. H.; Jackson-Lewis, V.; Przedborski, S.; Greene, L. A., Rapamycin Protects against Neuron Death in *In vitro* and *In Vivo* Models of Parkinson's Disease. *J. Neurosci.* **2010**, *30* (3), 1166-1175.
- [31] Spilman, P.; Podlutzkaya, N.; Hart, M. J.; Debnath, J.; Gorostiza, O.; Bredeken, D.; Richardson, A.; Strong, R.; Galvan, V., Inhibition of mTOR by rapamycin abolishes cognitive deficits and reduces amyloid-beta levels in a mouse model of Alzheimer's disease. *PLoS One* **2010**, *5* (4), e9979.
- [32] Santini, E.; Heiman, M.; Greengard, P.; Valjent, E.; Fissone, G., Inhibition of mTOR signaling in Parkinson's disease prevents L-DOPA-induced dyskinesia. *Sci Signal* **2009**, *2* (80), ra36.
- [33] Cirstea, D.; Hideshima, T.; Rodig, S.; Santo, L.; Pozzi, S.; Vallet, S.; Ikeda, H.; Perrone, G.; Gorgun, G.; Patel, K.; Desai, N.; Sportelli, P.; Kapoor, S.; Vall, S.; Mukherjee, S.; Munshi, N. C.; Anderson, K. C.; Raju, N., Dual inhibition of akt/mammalian target of rapamycin pathway by nanoparticle albumin-bound-rapamycin and perfosine induces antitumor activity in multiple myeloma. *Mol Cancer Ther* **2010**, *9* (4), 963-75.
- [34] Gu, J.; Ruppen, M. E.; Cai, P., Lipase-Catalyzed Regioselective Esterification of Rapamycin: Synthesis of Temsirolimus (CCI-779). *Org. Lett.* **2005**, *7* (18), 3945-3948.
- [35] Claessen, B. E.; Henriques, J. P.; Dangas, G. D., Clinical studies with sirolimus, zotarolimus, everolimus, and biolimus A9 drug-eluting stent systems. *Curr Pharm Des* **2010**, *16* (36), 4012-24.
- [36] Kirtane, A. J.; Leon, M. B., Clinical Use of Sirolimus-Eluting Stents. *Cardiovascular Drug Reviews* **2007**, *25* (4), 316-332.
- [37] Wagner, R.; Mollison, K. W.; Liu, L.; Henry, C. L.; Rosenberg, T. A.; Bamaung, N.; Tu, N.; Wiedeman, P. E.; Or, Y.; Luly, J. R., Rapamycin analogs with reduced systemic exposure. *Bioorganic & Medicinal Chemistry Letters* **2005**, *15* (23), 5340-5343.
- [38] Fujitani, Y.; Trifiloff, A., *In vivo* and *In vitro* Effects of SAR 943, a Rapamycin Analogue, on Airway Inflammation and Remodeling. *Am. J. Respir. Crit. Care Med.* **2003**, *167* (2), 193-198.
- [39] Strom, T.; Shokati, T.; Klawitter, J.; Klawitter, J.; Hoffman, K.; Schiebel, H.-M.; Christians, U., Structural identification of SAR-943 metabolites generated by human liver microsomes *in vitro* using mass spectrometry in combination with analysis of fragmentation patterns. *Journal of Mass Spectrometry* **2011**, *46* (7), 615-624.
- [40] Morisaki, M.; Arai, T., Identity of immunosuppressant FR-900520 with ascomycin. *J Antibiot (Tokyo)* **1992**, *45* (1), 126-8.
- [41] Gollnick, H.; Kaufmann, R.; Stough, D.; Heikkila, H.; Andriano, K.; Grinenko, A.; Jimenez, P., Pimecrolimus cream 1% in the long-term management of adult atopic dermatitis: prevention of flare progression. A randomized controlled trial. *Br J Dermatol* **2008**, *158* (5), 1083-93.
- [42] Sedrani, R.; Kallen, J. r.; Martin Cabrejas, L. M.; Papageorgiou, C. D.; Senia, F.; Rohrbach, S.; Wagner, D.; Thai, B.; Jutzi Eme, A.-M.; France, J.; Oberer, L.; Rihs, G.; Zenke, G.; Wagner, J. r., Sanglifehrin<sup>®</sup> Cyclophilin Interaction: Degradation Work, Synthetic Macrocyclic Analogues, X-ray Crystal Structure, and Binding Data. *Journal of the American Chemical Society* **2003**, *125* (13), 3849-3859.
- [43] Gaither, L. A.; Borawski, J.; Anderson, L. J.; Balabanis, K. A.; Devay, P.; Joberty, G.; Rau, C.; Schirle, M.; Bouwmeester, T.; Mickanin, C.; Zhao, S.; Vickers, C.; Lee, L.; Deng, G.; Baryza, J.; Fujimoto, R. A.; Lin, K.; Compton, T.; Wiedmann, B., Multiple cyclophilins involved in different cellular pathways mediate HCV replication. *Virology* **2009**, *397* (1), 43-55.
- [44] Immecke, S. N.; Baal, N.; Wilhelm, J.; Bechtel, J.; Knoche, A.; Bein, G.; Hackstein, H., The cyclophilin-binding agent Sanglifehrin A is a dendritic cell chemokine and migration inhibitor. *PLoS One* **2011**, *6* (3), e18406.
- [45] Kuglstatler, A.; Mueller, F.; Kuszniir, E.; Gsell, B.; Stihle, M.; Thoma, R.; Benz, J.; Aspeslet, L.; Freitag, D.; Hennig, M., Structural basis for the cyclophilin A binding affinity and immunosuppressive potency of E-ISA247 (voclosporin). *Acta Crystallographica Section D* **2010**, *67* (2), 119-123.
- [46] Brittain, D. E.; Griffiths-Jones, C. M.; Linder, M. R.; Smith, M. D.; McCusker, C.; Barlow, J. S.; Akiyama, R.; Yasuda, K.; Ley, S. V., Total synthesis of antascomycin B. *Angew Chem Int Ed Engl* **2005**, *44* (18), 2732-7.
- [47] Ley, S. V.; Tackett, M. N.; Maddess, M. L.; Anderson, J. C.; Brennan, P. E.; Cappi, M. W.; Heer, J. P.; Helgen, C.; Kori, M.; Kouklovsky, C.; Marsden, S. P.; Norman, J.; Osborn, D. P.; Palomero, M. A.; Pavey, J. B. J.; Pinel, C.; Robinson, L. A.; Schnaubelt, J.; Scott, J. S.; Spilling, C. D.; Watanabe, H.; Wesson, K. E.; Willis, M. C., Total Synthesis of Rapamycin. *Chemistry - A European Journal* **2009**, *15* (12), 2874-2914.
- [48] Sun, Y.; Hong, H.; Samborsky, M.; Mironenko, T.; Leadlay, P. F.; Haydock, S. F., Organization of the biosynthetic gene cluster in *Streptomyces* sp. DSM 4137 for the novel neuroprotectant polyketide meridamycin. *Microbiology* **2006**, *152* (Pt 12), 3507-15.
- [49] Liu, H.; Jiang, H.; Haldi, B.; Kulowski, K.; Muszynska, E.; Feng, X.; Summers, M.; Young, M.; Graziani, E.; Koehn, F.; Carter, G. T.; He, M., Rapid Cloning and Heterologous Expression of the Streptomyces Biosynthetic Gene Cluster Using a Versatile *Escherichia coli*†*Streptomyces* Artificial Chromosome Vector, pSBACaŠY. *Journal of Natural Products* **2009**, *72* (3), 389-395.
- [50] Park, J. W.; Park, S. R.; Han, A. R.; Ban, Y.-H.; Yoo, Y. J.; Kim, E. J.; Kim, E.; Yoon, Y. J., Generation of reduced macrolide analogs by regio-specific biotransformation. *J Antibiot* **2010**, *64* (1), 155-157.
- [51] Qu, X.; Jiang, N.; Xu, F.; Shao, L.; Tang, G.; Wilkinson, B.; Liu, W., Cloning, sequencing and characterization of the biosynthetic gene cluster of sanglifehrin A, a potent cyclophilin inhibitor. *Mol Biosyst* **2011**, *7* (3), 852-61.
- [52] Hui, K. K. W.; Liadis, N.; Robertson, J.; Kanungo, A.; Henderson, J. T., Calcineurin inhibition enhances motor neuron survival following injury. *Journal of Cellular and Molecular Medicine* **2010**, *14* (3), 671-686.
- [53] Park, K. K.; Liu, K.; Hu, Y.; Smith, P. D.; Wang, C.; Cai, B.; Xu, B.; Connolly, L.; Kramvis, I.; Sahin, M.; He, Z., Promoting axon regeneration in the adult CNS by modulation of the PTEN/mTOR pathway. *Science* **2008**, *322* (5903), 963-6.
- [54] Steiner, J. P.; Connolly, M. A.; Valentine, H. L.; Hamilton, G. S.; Dawson, T. M.; Hester, L.; Snyder, S. H., Neurotrophic actions of nonimmunosuppressive analogues of immunosuppressive drugs FK506, rapamycin and cyclosporin A. *Nat Med* **1997**, *3* (4), 421-8.
- [55] Gerard, M.; Deleersnijder, A.; Demuilemeester, J.; Debyser, Z.; Baekelandt, V., Unraveling the role of peptidyl-prolyl isomerases in neurodegeneration. *Mol Neurobiol* **2011**, *44* (1), 13-27.
- [56] Klettnar, A.; Herdegen, T., The immunophilin-ligands FK506 and V-10,367 mediate neuroprotection by the heat shock response. *Br J Pharmacol* **2003**, *138* (5), 1004-12.
- [57] Ruan, B.; Pong, K.; Jow, F.; Bowlby, M.; Crozier, R. A.; Liu, D.; Liang, S.; Chen, Y.; Mercado, M. L.; Feng, X.; Bennett, F.; von Schack, B.; McDonald, L.; Zaleska, M. M.; Wood, A.; Reinhart, P. H.; Magolda, R. L.; Skotnicki, J.; Pangalos, M. N.; Koehn, F. E.; Carter, G. T.; Abou-Gharbia, M.; Graziani, E. I., Binding of rapamycin analogs to calcium channels and FKBP52 contributes to their neuroprotective activities. *Proceedings of the National Academy of Sciences* **2008**, *105* (1), 33-38.
- [58] Liu, D.; McIlvain, H. B.; Fennell, M.; Dunlop, J.; Wood, A.; Zaleska, M. M.; Graziani, E. I.; Pong, K., Screening of immunophilin ligands by quantitative analysis of neurofilament expression and neurite outgrowth in cultured neurons and cells. *J Neurosci Methods* **2007**, *163* (2), 310-20.
- [59] Summers, M. Y.; Leighton, M.; Liu, D.; Pong, K.; Graziani, E. I., 3-Normeridamycin: A Potent Non-Immunosuppressive Immunophilin Ligand is Neuroprotective in Dopaminergic Neurons. *J Antibiot* **2006**, *59* (3), 184-189.
- [60] Revill, W. P.; Voda, J.; Reeves, C. R.; Chung, L.; Schirmer, A.; Ashley, G.; Camey, J. R.; Fardis, M.; Carreras, C. W.; Zhou, Y.; Feng, L.; Tucker, E.; Robinson, D.; Gold, B. G., Genetically engineered analogs of ascomycin for nerve regeneration. *J Pharmacol Exp Ther* **2002**, *302* (3), 1278-85.
- [61] Gold, B. G.; Armistead, D. M.; Wang, M. S., Non-FK506-binding protein-12 neuroimmunophilin ligands increase neurite elongation and accelerate nerve regeneration. *J Neurosci Res* **2005**, *80* (1), 56-65.
- [62] Birge, R. B.; Wadsworth, S.; Akakura, R.; Abeyinghe, H.; Kanojia, R.; MacLag, M.; Desbarats, J.; Escalante, M.; Singh, K.; Sundarababu, S.; Parris, K.; Childs, G.; August, A.; Siekierka, J.; Weinstein, D. E., A role for schwann cells in the neuroregenerative effects of a non-immunosuppressive fk506 derivative, jnj460. *Neuroscience* **2004**, *124* (2), 351-66.
- [63] Zhao, L.; Liu, H.; Wang, L.; Li, S., Modeling and synthesis of non-cyclic derivatives of GPI-1046 as potential FKBP ligands with neurotrophic properties. *Bioorganic & Medicinal Chemistry Letters* **2006**, *16* (16), 4385-4390.
- [64] Costantini, L. C.; Isacson, O., Immunophilin ligands and GDNF enhance neurite branching or elongation from developing dopamine neurons in culture. *Exp Neurol* **2000**, *164* (1), 60-70.
- [65] Costantini, L. C.; Chaturvedi, P.; Armistead, D. M.; McCaffrey, P. G.; Deacon, T. W.; Isacson, O., A Novel Immunophilin Ligand: Distinct Branching Effects on Dopaminergic Neurons in Culture and Neurotrophic

- Actions after Oral Administration in an Animal Model of Parkinson's Disease. *Neurobiology of Disease* **1998**, *5* (2), 97-106.
- [66] Wei, L.; Steiner, J. P.; Hamilton, G. S.; Wu, Y.-Q., Synthesis and neurotrophic activity of nonimmunosuppressant cyclosporin A derivatives. *Bioorganic & Medicinal Chemistry Letters* **2004**, *14* (17), 4549-4551.
- [67] Price, R. D.; Yamaji, T.; Yamamoto, H.; Higashi, Y.; Hanaka, K.; Yamazaki, S.; Ishiye, M.; Aramori, I.; Matsuoka, N.; Mutoh, S., FK1706, a novel non-immunosuppressive immunophilin: neurotrophic activity and mechanism of action. *European Journal of Pharmacology* **2005**, *509* (1), 11-19.
- [68] Yamazaki, S.; Yamaji, T.; Murai, N.; Yamamoto, H.; Price, R. D.; Matsuoka, N.; Mutoh, S., FK1706, a novel non-immunosuppressive immunophilin ligand, modifies the course of painful diabetic neuropathy. *Neuropharmacology* **2008**, *55* (7), 1226-1230.
- [69] Kupina, N. C.; Detloff, M. R.; Dutta, S.; Hall, E. D., Neuroimmunophilin Ligand V-10,367 Is Neuroprotective After 24-Hour Delayed Administration in a Mouse Model of Diffuse Traumatic Brain Injury. *J Cereb Blood Flow Metab* **2002**, *22* (10), 1212-1221.
- [70] Edlich, F.; Weiwad, M.; Wildemann, D.; Jarczowski, F.; Kilka, S.; Moutty, M.-C.; Jahreis, G.; Lucke, C.; Schmidt, W.; Striggow, F.; Fischer, G., The Specific FKBP38 Inhibitor N-(N',N'-Dimethylcarboxamidomethyl) cycloheximide Has Potent Neuroprotective and Neurotrophic Properties in Brain Ischemia. *J. Biol. Chem.* **2006**, *281* (21), 14961-14970.
- [71] Costantini, L. C.; Cole, D.; Chaturvedi, P.; Isacson, O., Immunophilin ligands can prevent progressive dopaminergic degeneration in animal models of Parkinson's disease. *Eur J Neurosci* **2001**, *13* (6), 1085-92.
- [72] Steiner, J. P.; Hamilton, G. S.; Ross, D. T.; Valentine, H. L.; Guo, H.; Connolly, M. A.; Liang, S.; Ramsey, C.; Li, J. H.; Huang, W.; Horwath, P.; Soni, R.; Fuller, M.; Sauer, H.; Nowotnik, A. C.; Suzdak, P. D., Neurotrophic immunophilin ligands stimulate structural and functional recovery in neurodegenerative animal models. *Proc Natl Acad Sci U S A* **1997**, *94* (5), 2019-24.
- [73] Kubota, M.; Kasahara, T.; Iwamoto, K.; Komori, A.; Ishiwata, M.; Miyachi, T.; Kato, T., Therapeutic implications of down-regulation of cyclophilin D in bipolar disorder. *Int J Neuropsychopharmacol* **2010**, *13* (10), 1355-68.
- [74] Minematsu, T.; Lee, J.; Zha, J.; Moy, S.; Kowalski, D.; Hori, K.; Ishibashi, K.; Usui, T.; Kamimura, H., Time-dependent inhibitory effects of (1R,9S,12S,13R,14S,17R,18E,21S,23S,24R,25S,27R)-1,14-dihydroxy-12-(E)-2-[(1R,3R,4R)-4-hydroxy-3-methoxycyclohexyl]-1-methylvinyl-23,25-dimethoxy-13, 19,21,27-tetramethyl-17-(2-oxopropyl)-11,28-dioxo-4-azatri-cyclo[22.3.1.0(4,9)]octacos-18-ene-2,3,10,16-tetrone (FK1706), a novel nonimmunosuppressive immunophilin ligand, on CYP3A4/5 activity in humans *in vivo* and *in vitro*. *Drug Metab Dispos* **2010**, *38* (2), 249-59.
- [75] Kawai, M.; Lane, B. C.; Hsieh, G. C.; Mollison, K. W.; Carter, G. W.; Luly, J. R., Structure-activity profiles of macrolactam immunosuppressant FK-506 analogues. *FEBS Lett* **1993**, *316* (2), 107-13.
- [76] Ocain, T. D.; Longhi, D.; Stefan, R. J.; Caccese, R. G.; Sehgal, S. N., *Biochem. Biophys. Res. Commun.* **1993**, *192* (null), 1340.
- [77] Armistead, D. M.; Badia, M. C.; Deiningner, D. D.; Duffy, J. P.; Saunders, J. O.; Tung, R. D.; Thomson, J. A.; DeCenzo, M. T.; Futer, O.; Livingston, D. J.; Murcko, M. A.; Yamashita, M. M.; Navia, M. A., Design, synthesis and structure of non-macrocyclic inhibitors of FKBP12, the major binding protein for the immunosuppressant FK506. *Acta Crystallogr D Biol Crystallogr* **1995**, *51* (Pt 4), 522-8.
- [78] Armistead, D. M., Methods and compositions for stimulating neurite growth. *WO 96/41609* **1996**.
- [79] Gemann, U. A. S.; Dlna; Mason, Valerie S.; Zelle, Robert E.; Duffy, John P.; Gahullo, Vincent; Armistead, David M.; Saunders, Jeffrey O.; Boger, Joshua; Harding, Matthew W., Cellular and biochemical characterization of VX-710 as a chemosensitizer: reversal of P-glycoprotein-mediated multidrug resistance *in vitro*. *Anti-Cancer Drugs* **1997**, *8*, 125-140.
- [80] Dey, S., Bircicodar. Vertex Pharmaceuticals. *Curr Opin Investig Drugs* **2002**, *3* (5), 818-23.
- [81] Harper, S.; Bilsland, J.; Young, L.; Bristow, L.; Boyce, S.; Mason, G.; Rigby, M.; Hewson, L.; Smith, D.; O'Donnell, R.; O'Connor, D.; Hill, R. G.; Evans, D.; Swain, C.; Williams, B.; Hefli, F., Analysis of the neurotrophic effects of GPI-1046 on neuron survival and regeneration in culture and *in vivo*. *Neuroscience* **1999**, *88* (1), 257-67.
- [82] Bocquet, A.; Lorent, G.; Fuks, B.; Grimee, R.; Talaga, P.; Daliers, J.; Klitgaard, H., Failure of GPI compounds to display neurotrophic activity *in vitro* and *in vivo*. *Eur J Pharmacol* **2001**, *415* (2-3), 173-80.
- [83] Zhao, L.; Huang, W.; Liu, H.; Wang, L.; Zhong, W.; Xiao, J.; Hu, Y.; Li, S., FK506-binding protein ligands: structure-based design, synthesis, and neurotrophic/neuroprotective properties of substituted 5,5-dimethyl-2-(4-thiazolidine)carboxylates. *J Med Chem* **2006**, *49* (14), 4059-71.
- [84] Graziani, F.; Aldegheri, L.; Terstappen, G. C., High Throughput Scintillation Proximity Assay for the Identification of FKBP-12 Ligands. *J Biomol Screen* **1999**, *4* (1), 3-7.
- [85] Rabinowitz, M.; Seneci, P.; Rossi, T.; Dal Cin, M.; Deal, M.; Terstappen, G., Solid-phase/solution-phase combinatorial synthesis of neuroimmunophilin ligands. *Bioorg Med Chem Lett* **2000**, *10* (10), 1007-10.
- [86] Sich, C.; Improta, S.; Cowley, D. J.; Guenet, C.; Merly, J. P.; Teufel, M.; Saudek, V., Solution structure of a neurotrophic ligand bound to FKBP12 and its effects on protein dynamics. *Eur J Biochem* **2000**, *267* (17), 5342-55.
- [87] Gerard, M.; Deleersnijder, A. I.; DaniÅels, V.; Schreurs, S.; Munck, S.; Reumers, V.; Pottel, H.; Engelborghs, Y.; Van den Haute, C.; Taymans, J.-M.; Debyser, Z.; Baekelandt, V., Inhibition of FK506 Binding Proteins Reduces  $\beta$ -Synuclein Aggregation and Parkinson's Disease-Like Pathology. *The Journal of Neuroscience* **2010**, *30* (7), 2454-2463.
- [88] Marshall, V. L.; Grosset, D. G., GPI-1485 (Guilford). *Curr Opin Investig Drugs* **2004**, *5* (1), 107-12.
- [89] Gold, B. G.; Densmore, V.; Shou, W.; and, M. M. M.; Gordon, H. S., Immunophilin FK506-Binding Protein 52 (Not FK506-Binding Protein 12) Mediates the Neurotrophic Action of FK506. *J. Pharmacol. Exper. Therap.* **1999**, *289* (3), 1202-1210.
- [90] Cole, D. G. O., Stephan., Pharmacological activities of neurophilin ligands. *immunophilins in the Brain. FKBP Ligands: Novel Strategies for the Treatment of Neurodegenerative Disorders*, proceedings from the conference on neuroimmunophilins, 1st.schlagenbad.germany. **1999**, 109-116.
- [91] Polydefkis, M.; Sirdofsky, M.; Hauer, P.; Petty, B. G.; Murinson, B.; McArthur, J. C., Factors influencing nerve regeneration in a trial of fimmecodar dime-sylate. *Neurology* **2006**, *66* (2), 259-61.
- [92] Hahn, K.; Sirdofsky, M.; Brown, A.; Ebenezer, G.; Hauer, P.; Miller, C.; Polydefkis, M., Collateral sprouting of human epidermal nerve fibers following intracutaneous axotomy. *J Peripher Nerv Syst* **2006**, *11* (2), 142-7.
- [93] Norville, I. H.; O'Shea, K.; Sarkar-Tyson, M.; Zheng, S.; Titball, R. W.; Varani, G.; Harmer, N. J., The structure of a Burkholderia pseudomallei immunophilin-inhibitor complex reveals new approaches to antimicrobial development. *Biochem J* **437** (3), 413-22.
- [94] Shim, S.; Yuan, J. P.; Kim, J. Y.; Zeng, W.; Huang, G.; Milshchey, A.; Kern, D.; Muallem, S.; Ming, G.-I.; Worley, P. F., Peptidyl-Prolyl Isomerase FKBP52 Controls Chemotropic Guidance of Neuronal Growth Cones via Regulation of TRPC1 Channel Opening. *Neuron* **2009**, *64* (4), 471-483.
- [95] Quintá, H. R.; Maschi, D.; Gomez-Sanchez, C.; Pwien-Pilipuk, G.; Galigniana, M. D., Subcellular rearrangement of hsp90-binding immunophilins accompanies neuronal differentiation and neurite outgrowth. *Journal of Neurochemistry* **2010**, *115* (3), 716-734.
- [96] Chambraud, B.; Sardin, E.; Giustiniani, J.; Donnane, O.; Schumacher, M.; Goedert, M.; Baulieu, E. E., A role for FKBP52 in Tau protein function. *Proc Natl Acad Sci U S A* **2010**, *107* (6), 2658-63.
- [97] Jinwal, U. K.; Koren, J.; Borysov, S. I.; Schmidt, A. B.; Abisambra, J. F.; Blair, L. J.; Johnson, A. G.; Jones, J. R.; Shults, C. L.; O'Leary, J. C.; 3rd; Jin, Y.; Buchner, J.; Cox, M. B.; Dickey, C. A., The Hsp90 cochaperone, FKBP51, increases Tau stability and polymerizes microtubules. *J Neurosci* **2010**, *30* (2), 591-9.
- [98] Chambraud, B.; Belabes, H.; Fontaine-Lenoir, V.; Fellous, A.; Baulieu, E. E., The immunophilin FKBP52 specifically binds to tubulin and prevents microtubule formation. *FASEB J* **2007**, *21* (11), 2787-97.
- [99] Huse, M.; Chen, Y. G.; Massague, J.; Kuriyan, J., Crystal structure of the cytoplasmic domain of the type I TGF beta receptor in complex with FKBP12. *Cell* **1999**, *96* (3), 425-36.
- [100] Ahearn, I. M.; Tsai, F. D.; Court, H.; Zhou, M.; Jennings, B. C.; Ahmed, M.; Fehrenbacher, N.; Linder, M. E.; Phillips, M. R., FKBP12 Binds to Acetylated H-Ras and Promotes Depalmitoylation. *Molecular Cell* **2011**, *41* (2), 173-185.
- [101] Gerard, M.; Debyser, Z.; Desender, L.; Kahle, P. J.; Baert, J.; Baekelandt, V.; Engelborghs, Y., The aggregation of alpha-synuclein is stimulated by FK506 binding proteins as shown by fluorescence correlation spectroscopy. *FASEB J* **2006**, *20* (3), 524-6.
- [102] Deleersnijder, A.; Van Rompuy, A. S.; Desender, L.; Pottel, H.; Buee, L.; Debyser, Z.; Baekelandt, V.; Gerard, M., Comparative analysis of different peptidyl-prolyl isomerases reveals FK506-binding protein 12 as the most potent enhancer of {alpha}-synuclein aggregation. *J Biol Chem* **2011**.
- [103] Smalil, S. S.; Stellato, K. A.; Burnett, P.; Thomas, A. P.; Gaspers, L. D., Cyclosporin A inhibits inositol 1,4,5-trisphosphate-dependent Ca<sup>2+</sup> signals by enhancing Ca<sup>2+</sup> uptake into the endoplasmic reticulum and mitochondria. *J Biol Chem* **2001**, *276* (26), 23329-40.
- [104] Bultynck, G.; De Smet, P.; Weidema, A. F.; Ver Heyen, M.; Maes, K.; Callewaert, G.; Missiaen, L.; Parys, J. B.; De Smedt, H., Effects of the immunosuppressant FK506 on intracellular Ca<sup>2+</sup> release and Ca<sup>2+</sup> accumulation mechanisms. *J Physiol* **2000**, *525* Pt 3, 681-93.
- [105] Bilmen, J. G.; Woolton, L. L.; Michelangeli, F., The inhibition of the sarcoplasmic/endoplasmic reticulum Ca<sup>2+</sup>-ATPase by macrocyclic lactones and cyclosporin A. *Biochem J* **2002**, *366* (Pt 1), 255-63.
- [106] Rosado, J. A.; Pariente, J. A.; Salido, G. M.; Redondo, P. C., SERCA2b Activity Is Regulated by Cyclophilins in Human Platelets. *Arterioscler Thromb Vasc Biol* **2010**, *30* (3), 419-425.
- [107] Caporello, E.; Nath, A.; Slevin, J.; Galey, D.; Hamilton, G.; Williams, L.; Steiner, J. P.; Haughey, N. J., The immunophilin ligand GPI1046 protects neurons from the lethal effects of the HIV-1 proteins gp120 and Tat by modulating endoplasmic reticulum calcium load. *J Neurochem* **2006**, *98* (1), 146-55.
- [108] Goel, M.; Garcia, R.; Estacion, M.; Schilling, W. P., Regulation of Drosophila TRPL channels by immunophilin FKBP59. *J Biol Chem* **2001**, *276* (42), 38762-73.
- [109] Sinkins, W. G.; Goel, M.; Estacion, M.; Schilling, W. P., Association of immunophilins with mammalian TRPC channels. *J Biol Chem* **2004**, *279* (33), 34521-9.

- [110] Gkika, D.; Topala, C. N.; Hoenderop, J. G. J.; Bindels, R. J. M., The immunophilin FKBP52 inhibits the activity of the epithelial Ca<sup>2+</sup> channel TRPV5. *Am J Physiol Renal Physiol* **2006**, *290* (5), F1253-1259.
- [111] Arceci, R. J.; Slieglitz, K.; Bierer, B. E., Immunosuppressants FK506 and rapamycin function as reversal agents of the multidrug resistance phenotype. *Blood* **1992**, *80* (6), 1528-36.
- [112] Guo, C.; Reich, S.; Showalter, R.; Villafranca, E.; Dong, L., A concise synthesis of AG5473/5507 utilizing N-acyliminium ion chemistry. *Tetrahedron Letters* **2000**, *41* (28), 5307-5311.
- [113] Hudack R A Jr, B. N., Guo C, Deal J, Dong L, Fay LK, Caprathe B, Chatterjee A, Vanderpool D, Bigge C, Showalter R, Bender S, Augelli-Szafran CE, Lunney E, Hou X., Design, synthesis, and biological activity of novel polycyclic aza-amide FKBP12 ligands. *J. Med. Chem* **2006**, 1202-1206.
- [114] Guo, C.; Dong, L.; Kephart, S.; Hou, X., An efficient synthesis of sulfamides. *Tetrahedron Letters* **2010**, *51* (21), 2909-2913.
- [115] Shuker, S. B.; Hajduk, P. J.; Meadows, R. P.; Fesik, S. W., Discovering high-affinity ligands for proteins: SAR by NMR. *Science* **1996**, *274* (5292), 1531-4.
- [116] Röhrig, Christoph H.; Overhand, C. L. J.-Y. G. G. S. M., Fragment-Based Synthesis and SAR of Modified FKBP Ligands: Influence of Different Linking on Binding Affinity. *ChemMedChem* **2007**, *2* (7), 1054-1070.
- [117] Stebbins, J. L.; Zhang, Z.; Chen, J.; Wu, B.; Emdadi, A.; Williams, M. E.; Cashman, J.; Pellicchia, M., Nuclear Magnetic Resonance Fragment-Based Identification of Novel FKBP12 Inhibitors. *J. Med. Chem.* **2007**.
- [118] Blackburn, E. A.; Maclean, J. K.; Sherborne, B. S.; Walkinshaw, M. D., Estimating the affinity of protein-ligand complex from changes to the charge-state distribution of a protein in electrospray ionization mass spectrometry. *Biochem Biophys Res Commun* **2010**, *403* (2), 190-3.
- [119] Cioffi, D. L.; Hubler, T. R.; Scammell, J. G., Organization and function of the FKBP52 and FKBP51 genes. *Current Opinion in Pharmacology* **2011**, *In Press, Corrected Proof*.
- [120] Sivits, J. C.; Storer, C. L.; Galigniana, M. D.; Cox, M. B., Regulation of steroid hormone receptor function by the 52-kDa FK506-binding protein (FKBP52). *Curr Opin Pharmacol* **2011**.
- [121] Yong, W.; Bao, S.; Chen, H.; Li, D.; Sanchez, E. R.; Shou, W., Mice Lacking Protein Phosphatase 5 Are Defective in Ataxia Telangiectasia Mutated (ATM)-mediated Cell Cycle Arrest. *J. Biol. Chem.* **2007**, *282* (20), 14690-14694.
- [122] Attwood, B. K.; Bourgognon, J. M.; Patel, S.; Mucha, M.; Schiavon, E.; Skrzypiec, A. E.; Young, K. W.; Shiosaka, S.; Korostynski, M.; Piechota, M.; Przewlocki, R.; Pawlak, R., Neurospins cleaves EphB2 in the amygdala to control anxiety. *Nature* **2011**, *473* (7347), 372-5.
- [123] Jaaskelainen, T.; Makkonen, H.; Palvimo, J. J., Steroid up-regulation of FKBP51 and its role in hormone signaling. *Curr Opin Pharmacol* **2011**.
- [124] Scharf, S. H.; Liebl, C.; Binder, E. B.; Schmidt, M. V.; Müller, M. B., Expression and regulation of the Fkbp5 gene in the adult mouse brain. *PLoS One* **6** (2), e16883.
- [125] Binder, E. B., The role of FKBP5, a co-chaperone of the glucocorticoid receptor in the pathogenesis and therapy of affective and anxiety disorders. *Psychoneuroendocrinology* **2009**, *34* (Supplement 1), S186-S195.
- [126] Zou, Y.-F.; Wang, F.; Feng, X.-L.; Li, W.-F.; Tao, J.-H.; Pan, F.-M.; Huang, F.; Su, H., Meta-analysis of FKBP5 gene polymorphisms association with treatment response in patients with mood disorders. *Neuroscience Letters* **2010**, *484* (1), 56-61.
- [127] Hartmann, J.; Wagner, K. V.; Liebl, C.; Scharf, S. H.; Wang, X.-D.; Wolf, M.; Hausch, F.; Rein, T.; Schmidt, U.; Touma, C.; Cheung-Flynn, J.; Cox, M. B.; Smith, D. F.; Holsboer, F.; Müller, M. B.; Schmidt, M. V., The involvement of FK506-binding protein 51 (FKBP5) in the behavioral and neuroendocrine effects of chronic social defeat stress. *Neuropharmacology* **2011**, *In Press, Corrected Proof*.
- [128] Touma, C.; Gassen, N. C.; Herrmann, L.; Cheung-Flynn, J.; Büll, D. R.; Ionescu, I. A.; Heinzmann, J. M.; Knapman, A.; Siebertz, A.; Depping, A. M.; Hartmann, J.; Hausch, F.; Schmidt, M. V.; Holsboer, F.; Ising, M.; Cox, M. B.; Schmidt, U.; Rein, T., FKBP5 shapes stress responsiveness: Modulation of neuroendocrine reactivity and coping behavior. *Biological Psychiatry* **2011**, *In Press, Corrected Proof*.
- [129] Romano S, M. M., Romano MF, FKBP51 and the NF- $\kappa$ B regulatory pathway in cancer. *Current Opinion in Pharmacology* **2011**, 1-6.
- [130] Li, L.; Lou, Z.; Wang, L., The role of FKBP5 in cancer aetiology and chemoresistance. *Br J Cancer* **2010**, *104* (1), 19-23.
- [131] Periyasamy, S.; Hinds, T., Jr.; Shemshedini, L.; Shou, W.; Sanchez, E. R., FKBP51 and Cyp40 are positive regulators of androgen-dependent prostate cancer cell growth and the targets of FK506 and cyclosporin A. *Oncogene* **2010**, *29* (11), 1691-1701.
- [132] Ni, L.; Yang, C. S.; Gioeli, D.; Frierson, H.; Toff, D. O.; Paschal, B. M., FKBP51 Promotes Assembly of the Hsp90 Chaperone Complex and Regulates Androgen Receptor Signaling in Prostate Cancer Cells. *Mol Cell Biol* **2010**, *30* (5), 1243-53.
- [133] Romano, S.; D'Angelillo, A.; Pacelli, R.; Staibano, S.; De Luna, E.; Bisogni, R.; Eskelinen, E. L.; Mascolo, M.; Cali, G.; Arra, C.; Romano, M. F., Role of FK506-binding protein 51 in the control of apoptosis of irradiated melanoma cells. *Cell Death Differ* **2010**, *17* (1), 145-57.
- [134] Bouwmeester, T.; Bauch, A.; Ruffner, H.; Angrand, P. O.; Bergamini, G.; Croughton, K.; Cruciat, C.; Eberhard, D.; Gagneur, J.; Ghidelli, S.; Hopf, C.; Huhse, B.; Mangano, R.; Michon, A. M.; Schirle, M.; Schlegl, J.; Schwab, M.; Stein, M. A.; Bauer, A.; Casari, G.; Drewes, G.; Gavin, A. C.; Jackson, D. B.; Joberty, G.; Neubauer, G.; Rick, J.; Kuster, B.; Superti-Furga, G., A physical and functional map of the human TNF- $\alpha$ /NF- $\kappa$ B signal transduction pathway. *Nat Cell Biol* **2004**, *6* (2), 97-105.
- [135] Pei, H.; Li, L.; Fridley, B. L.; Jenkins, G. D.; Kalari, K. R.; Lingle, W.; Petersen, G.; Lou, Z.; Wang, L., FKBP51 Affects Cancer Cell Response to Chemotherapy by Negatively Regulating Akt. *Cancer Cell* **2009**, *16* (3), 259-266.
- [136] Riggs, D. L.; Roberts, P. J.; Chirillo, S. C.; Cheung-Flynn, J.; Prapanich, V.; Ratajczak, T.; Gaber, R.; Picard, D.; Smith, D. F., The Hsp90-binding peptidylprolyl isomerase FKBP52 potentiates glucocorticoid signaling *in vivo*. *Embo J* **2003**, *22* (5), 1158-67.
- [137] Davies, T. H.; Ning, Y. M.; Sanchez, E. R., Differential control of glucocorticoid receptor hormone-binding function by tetratricopeptide repeat (TPR) proteins and the immunosuppressive ligand FK506. *Biochemistry* **2005**, *44* (6), 2030-8.
- [138] Westberry, J. M.; Sadosky, P. W.; Hubler, T. R.; Gross, K. L.; Scammell, J. G., Glucocorticoid resistance in squirrel monkeys results from a combination of a transcriptionally incompetent glucocorticoid receptor and overexpression of the glucocorticoid receptor co-chaperone FKBP51. *J Steroid Biochem Mol Biol* **2006**, *100* (1-3), 34-41.
- [139] Kralli, A.; Yamamoto, K. R., An FK506-sensitive transporter selectively decreases intracellular levels and potency of steroid hormones. *J Biol Chem* **1996**, *271* (29), 17152-6.
- [140] Marsaud, V.; Mercier-Bodard, C.; Fortin, D.; Le Bihan, S.; Renoir, J. M., Dexamethasone and triamcinolone acetonide accumulation in mouse fibroblasts is differently modulated by the immunosuppressants cyclosporin A, FK506, rapamycin and their analogues, as well as by other P-glycoprotein ligands. *J Steroid Biochem Mol Biol* **1998**, *66* (1-2), 11-25.
- [141] Bracher, A.; Kozany, C.; Thost, A. K.; Hausch, F., Structural characterization of the PPIase domain of FKBP51, a co-chaperone of human Hsp90. *Acta Crystallogr D Biol Crystallogr* **67** (Pt 6), 549-59.
- [142] Kozany, C.; März, A.; Kress, C.; Hausch, F., Fluorescent Probes to Characterise FK506-Binding Proteins. *ChemBioChem* **2009**, *10* (8), 1402-1410.
- [143] Bell, A.; Monaghan, P.; Page, A. P., Peptidyl-prolyl cis-trans isomerases (immunophilins) and their roles in parasite biochemistry, host-parasite interaction and antiparasitic drug action. *Int J Parasitol* **2006**, *36* (3), 261-76.
- [144] Kohler, R.; Fanghanel, J.; König, B.; Lüneberg, E.; Frosch, M.; Rahfeld, J. U.; Hilgenfeld, R.; Fischer, G.; Hacker, J.; Steinert, M., Biochemical and functional analyses of the Mip protein: influence of the N-terminal half and of peptidylprolyl isomerase activity on the virulence of Legionella pneumophila. *Infect Immun* **2003**, *71* (8), 4389-97.
- [145] Moro, A.; Ruiz-Cabello, F.; Fernandez-Cano, A.; Stock, R. P.; Gonzalez, A., Secretion by Trypanosoma cruzi of a peptidyl-prolyl cis-trans isomerase involved in cell infection. *EMBO J* **1995**, *14* (11), 2483-90.
- [146] Oz, H. S.; Hughes, W. T.; Thomas, E. K.; McClain, C. J., Effects of immunomodulators on acute Trypanosoma Cruzi infection in mice. *Med Sci Monit* **2002**, *8* (6), BR208-11.
- [147] Ceymann, A.; Horstmann, M.; Ehses, P.; Schweimer, K.; Paschke, A. K.; Steinert, M.; Faber, C., Solution structure of the Legionella pneumophila Mip-rapamycin complex. *BMC Struct Biol* **2008**, *8*, 17.
- [148] Juli, C.; Sippel, M.; Jager, J.; Thiele, A.; Weiwad, M.; Schweimer, K.; Rosch, P.; Steinert, M.; Sottriffer, C. A.; Holzgrabe, U., Pipecolic Acid Derivatives As Small-Molecule Inhibitors of the Legionella MIP Protein. *J Med Chem* **2010**.
- [149] Norville, I. H.; O'Shea, K.; Sarkar-Tyson, M.; Zheng, S.; Tibball, R. W.; Varani, G.; Harmer, N. J., The structure of a Burkholderia pseudomallei immunophilin-inhibitor complex reveals new approaches to antimicrobial development. *Biochem J* **2011**, *437* (3), 413-22.
- [150] Monaghan, P.; Fardis, M.; Revill, W. P.; Bell, A., Antimalarial effects of macrolactones related to FK520 (ascmycin) are independent of the immunosuppressive properties of the compounds. *J Infect Dis* **2005**, *191* (8), 1342-9.
- [151] Rotonda, J.; Burbaum, J. J.; Chan, H. K.; Marcy, A. I.; Becker, J. W., Improved calcineurin inhibition by yeast FKBP12-drug complexes. Crystallographic and functional analysis. *J Biol Chem* **1993**, *268* (11), 7607-9.
- [152] Kumar, R.; Adams, B.; Musiyenko, A.; Shulyayeva, O.; Barik, S., The FK506-binding protein of the malaria parasite, Plasmodium falciparum, is a FK506-sensitive chaperone with FK506-independent calcineurin-inhibitory activity. *Mol Biochem Parasitol* **2005**, *141* (2), 163-73.
- [153] Hopkins, S.; Scorneaux, B.; Huang, Z.; Murray, M. G.; Wring, S.; Smitley, C.; Harris, R.; Erdmann, F.; Fischer, G.; Ribell, Y., SCY-635, a novel nonimmunosuppressive analog of cyclosporine that exhibits potent inhibition of hepatitis C virus RNA replication *in vitro*. *Antimicrob Agents Chemother* **2010**, *54* (2), 660-72.
- [154] Baumgrass, R.; Zhang, Y.; Erdmann, F.; Thiel, A.; Weiwad, M.; Radbruch, A.; Fischer, G., Substitution in position 3 of cyclosporin A abolishes the cyclophilin-mediated gain-of-function mechanism but not immunosuppression. *J Biol Chem* **2004**, *279* (4), 2470-9.
- [155] Puyang, X.; Poulin, D. L.; Mathy, J. E.; Anderson, L. J.; Ma, S.; Fang, Z.; Zhu, S.; Lin, K.; Fujimoto, R.; Compton, T.; Wiedmann, B., Mechanism of Resistance of Hepatitis C Virus Replicons to Structurally Distinct

- Cyclophilin Inhibitors. *Antimicrob. Agents Chemother.* **2010**, *54* (5), 1981-1987.
- [156] Goto, K.; Watashi, K.; Inoue, D.; Hijikata, M.; Shimotohno, K., Identification of cellular and viral factors related to anti-hepatitis C virus activity of cyclophilin inhibitor. *Cancer Science* **2009**, *100* (10), 1943-1950.
- [157] Gregory, M. A.; Bobardt, M.; Oheid, S.; Chatterji, U.; Coates, N. J.; Foster, T.; Gallay, P.; Leyssen, P.; Moss, S. J.; Neyts, J.; Nur-e-Alam, M.; Paeshuyse, J.; Pirace, M.; Sulhar, D.; Warneck, T.; Zhang, M.-Q.; Wilkinson, B., Preclinical Characterization of Naturally Occurring Polyketide Cyclophilin Inhibitors from the Sanglifehrin Family. *Antimicrob. Agents Chemother.* **2011**, *55* (5), 1975-1981.
- [158] Morohashi, K.; Sahara, H.; Watashi, K.; Iwabata, K.; Sunoki, T.; Kuramochi, K.; Takakusagi, K.; Miyashita, H.; Sato, N.; Tanabe, A.; Shimotohno, K.; Kobayashi, S.; Sakaguchi, K.; Sugawara, F., Cyclosporin A Associated Helicase-Like Protein Facilitates the Association of Hepatitis C Virus RNA Polymerase with Its Cellular Cyclophilin B. *PLoS ONE* **2011**, *6* (4), e18285.
- [159] Coelmont, L.; Hanoulle, X.; Chatterji, U.; Berger, C.; Snoeck, J.; Bobardt, M.; Lim, P.; Vliegen, I.; Paeshuyse, J.; Vuagniaux, G. g.; Vandamme, A.-M.; Bartschlager, R.; Gallay, P.; Lippens, G.; Neyts, J., DEB025 (Alisporivir) Inhibits Hepatitis C Virus Replication by Preventing a Cyclophilin A Induced Cis-Trans Isomerisation in Domain II of NSSA. *PLoS ONE* **2010**, *5* (10), e13687.
- [160] Crabbe, R.; Vuagniaux, G.; Dumont, J. M.; Nicolas-Metral, V.; Marfurt, J.; Novaroli, L., An evaluation of the cyclophilin inhibitor Debio 025 and its potential as a treatment for chronic hepatitis C. *Expert Opin Investig Drugs* **2009**, *18* (2), 211-20.
- [161] Flisiak, R.; Dumont, J. M.; Crabbe, R., Cyclophilin inhibitors in hepatitis C viral infection. *Expert Opin Investig Drugs* **2007**, *16* (9), 1345-54.
- [162] Simon, N.; Dailly, E.; Combes, O.; Malaurie, E.; Lemaire, M.; Tillement, J. P.; Urien, S., Role of lipoproteins in the plasma binding of SDZ PSC 833, a novel multidrug resistance-reversing cyclosporin. *Br J Clin Pharmacol* **1998**, *45* (2), 173-5.
- [163] Suzuki, J.; Jin, Z.-G.; Meoli, D. F.; Matoba, T.; Berk, B. C., Cyclophilin A Is Secreted by a Vesicular Pathway in Vascular Smooth Muscle Cells. *Circulation Research* **2006**, *98* (6), 811-817.
- [164] Arora, K.; Gwinn, W. M.; Bower, M. A.; Watson, A.; Okwumabua, I.; MacDonald, H. R.; Bukrinsky, M. I.; Constant, S. L., Extracellular cyclophilins contribute to the regulation of inflammatory responses. *J Immunol* **2005**, *175* (1), 517-22.
- [165] Malesevic, M.; Kuhling, J.; Erdmann, F.; Balsley, M. A.; Bukrinsky, M. I.; Constant, S. L.; Fischer, G., A cyclosporin derivative discriminates between extracellular and intracellular cyclophilins. *Angew Chem Int Ed Engl* **2010**, *49* (1), 213-5.
- [166] Zhang, Y.; Erdmann, F.; Baumgrass, R.; Schutkowski, M.; Fischer, G., Unexpected side chain effects at residue 8 of cyclosporin A derivatives allow photoswitching of immunosuppression. *J Biol Chem* **2005**, *280* (6), 4842-50.
- [167] Balsley, M. A.; Malesevic, M.; Stemmy, E. J.; Giggley, J.; Jurjus, R. A.; Herzog, D.; Bukrinsky, M. I.; Fischer, G.; Constant, S. L., A cell-impermeable cyclosporine A derivative reduces pathology in a mouse model of allergic lung inflammation. *J Immunol* **2010**, *185* (12), 7663-70.
- [168] Giorgio, V.; Soriano, M. E.; Basso, E.; Bisetto, E.; Lippe, G.; Forte, M. A.; Bernardi, P., Cyclophilin D in mitochondrial pathophysiology. *Biochim Biophys Acta* **2010**, *1797* (6-7), 1113-8.
- [169] Fujimoto, K.; Chen, Y.; Polonsky, K. S.; Dom, G. W., 2nd, Targeting cyclophilin D and the mitochondrial permeability transition enhances beta-cell survival and prevents diabetes in Pdx1 deficiency. *Proc Natl Acad Sci U S A* **2010**, *107* (22), 10214-9.
- [170] Piot, C.; Croisille, P.; Staat, P.; Thibault, H.; Rioufol, G.; Newton, N.; Elbelghiti, R.; Chung, T. T.; Bonnefoy, E.; Angoulvant, D.; Macia, C.; Raczka, F.; Sportouch, C.; Gahide, G.; Finet, G.; Andre-Fouet, X.; Revel, D.; Kirkorian, G.; Monassier, J. P.; Derumeaux, G.; Ovize, M., Effect of cyclosporine on reperfusion injury in acute myocardial infarction. *N Engl J Med* **2008**, *359* (5), 473-81.
- [171] Merlini, L.; Angelin, A.; Tiepolo, T.; Braghetta, P.; Sabatelli, P.; Zamparelli, A.; Ferlini, A.; Maraldi, N. M.; Bonaldo, P.; Bernardi, P., Cyclosporin A corrects mitochondrial dysfunction and muscle apoptosis in patients with collagen VI myopathies. *Proc Natl Acad Sci U S A* **2008**, *105* (13), 5225-9.
- [172] Seizer, P.; Ochmann, C.; Schonberger, T.; Zach, S.; Rose, M.; Borst, O.; Klingel, K.; Kandolf, R.; MacDonald, H. R.; Nowak, R. A.; Engelhardt, S.; Lang, F.; Gawaz, M.; May, A. E., Disrupting the EMMPRIN (CD147)-Cyclophilin A Interaction Reduces Infarct Size and Preserves Systolic Function After Myocardial Ischemia and Reperfusion. *Arterioscler Thromb Vasc Biol* **2011**, *31* (6), 1377-1386.
- [173] Kajitani, K.; Fujihashi, M.; Kobayashi, Y.; Shimizu, S.; Tsujimoto, Y.; Miki, K., Crystal structure of human cyclophilin D in complex with its inhibitor, cyclosporin A at 0.96-A resolution. *Proteins* **2008**, *70* (4), 1635-9.
- [174] Malouire, S.; Dube, H.; Selwood, D.; Crompton, M., Mitochondrial targeting of cyclosporin A enables selective inhibition of cyclophilin-D and enhanced cytoprotection after glucose and oxygen deprivation. *Biochemical Journal* **2010**, *425* (1), 137-148.
- [175] Guichou, J. F.; Viaud, J.; Mettling, C.; Subra, G.; Lin, Y. L.; Chavanieu, A., Structure-based design, synthesis, and biological evaluation of novel inhibitors of human cyclophilin A. *J Med Chem* **2006**, *49* (3), 900-10.
- [176] Gaali, S.; Kozany, C.; Hoogeland, B.; Klein, M.; Hausch, F., Facile Synthesis of a Fluorescent Cyclosporin A Analogue To Study Cyclophilin 40 and Cyclophilin 18 Ligands. *ACS Medicinal Chemistry Letters* **2010**, *1* (9), 536-539.
- [177] Guo, H. X.; Wang, F.; Yu, K. Q.; Chen, J.; Bai, D. L.; Chen, K. X.; Shen, X.; Jiang, H. L., Novel cyclophilin D inhibitors derived from quinoxaline exhibit highly inhibitory activity against rat mitochondrial swelling and Ca<sup>2+</sup> uptake/release. *Acta Pharmacol Sin* **2005**, *26* (10), 1201-11.
- [178] Li, J.; Chen, J.; Zhang, L.; Wang, F.; Gui, C.; Qin, Y.; Xu, Q.; Liu, H.; Nan, F.; Shen, J.; Bai, D.; Chen, K.; Shen, X.; Jiang, H., One novel quinoxaline derivative as a potent human cyclophilin A inhibitor shows highly inhibitory activity against mouse spleen cell proliferation. *Bioorg Med Chem* **2006**, *14* (16), 5527-34.
- [179] Li, J.; Chen, J.; Gui, C.; Zhang, L.; Qin, Y.; Xu, Q.; Zhang, J.; Liu, H.; Shen, X.; Jiang, H., Discovering novel chemical inhibitors of human cyclophilin A: virtual screening, synthesis, and bioassay. *Bioorg Med Chem* **2006**, *14* (7), 2209-24.
- [180] Li, J.; Zhang, J.; Chen, J.; Luo, X.; Zhu, W.; Shen, J.; Liu, H.; Shen, X.; Jiang, H., Strategy for discovering chemical inhibitors of human cyclophilin A: focused library design, virtual screening, chemical synthesis and bioassay. *J Comb Chem* **2006**, *8* (3), 326-37.
- [181] Ni, S.; Yuan, Y.; Huang, J.; Mao, X.; Lv, M.; Zhu, J.; Shen, X.; Pei, J.; Lai, L.; Jiang, H.; Li, J., Discovering potent small molecule inhibitors of cyclophilin A using de novo drug design approach. *J Med Chem* **2009**, *52* (17), 5295-8.
- [182] Li, J.; Tan, Z.; Tang, S.; Hewlett, I.; Pang, R.; He, M.; He, S.; Tian, B.; Chen, K.; Yang, M., Discovery of dual inhibitors targeting both HIV-1 capsid and human cyclophilin A to inhibit the assembly and uncoating of the viral capsid. *Bioorg Med Chem* **2009**, *17* (8), 3177-88.
- [183] Tan, Z.; Li, J.; Pang, R.; He, S.; He, M.; Tang, S.; Hewlett, I.; Yang, M., Screening and evaluation of thiourea derivatives for their HIV capsid and human cyclophilin A inhibitory activity. *Med Chem Res* **2011**, *20*, 314-320.
- [184] Mori, T.; Hidaka, M.; Lin, Y. C.; Yoshizawa, I.; Okabe, T.; Egashira, S.; Kojima, H.; Nagano, T.; Koketsu, M.; Takamiya, M.; Uchida, T., A dual inhibitor against prolyl isomerase Pnl and cyclophilin discovered by a novel real-time fluorescence detection method. *Biochem Biophys Res Commun* **2011**, *406* (3), 439-43.
- [185] Yang, Y.; Moir, E.; Kontopidis, G.; Taylor, P.; Wear, M. A.; Malone, K.; Dunsmore, C. J.; Page, A. P.; Turner, N. J.; Walkinshaw, M. D., Structure-based discovery of a family of synthetic cyclophilin inhibitors showing a cyclosporin-A phenotype in *Caenorhabditis elegans*. *Biochem Biophys Res Commun* **2007**, *363* (4), 1013-9.
- [186] Dunsmore, C. J.; Malone, K. J.; Bailey, K. R.; Wear, M. A.; Florance, H.; Shirran, S.; Barran, P. E.; Page, A. P.; Walkinshaw, M. D.; Turner, N. J., Design and synthesis of conformationally constrained cyclophilin inhibitors showing a cyclosporin-A phenotype in *C. elegans*. *Chembiochem* **2011**, *12* (5), 802-10.
- [187] Dearmond, P. D.; West, G. M.; Anbalagan, V.; Campa, M. J.; Patz, E. F., Jr.; Fitzgerald, M. C., Discovery of novel cyclophilin A ligands using an H/D exchange- and mass spectrometry-based strategy. *J Biomol Screen* **2011**, *15* (9), 1051-62.
- [188] Clavaud, C.; Heckenroth, M.; Stricane, C.; Lelaït, M. A.; Menez, A.; Dugave, C., Combinatorial self-assembly of cyclophilin hCyp-18 ligands through rhenium coordination. *Chembiochem* **2006**, *7* (9), 1352-5.
- [189] Clavaud, C.; Le Gal, J.; Thai, R.; Moutiez, M.; Dugave, C., Dynamic combinatorial self-assembly of cyclophilin hCyp-18 ligands through oxorhenium coordination. *Chembiochem* **2008**, *9* (11), 1823-9.
- [190] Daum, S.; Schumann, M.; Mathea, S.; Aumuller, T.; Balsley, M. A.; Constant, S. L.; de Lacroix, B. F.; Kruska, F.; Braun, M.; Schiene-Fischer, C., Isoform-specific inhibition of cyclophilins. *Biochemistry* **2009**, *48* (26), 6268-77.
- [191] Kofron, J. L.; Kuzmic, P.; Kishore, V.; Colon-Bonilla, E.; Rich, D. H., Determination of kinetic constants for peptidyl prolyl cis-trans isomerases by an improved spectrophotometric assay. *Biochemistry* **1991**, *30* (25), 6127-34.
- [192] Mori, T.; Itami, S.; Yanagi, T.; Tataru, Y.; Takamiya, M.; Uchida, T., Use of a Real-Time Fluorescence Monitoring System for High-Throughput Screening for Prolyl Isomerase Inhibitors. *J Biomol Screen* **2009**, *14* (4), 419-424.
- [193] Liu, J.; Chen, C. M.; Walsh, C. T., Human and *Escherichia coli* cyclophilins: sensitivity to inhibition by the immunosuppressant cyclosporin A correlates with a specific tryptophan residue. *Biochemistry* **1991**, *30* (9), 2306-10.
- [194] Park, S. T.; Aldape, R. A.; Futer, O.; Decenzo, M. T.; Livingston, D. J., PPLase catalysis by human FK506-binding protein proceeds through a conformational twist mechanism. *Journal of Biological Chemistry* **1992**, *267*, 3316 - 3324.
- [195] Carreras, C. W.; Fu, H.; Santi, D. V., An FKBP12 binding assay based upon biofilylated FKBP12. *Anal Biochem* **2001**, *298* (1), 57-61.
- [196] Banaszynski, L. A.; Liu, C. W.; Wandless, T. J., Characterization of the FKBP-rapamycin-FRB ternary complex. *J Am Chem Soc* **2005**, *127* (13), 4715-21.
- [197] Mahendrarajah, K.; Dalby, P. A.; Wilkinson, B.; Jackson, S. E.; Main, E. R., A high-throughput fluorescence chemical denaturation assay as a general screen for protein-ligand binding. *Anal Biochem* **2011**, *411* (1), 155-7.
- [198] West, G. M.; Thompson, J. W.; Soderblom, E. J.; Dubois, L. G.; Dearmond, P. D.; Moseley, M. A.; Fitzgerald, M. C., Mass spectrometry-based thermal shift assay for protein-ligand binding analysis. *Anal Chem* **2010**, *82* (13), 5573-81.

- [199] Luker, K. E.; Smith, M. C.; Luker, G. D.; Gammon, S. T.; Piwnica-Worms, H.; Piwnica-Worms, D., Kinetics of regulated protein-protein interactions revealed with firefly luciferase complementation imaging in cells and living animals. *Proc Natl Acad Sci U S A* **2004**, *101* (33), 12288-93.
- [200] Corson, T. W.; Aberle, N.; Crews, C. M., Design and Applications of Bifunctional Small Molecules: Why Two Heads Are Better Than One. *ACS Chem. Biol.* **2008**.
- [201] Fegan, A.; White, B.; Carlson, J. C.; Wagner, C. R., Chemically controlled protein assembly: techniques and applications. *Chem Rev* **2010**, *110* (6), 3315-36.
- [202] Biggar, S. R.; Crabtree, G. R., Cell signaling can direct either binary or graded transcriptional responses. *Embo J* **2001**, *20* (12), 3167-76.
- [203] Biggar, S. R.; Crabtree, G. R., Chemically regulated transcription factors reveal the persistence of repressor-resistant transcription after disrupting activator function. *J Biol Chem* **2000**, *275* (33), 25381-90.
- [204] Rivera, V. M.; Clackson, T.; Natesan, S.; Pollock, R.; Amara, J. F.; Keenan, T.; Magari, S. R.; Phillips, T.; Courage, N. L.; Cerasoli, F., Jr.; Holt, D. A.; Gilman, M., A humanized system for pharmacologic control of gene expression. *Nat Med* **2006**, *2* (9), 1028-32.
- [205] Ye, X.; Rivera, V. M.; Zolnick, P.; Cerasoli, F., Jr.; Schnell, M. A.; Gao, G.; Hughes, J. V.; Gilman, M.; Wilson, J. M., Regulated delivery of therapeutic proteins after *in vivo* somatic cell gene transfer. *Science* **1999**, *283* (5398), 88-91.
- [206] Kohler, J. J.; Bertozzi, C. R., Regulating cell surface glycosylation by small molecule control of enzyme localization. *Chem Biol* **2003**, *10* (12), 1303-11.
- [207] Robinson, M. S.; Sahlender, D. A.; Foster, S. D., Rapid inactivation of proteins by rapamycin-induced rerouting to mitochondria. *Dev Cell* **2010**, *18* (2), 324-31.
- [208] Komatsu, T.; Kukuljansky, I.; McCaffery, J. M.; Ueno, T.; Varela, L. C.; Inoue, T., Organelle-specific, rapid induction of molecular activities and membrane tethering. *Nat Meth* **2010**, *7* (3), 206-208.
- [209] Liberles, S. D.; Diver, S. T.; Austin, D. J.; Schreiber, S. L., Inducible gene expression and protein translocation using nontoxic ligands identified by a mammalian three-hybrid screen. *Proc Natl Acad Sci U S A* **1997**, *94* (15), 7825-30.
- [210] Stankunas, K.; Bayle, J. H.; Gestwicki, J. E.; Lin, Y. M.; Wandless, T. J.; Crabtree, G. R., Conditional protein alleles using knockin mice and a chemical inducer of dimerization. *Mol Cell* **2003**, *12* (6), 1615-24.
- [211] Luengo, J. I.; Yamashita, D. S.; Dunnington, D.; Beck, A. K.; Rozamus, L. W.; Yen, H. K.; Bossard, M. J.; Levy, M. A.; Hand, A.; Newman-Tarr, T.; et al., Structure-activity studies of rapamycin analogs: evidence that the C-7 methoxy group is part of the effector domain and positioned at the FKBP12-FRAP interface. *Chem Biol* **1995**, *2* (7), 471-81.
- [212] Pollock, R.; Giel, M.; Linher, K.; Clackson, T., Regulation of endogenous gene expression with a small-molecule dimerizer. *Nat Biotechnol* **2002**, *20* (7), 729-33.
- [213] Inoue, T.; Heo, W. D.; Grimley, J. S.; Wandless, T. J.; Meyer, T., An inducible translocation strategy to rapidly activate and inhibit small GTPase signaling pathways. *Nat Methods* **2005**, *2* (6), 415-8.
- [214] Chong, H.; Ruchatz, A.; Clackson, T.; Rivera, V. M.; Vile, R. G., A system for small-molecule control of conditionally replication-competent adenoviral vectors. *Mol Ther* **2002**, *5* (2), 195-203.
- [215] Kapova, A. Y.; Tervo, D. G.; Gray, N. W.; Svoboda, K., Rapid and reversible chemical inactivation of synaptic transmission in genetically targeted neurons. *Neuron* **2005**, *48* (5), 727-35.
- [216] Indraccolo, S.; Moserle, L.; Tisato, V.; Gola, E.; Minuzzo, S.; Roni, V.; Persano, L.; Chicco-Bianchi, L.; Amadori, A., Gene therapy of ovarian cancer with IFN-alpha-producing fibroblasts: comparison of constitutive and inducible vectors. *Gene Ther* **2006**, *13* (12), 953-65.
- [217] Vogel, R.; Mammeri, H.; Mallet, J., Lentiviral vectors mediate nonimmunosuppressive rapamycin analog-induced production of secreted therapeutic factors in the brain: regulation at the level of transcription and exocytosis. *Hum Gene Ther* **2008**, *19* (2), 167-78.
- [218] Clemons, P. A.; Gladstone, B. G.; Seth, A.; Chao, E. D.; Foley, M. A.; Schreiber, S. L., Synthesis of Calcineurin-Resistant Derivatives of FK506 and Selection of Compensatory Receptors. *Chemistry & Biology* **2002**, *9* (1), 49-61.
- [219] Spencer, D. M.; Wandless, T. J.; Schreiber, S. L.; Crabtree, G. R., Controlling signal transduction with synthetic ligands. *Science* **1993**, *262* (5136), 1019-24.
- [220] Luo, Z.; Zivion, G.; Belshaw, P. J.; Vavvas, D.; Marshall, M.; Avruhc, J., Oligomerization activates c-Raf-1 through a Ras-dependent mechanism. *Nature* **1996**, *383* (6596), 181-5.
- [221] Belshaw, P. J.; Spencer, D. M.; Crabtree, G. R.; Schreiber, S. L., Controlling programmed cell death with a cyclophilin-cyclosporin-based chemical inducer of dimerization. *Chem Biol* **1996**, *3* (9), 731-8.
- [222] Amara, J. F.; Clackson, T.; Rivera, V. M.; Guo, T.; Keenan, T.; Natesan, S.; Pollock, R.; Yang, W.; Courage, N. L.; Holt, D. A.; Gilman, M., A versatile synthetic dimerizer for the regulation of protein-protein interactions. *Proc Natl Acad Sci U S A* **1997**, *94* (20), 10618-23.
- [223] Keenan, T. Y. D.; Courage, N. L.; Rollins, C. T.; Pavone, M. E.; Rivera, V. M.; Yang, W.; Guo, T.; Amara, J. F.; Clackson, T.; Gilman, M.; Holt, D. A., Synthesis and activity of bivalent FKBP12 ligands for the regulated dimerization of proteins. *Bioorganic & Medicinal Chemistry Letters* **1998**, *6* (8), 1309-1335.
- [224] Clackson, T.; Yang, W.; Rozamus, L. W.; Hatada, M.; Amara, J. F.; Rollins, C. T.; Stevenson, L. F.; Magari, S. R.; Wood, S. A.; Courage, N. L.; Lu, X.; Cerasoli, F., Jr.; Gilman, M.; Holt, D. A., Redesigning an FKBP-ligand interface to generate chemical dimerizers with novel specificity. *Proc Natl Acad Sci U S A* **1998**, *95* (18), 10437-42.
- [225] Nourse, M. B.; Rolle, M. W.; Pabon, L. M.; Murry, C. E., Selective control of endothelial cell proliferation with a synthetic dimerizer of FGF receptor-1. *Lab Invest* **2007**, *87* (8), 828-35.
- [226] Belshaw, P. J.; Schoepfer, J. G.; Liu, K.-Q.; Morrison, K. L.; Schreiber, S. L., Rational Design of Orthogonal Receptor-Ligand Combinations. *Angewandte Chemie International Edition in English* **1995**, *34* (19), 2129-2132.
- [227] Belshaw, P. J.; Schreiber, S. L., Cell-Specific Calcineurin Inhibition by a Modified Cyclosporin. *Journal of the American Chemical Society* **1997**, *119* (7), 1805-1806.
- [228] Yang, X.; Chang, H. Y.; Baltimore, D., Autoproteolytic activation of procaspases by oligomerization. *Mol Cell* **1998**, *1* (2), 319-25.
- [229] Li, Z. Y.; Otto, K.; Richard, R. E.; Ni, S.; Kirillova, I.; Fausto, N.; Blau, C. A.; Lieber, A., Dimerizer-induced proliferation of genetically modified hepatocytes. *Mol Ther* **2002**, *5* (4), 420-6.
- [230] Trujillo, M. E.; Pajvani, U. B.; Scherer, P. E., Apoptosis through targeted activation of caspase 8 ("ATTAC-mice"): novel mouse models of inducible and reversible tissue ablation. *Cell Cycle* **2005**, *4* (9), 1141-5.
- [231] Pajvani, U. B.; Trujillo, M. E.; Combs, T. P.; Iyengar, P.; Jelicks, L.; Roth, K. A.; Kitsis, R. N.; Scherer, P. E., Fat apoptosis through targeted activation of caspase 8: a new mouse model of inducible and reversible lipodystrophy. *Nat Med* **2005**, *11* (7), 797-803.
- [232] Landskroner-Eiger, S.; Park, J.; Israel, D.; Pollard, J. W.; Scherer, P. E., Morphogenesis of the developing mammary gland: Stage-dependent impact of adipocytes. *Developmental Biology* **2011**, *344* (2), 968-978.
- [233] Tsuruma, K.; Nakagawa, T.; Shirakura, H.; Hayashi, N.; Uehara, T.; Nomura, Y., Regulation of procaspase-2 by glucocorticoid modulatory element-binding protein 1 through the interaction with caspase recruitment domain. *Biochem Biophys Res Commun* **2004**, *325* (4), 1246-51.
- [234] Burnett, S. H.; Beus, B. J.; Avdiushko, R.; Qualls, J.; Kaplan, A. M.; Cohen, D. A., Development of peritoneal adhesions in macrophage depleted mice. *J Surg Res* **2006**, *131* (2), 296-301.
- [235] Burnett, S. H.; Kershen, E. J.; Zhang, J.; Zeng, L.; Straley, S. C.; Kaplan, A. M.; Cohen, D. A., Conditional macrophage ablation in transgenic mice expressing a Fas-based suicide gene. *Journal of Leukocyte Biology* **2004**, *75* (4), 612-623.
- [236] Ho, S. N.; Biggar, S. R.; Spencer, D. M.; Schreiber, S. L.; Crabtree, G. R., Dimeric ligands define a role for transcriptional activation domains in reinitiation. *Nature* **1996**, *382* (6594), 822-6.
- [237] Rivera, V. M., Controlling gene expression using synthetic ligands. *Methods* **1998**, *14* (4), 421-9.
- [238] Licitra, E. J.; Liu, J. O., A three-hybrid system for detecting small ligand-protein receptor interactions. *Proc Natl Acad Sci U S A* **1996**, *93* (23), 12817-21.
- [239] Althoff, E. A.; Cornish, V. W., A bacterial small-molecule three-hybrid system. *Angew Chem Int Ed Engl* **2002**, *41* (13), 2327-30.
- [240] Czaplinski, J. L.; Schelle, M. W.; Miller, L. W.; Laughlin, S. T.; Kohler, J. J.; Cornish, V. W.; Bertozzi, C. R., Conditional Glycosylation in Eukaryotic Cells Using a Biocompatible Chemical Inducer of Dimerization. *J. Am. Chem. Soc.* **2008**.
- [241] Jullien, N.; Goddard, I.; Selmi-Ruby, S.; Fina, J. L.; Cremer, H.; Herman, J. P., Conditional transgenesis using Dimerizable Cre (DiCre). *PLoS One* **2007**, *2* (12), e1355.
- [242] Gray, D. C.; Mahrus, S.; Wells, J. A., Activation of Specific Apoptotic Caspases with an Engineered Small-Molecule-Activated Protease. *Cell* **2010**, *142* (4), 637-646.
- [243] Holsinger, L. J.; Spencer, D. M.; Austin, D. J.; Schreiber, S. L.; Crabtree, G. R., Signal transduction in T lymphocytes using a conditional allele of Sos. *Proc Natl Acad Sci U S A* **1995**, *92* (21), 9810-4.
- [244] Graef, I. A.; Holsinger, L. J.; Diver, S.; Schreiber, S. L.; Crabtree, G. R., Proximity and orientation underlie signaling by the non-receptor tyrosine kinase ZAP70. *Embo J* **1997**, *16* (18), 5618-28.
- [245] Ng, Y.; Ramm, G.; Lopez, J. A.; James, D. E., Rapid activation of Akt2 is sufficient to stimulate GLUT4 translocation in 3T3-L1 adipocytes. *Cell Metab* **2008**, *7* (4), 348-56.
- [246] Patury, S.; Geda, P.; Dobry, C. J.; Kumar, A.; Gestwicki, J. E., Conditional nuclear import and export of yeast proteins using a chemical inducer of dimerization. *Cell Biochem Biophys* **2009**, *53* (3), 127-34.
- [247] Xu, T.; Johnson, C. A.; Gestwicki, J. E.; Kumar, A., Conditionally controlling nuclear trafficking in yeast by chemical-induced protein dimerization. *Nat Protoc* **2010**, *5* (11), 1831-43.
- [248] Haruki, H.; Nishikawa, J.; Laemmli, U. K., The anchor-away technique: rapid, conditional establishment of yeast mutant phenotypes. *Mol Cell* **2008**, *31* (6), 925-32.
- [249] Mootz, H. D.; Blum, E. S.; Muir, T. W., Activation of an Autoregulated Protein Kinase by Conditional Protein Splicing. *Angewandte Chemie International Edition* **2004**, *43* (39), 5189-5192.
- [250] Mootz, H. D.; Muir, T. W., Protein Splicing Triggered by a Small Molecule. *Journal of the American Chemical Society* **2002**, *124* (31), 9044-9045.

- [251] Zhu, S.; Zhang, H.; Matunis, M. J., SUMO modification through rapamycin-mediated heterodimerization reveals a dual role for Ubc9 in targeting RanGAP1 to nuclear pore complexes. *Exp Cell Res* **2006**, *312* (7), 1042-9.
- [252] Zinnik, S.; Gaestel, M.; Niedenthal, R., Mutually exclusive STAT1 modifications identified by Ubc9/substrate dimerization-dependent SUMOylation. *Nucleic Acids Res* **2009**, *37* (4), e30.
- [253] Rollins, C. T.; Rivera, V. M.; Woolfson, D. N.; Keenan, T.; Hatada, M.; Adams, S. E.; Andrade, L. J.; Yaeger, D.; van Schravendijk, M. R.; Holt, D. A.; Gilman, M.; Clackson, T., A ligand-reversible dimerization system for controlling protein-protein interactions. *Proc Natl Acad Sci U S A* **2000**, *97* (13), 7096-101.
- [254] Rivera, V. M.; Wang, X.; Wardwell, S.; Courage, N. L.; Volchuk, A.; Keenan, T.; Holt, D. A.; Gilman, M.; Orsi, L.; Cerasoli, F., Jr.; Rothman, J. E.; Clackson, T., Regulation of protein secretion through controlled aggregation in the endoplasmic reticulum. *Science* **2000**, *287* (5454), 826-30.
- [255] Janse, D. M.; Crossas, B.; Finley, D.; Church, G. M., Localization to the proteasome is sufficient for degradation. *J Biol Chem* **2004**, *279* (20), 21415-20.
- [256] Pratt, M. R.; Schwartz, E. C.; Muir, T. W., Small-molecule-mediated rescue of protein function by an inducible proteolytic shunt. *Proc Natl Acad Sci U S A* **2007**, *104* (27), 11209-14.
- [257] Lau, H. D.; Yaegashi, J.; Zaro, B. W.; Pratt, M. R., Precise Control of Protein Concentration in Living Cells. *Angewandte Chemie International Edition* **2010**, *49* (45), 8458-8461.
- [258] Stankunas, K.; Bayle, J. H.; Havranek, J. J.; Wandless, T. J.; Baker, D.; Crabtree, G. R.; Gestwicki, J. E., Rescue of Degradation-Prone Mutants of the FK506-Rapamycin Binding (FRB) Protein with Chemical Ligands. *Chembiochem* **2007**, *8* (10), 1162-9.
- [259] Banaszynski, L. A.; Chen, L.-c.; Maynard-Smith, L. A.; Ooi, A. G. L.; Wandless, T. J., A Rapid, Reversible, and Tunable Method to Regulate Protein Function in Living Cells Using Synthetic Small Molecules. *Cell* **2006**, *126* (5), 995-1004.
- [260] Grimley, J. S.; Chen, D. A.; Banaszynski, L. A.; Wandless, T. J., Synthesis and analysis of stabilizing ligands for FKBP-derived destabilizing domains. *Bioorg Med Chem Lett* **2008**, *18* (2), 759-61.
- [261] Armstrong, C. M.; Goldberg, D. E., An FKBP destabilization domain modulates protein levels in *Plasmodium falciparum*. *Nat Methods* **2007**, *4* (12), 1007-9.
- [262] Herm-Gotz, A.; Agop-Nersesian, C.; Munter, S.; Grimley, J. S.; Wandless, T. J.; Frischknecht, F.; Meissner, M., Rapid control of protein level in the apicomplexan *Toxoplasma gondii*. *Nat Methods* **2007**, *4* (12), 1003-5.
- [263] Chu, B. W.; Banaszynski, L. A.; Chen, L. C.; Wandless, T. J., Recent progress with FKBP-derived destabilizing domains. *Bioorg Med Chem Lett* **2008**, *18* (22), 5941-4.
- [264] Bonger, K. M.; Chen, L. C.; Liu, C. W.; Wandless, T. J., Small-molecule displacement of a cryptic degron causes conditional protein degradation. *Nat Chem Biol* **2011**, *7* (8), 531-7.
- [265] Marks, K. M.; Braun, P. D.; Nolan, G. P., A general approach for chemical labeling and rapid, spatially controlled protein inactivation. *Proc Natl Acad Sci U S A* **2004**, *101* (27), 9982-7.
- [266] Schneckloth, J. S., Jr.; Crews, C. M., Chemical approaches to controlling intracellular protein degradation. *Chembiochem* **2005**, *6* (1), 40-6.
- [267] Sadowski, O.; Jaikaran, A. S.; Samanta, S.; Fabian, M. R.; Dowling, R. J.; Sonenberg, N.; Woolley, G. A., A collection of caged compounds for probing roles of local translation in neurobiology. *Bioorg Med Chem* **2010**, *18* (22), 7746-52.
- [268] Umeda, N.; Ueno, T.; Pohlmeier, C.; Nagano, T.; Inoue, T., A photocleavable rapamycin conjugate for spatiotemporal control of small GTPase activity. *J Am Chem Soc* **2011**, *133* (1), 12-4.
- [269] Karginov, A. V.; Zou, Y.; Shirvanyants, D.; Kota, P.; Dokholyan, N. V.; Young, D. D.; Hahn, K. M.; Deiters, A., Light Regulation of Protein Dimerization and Kinase Activity in Living Cells Using Photocaged Rapamycin and Engineered FKBP. *J Am Chem Soc* **2011**.
- [270] Marinec, P. S.; Chen, L.; Barr, K. J.; Mutz, M. W.; Crabtree, G. R.; Gestwicki, J. E., FK506-binding protein (FKBP) partitions a modified HIV protease inhibitor into blood cells and prolongs its lifetime *in vivo*. *Proceedings of the National Academy of Sciences* **2009**, *106* (5), 1336-1341.
- [271] Braun, P. D.; Barglow, K. T.; Lin, Y. M.; Akompong, T.; Briesewitz, R.; Ray, G. T.; Haldar, K.; Wandless, T. J., A bifunctional molecule that displays context-dependent cellular activity. *J Am Chem Soc* **2003**, *125* (25), 7575-80.
- [272] Sellmyer, M. A.; Stankunas, K.; Briesewitz, R.; Crabtree, G. R.; Wandless, T. J., Engineering small molecule specificity in nearly identical cellular environments. *Bioorg Med Chem Lett* **2007**, *17* (10), 2703-5.
- [273] Robers, M.; Pinson, P.; Leong, L.; Batchelor, R. H.; Gee, K. R.; Machleidt, T., Fluorescent labeling of proteins in living cells using the FKBP12 (F36V) tag. *Cytometry A* **2009**, *75* (3), 207-24.
- [274] Davis, T. L.; Walker, J. R.; Campagna-Slater, V.; Finerty, P. J.; Paramanathan, R.; Bernstein, G.; MacKenzie, F.; Tempel, W.; Ouyang, H.; Lee, W. H.; Eisenmesser, E. Z.; Dhe-Paganon, S., Structural and biochemical characterization of the human cyclophilin family of peptidyl-prolyl isomerases. *PLoS Biol* **2010**, *8* (7), e1000439.
- [275] Blau, C. A.; Peterson, K. R.; Drachman, G.; Spencer, D. M. A proliferation switch for genetically modified cells. *Proceedings of the National Academy of Sciences* **1997**, *94* (7), 3076-3081.
- [276] Nör, J.; Hu, Y.; Song, W.; Spencer, D. M.; Núñez, G., Ablation of microvessels *in vivo* upon dimerization of iCaspase-9. *Gene Therapy* **2002**, *9* (7), 444-451.
- [277] Romano, S.; D'Angelillo, A.; Staibano, S.; Iardi, G.; Romano, M. F. FK506-binding protein 51 is a possible novel tumoral marker. *Cell Death and Disease* **2010**, *1*, e55.
- [278] Hamilton, G.S., Norman, M.H., Wu, Y.-Q., Carboxylic acids and carboxylic acid isomers of N-heterocyclic compounds, *WO0032588*, **2000**.
- [279] Cooper, M. E., Donald, D. K., Hardern, D. N., Macrocyclic compounds, *US5376663*, **1994**.

### 1.2.2 Aim of Manuscripts 2 and 3

X-ray co-crystal structures of FK506 with FKBP51 (305R) and FKBP52 (in preparation) revealed that the pyranose group of FK506 (**1**) is in close proximity and contacts the 80s loop. SAR studies around the pyranose sub-structure have shown that the methyl group at C<sup>11</sup> of FK506 analogs is important while the pyranose ring oxygen is dispensable for binding to FKBP12 (**Table 2**)<sup>50-52</sup>. The above SAR conclusion is consistent with the FK506-FKBP51 and FK506-FKBP52 co-crystal structures where the pyranose oxygen does not seem to be involved as a hydrogen bond acceptor while the C<sup>11</sup>-methyl fills the small hydrophobic cavity<sup>102</sup>. The exocyclic hydroxyl group present in FK506 at C<sup>10</sup> engages in a hydrogen bond with Asp<sup>68</sup> of FKBP51/52 which is absent in the co-crystal structures of the non-immunosuppressive analogs with FKBP51 and FKBP52. The crystal structures further revealed that the pocket outlined by the 80s loop is more open and there could be a potential hydrogen bond interaction partner (S<sup>118</sup>). Taking these as structural starting points we decided to follow two different approaches to target the 80s loop of FKBP51 and FKBP52 to gain affinity and selectivity. The patent applications of the compounds and the treatment for which these compounds can be useful have been filed.

➤ **Pipicolate-diketoamides for treatment of psychiatric disorders.**

**Gopalakrishnan R**, Hausch, F. (Patent No. **EP-11075275.5**)

➤ “Reprinted (adapted) with permission from **Ranganath Gopalakrishnan et al. Evaluation of Synthetic FK506 Analogs as Ligands for the FK506-Binding Proteins 51 and 52**, Journal of Medicinal Chemistry, March 29, 2012, DOI: 10.1021/jm201746x. Copyright (2012) American Chemical Society.”

➤ **Pipicolate-sulfonamides for treatment of psychiatric disorders.** **Gopalakrishnan R**, Hausch, F. (Patent No. **EP-11195970.6**)

➤ “Reprinted (adapted) with permission from **Ranganath Gopalakrishnan et al. Exploration of Pipicolate Sulfonamides as Binders of the FK506-Binding Proteins 51 and 52**, Journal of Medicinal Chemistry, March 29, 2012, DOI: 10.1021/jm201747c. Copyright (2012) American Chemical Society.”

### 1.2.2.1 Evaluation of Synthetic FK506 Analogs as Ligands for FKBP51 and FKBP52 (Manuscript-2)

In this manuscript we report the co-crystal structure of FKBP51 with a simplified  $\alpha$ -ketoamide analog derived from FK506 and the first structure-activity relationship analysis for FKBP51 and FKBP52 based on this compound. Further, the tert-pentyl group of this ligand was systematically replaced by a cyclohexyl ring system which more closely resembles the pyranose ring in the high affinity ligands Rapamycin and FK506. The compounds in this series had various alkyl substituents at the C<sup>11</sup> position. The interaction with FKBP5s was found to be surprisingly tolerant to the stereochemistry of the attached cyclohexyl substituents. The molecular basis for this tolerance was elucidated by X-ray co-crystallography.

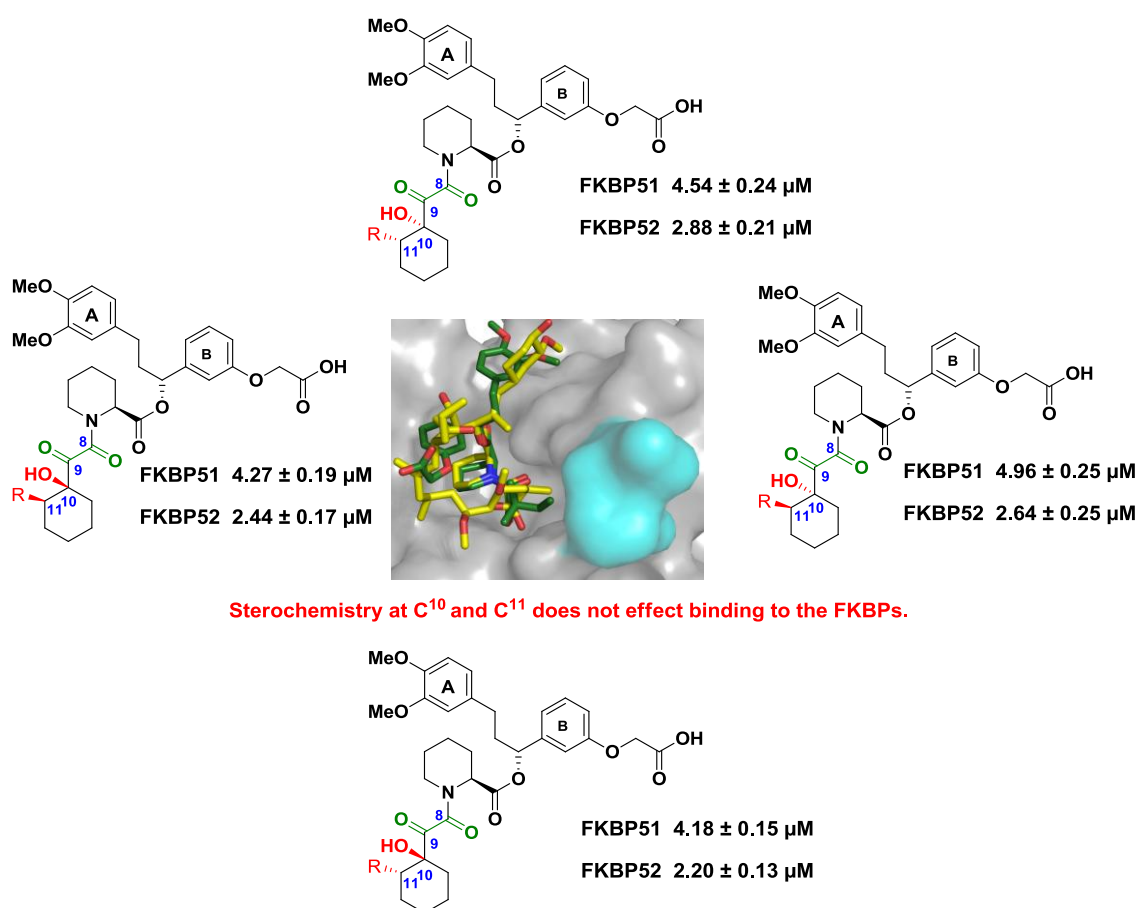


**Figure 13:** Prototypical pyranose containing FK506 analogs

**Own Contributions:**

In the manuscript, my personal contributions have been the following:

1. Partial optimization of synthesis protocol (Scheme-1) and synthesis of analogs 6a, 6b, 6e, 6f in **Table 1** of the manuscript.
2. Establishment of the synthesis protocol (Scheme-2) and optimization of synthesis protocol (Supp. Scheme-S1, S5 and partially S3) for the synthesis of  $\alpha$ -keto acids and further incorporation into the corresponding  $\alpha$ -ketoamides (Scheme-3). Synthesis and purification of all intermediates and compounds (**3a\***- **3j\***) followed by structural characterization of all the compounds in **Table 1 and 2**.
3. Characterization of the final compounds in the fluorescence polarization assay together with B. Hoogeland and C. Kozany. Data analysis of the tested compounds.

**Evaluation of Synthetic FK506 Analogs as Ligands for FKBP51 and FKBP52**

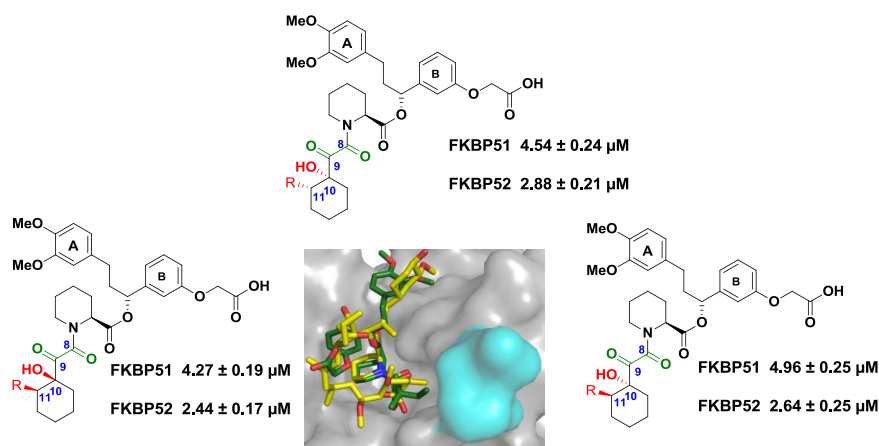
**Ranganath Gopalakrishnan**<sup>1</sup>, Christian Kozany<sup>1</sup>, Steffen Gaali<sup>1</sup>, Christoph Kress<sup>1</sup>, Bastiaan Hoogeland<sup>1</sup>, Andreas Bracher<sup>2</sup>, Felix Hausch<sup>1\*</sup>.

<sup>1</sup>Max Planck Institute of Psychiatry, Kraepelinstr. 2, 80804 Munich, Germany,

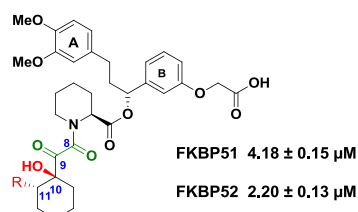
<sup>2</sup>Max Planck Institute of Biochemistry, Am Klopferspitz 18, 82152, Martinsried, Germany

Correspondance: Email: [hausch@mpipsykl.mpg.de](mailto:hausch@mpipsykl.mpg.de), phone: +49(89)30622640, fax: +49(89)30622610

**Abstract:** The FK506-binding proteins (FKBP) 51 and 52 are co-chaperones that modulate the signal transduction of steroid hormone receptors. Both proteins have been implicated in prostate cancer. Furthermore, single nucleotide polymorphisms in the gene encoding FKBP51 have been associated with a variety of psychiatric disorders. Rapamycin and FK506 are two macrocyclic natural products that bind to these proteins indiscriminately, but with nanomolar affinity. We here report the co-crystal structure of FKBP51 with a simplified  $\alpha$ -ketoamide analog derived from FK506 and the first structure-activity relationship analysis for FKBP51 and FKBP52 based on this compound. In particular, the tert-pentyl group of this ligand was systematically replaced by a cyclohexyl ring system which more closely resembles the pyranose ring in the high affinity ligands rapamycin and FK506. The interaction with FKBP51 was found to be surprisingly tolerant to the stereochemistry of the attached cyclohexyl substituents. The molecular basis for this tolerance was elucidated by X-ray co crystallography.



**Stereochemistry at C<sup>10</sup> and C<sup>11</sup> does not effect binding to the FKBP5s.**



## Introduction:

Immunosuppressant natural products like FK506 (Fig. 1a) and rapamycin bind with high affinity to immunophilins of the FKBP (FK506 binding protein) family, which often also possess peptidyl-propyl isomerase (PPIase) activity. The best-characterized member of the FKBP family is FKBP12, a 12kD protein, which consists only of the FK506-binding domain. FKBP12-FK506 and FKBP12-rapamycin complexes create binding surfaces for binding to calcineurin (CaN) and mTOR, respectively<sup>1</sup>. The inhibition of the latter proteins mediates the immunosuppressive action of the two natural products. FKBP12 has also been shown to modulate the ryanodine receptor (RyR) channels and to bind to the transforming growth factor  $\beta$  receptor I. FK506 inhibits these interactions consistent with a shared common binding site<sup>2</sup>.

The higher molecular weight FKBP homologs FKBP51 and FKBP52 act as co-chaperones for the heat shock protein 90 (Hsp90). In the Hsp90 heterocomplex FKBP51 and FKBP52 have been shown to modulate signal transduction by the glucocorticoid receptor in a mutually antagonistic direction<sup>3-5</sup>. FK506 was shown to inhibit the proliferation of prostate cancer cells. This was attributed to blockade of the enhancing effect of FKBP51 on the androgen receptor in these cells<sup>6,7</sup>. Numerous human genetic studies have shown that single nucleotide polymorphisms in the gene encoding FKBP51 are associated with a variety of psychiatric disorders<sup>8</sup>. Very recently, several independent studies using knockdown or knockout mice strongly supported an important role of FKBP51 in stress-coping behaviour<sup>9-12</sup>. These findings have rendered FKBP51 as a novel target for treatment of psychiatric disorders. However, neither FK506 nor rapamycin can be used as a tool to investigate the roles of individual FKBP51 in mammalian system due to strong off-target effects and lack of selectivity. Thus, non-immunosuppressive and selective inhibitors for the large FKBP homologs FKBP51 and FKBP52 are required.

At the end of the last millennium various sub-classes of high affinity FKBP12 ligands were described which were devoid of the immunosuppressive activity present in FK506 and rapamycin<sup>13,14</sup>.  $\alpha$ -Ketoamide derivatives without the effector region were the most widely studied series exemplified by compound 2a<sup>15</sup> (Fig. 1). For FKBP12 the tert-pentyl group in 2a was found to be a good surrogate for the pyranose group in FK506 and rapamycin<sup>16</sup>. While the high affinity of the natural products FK506 and rapamycin were retained for the larger FKBP51 and FKBP52, the binding affinity of 2a for the larger FKBP51 and FKBP52 was substantially weaker<sup>17</sup>. We thus first set out for a basic characterization of the structure-activity relationship of 2a. To analyze the

interactions with the 80s loop in more detail we then substituted the tert-pentyl group in 2a with cyclohexyl analogs which more closely mimic the pyranose group in the high affinity natural product ligands (Fig. 1c).

## Result and Discussion

### Crystal structure of the 2a-FKBP51 complex

As a structural starting point for a rational design the co-crystal structure of 2a, the only synthetic ligand known for FKBP51, was solved in complex with the FK506-binding domain of FKBP51 at 1.5 Å resolution (Fig. 1d and 1e). Upon binding of compound 2a FKBP51 adopts a very similar conformation as found in the FK506 complex<sup>18</sup> (Fig. 1d). Most active site residues are virtually superimposable in the two co-crystal structures. Compared to the FK506 complex (3O5R), Phe<sup>77</sup> moves into the binding pocket, while Asp<sup>68</sup> and the tip of the 80s loop (Leu<sup>119</sup>-Lys<sup>122</sup>) move outward in the FKBP51-2a complex, the latter in part due to crystal contacts with a neighboring FKBP51 molecule.

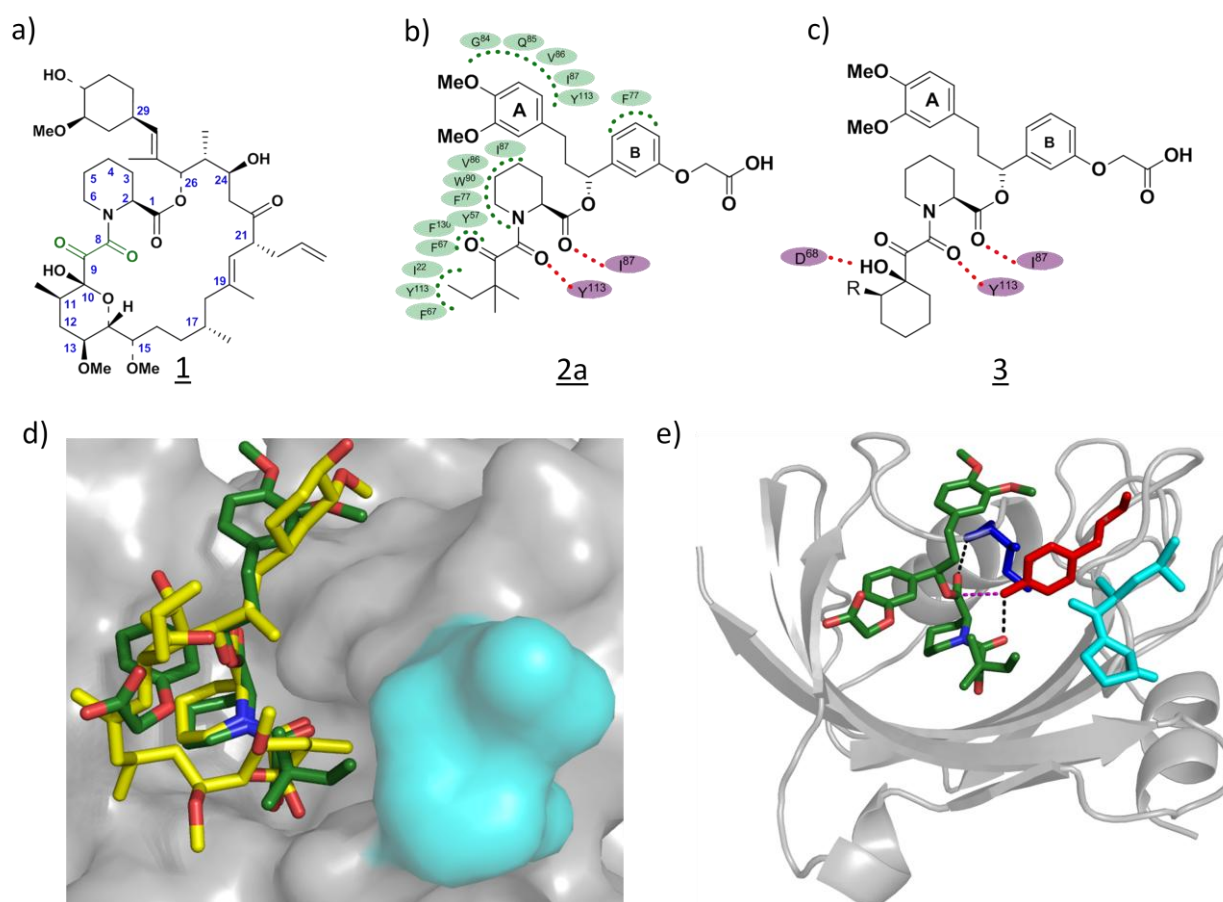


**Fig. 1** Natural and synthetic FKBP ligands: (a) Structure of FK506 (**1**), (b) prototypic synthetic ligand of FKBP51 **2a**, which is devoid of immunosuppressive activity (hydrophobic contacts with FKBP51 are indicated in green, hydrogen bonds are represented as pink dotted lines), (c) prototypic cyclohexyl-substituted ligand **3**, (d, e) binding mode of **2a** with FKBP51, (d) surface representation of FKBP51 in complex with **2a** (green). FK506 bound to FKBP51 (3O5R) is superimposed in yellow. (e) Ribbon representation of FKBP51 showing the conserved H-bonds between O<sup>1</sup>-**2a** and HN-Ile<sup>87</sup> (dark blue) and between O<sup>8</sup>-**2a** and HO-Tyr<sup>113</sup> (red) as black dotted lines. Leu<sup>119</sup> and Pro<sup>120</sup> at the top of the 80s loop are colored in cyan. The dipolar interaction between OH-Tyr<sup>113</sup> and C<sup>1</sup>-carbonyl is shown as a dotted line in magenta.

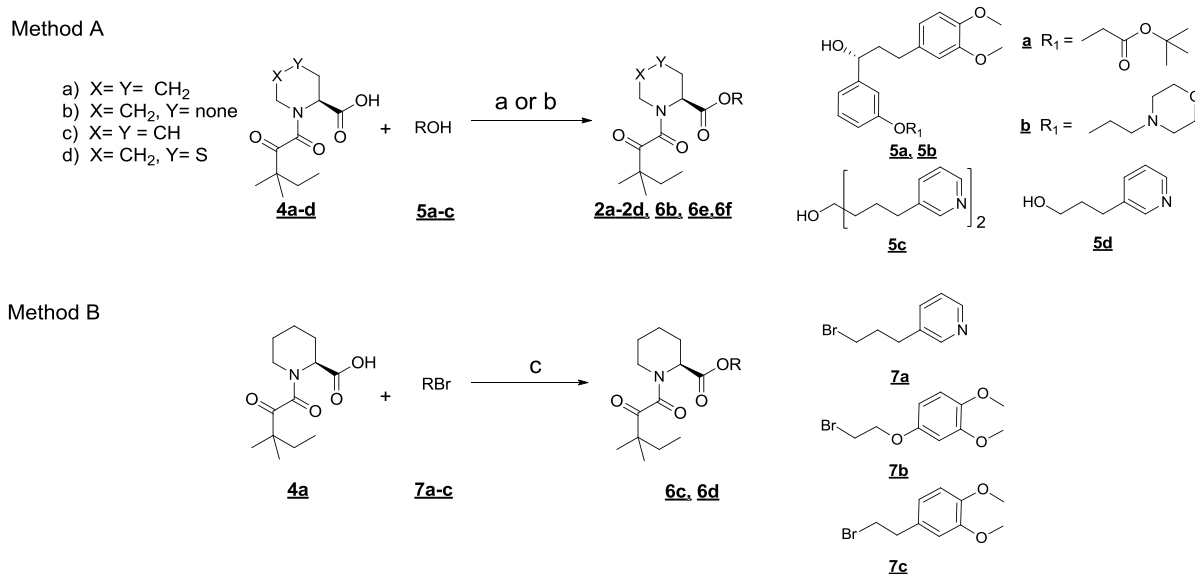
The core interactions of FK506 are conserved for **2a** with the common pipercolate ring sitting atop the indole of Trp<sup>90</sup>, which forms the floor of the FKBP binding pocket. The C<sup>1</sup>-carbonyl of the pipercolate forms a hydrogen bond with the backbone amide of Ile<sup>87</sup> ( $d = 2.92 \text{ \AA}$ ), while the C<sup>8</sup>-carbonyl of the  $\alpha$ -ketoamide engages in a hydrogen bond with the hydroxyl group of Tyr<sup>113</sup> ( $d = 2.65 \text{ \AA}$ ). The latter approaches the C<sup>1</sup>-carbonyl at an angle of  $107^\circ$  and below van-der-Waals distance ( $3.17 \text{ \AA}$ ) consistent with an attractive dipolar interaction<sup>19</sup>. The C<sup>9</sup>-keto oxygen of **2a** occupies a position similar to the keto group of FK506, while the hydrogen bond with Asp<sup>68</sup> seen in 3O5R is no longer conserved owing to the absence of the corresponding hydroxyl group in compound **2a**. The tert-pentyl group of compound **2a** sits in pocket formed by the 80s loop (Ser<sup>118</sup>-Ile<sup>122</sup>) which is occupied by the pyranose group of FK506 in the FK506-FKBP51 complex. Compared to a similar compound (SB3) in a complex with FKBP12 (1FKG<sup>16</sup>) the ethyl of the tert-pentyl group is rotated by  $180^\circ$  and faces the 80s loop. The dimethoxyaryl group (ring A) of **2a** sits in a cradle formed by residues Gly<sup>84</sup>-Ile<sup>87</sup> and Tyr<sup>113</sup> and engages in van-der-Waals contacts with Glu<sup>20</sup> from a neighboring FKBP51 molecule in the crystal. The acetyloxyaryl group (ring B) stacks on top of the edge of Phe<sup>77</sup> and its carboxyl moiety forms electrostatically enhanced hydrogen bonds with Lys<sup>108</sup> and Arg<sup>31</sup> from a neighboring molecule.

### Structure-activity relationship (SAR) of the pipercolate core and ester substituent

So far virtually nothing is known about the interaction of the large FKBP51 and FKBP52 with small molecule ligands. To the best of our knowledge only one and three synthetic ligands have been described for FKBP51 and FKBP52, respectively<sup>17,20,21</sup>.

As a first characterization of the recognition properties of FKBP51 and FKBP52 we engaged on a basic structure-activity relationship analysis of the prototypic ligand **2a**. The analogs of **2a** (Tab. 1) were synthesized by esterification or by alkylation of the C<sup>1</sup> carboxylate of the

building blocks **4a-d** as outlined in Scheme 1 or Scheme S4. The latter were prepared from the corresponding pipercolate analogs by N-oxalylolation, introduction of the tert-pentyl moiety followed by deprotection of the C<sup>1</sup> carboxylate (scheme S3)<sup>16</sup>. The 4,5-dehydropipercolate building block **4c** was synthesized from allyl glycine in four steps (scheme S2 and S3)<sup>22</sup>. Building block **5a** was obtained in 98% enantiomeric excess and 94% yield by a Noyori-catalyzed enantioselective reduction of the known keto precursor **13a** (Scheme S1)<sup>15</sup>. Building blocks **5b** (Scheme S1) and **5c** were synthesized as described<sup>23</sup>.



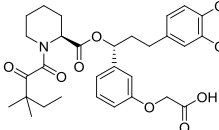
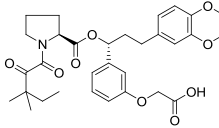
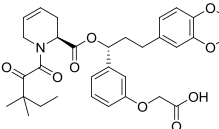
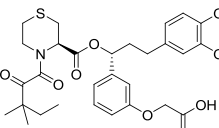
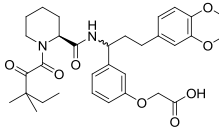
**Scheme 1:** General synthesis protocol of compounds **2a-2d**, **6a-6h**. <sup>a</sup> Reagent and conditions : (a) DCC, DMAP, rt, 12h. (b) (i) DCC, DMAP, rt, 12h. (ii) 20% TFA in DCM, rt, 6h, (c) DIPEA, toluene, reflux, 40h.

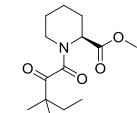
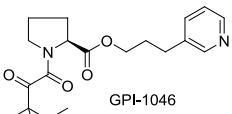
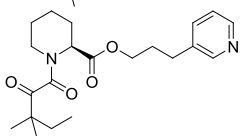
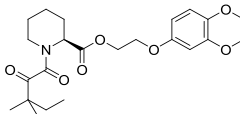
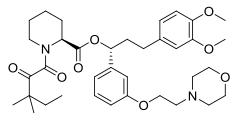
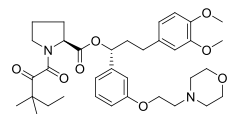
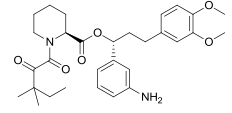
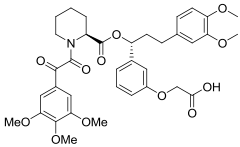
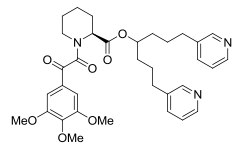
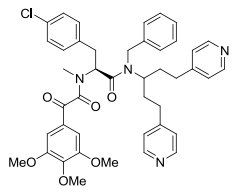
In an initial SAR analysis we explored the contributions of individual substructures in **2a** by first focusing on the pipercolate core. Replacement by a proline (**2b**) or a 4,5-dehydropipercolinic acid (**2c**) decreased the affinity for FKBP5 4-6 fold while thiomorpholine-3-carboxylic acid (**2d**) abrogated detectable binding to the large FKBP5s. Since even small changes at the core diminished affinity we kept the pipercolate core constant in all further derivatives. We then replaced the pipercolate C<sup>1</sup> ester by an amide (**2e**) which completely abolished binding to larger FKBP5s. This was anticipated since the additional hydrogen bond donor would point to the hydrophobic tert-pentyl group of **2e** when bound in a homologous binding mode as **2a**.

We next explored the requirements of the ester “top” group. Smaller substituents like in **6a-6d** resulted in analogs with 7-100 fold lower affinity for FKBP12 and no activity for larger FKBP5s

as compared to **2a**. Compound **6b** (also called GPI-1046<sup>24</sup>) has been reported as one of the most potent and advanced inhibitors for FKBP12. Similar to the corresponding pipercolate analog **6c**, GPI-1046 (**6b**) had no binding to larger FKBP5s and micromolar affinity to FKBP12 in the fluorescence polarization assay which is consistent with the discrepancies previously observed as reviewed by Gaali. et.al for GPI-1046 by others<sup>1</sup>. To eliminate the negative charge in **2a** we exchanged the free acid moiety by a morpholine group (**6e**) which increased affinity 2-4 fold and induced a slight preference for FKBP52 vs. FKBP51. In contrast to the carboxylic acid analog **2b**, the morpholine-containing proline derivative **6f** retained detectable but three-fold reduced binding. Replacement of the oxyacetyl group in **6g** by an amine resulted in compound having similar affinity.

Table-1

Compd. No	Structure	Purity	FKBP12	FKBP51FK1	
				FKBP52FK1	FKBP52FK1
			IC <sub>50</sub> ( $\mu$ M)		
<b>2a</b>		> 99%	0.17 $\pm$ 0.05	8.36 $\pm$ 0.98	10.5 $\pm$ 1.5
<b>2b</b>		> 99%	0.80 $\pm$ 0.05	51.5 $\pm$ 31.9	41.6 $\pm$ 15.8
<b>2c</b>		> 99%	0.55 $\pm$ 0.06	32.73 $\pm$ 12.3	49.2 $\pm$ 24.6
<b>2d</b>		> 98%	1.29 $\pm$ 0.14	>100	>100
<b>2e</b>		> 99%	3.38 $\pm$ 0.54	>100	>100

<b>6a</b>		> 99%	$17.1 \pm 2.7$	>100	>100
<b>6b</b>		> 99%	$1.24 \pm 0.33$	>100	>100
<b>6c</b>		> 99%	$2.11 \pm 0.20$	>150	>150
<b>6d</b>		> 99%	$2.45 \pm 0.44$	>100	>100
<b>6e</b>		> 99%	$0.10 \pm 0.02$	$4.15 \pm 1.45$	$2.8 \pm 1.10$
<b>6f</b>		> 99%	$1.05 \pm 0.09$	$15.34 \pm 1.94$	$5.55 \pm 1.16$
<b>6g</b>		$\geq 98\%$	$0.10 \pm 0.05$	$3.8 \pm 1.05$	$1.07 \pm 0.84$
<b>6h</b>		> 99%	$0.15 \pm 0.02$	$19.3 \pm 6.6$	$11.6 \pm 1.6$
<b>6i</b>		>98%	$0.017 \pm 0.020$	$8.52 \pm 2.81$	$7.37 \pm 3.28$
<b>6j</b>		> 99%	>100	>100	>100

---

Table-1 Purity of the compounds was confirmed by using HPLC. Binding affinities to FKBP12, FKBP51 (FK1 domain) and FKBP52 (FK1 domain) were determined by a fluorescence polarization assay<sup>17</sup>.

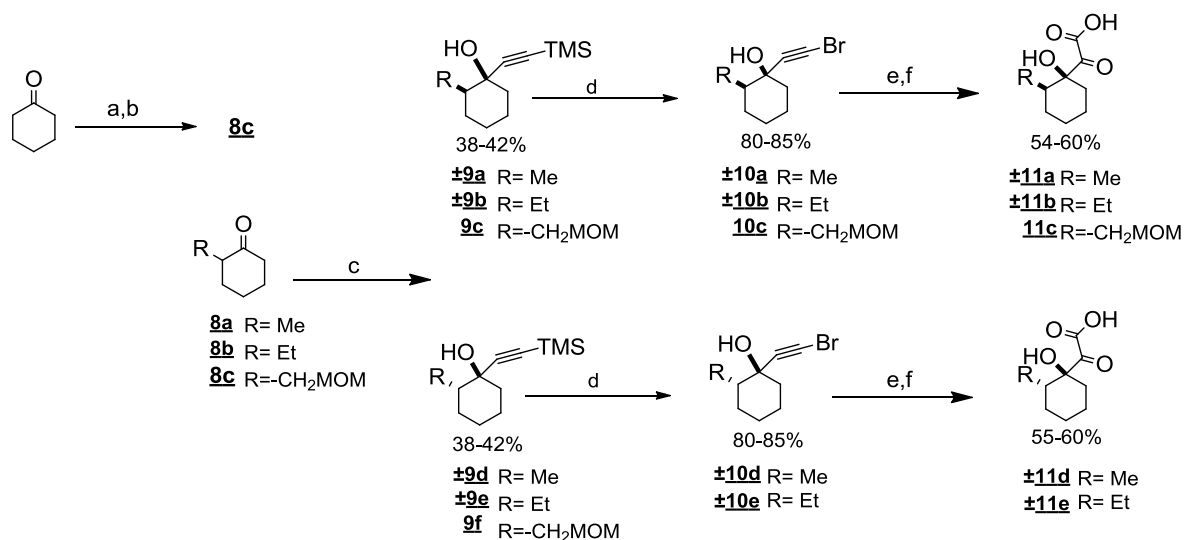
Finally, we replaced the tert-pentyl group with 3,4,5-trimethoxyphenyl in **6h** (scheme S6) which led to a two-fold decrease in affinity for FKBP51 while having equivalent binding for FKBP12 and FKBP52. Additionally, two FK506 analogs that had been evaluated in the clinic were tested for their binding to the larger FKBP<sup>1</sup>. Biricodar (VX-710, **6i**) potently bound to FKBP12 while displaying moderate affinity for the larger FKBP<sup>1</sup>s. In contrast, the related Timcodar (VX-853, **6j**) which lacks the pipicolate core had no binding affinity for any FKBP<sup>1</sup>s, consistent with the SAR data observed above.

### Exploration of pyranose/tert-pentyl analogs

A three-dimensional alignment of FKBP12 and the FK506-binding domains of FKBP51 and FKBP52 revealed that the core residues of the binding pockets are highly conserved. The largest differences were found in the adjacent 40s and 80s loops (residues 71-76 and 118-122 for FKBP51, respectively). The 80s loop of FKBP51 further contains Leu<sup>119</sup> which is replaced by Pro<sup>119</sup> in FKBP52. Cellular studies have shown the residue at position 119 to be a major functional determinant for the effect on steroid hormone receptors<sup>25</sup>. Optimization of interactions with this part of the protein thus could impart selectivity and functional efficacy towards steroid hormone receptor for the large FKBP<sup>1</sup>s. We therefore decided to investigate the interaction with this part of the protein in more detail.

The X-ray structure of FK506 with FKBP12(1FKJ)<sup>26</sup>, with the FK1 domains of FKBP51(PDB code 3O5R)<sup>18</sup> and FKBP52 (manuscript in preparation) revealed that the pyranose group in FK506 (**1**) contacts the 80s loop. SAR studies around the pyranose group have shown that the methyl group at C<sup>11</sup> of FK506 analogs is important while the pyranose ring oxygen is dispensable for binding to FKBP12<sup>27-29</sup>. This is consistent with the FK506-FKBP51 co-crystal structure where the C<sup>11</sup>-methyl fills a small hydrophobic cavity, while the pyranose ring oxygen of FK506 does not seem to act as a hydrogen bond acceptor<sup>18</sup>. The pyranose of FK506 further contains an exocyclic hydroxyl group at C<sup>10</sup> that engages in a hydrogen bond with Asp<sup>68</sup> of FKBP51. This could contribute to the higher affinity observed for the natural product. The **2a**-FKBP51 co-crystal structure shows that the tert-pentyl group in **2a** occupies the same subpocket below the 80s loop as the pyranose ring in FK506. We therefore decided to replace

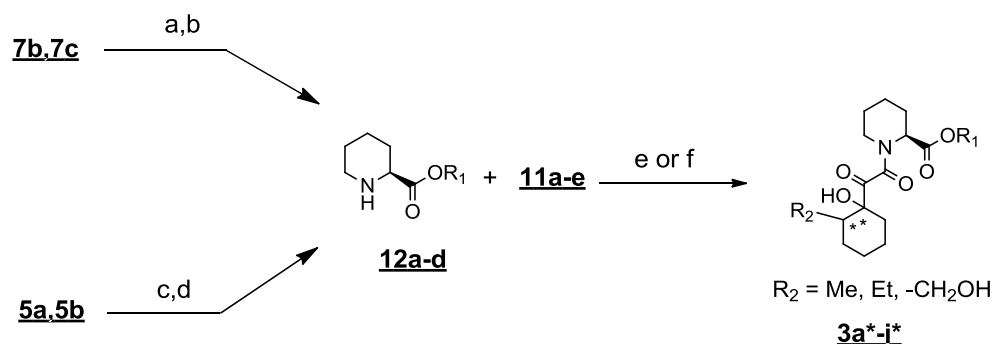
the tert-pentyl group in **2a** with cyclohexyl derivatives that more closely resembled the pyranose in the high-affinity ligand FK506 (**1**). The first series of compounds investigated had a methyl substituent (**3a**) at C<sup>11</sup> as in FK506. The FK506-FKBP51 crystal structure (305R) further revealed that the 80s subpocket in the large FKBP is more open and has a potential hydrogen bond interaction partner (S<sup>118</sup>) in its vicinity. We therefore also prepared cyclohexyl analogs with larger or hydrophilic C<sup>11</sup> substituents.



**Scheme 2:** General synthesis protocol of diketo acids **11a-e**.<sup>a</sup> Reagent and conditions : (a) L-threonine, MgSO<sub>4</sub>, HCHO, THF, 5 days. (b) MOMCl, DIPEA, DCM 12h. (c) TMS acetylene, n-BuLi, -78°C, 2h. (d) N-bromosuccinimide, AgNO<sub>3</sub>, acetone, 2h. (e) KMnO<sub>4</sub>, pH 7 (MgSO<sub>4</sub>, NaHCO<sub>3</sub>), MeOH: H<sub>2</sub>O: 1:1, 0°C to room temperature, 1h. (f) 1M LiOH, MeOH, 6h.

A four step synthesis scheme for the  $\alpha$ -keto acids **11a-b** and **11d-e** was set up starting from the corresponding racemic cyclohexanones **8a** or **8b** (Scheme 2). Alternatively, for **11c** the enantiopure MOM-protected 2-hydroxymethyl cyclohexanone **8c** was used. The latter was obtained in two steps from cyclohexanone by an organocatalyzed formylation<sup>30,31</sup>. TMS acetylene was reacted with **8a-c** to obtain the cis and trans diastereomers **9a- 9f**<sup>32</sup> (stereochemistry assigned by NMR<sup>33</sup>) in nearly equal amounts which could be separated using column chromatography. N-bromosuccinimide was used to cleave the TMS group and introduce the bromide at the terminal alkynes (**10a-e**)<sup>34</sup> followed by oxidation of the activated alkynes by KMnO<sub>4</sub> to yield the corresponding  $\alpha$ -keto esters<sup>35-38</sup>. These were further hydrolysed to give the  $\alpha$ -keto acids **11a-b** and **11d-e**, as racemic mixtures, and enantiopure **11c**.

The  $\alpha$ -keto acids (**11a-e**) were coupled with the piperocolic acid building blocks **12a-d** as outlined in Scheme 3 to give compounds **3a-3g** and **3i-3j** as mixture of diastereomers and **3h** as a single pure diastereomers. The affinities for FKBP5s were either tested as mixture of diastereomers (**3a-3g**, **3i-3j**) or after diastereomeric separation using preparative HPLC (Table-2).



**Scheme 3:** General synthesis protocol of compounds **3a-3j**. <sup>a</sup> Reagent and conditions : (a) (S)-1-Boc-piperidine-2-carboxylic acid,  $K_2CO_3$ , KI, 60°C, 12h. (b) 20% TFA in DCM, rt, 2h. (c) (S)-1-Fmoc-piperidine-2-carboxylic acid, DCC, DMAP, rt, 12h. (d) 20% 4-methylpiperidine in DCM, rt, 4h. (e) **11a-e**, HATU, DIPEA, rt, 16h. (f) (i) **11a-e**, HATU, DIPEA, rt, 16h. (ii) 20% TFA in DCM, rt, 6h.

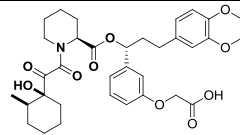
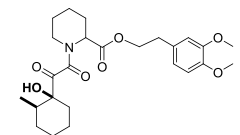
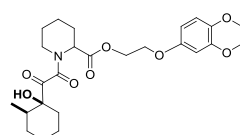
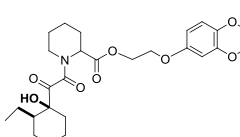
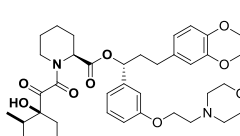
Introduction of the FK506-like cyclohexyl moiety in **3a** increased affinity for FKBP5s two-fold compared to **2a** indicating that the cyclohexyl moiety might indeed better interact with the 80s loop than the tert-pentyl group. We next explored the influence of the ester “top” group in the context of the cyclohexyl substituent. Removing the acetyloxyaryl ring (ring B) as in **3c** reduced the affinity for FKBP5s by 6 fold. This is in contrast to the results observed for the C<sup>11</sup>-ethyl analog **3d** and the corresponding tert-pentyl containing substance **6d**. Further shortening of the linker connecting the dimethoxyaryl moiety (ring A) as in **3b** substantially decreased affinity for all FKBP5s. This indicates that the linker length is critical for optimal positioning of the dimethoxyaryl moiety, at least in the cyclohexyl series. Similar to the tert-pentyl series, replacement of the carboxylate by a morpholine in compounds **3e** and **3g** increased affinity for FKBP5s and induced a slight preference for FKBP52 compared to FKBP51.

We next investigated the role of the C<sup>11</sup> substituent on the cyclohexyl moiety. The C<sup>11</sup>-methyl (**3a\***), C<sup>11</sup>-ethyl (**3f\***) and C<sup>11</sup>-hydroxymethyl derivative (**3h**) had similar binding for the larger FKBP5s while the affinity for FKBP12 was reduced. Importantly, however, we also found that the diastereomeric mixtures **3i\*** and **3j\*** had almost equivalent binding to FKBP5s as their FK506-like counterparts **3a\*** and **3f\***. This was somewhat surprising since in the “unnatural”

diastereomers **3i\*** and **3j\*** the Asp<sup>68</sup>-HO<sup>10</sup> hydrogen bond and hydrophobic 80s loop contacts of the C<sup>11</sup>-substituent are not possible at the same time. To further investigate the influence of stereochemistry and the substitution pattern at the cyclohexyl ring in more detail we separated the individual diastereomers **3a-1**, **3a-2**, **3i-1**, **3i-2**, **3f-1** and **3f-2**.

Again, these diastereomers had almost equivalent binding to the proteins. These observation led us to conclude that the stereochemistry around the pyranose group in FK506/rapamycin like ligands is not as important for activity as previously thought and that the 80s loop is flexible enough to accommodate the small stereo chemical changes in the active site.

**Table-2**

Compd. No.	R1	FKBP12	FKBP51FK1	FKBP52FK1
		IC <sub>50</sub> (μM)		
<b>3a*</b>		0.055 ± 0.004	4.20 ± 0.11	2.13 ± 0.21
<b>3b*</b>		2.2 ± 0.5	>100	>100
<b>3c*</b>		0.31 ± 0.04	29.39 ± 8.5	11.7 ± 6.4
<b>3d*</b>		2.78 ± 0.02	>100	>100
<b>3e*</b>		0.057 ± 0.004	2.02 ± 0.14	0.89 ± 0.06

<b>3f*</b>	The structure of 3f* features a piperidine ring connected via a carbonyl group to a chiral center. This chiral center is also bonded to a cyclohexane ring with a hydroxyl group and a 4-(3,4,5-trimethoxyphenyl)oxyacetate group.	$0.32 \pm 0.025$	$3.9 \pm 1.2$	$9.5 \pm 1.3$
<b>3f-1</b>	The structure of 3f-1 is identical to 3f* but with a different stereochemistry at the chiral center.	$0.128 \pm 0.03$	$5.8 \pm 0.6$	$4.2 \pm 0.3$
<b>3f-2</b>	The structure of 3f-2 is identical to 3f* but with a different stereochemistry at the chiral center.	$0.343 \pm 0.09$	$3.9 \pm 0.6$	$3.5 \pm 0.6$
<b>3g*</b>	The structure of 3g* is similar to 3f* but includes a morpholine ring connected to the chiral center via an ether linkage.	$0.47 \pm 0.06$	$9.66 \pm 0.83$	$3.72 \pm 1.02$
<b>3h</b>	The structure of 3h is similar to 3f* but has a different stereochemistry at the chiral center.	$0.507 \pm 0.08$	$8.5 \pm 0.6$	$6.2 \pm 0.5$
<b>3i*</b>	The structure of 3i* is similar to 3f* but has a different stereochemistry at the chiral center.	$0.055 \pm 0.004$	$4.13 \pm 0.20$	$2.64 \pm 0.19$
<b>3a-1</b>	The structure of 3a-1 is similar to 3f* but has a different stereochemistry at the chiral center.	$0.056 \pm 0.004$	$4.27 \pm 0.19$	$2.44 \pm 0.17$
<b>3a-2</b>	The structure of 3a-2 is similar to 3f* but has a different stereochemistry at the chiral center.	$0.048 \pm 0.006$	$4.54 \pm 0.24$	$2.88 \pm 0.21$
<b>3i-1</b>	The structure of 3i-1 is similar to 3f* but has a different stereochemistry at the chiral center.	$0.049 \pm 0.005$	$4.18 \pm 0.15$	$2.20 \pm 0.13$
<b>3i-2</b>	The structure of 3i-2 is similar to 3f* but has a different stereochemistry at the chiral center.	$0.063 \pm 0.003$	$4.96 \pm 0.25$	$2.64 \pm 0.25$

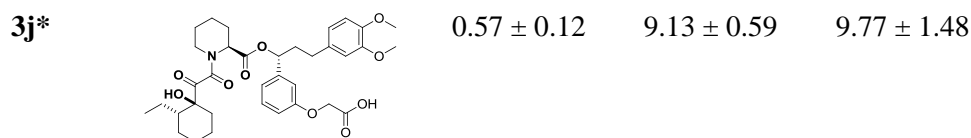
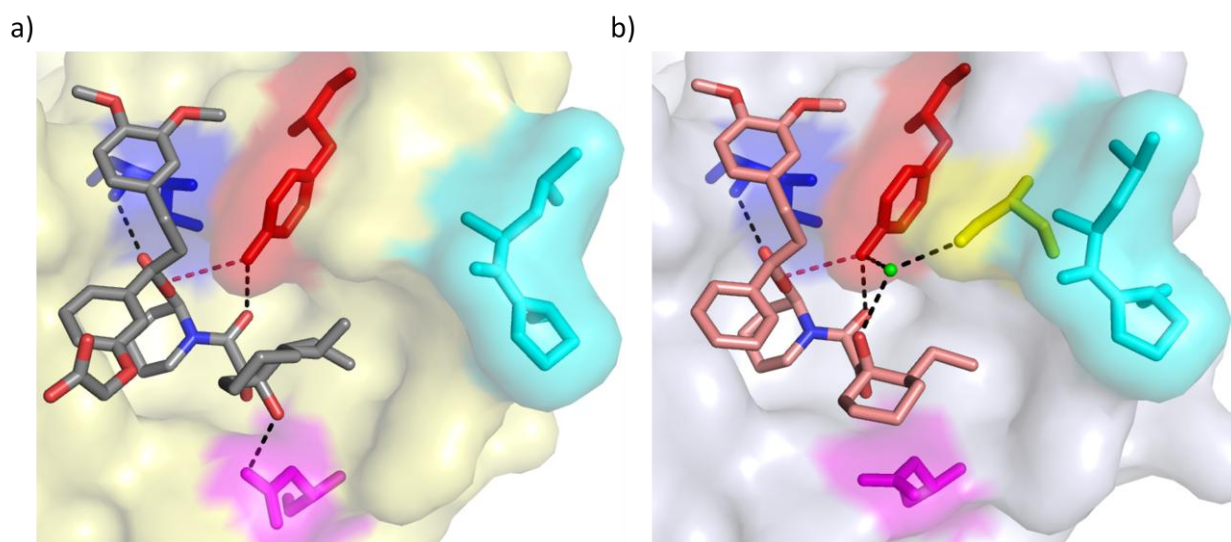


Table-2: \*Mixture of diastereomers. Binding affinity to FKBP12, FKBP51 (FK1 domain) and FKBP52 (FK1 domain) determined by fluorescence polarization assay<sup>17</sup>.

### Crystal structures of **3f-1** and **3f-2**

To understand the unexpected binding of the non-canonical diastereomers we solved the co-crystal structure of both **3f-1** and **3f-2** with the FK506-binding domain of FKBP51 (Fig. 2). Depending on whether the complexes were crystallized or the compounds were added to pre-formed crystals, different crystal forms were obtained. In both co-crystal lattices the ligands engaged Glu<sup>20</sup>, Arg<sup>31</sup> and Lys<sup>108</sup> of a neighboring FKBP51 molecule, similar to the crystal contacts observed for **2a** (see above).

Upon binding of compound **3f-1** or **3f-2** FKBP51 adopts the same structure as found in FKBP51 complexed with **1** and **2a**. Likewise, the binding modes for the pipecolate, the ester “top” group and the  $\alpha$ -keto amide of **3f-1** or **3f-2** were almost perfectly superimposable to those found for **2a** in complex with FKBP51. In particular the hydrogen bond network and the dipolar interaction comprising Ile<sup>87</sup>-NH, C<sup>1</sup>=O, Tyr<sup>113</sup>-OH and C<sup>8</sup>=O is conserved. In **3f-1** a hydrogen bond of C<sup>10</sup>-OH with Asp<sup>68</sup> ( $d = 2.75 \text{ \AA}$ ) is formed similar to the one observed for the pyranose group of FK506 (PDB code 3O5R). However, the cyclohexyl group in **3f-1** is slightly lifted out of the binding pocket and slightly rotated likely to relieve a steric clash of the larger C<sup>11</sup> substituent. For the C<sup>11</sup> substituent two orientations seem to be possible which occupy similar positions like the ethyl group of the tert-pentyl moiety in **2a** (Fig. 2a). In the case of **3f-2** the cyclohexyl moiety is rotated by 180° which allows the C<sup>11</sup> ethyl substituent to occupy almost an identical position as for **3f-1** indicating that this hydrophobic interaction might be rather important (Fig. 2b). In this conformation the hydrogen bond with Asp<sup>68</sup> is no longer possible but the C<sup>10</sup>-OH now forms water-mediated hydrogen bonds to Tyr<sup>113</sup> and Ser<sup>118</sup>. This water network might provide the binding energy to compensate for the loss of the C<sup>10</sup>-OH...Asp<sup>68</sup> H-bond.



**Fig. 2** X-ray crystal structure of **3f-1** and **3f-2** in the FK506-binding domain of FKBP51. The hydrogen bonds between O<sup>1</sup> and HN-Ile<sup>87</sup> (shadowed blue) and between O<sup>8</sup> and HO-Tyr<sup>113</sup> (shadowed red) are represented as dotted black lines. The dipolar interaction between OH-Tyr<sup>113</sup> and C<sup>1</sup> carbonyl is indicated by a dotted pink line. Leu<sup>119</sup> and Pro<sup>120</sup> of the 80s-loop are indicated in cyan. (a) Binding mode of **3f-1** in the active site of FKBP51. The additional hydrogen bond between HO<sup>10</sup>-**3f-1** and O-Asp<sup>68</sup> (shadowed magenta) is shown as dotted black line. (b) Binding mode of **3f-2** in the active site of FKBP51. The hydrogen bond network formed by a water molecule (green) with Tyr<sup>113</sup> and Ser<sup>118</sup> (yellow) of FKBP51 and with C<sup>10</sup>-OH of **3f-2** complex is indicated by a dotted black line.

## Conclusion:

This study for the first time describes a detailed structure-activity relationship of ligands for the larger FKBP51 and FKBP52. Though SAR of  $\alpha$ -ketoamides for FKBP12 has been extensively documented this is the first instance where a direct comparison of binding trends between FKBP12 and larger FKBP51 and FKBP52 have been studied. X-ray co-crystal structure of **2a** was obtained as the starting point, followed by a systematic exploration of the contributions of each substituent on affinity to FKBP51 or FKBP52. Larger top groups as in **2a** and **6e** were found to have better binding affinity, while the pipercolic core (**2a**) was found to be essential. The tert-pentyl group in **2a** was further substituted by a cyclohexyl group which mimicked the pyranose in FK506 and rapamycin. From the binding studies and X-ray co-crystal structure of the diastereomers (**3f-1** and **3f-2**) we can conclude that the FKBP51 and FKBP52 are tolerant towards change of the stereochemistry around the cyclohexyl (pyranose) substituents. These co-crystal structures also suggest that multiple molecular binding modes are possible for the 80s loop interaction which is in line with the high flexibility of this region.

**Experimental section:**

**Chemistry:** Chromatographic separations were performed either by manual flash chromatography or by automated flash chromatography using an Interchim Puriflash 430 with an UV detector. Organic phases were dried over MgSO<sub>4</sub>, and the solvents were removed under reduced pressure. Merck F-254 (thickness 0.25mm) commercial plates were used for analytical TLC to follow the progress of reactions. Silica gel 60 (Merck 70-230 mesh) was used for manual column chromatography. Unless otherwise specified, <sup>1</sup>H NMR spectra, <sup>13</sup>C NMR spectra, 2D HSQC, HMBC and COSY of all intermediates were obtained from the Department of Chemistry and Pharmacy, LMU, on a Bruker AC 300, a Bruker XL 400, or a Bruker AMX 600 at room temperature. Chemical shifts for <sup>1</sup>H or <sup>13</sup>C are given in ppm (δ) relative to tetramethylsilane (TMS) as internal standard. Mass spectra (m/z) were recorded on a Thermo Finnigan LCQ DECA XP Plus mass spectrometer at the Max Planck Institute of Psychiatry, while the high resolution mass spectrometry was carried out at MPI for Biochemistry (Microchemistry Core facility) on Varian Mat711 mass spectrometer. The purity of the compounds was verified by reversed phase HPLC.

**HPLC conditions for product analysis: Column:** Jupiter 4 μm Proteo 90 A, 250 x 4.6 mm, Phenomenex, Torrance, USA, **Wavelength:** 224nm, 280nm **Flow rate:** 1ml/min, **Buffer A:** 0.1% TFA in 5% MeCN/Water, **Buffer B:** 0.1% TFA in 95% MeCN/water. **Gradient A** After 1 min elution with 100% buffer A, linear gradient of 0-100% buffer B for 30 min.

**LCMS conditions for product analysis: Column:** YMC Pack Pro C8, 100 x 4.6 mm, 3μm **Wavelength:** 224nm, 280nm **Flow rate:** 1ml/min, **Buffer A:** 0.1% HCOOH in 5% MeCN/water, **Buffer B:** 0.1% HCOOH in 95% MeCN/water. **Gradient A:** 1min 100% buffer A, then linear gradient of 0-100% buffer B for 11 min.

**Preparative HPLC for diastereomer separation:** Compound was dissolved in 40% buffer B and the purification was carried out with a injection loop volume of 2ml, **Column:** Jupiter 10μm Proteo 90 A, 250 x 21.7 mm, 10micron Phenomenex, Torrance, USA, **Wavelength:** 224nm, **Flow rate:** 25ml/min, **Buffer A:** 0.1% TFA in 5% MeOH/Water, **Buffer B:** 0.1% TFA in 95% MeOH/water..

***Synthesis of (S)-methyl 1-(3,3-dimethyl-2-oxopentanoyl)piperidine-2-carboxylate (4a)***

The compound was prepared as described previously<sup>16</sup>.

**Synthesis of (S)-methyl 1-(3,3-dimethyl-2-oxopentanoyl)pyrrolidine-2-carboxylate (4b)**

Prepared from the methyl ester of L-Proline in an analogous manner to **4a**.

**General Method A.**

A solution of alcohol **5a-c**, carboxylic acid **4a-d** and DMAP in DCM at room temperature was treated with DCC. After stirring for 12 h the mixture was diluted with EtOAc and filtered through a plug of celite. The filtrate was concentrated and the crude material flash chromatographed to afford the product.

**General Method B.**

A solution of bromide **7a-c** and carboxylic acid **4a** or **4b** was treated with DIPEA in toluene at reflux for 40 h. Afterwards, the mixture was diluted with EtOAc (30ml) and filtered through a plug of celite. The filtrate was concentrated and the crude material flash chromatographed to afford the product.

**Synthesis of 2-(3-((R)-3-(3,4-dimethoxyphenyl)-1-((S)-1-(3,3-dimethyl-2-oxopentanoyl)piperidine-2-carboxyloxy)propyl)phenoxy)acetic acid 2a**

The compound was prepared as described previously<sup>17</sup>

**Synthesis of 2-(3-((R)-3-(3,4-dimethoxyphenyl)-1-((S)-1-(3,3-dimethyl-2-oxopentanoyl)pyrrolidine-2-carboxyloxy)propyl)phenoxy)acetic acid 2b**

General method A was used for coupling of alcohol **5a** (75.9mg, 0.188 mmol) and acid **4b** (50 mg, 0.207 mmol) using DMAP (2.5 mg, 0.0207 mmol) and DCC (43mg, 0.207 mmol). The crude product was chromatographed using Hexane: EtOAc 3: 1 to afford **ester 2**.

TLC (Hexane: EtOAc 3:1): R<sub>f</sub> = 0.19.

HPLC (Gradient A) retention time= 30.1-30.4min

HRMS 626.3229 [M + H]<sup>+</sup>, calculated 626.3250 [M + H]<sup>+</sup>.

**Ester 2** was treated with 20% TFA in DCM at room temperature. The mixture was stirred for 6h. TFA and DCM were evaporated under reduced pressure to yield the free acid **2b** (22.6mg, 0.039mmol, 21%) over two steps.

TLC (Hexane: EtOAc: MeOH: AcOH: 6:3: 0.5: 0.5): R<sub>f</sub> = 0.25.

HPLC (Gradient A) retention time= 24.8-25.2min

<sup>1</sup>H NMR (600 MHz, CDCl<sub>3</sub>) δ= 0.79 (t, 3H, J= 7.2Hz), 1.14 (s, 3H), 1.16 (s, 3H), 1.59-1.70 (s, 2H), 1.89-2.05 (m, 4H), 2.15-2.24 (m, 2H), 2.48-2.60 (m, 2H), 3.44-3.70 (m, 2H), 3.80 (s, 3H),

3.82 (s, 3H), 4.55 (s, 2H), 4.58-4.61(m, 1H), 5.66-5.72 (m, 1H), 6.62-6.66 (m, 2H), 6.74 (d, 1H, J= 8.4Hz), 6.78-6.81 (m, 1H), 6.85- 6.89 (m, 2H), 7.18-7.21 (m, 1H).

$^{13}\text{C}$  NMR (150 MHz,  $\text{CDCl}_3$ )  $\delta$ = 9.05, 23.20, 23.76, 24.99, 29.89, 31.36, 32.33, 38.26, 47.05, 47.46, 56.04, 58.78, 65.74, 76.39, 111.52, 112.03, 112.56, 114.58, 119.63, 120.39, 129.86, 133.76, 141.91, 147.48, 149.02, 158.05, 163.74, 165.53, 170.83, 207.13.

MS (ESI) m/z: found Rt 11.52 min. (Method LCMS), 592.32  $[\text{M} + \text{Na}]^+$ .

HRMS 570.3268 $[\text{M} + \text{H}]^+$ , calculated 570.3225  $[\text{M} + \text{H}]^+$ .

**Synthesis of 2-(3-((R)-3-(3,4-dimethoxyphenyl)-1-((S)-1-(3,3-dimethyl-2-oxopentanoyl)-1,2,3,6-tetrahydropyridine-2-carbonyloxy)propyl)phenoxy)acetic acid 2c**

General method A was used for coupling of alcohol **5a** (71.7mg, 0.178 mmol) and acid **4c** (50 mg, 0.19 mmol) using DMAP (2.4 mg, 0.0196 mmol) and DCC (39.2 mg, 0.19 mmol). The crude product was chromatographed using Hexane: EtOAc 3: 1 to afford ester **3** (115mg, 0.180 mmol, 91%)

TLC (Hexane: EtOAc 1: 1): Rf = 0.8.

HPLC (Gradient A) retention time= 30.2-30.6min

$^1\text{H}$  NMR (300 MHz,  $\text{CDCl}_3$ )  $\delta$ = 0.77-0.91 (m, 3H), 1.12 (d, 2H, J= 4.2Hz), 1.21 (s, 3H), 1.22 (s, 3H), 1.47 (s, 9H), 1.96-2.08 (m, 1H), 2.15-2.28 (m, 1H), 2.44-2.62 (m, 3H), 2.66-2.83 (m, 1H), 3.72-4.00 (m, 8H), 4.34-4.47 (m, 1H), 4.52 (s, 2H), 5.48-5.59 (m, 1H), 5.69-5.86 (m, 2H), 6.64-6.67 (m, 2H), 6.75-6.87 (m, 3H), 6.92 (d, 1H, J= 7.8Hz), 7.21-7.27 (m, 1H).

$^{13}\text{C}$  NMR (75 MHz,  $\text{CDCl}_3$ )  $\delta$ = 9.00, 23.54, 23.69, 26.21, 28.24, 31.36, 32.71, 38.21, 43.15, 46.9, 54.6, 56.03, 56.14, 65.95, 76.87, 82.52, 111.57, 111.99, 113.24, 114.50, 119.94, 120.40, 122.61, 124.07, 129.90, 133.65, 141.50, 147.56, 149.11, 158.32, 167.42, 168.07, 169.61, 207.48.

HRMS 582.2601 $[\text{M} - \text{tBu} + \text{H}]^+$ , 660.3110  $[\text{M} + \text{Na}]^+$ , calculated 582.2625  $[\text{M} - \text{tBu} + \text{H}]^+$ , 660.3143 $[\text{M} + \text{Na}]^+$ .

**Ester 3** (100 mg, 0.157 mmol) was treated with 20% TFA in DCM at room temperature. The mixture was stirred for 6h. TFA and DCM were evaporated under reduced pressure to yield the free acid **2c** (61mg, 0.104mmol, 67%).

TLC (Hexane: EtOAc: AcOH: 5:5: 0.5): Rf = 0.35.

HPLC (Gradient A) retention time= 25.4-25.9min

$^1\text{H}$  NMR (300 MHz,  $\text{CDCl}_3$ )  $\delta$ = 0.89 (t, 3H, J= 7.5 Hz), 1.22 (s, 3H), 1.23 (s, 3H), 1.67-1.75 (m, 3H), 1.99-2.29 (m, 2H), 2.51-2.64 (m, 3H), 3.73 (t, 1H, J= 18.8 Hz), 3.85 (s, 3H), 3.86 (s,

3H), 3.97 (d, 1H, J= 18.7 Hz), 4.37-4.38 (m, 1H), 4.68 (s, 2H), 5.50-5.89 (m, 3H), 6.66 (s, 1H), 6.69 (s, 1H), 6.77-6.81 (m, 1H), 6.83- 6.94 (m, 3H), 7.17-7.24 (m, 1H).

$^{13}\text{C}$  NMR (75 MHz,  $\text{CDCl}_3$ )  $\delta$ = 9.06, 23.56, 23.66, 27.38, 29.37, 31.44, 32.73, 38.31, 43.26, 54.75, 56.10, 56.17, 65.36, 76.88, 111.64, 112.06, 112.82, 114.92, 120.48, 122.57, 123.98, 125.53, 130.07, 133.61, 141.88, 147.63, 149.14, 158.07, 167.34, 169.54, 172.76, 207.48.

MS (ESI) m/z: found Rt 11.12 min. (Method LCMS), 604.92  $[\text{M} + \text{Na}]^+$ .

HRMS 582.3266  $[\text{M} + \text{H}]^+$ , calculated 582.3225  $[\text{M} + \text{H}]^+$ .

***Synthesis of 2-(3-((R)-3-(3,4-dimethoxyphenyl)-1-((R)-4-(3,3-dimethyl-2-oxopentanoyl)thiomorpholine-3-carboxyloxy)propyl)phenoxy)acetic acid 2d***

General method A was used for coupling of alcohol **5a** (67mg, 0.166 mmol) and acid **4d** (50 mg, 0.183 mmol) using DMAP (2.2 mg, 0.018 mmol) and DCC (38 mg, 0.183 mmol). The crude product was chromatographed using Hexane: EtOAc 3: 1 to afford ester 4 (104mg, 0.158 mmol, 87%)

TLC (Hexane: EtOAc 1: 1): Rf = 0.80.

HPLC (Gradient A) retention time= 30.2-30.6min

$^1\text{H}$  NMR (600 MHz,  $\text{CDCl}_3$ )  $\delta$ = 0.83-0.86 (m, 3H), 1.19 (s, 3H), 1.21 (s, 3H), 1.44 (s, 9H), 1.56-1.63 (m, 1H), 1.68-1.76 (m, 1H), 2.01-2.08 ((m, 1H), 2.20-2.26 (m, 1H), 2.33-2.38 (m, 1H), 2.51-2.65 (m, 2H), 2.71-2.81 (m, 1H), 2.91-3.03 (m, 1H), 3.08-3.27 (m, 1H), 3.51-3.58 (m, 2H), 3.81 (s, 3H), 3.82 (s, 3H), 4.48 (s, 2H), 5.55-5.56 (m, 1H), 5.74-5.84 (m, 1H), 6.65-6.68 (m, 2H), 6.74-6.76 (m, 1H), 6.79 (d, 1H, J= 8Hz), 6.86 (s, 1H), 6.92 (d, 1H, J= 8.2Hz), 7.20-7.25 (m, 1H).

$^{13}\text{C}$  NMR (150 MHz,  $\text{CDCl}_3$ )  $\delta$ = 8.92, 23.05, 23.84, 27.37, 28.23, 28.72, 31.36, 32.64, 38.23, 45.60, 47.00, 51.72, 56.02, 56.12, 65.96, 77.37, 82.56, 111.55, 112.03, 113.46, 114.37, 119.98, 120.41, 129.94, 133.71, 141.32, 147.54, 149.07, 158.33, 167.87, 168.05, 171.27, 207.64.

HRMS 602.2355  $[\text{M} - \text{tBu} + \text{H}]^+$ , 658.3018  $[\text{M} + \text{H}]^+$ , calculated 602.2346  $[\text{M} - \text{tBu} + \text{H}]^+$ , 658.3072  $[\text{M} + \text{H}]^+$ .

**Ester 4** (100 mg, 0.152 mmol) was treated with 20% TFA in DCM at room temperature. The mixture was stirred for 6h. TFA and DCM were evaporated under reduced pressure to yield the free acid **2d** (58.1mg, 0.096mmol, 64%).

TLC (Hexane: EtOAc: AcOH: 5:5: 0.5): Rf = 0.42.

HPLC (Gradient A) retention time= 25.2-25.7min

$^1\text{H}$  NMR (600 MHz,  $\text{CDCl}_3$ )  $\delta$ = 0.84-0.87 (m, 3H), 1.17 (s, 3H), 1.20 (s, 3H), 1.55-1.76 (m, 2H), 2.05-2.10 (m, 1H), 2.21-2.28 (m, 1H), 2.34-2.41 (m, 1H), 2.56-2.69 (m, 2H), 2.74-2.84 (m, 1H), 2.92-3.04 (m, 1H), 3.10-3.24 (m, 1H), 3.50-3.59 (m, 2H), 3.82 (s, 3H), 3.84 (s, 3H), 4.64 (s, 2H), 5.56-5.57 (m, 1H), 5.76-5.83 (m, 1H), 6.65-6.69 (m, 2H), 6.75-6.76 (m, 1H), 6.80-6.86 (m, 2H), 6.91 (d, 1H,  $J$ = 7.8 Hz), 7.21-7.25 (m, 1H).

$^{13}\text{C}$  NMR (150 MHz,  $\text{CDCl}_3$ )  $\delta$ = 8.91, 23.04, 23.81, 27.38, 28.76, 31.42, 32.65, 38.30, 45.67, 47.06, 51.96, 56.08, 56.14, 65.30, 80.28, 111.61, 112.11, 112.44, 114.87, 130.11, 133.65, 141.72, 147.56, 149.08, 158.02, 167.78, 168.02, 173.02, 207.55.

MS (ESI)  $m/z$ : found Rt 11.85 min. (Method LCMS), 624.45  $[\text{M} + \text{Na}]^+$ .

HRMS 602.2379  $[\text{M} + \text{H}]^+$ , calculated 602.2346  $[\text{M} + \text{H}]^+$ .

***Synthesis of 2-(3-(3-(3,4-dimethoxyphenyl)-1-((S)-1-(3,3-dimethyl-2-oxopentanoyl)piperidine-2-carboxamido)propyl)phenoxy)acetic acid (mixture of diastereomers) 2e***

General method A was used for coupling of amine **19** (71.5mg, 0.178 mmol) and acid **4a** (50 mg, 0.195 mmol) using DMAP (2.3 mg, 0.019 mmol) and DCC (40 mg, 0.195 mmol). The crude product was chromatographed using Hexane: EtOAc 1: 1 to afford ester **5** (110mg, 0.172 mmol, 96%)

TLC (Hexane: EtOAc 1: 1):  $R_f$  = 0.7.

HPLC (Gradient A) retention time= 28.2-28.8min

$^1\text{H}$  NMR (300 MHz,  $\text{CDCl}_3$ )  $\delta$ = 0.82-0.92 (m, 3H), 1.18-1.26 (m, 6H), 1.46 (s, 9H), 1.57-1.75 (m, 5H), 2.23-2.70 (m, 3H), 3.16-3.38 (m, 1H), 3.83 (s, 3H), 3.84 (s, 3H), 4.43-4.45 (m, 2H), 4.87-4.96 (m, 1H), 5.06 (t, 1H,  $J$ = 6Hz), 6.63-6.96 (m, 6H), 7.19-7.28 (m, 1H).

$^{13}\text{C}$  NMR (75 MHz,  $\text{CDCl}_3$ )  $\delta$ = 8.94, 9.03, 20.60, 21.21, 22.92, 22.96, 23.33, 23.39, 23.44, 23.72, 25.26, 25.36, 28.37, 32.66, 32.89, 32.91, 38.45, 38.78, 44.59, 44.64, 46.77, 46.80, 51.59, 53.43, 53.46, 56.02, 56.11, 60.55, 65.91, 82.46, 111.55, 112.07, 113.32, 113.58, 119.72, 119.77, 120.36, 120.38, 130.01, 130.10, 133.93, 134.00, 143.95, 147.48, 149.06, 149.08, 158.42, 158.46, 166.64, 166.74, 168.08, 169.00, 169.17, 171.27, 207.98, 208.01, 210.02, 210.31.

HRMS 639.3611  $[\text{M} + \text{H}]^+$ , calculated 639.3665  $[\text{M} + \text{H}]^+$ .

**Ester 5** (110 mg, 0.172 mmol) was treated with 20% TFA in DCM at room temperature. The mixture was stirred for 6h. TFA and DCM were evaporated under reduced pressure to yield the free acid **2e** (40mg, 0.068mmol, 40%).

TLC (Hexane: EtOAc: AcOH 5: 5: 0.5):  $R_f$  = 0.19.

HPLC (Gradient A) retention time= 26.2-26.8 min

$^1\text{H}$  NMR (600 MHz,  $\text{CDCl}_3$ )  $\delta$ = 0.86-0.94 (m, 3H), 1.08-1.16 (m, 6H), 1.42 (s, 9H), 1.49-1.65 (m, 5H), 2.20-2.60 (m, 3H), 3.05-3.40 (m, 1H), 3.79 (s, 3H), 3.80 (s, 3H), 4.46-4.49 (m, 2H), 4.86-4.96 (m, 1H), 5.07 (t, 1H,  $J$ = 6Hz), 6.63-6.95 (m, 6H), 7.20-7.28 (m, 1H).

$^{13}\text{C}$  NMR (150 MHz,  $\text{CDCl}_3$ )  $\delta$ = 8.94, 9.03, 20.60, 21.21, 22.92, 22.96, 23.33, 23.39, 23.44, 23.72, 25.26, 25.36, 32.66, 32.89, 32.91, 38.45, 38.78, 44.59, 44.64, 46.77, 46.80, 51.59, 53.43, 53.46, 56.02, 56.11, 60.55, 65.91, 111.55, 112.07, 113.32, 113.58, 119.72, 119.77, 120.36, 120.38, 130.01, 130.10, 133.93, 134.00, 143.95, 147.48, 149.06, 149.08, 158.42, 158.46, 166.64, 166.74, 168.08, 169.00, 169.17, 171.27, 207.98, 208.01, 210.02, 210.31.

MS (ESI)  $m/z$ : found Rt 11.01 min. (Method LCMS), 583.28  $[\text{M} + \text{H}]^+$ , 605.60  $[\text{M} + \text{Na}]^+$ .

HRMS 583.3577  $[\text{M} + \text{H}]^+$ , calculated 583.3541  $[\text{M} + \text{H}]^+$ .

### ***Synthesis of (S)-methyl 1-(3,3-dimethyl-2-oxopentanoyl)piperidine-2-carboxylate 6a***

The compound was prepared as described previously<sup>16</sup>.

TLC (Hexane : EtOAc 8: 2):  $R_f$  = 0.40, Yield- 640mg (73%).

HPLC (Gradient A) retention time= 22.8-23.1 min

$^1\text{H}$  NMR (400 MHz,  $\text{CDCl}_3$ )  $\delta$ = 0.83 (dt, 3H,  $J$ = 1.2, 7.2Hz), 1.14 (s, 3H), 1.17 (s, 3H), 1.26-1.50 (m, 2H), 1.58-1.74 (m, 5H), 2.24 (d, 1H,  $J$ = 14Hz), 3.12-3.19 (m, 1H), 3.33 (d, 1H,  $J$ = 13.8Hz), 3.70 (s, 3H), 5.20 (d, 1H,  $J$ = 5.6Hz).

$^{13}\text{C}$  NMR (100 MHz,  $\text{CDCl}_3$ )  $\delta$ = 8.69, 21.11, 22.85, 23.54, 24.82, 26.27, 32.45, 43.89, 46.70, 51.06, 52.35, 167.49, 170.77, 207.77.

MS (ESI)  $m/z$ : found Rt 12.94 min. (Method LCMS), 270.30  $[\text{M} + \text{H}]^+$ , 292.24  $[\text{M} + \text{Na}]^+$ .  
calculated 270.28  $[\text{M} + \text{H}]^+$ , 292.15  $[\text{M} + \text{Na}]^+$ .

### ***Synthesis of (S)-3-(pyridin-3-yl)propyl 1-(3,3-dimethyl-2-oxopentanoyl)pyrrolidine-2-carboxylate 6b***

General method A was used for coupling of alcohol **5d** (34mg, 0.249 mmol) and acid **4b** (60 mg, 0.248 mmol) using DMAP (3.3 mg, 0.027 mmol) and DCC (65.8 mg, 0.298 mmol). The crude product was chromatographed using DCM: MeOH 9.3: 0.7 to afford **6b** (52mg, 0.144 mmol, 57%).

TLC (DCM: MeOH 9.7:0.3):  $R_f$  = 0.39.

HPLC (Gradient A) retention time= 14.87-15.26 min

$^1\text{H}$  NMR (400 MHz,  $\text{CDCl}_3$ )  $\delta$ = 0.85 (t, 3H,  $J$  = 7.6 Hz), 1.20 (s, 3H), 1.24 (s, 3H), 1.64-1.71 (m, 2H), 1.91-2.04 (m, 5H), 2.19-2.30 (m, 1H), 2.66-2.73 (m, 2H), 3.40-3.54 (m, 2H), 4.08-4.20 (m, 2H), 4.49-4.52 (m, 1H), 7.19-7.23 (m, 1H), 7.50-7.53 (m, 1H), 8.45 (s, 2H).

$^{13}\text{C}$  NMR (100 MHz,  $\text{CDCl}_3$ )  $\delta$ = 8.92, 23.10, 23.70, 24.87, 29.17, 29.92, 32.34, 33.93, 46.94, 47.17, 58.33, 64.18, 123.37, 135.98, 147.54, 149.83, 165.14, 171.41, 206.98

MS (ESI)  $m/z$ : found Rt 9.51 min. (Method LCMS), 361.35  $[\text{M} + \text{H}]^+$ ,

HRMS 361.2299  $[\text{M} + \text{H}]^+$ , calculated 361.2249  $[\text{M} + \text{H}]^+$ .

***Synthesis of (S)-3-(pyridin-3-yl)propyl-(3,3-dimethyl-2-oxopentanoyl)piperidine-2-carboxylate 6c***

General method B was used for reacting the bromide 7a (37.8mg, 0.19mmol) and acid 4a (48.5 mg, 0.19 mmol) using DIPEA (24.7 mg, 0.23 mmol). The crude product was chromatographed using DCM: MeOH 9.3: 0.7 to afford 6c (45mg, 0.12 mmol, 64%)

TLC (DCM: MeOH 9.7:0.3):  $R_f$  = 0.30,

HPLC (Gradient A) retention time- 16.9-17.4min

$^1\text{H}$  NMR (300 MHz,  $\text{CDCl}_3$ )  $\delta$ = 0.82 (t, 3H,  $J$  = 7.5 Hz), 1.16 (d, 6H,  $J$  = 9.3 Hz), 1.36 (s, 2H), 1.59-1.70 (m, 4H), 1.87-1.95 (m, 2H), 2.23 (d, 2H,  $J$  = 14.16 Hz), 2.65 (t, 2H,  $J$  = 7.9 Hz), 3.15-3.31 (m, 2H), 4.12 (t, 2H,  $J$  = 8.0 Hz), 5.21 (d, 1H,  $J$  = 5.3 Hz), 7.46 (d, 2H,  $J$  = 7.8 Hz), 8.40 (s, 2H).

MS (ESI)  $m/z$ : found Rt 4.80 min. (Method LCMS), 375.39  $[\text{M} + \text{H}]^+$ ,

HRMS 375.2642  $[\text{M} + \text{H}]^+$ , calculated 375.2606  $[\text{M} + \text{H}]^+$ .

***Synthesis of (S)-2-(3,4-dimethoxyphenoxy)ethyl 1-(3,3-dimethyl-2-oxopentanoyl)piperidine - 2-carboxylate 6d***

General method B was used for reacting the bromide 7b (50mg, 0.19mmol) and acid 4a (50mg, 0.196mmol) using DIPEA (24.7mg, 0.23mmol). The crude product was chromatographed using Hexane: EtOAc 4:1 to afford 6d (70mg, 0.16mmol, 84%).

TLC (Hexane: EtOAc 4:1):  $R_f$  = 0.45.

HPLC (Gradient A) retention time= 25.8-26.4 min

$^1\text{H}$  NMR (300 MHz,  $\text{CDCl}_3$ )  $\delta$ = 0.86 (t, 3H,  $J$ =7.5Hz), 1.16 (s, 3H), 1.20 (s, 3H), 1.58-1.79 (m, 7H), 2.33 (d, 1H,  $J$ = 14.1 Hz), 3.18-3.28 (m, 1H), 3.38 (d, 1H,  $J$ = 13.2 Hz), 3.82 (s, 3H), 3.84 (s, 3H), 4.13 (t, 2H,  $J$ = 4.8 Hz), 4.44-4.56 (m, 2H), 5.30 (d, 1H,  $J$ = 5.1Hz), 6.37 (dd, 1H,  $J$ = 2.7, 8.7 Hz), 6.50 (d, 1H,  $J$ = 4.05 Hz), 6.76 (d, 1H,  $J$ = 8.7 Hz).

$^{13}\text{C}$  NMR (75 MHz,  $\text{CDCl}_3$ )  $\delta$ = 8.94, 21.37, 23.07, 23.87, 25.11, 26.62, 32.07, 44.19, 46.94, 51.42, 56.08, 56.64, 63.90, 66.50, 101.31, 104.22, 112.03, 144.16, 150.15, 153.16, 167.74, 170.59, 207.98.

MS (ESI) m/z: found Rt 11.77 min. (Method LCMS), 436.37  $[\text{M} + \text{H}]^+$ , 458.39  $[\text{M} + \text{Na}]^+$ .

HRMS 436.2627  $[\text{M} + \text{H}]^+$ , calculated 436.2657  $[\text{M} + \text{H}]^+$ .

***Synthesis of (S)-((R)-3-(3,4-dimethoxyphenyl)-1-(3-(2-morpholinoethoxy)phenyl)propyl)-1-(3,3-dimethyl-2-oxopentanoyl)piperidine-2-carboxylate 6e***

General method A was used for coupling of alcohol **5b** (95mg, 0.235 mmol) and acid **4a** (60 mg, 0.235 mmol) using DMAP (3.1 mg, 0.026 mmol) and DCC (62.1 mg, 0.282 mmol). The crude product was chromatographed using DCM: MeOH 9.3: 0.7 to afford **6e** (51mg, 0.079 mmol, 34%)

TLC (DCM: MeOH 9.7:0.3): Rf = 0.62.

HPLC (Gradient A) retention time= 18.87-19.32 min

$^1\text{H}$  NMR (400 MHz,  $\text{CDCl}_3$ )  $\delta$ = 0.87 (t, 3H, J= 7.6 Hz), 1.19 (s, 3H), 1.21 (s, 3H), 1.56-1.76 (m, 7H), 1.99-2.08 (m, 1H), 2.19-2.37 (m, 2H), 2.47-2.59 (m, 6H), 2.80 (t, 2H, J= 5.2 Hz), 3.14 (dt., 1H, J= 3.2, 13.2 Hz), 3.34 (d, 1H, J= 13.2 Hz), 3.73 (t, 4H, J= 4.4 Hz), 3.84 (s, 3H), 3.85 (s, 3H), 4.11 (t, 2H, J= 5.6 Hz), 5.30 (d, 1H, J= 5.2 Hz), 5.75 (q, 1H, J= 2.4, 5.6 Hz), 6.65-6.68 (m, 2H), 6.75-6.78 (m, 1H), 6.81-6.84 (m, 1H), 6.87-6.92 (m, 2H), 7.22-7.26 (m, 1H).

$^{13}\text{C}$  NMR (100 MHz,  $\text{CDCl}_3$ )  $\delta$ = 8.74, 21.18, 23.09, 23.49, 24.94, 26.41, 31.24, 32.45, 38.01, 44.12, 46.66, 51.23, 54.04, 55.80, 55.89, 57.63, 65.68, 66.81, 77.02, 111.25, 111.69, 113.01, 114.20, 119.04, 120.11, 129.64, 133.43, 141.31, 147.29, 148.83, 158.82, 167.19, 169.65, 207.76.

MS (ESI) m/z: found Rt 10.90 min. (Method LCMS), 639.45  $[\text{M} + \text{H}]^+$ .

HRMS 639.3566  $[\text{M} + \text{H}]^+$ , calculated 639.3567  $[\text{M} + \text{H}]^+$ .

***Synthesis of (S)-((R)-3-(3,4-dimethoxyphenyl)-1-(3-(2-morpholinoethoxy)phenyl)propyl)-1-(3,3-dimethyl-2-oxopentanoyl)pyrrolidine-2-carboxylate 6f***

General method A was used for coupling of alcohol **5b** (50mg, 0.124 mmol) and acid **4b** (30 mg, 0.124 mmol) using DMAP (1.6 mg, 0.013 mmol) and DCC (33 mg, 0.149 mmol). The crude product was chromatographed using DCM: MeOH 9.3: 0.7 to afford **6f** (45mg, 0.072 mmol, 59%)

TLC (DCM: MeOH 9.7:0.3): R<sub>f</sub> = 0.38.

HPLC (Gradient A) retention time= 18.79-19.19 min

<sup>1</sup>H NMR (400 MHz, CDCl<sub>3</sub>) δ= 0.81-0.86 (m, 3H), 1.19-1.22 (m, 6H), 1.56-1.75 (m, 3H), 1.89-2.01 (m, 4H), 2.17-2.25 (m, 1H), 2.45-2.61 (m, 6H), 2.79 (s, 2H), 3.45-3.54 (m, 2H), 3.72 (t, 4H, J= 4.8 Hz), 3.83 (s, 3H), 3.85 (s, 3H), 4.11 (t, 2H, J= 5.6 Hz), 4.56-4.66 (m, 1H), 5.65-5.77 (m, 1H), 6.64-6.66 (m, 1H), 6.67 (s, 1H), 6.75-6.77 (m, 1H), 6.79-6.84 (m, 1H), 6.88-6.90 (m, 2H), 7.20-7.25 (m, 1H).

<sup>13</sup>C NMR (100 MHz, CDCl<sub>3</sub>) δ= 8.92, 23.23, 23.59, 24.93, 31.07, 32.20, 33.93, 38.04, 46.86, 47.14, 49.06, 54.04, 55.81, 57.63, 65.67, 66.85, 76.19, 111.21, 111.79, 112.70, 114.08, 118.75, 120.11, 129.50, 133.63, 141.48, 147.21, 148.78, 158.78, 165.04, 170.62, 207.01.

MS (ESI) m/z: found Rt 10.59 min. (Method LCMS), 625.47 [M + H]<sup>+</sup>,

HRMS 625.3421 [M + H]<sup>+</sup> calculated 625.3411 [M + H]<sup>+</sup>.

*(S)-((R)-1-(3-aminophenyl)-3-(3,4-dimethoxyphenyl)propyl) 1-(3,3-dimethyl-2-oxopentanoyl)piperidine-2-carboxylate **6g***

Obtained from Cayman Chemicals, Compound name: SLF, Cat no. 1000974.

*Synthesis of 2-(3-((R)-3-(3,4-dimethoxyphenyl)-1-((S)-1-(2-oxo-2-(3,4,5-trimethoxyphenyl)acetyl)piperidine-2-carboxyloxy)propyl)phenoxy)acetic acid **6h***

To a stirred solution of the **12c** (51mg, 0.1mmol) in DCM under argon was added sequentially *N,N*-Diisopropyl-ethylamine (DIPEA) (15.7mg, 0.125mmol) to which was added **22** (26mg, 0.1mmol). The reaction mixture was stirred for 1h at room temperature. Saturated NH<sub>4</sub>Cl solution was added to the reaction and the solution was stirred for 10 min. The organic phase was separated and the aqueous phase was extracted with ethyl acetate (3x 100ml). The combined organic phases were washed with brine (10ml), dried over MgSO<sub>4</sub> and the residual solid was purified by column chromatography using Hexane : EtOAc 4:1 to afford **ester 6** (35.8mg, 0.048mmol, 49%).

TLC (Hexane: EtOAc 4:1): R<sub>f</sub> = 0.45.

HPLC (Gradient A) retention time= 18.92-19.16min

<sup>1</sup>H NMR (600 MHz, CDCl<sub>3</sub>) δ= 1.48 (s, 9H), 1.58-1.66 (m, 1H), 1.78-1.85 (m, 3H), 2.06-2.12 (m, 1H), 2.24-2.30 (m, 2H), 2.44 (d, 1H, J= 12.6 Hz), 2.52-2.57 (m, 1H), 2.59-2.64 (m, 1H), 3.27 (t, 1H, J= 12.6 Hz), 3.48 (d, 1H, J= 12.6Hz), 3.82 (s, 6H), 3.85 (s, 6H), 3.92 (s, 3H), 4.52 (s, 2H), 5.41 (d, 1H, J= 4.8Hz), 5.73 (t, 1H, J= 6.6Hz), 6.63-6.70 (m, 3H), 6.76-6.81 (m, 2H), 6.90 (s, 1H), 6.95 (d, 1H, J= 7.8 Hz), 7.09 (s, 1H), 7.28-7.35 (m, 1H).

**Ester 6** (35.8mg, 0.048mmol) was treated with 20% TFA in DCM at room temperature. The mixture was stirred for 6h. TFA and DCM were evaporated under reduced pressure to yield the free acid **6h** (30.9mg, 0.045mmol, 96%).

TLC (Hexane: EtOAc: AcOH 5:5: 0.5): Rf = 0.37.

HPLC (Gradient A) retention time= 23.8-24.6min

$^1\text{H}$  NMR (600 MHz,  $\text{CDCl}_3$ )  $\delta$ = 1.50-1.56 (m, 1H), 1.61-1.66(m, 1H), 1.83-1.91 (m, 2H), 1.98-2.10 (m, 2H), 2.22-2.28 (m, 1H), 2.42 (d, 1H, J= 13.8 Hz), 2.56-2.61 (m, 1H), 2.64-2.69 (m, 1H), 3.25-3.30 (m, 1H), 3.45 (d, 1H, J= 12 Hz), 3.71 (s, 6H), 3.84 (s, 3H), 3.85 (s, 3H), 3.88 (s, 3H), 4.58 (s, 2H), 5.40 (d, 1H, J= 5.4 Hz), 5.56-5.66 (m, 1H), 6.66-6.67 (m, 2H), 6.75-6.78 (m, 1H), 6.82 (d, 1H, J= 7.8 Hz), 6.87-6.88 (m, 2H), 7.16 (s, 2H), 7.22 (t, 1H, j= 7.8Hz).

$^{13}\text{C}$  NMR 150 MHz,  $\text{CDCl}_3$ )  $\delta$ = 24.84, 28.41, 28.44, 31.65, 38.45, 44.56, 52.17, 56.06, 56.14, 56.39, 61.14, 77.40, 107.09, 111.43, 111.58, 111.89, 114.92, 119.85, 120.41, 127.87, 129.85, 133.48, 142.25, 144.19, 147.64, 149.15, 153.63, 158.17, 168.36, 170.23, 177.39, 190.70

MS (ESI) m/z: found Rt 13.29 min. (Method LCMS), 702.22  $[\text{M} + \text{Na}]^+$ .

HRMS 680.3277  $[\text{M} + \text{H}]^+$ , calculated 680.3129  $[\text{M} + \text{H}]^+$ .

***Synthesis of (S)-1,7-di(pyridin-3-yl)heptan-4-yl 1-(3,3-dimethyl-2-oxopentanoyl)piperidi ne-2-carboxylate (Biricodar) 6i***

The compound was prepared as described previously<sup>23,39</sup>.

***Timcodar 6j***

Obtained from the group of Dr. Edwin Sanchez.

***Synthesis of (S)-2-((MOM)methyl)cyclohexanone 8c***

The (S)-2-(hydroxymethyl)cyclohexanone was prepared as already described<sup>31</sup>. To this compound (1.5g, 11.7 mmol) in DCM was added *N,N*-Diisopropyl-ethylamine(3.7g, 29.3 mmol). The mixture was stirred at 0°C for 5 min before MOM-Cl (2g, 25.7 mmol) was added. After stirring for 3h the mixture was concentrated under reduced pressure and subjected to purification by column chromatography using Hexane: EtOAc 8:2 to afford **8c** (1.8g, 10.5 mmol, 90%) as a colorless liquid.

TLC (Hexane: EtOAc 8:2): Rf = 0.45

$^1\text{H}$  NMR (300 MHz,  $\text{CDCl}_3$ )  $\delta$ = 1.36-1.49 (m, 1H), 1.54-1.71 (m, 2H), 1.77-1.89 (m, 1H), 1.95-2.06 (m, 1H), 2.13-2.38 (m, 3H), 2.50-2.60 (m, 1H), 3.29 (s, 3H), 3.41-3.47 (m, 1H), 3.75-3.80 (m, 1H), 4.58 (d, 2H,  $J$ = 2.1 Hz).

$^{13}\text{C}$  NMR (75 MHz,  $\text{CDCl}_3$ )  $\delta$ = 24.63, 27.62, 31.16, 41.99, 50.67, 55.08, 66.72, 96.62, 211.13

MS (ESI)  $m/z$ : 195.67  $[\text{M} + \text{Na}]^+$ , calculated 195.10  $[\text{M} + \text{Na}]^+$ .

***General procedure for the synthesis of 2-alkyl-1-((trimethylsilyl)ethynyl)cyclohexanol 9***

The THF solution of lithium reagent was generated by treating trimethylsilylacetylene (3ml, 21.4 mmol) with *n*-BuLi (2M in hexane, 11.6ml) at  $-78^\circ\text{C}$ . The solution was stirred for 0.5h at that temperature. To this a solution of 2-alkylcyclohexanone (**8a-8c**) (17.8 mmol) in THF (5ml) was added and stirred for an additional 2h. Then the solution was quenched by addition of a saturated aqueous  $\text{NH}_4\text{Cl}$  solution. The organic phase was separated and the aqueous phase was extracted with ethyl acetate (3x 100ml). The combined organic phases were washed with brine (30ml) and dried over  $\text{MgSO}_4$ . The solution was concentrated and then flash chromatographed using Hexane: EtOAc 9:1 to afford each of the two diastereomers **9a-9f**.

***(1S,2R)-2-Methyl-1-((trimethylsilyl)ethynyl)cyclohexanol and (1R,2S)-2-Methyl-1-((trimethylsilyl)ethynyl)cyclohexanol 9a***

Compound **9a** (1.2g, 33%) was obtained from **8a** (2g) as a colorless liquid.

TLC (Hexane: EtOAc 9:1):  $R_f$  = 0.36

$^1\text{H}$  NMR (300 MHz,  $\text{CDCl}_3$ )  $\delta$ = 0.17(s, 9H), 1.06(d, 3H,  $J$  = 6.9 Hz), 1.23-1.33 (m, 1H), 1.48-1.71 (m, 7p), 1.95-2.02 (m, 1P).

$^{13}\text{C}$  NMR (75 MHz,  $\text{CDCl}_3$ )  $\delta$ = 0.01, 16.00, 21.06, 25.02, 29.15, 39.15, 40.48, 69.77, 86.95, 110.61

HRMS 193.1390  $[\text{M} - \text{OH}]^+$ , calculated 193.1413  $[\text{M} - \text{OH}]^+$ .

***(1S,2R)-2-Ethyl-1-((trimethylsilyl)ethynyl)cyclohexanol and (1R,2S)-2-Ethyl-1-((trimethylsilyl)ethynyl)cyclohexanol 9b***: Compound **9b** (1.65g, 46%) was obtained from **8b** (2.2g) as a colorless liquid.

TLC (Hexane: EtOAc 9:1):  $R_f$  = 0.40

$^1\text{H}$  NMR (300 MHz,  $\text{CDCl}_3$ )  $\delta$ = 0.17(s, 9H), 0.86-0.96 (m, 6H), 1.12-2.42 (m, 22H).

$^{13}\text{C}$  NMR (75 MHz,  $\text{CDCl}_3$ )  $\delta$ = 0.024, 11.68, 12.30, 21.23, 22.88, 24.80, 25.46, 28.00, 33.28, 39.47, 41.94, 47.47, 52.31, 70.32, 87.09, 110.85.

HRMS 208.2069  $[\text{M} - \text{OH}]^+$ , calculated 208.1569  $[\text{M} - \text{OH}]^+$ .

**(1S,2S)-2-((methoxymethoxy)methyl)-1-((trimethylsilyl)ethynyl)cyclohexanol 9c:**

Compound 9c (2.1g, 46%) was obtained from 8c (3g) as a colorless liquid.

TLC (Hexane: EtOAc 9:1): R<sub>f</sub> = 0.45

<sup>1</sup>H NMR (300 MHz, CDCl<sub>3</sub>) δ= 0.17(s,9H), 1.31-2.04 (m, 9H), 3.40(s, 3H), 3.58 (dd, 1H, J = 2.4, 9.3 Hz), 4.26 (dd, 1H, J = 3.6, 9.6 Hz), 4.64 (dd, 2H, J = 6.6, 10.8 Hz).

<sup>13</sup>C NMR (75 MHz, CDCl<sub>3</sub>) δ= 0.00, 20.70, 24.67, 25.57, 39.18, 45.07, 55.41, 69.77, 70.75, 87.06, 96.54, 110.30.

HRMS 254.2134 [M - OH]<sup>+</sup>, calculated 254.2124 [M - OH]<sup>+</sup>.

***(1R,2R)-2-Methyl-1-((trimethylsilyl)ethynyl)cyclohexanol and (1S,2S)-2-Methyl-1-((trimethylsilyl)ethynyl)cyclohexanol 9d***

Compound 9d (1.1 g, 31%) was obtained from 8a (2g) as a colorless liquid.

TLC (Hexane: EtOAc 9:1): R<sub>f</sub> = 0.32

<sup>1</sup>H NMR (300 MHz, CDCl<sub>3</sub>) δ= 0.18 (s,9H), 1.04 (d, 3H, J = 6.6 Hz), 1.17-1.32 (m, 2H), 1.41-1.73 (m, 6H), 1.96-2.02 (m, 1H).

<sup>13</sup>C NMR (75 MHz, CDCl<sub>3</sub>) δ= 0.02, 16.03, 24.29, 25.50, 32.29, 40.63, 42.53, 73.42, 90.63, 106.80.

HRMS 193.1278 [M - OH]<sup>+</sup>, calculated 193.1413 [M - OH]<sup>+</sup>.

***(1R,2R)-2-Ethyl-1-((trimethylsilyl)ethynyl)cyclohexanol and (1S,2S)-2-Ethyl-1-((trimethylsilyl)ethynyl)cyclohexanol 9e***

Compound 9e (1.3g, 37%) was obtained from 8b (2.2g) as a colorless liquid.

TLC (Hexane: EtOAc 9:1): R<sub>f</sub> = 0.37

<sup>1</sup>H NMR (300 MHz, CDCl<sub>3</sub>) δ= 0.19(s,9H), 0.94 (t, 3H, J= 7.2Hz), 1.04-1.30 (m, 4H), 1.43-1.74 (m, 4H), 1.80-2.01 (m, 3H).

<sup>13</sup>C NMR (75 MHz, CDCl<sub>3</sub>) δ= 0.03, 11.93, 21.73, 24.15, 25.49, 28.36, 41.11, 49.56, 73.04, 90.46, 107.33.

HRMS 208.2069 [M - OH]<sup>+</sup>, calculated 208.1569 [M - OH]<sup>+</sup>.

***(1R,2S)-2-((methoxymethoxy)methyl)-1-((trimethylsilyl)ethynyl)cyclohexanol 9f***

Compound 9f (1.9g, 41%) was obtained from 8c (3g) as a colorless liquid.

TLC (Hexane: EtOAc 9:1): R<sub>f</sub> = 0.40

$^1\text{H}$  NMR (300 MHz,  $\text{CDCl}_3$ )  $\delta$ = 0.18 (s, 9H), 1.03-1.29 (m, 2H), 1.46-1.55 (m, 3H), 1.67-1.71 (m, 2H), 1.80-1.90 (m, 1H), 2.02-2.06 (m, 1H), 3.41 (s, 3H), 3.48 (dd, 1H,  $J$ = 4.2, 9.6 Hz) 3.87 (t, 1H,  $J$ = 9.9 Hz), 4.64 (s, 2H).

$^{13}\text{C}$  NMR (75 MHz,  $\text{CDCl}_3$ )  $\delta$ = 0.04, 23.16, 24.94, 26.29, 39.48, 46.06, 55.59, 71.68, 72.87, 90.49, 96.49, 106.78.

HRMS 254.2134  $[\text{M} - \text{OH}]^+$ , calculated 254.2124  $[\text{M} - \text{OH}]^+$ .

***General procedure for the synthesis of 2-alkyl-1-(bromoethynyl)cyclohexanol 10***

To solution of **9a-e** (1.3 mmol), N-bromosuccinimide (1.5 mmol) and  $\text{AgNO}_3$  (0.5 mmol) in acetone (10 ml) was added and the resulting solution was stirred in darkness for 2h at room temperature. Acetone was evaporated under reduced pressure and the solids were removed by filtration through a celite pad (washing with ether). The combined organic phase were concentrated and subjected to purification by column chromatography using Hexane: EtOAc 9:1 to yield **10a-e** as yellow liquids.

***(1S,2R)-1-(Bromoethynyl)-2-methylcyclohexanol and (1R,2S)-1-(Bromoethynyl)-2-methylcyclohexanol 10a***

Compound **10a** (256 mg, 91%) was obtained from **9a** (273mg) as a yellow liquid.

TLC (Hexane: EtOAc 9:1):  $R_f$  = 0.30

$^1\text{H}$  NMR (300 MHz,  $\text{CDCl}_3$ )  $\delta$ = 1.06 (d, 3H,  $J$  = 6.9 Hz), 1.29-1.73 (m, 8H), 1.97-2.04 (m, 1H).

$^{13}\text{C}$  NMR (75 MHz,  $\text{CDCl}_3$ )  $\delta$ = 16.05, 20.94, 24.95, 29.09, 39.17, 40.52, 43.04, 70.79, 84.60.

HRMS  $m/z$  199.0193, 201.0169  $[\text{M} - \text{OH}]^+$ , calculated 199.0122, 201.0102  $[\text{M} - \text{OH}]^+$ .

***(1S,2R)-1-(Bromoethynyl)-2-ethylcyclohexanol and (1R,2S)-1-(Bromoethynyl)-2-ethylcyclohexanol 10b***

Compound **10b** (264 mg, 88%) was obtained from **9b** (292 mg) as a yellow liquid.

TLC (Hexane: EtOAc 9:1):  $R_f$  = 0.36

$^1\text{H}$  NMR (300 MHz,  $\text{CDCl}_3$ )  $\delta$ = 0.96 (d, 3H,  $J$  = 7.2 Hz), 1.13-1.30 (m, 3H), 1.36-1.45 (m, 1H), 1.50-1.74 (m, 5H), 1.83-2.02 (m, 2H).

$^{13}\text{C}$  NMR (75 MHz,  $\text{CDCl}_3$ )  $\delta$ = 12.17, 21.10, 23.03, 24.81, 25.35, 39.55, 43.17, 47.78, 71.39, 84.74.

HRMS  $m/z$  213.0268, 215.0245  $[\text{M} - \text{OH}]^+$ , calculated 213.0279, 215.0259  $[\text{M} - \text{OH}]^+$ .

***(1S,2S)-1-(Bromoethynyl)-2-((methoxymethoxy)methyl)cyclohexanol 10c***

Compound **10c** (327 mg, 90%) was obtained from **9c** (350mg) as a yellow liquid.

TLC (Hexane: EtOAc 9:1): R<sub>f</sub> = 0.39

<sup>1</sup>H NMR (300 MHz, CDCl<sub>3</sub>) δ= 1.33-2.07 (m, 9H), 3.41(s, 3H), 3.59 (dd, 1H, J = 2.4, 9.6 Hz), 4.24 (dd, 1H, J = 3.3, 9.6 Hz), 4.65 (dd, 2H, J = 6.6, 13.2 Hz).

<sup>13</sup>C NMR (75 MHz, CDCl<sub>3</sub>) δ= 20.61, 24.67, 25.51, 39.17, 43.23, 45.09, 55.39, 70.66, 70.87, 84.39, 96.51.

HRMS m/z 259.0104, 261.0123[M - OH]<sup>+</sup>, calculated 259.0334, 261.0314 [M - OH]<sup>+</sup>.

***(1R,2R)-1-(Bromoethynyl)-2-methylcyclohexanol and (1S,2S)-1-(Bromoethynyl)-2-methylcyclohexanol 10d***

Compound **10d** (254 mg, 90%) was obtained from **9d** (270mg) as a yellow liquid.

TLC (Hexane: EtOAc 9:1): R<sub>f</sub> = 0.28

<sup>1</sup>H NMR (300 MHz, CDCl<sub>3</sub>) δ= 1.05 (d, 3H, J= 6.6 Hz), 1.20-1.29 (m, 2H), 1.48-1.75 (m, 6H), 2.00-2.05 (m, 1H).

<sup>13</sup>C NMR (75 MHz, CDCl<sub>3</sub>) δ= 16.66, 24,18, 25.43, 32.16, 40.63, 42.73, 45.35, 74.40, 81.18.

HRMS m/z 199.0193, 201.0169 [M - OH]<sup>+</sup>, calculated 199.0122, 201.0102 [M - OH]<sup>+</sup>.

***(1R,2R)-1-(Bromoethynyl)-2-ethylcyclohexanol and (1S,2S)-1-(Bromoethynyl)-2-ethylcyclohexanol 10e***

Compound **10e** (267 mg, 89%) was obtained from **9e** (292 mg) as a yellow liquid.

TLC (Hexane: EtOAc 9:1): R<sub>f</sub> = 0.32

<sup>1</sup>H NMR (300 MHz, CDCl<sub>3</sub>) δ= 0.97 (d, 3H, J = 7.2 Hz ), 1.09-1.25 (m, 3H), 1.36-1.76 (m, 6H), 1.87-2.03 (m, 2H).

<sup>13</sup>C NMR (75 MHz, CDCl<sub>3</sub>) δ= 12.57, 23.15, 24.97, 25.68, 25.55, 40.51, 45.60, 48.11, 75.20, 81.16.

HRMS m/z 213.0361, 215.0340 [M - OH]<sup>+</sup>, calculated 213.0279, 215.0259 [M - OH]<sup>+</sup>.

***General procedure for the synthesis of α-ketoesters of 11a-e***

To a solution of **10a-e** (1.08 mmol) in MeOH (5ml) was added a solution of NaHCO<sub>3</sub> (45.5 mg, 0.54 mmol) and MgSO<sub>4</sub> (261mg, 2.16 mmol) in water (5ml) at 0°C. The mixture was stirred for 10 min vigorously before KMnO<sub>4</sub> (513mg, 3.25 mmol) was added. The mixture was allowed to warm to room temperature and stirred at this temperature for 1h. The solids were removed by filtration through celite pad and washed with ethyl acetate. The organic phase was separated

and the aqueous phase was extracted with ethyl acetate (3x 100ml). The combined organic phases were washed with brine (30ml) and dried over MgSO<sub>4</sub>. The solution was concentrated and then flash chromatographed using Hexane: EtOAc 9:1 to afford the corresponding  $\alpha$ -ketoesters of **11a-e**.

***Methyl 2-((1S,2R)-1-hydroxy-2-methylcyclohexyl)-2-oxoacetate and Methyl 2-((1R,2S)-1-hydroxy-2-methylcyclohexyl)-2-oxoacetate***

The corresponding  $\alpha$ -ketoester of **11a** (117 mg, 65%) was obtained from **10a** (235 mg) as an oily liquid.

TLC (Hexane: EtOAc 9:1): R<sub>f</sub> = 0.61

<sup>1</sup>H NMR (300 MHz, CDCl<sub>3</sub>)  $\delta$ = 0.81 (d, 3H, J = 6.6 Hz), 1.25-1.90 (m, 8H), 2.03- 2.16 (m, 1H), 3.90 (s, 3H).

<sup>13</sup>C NMR (75 MHz, CDCl<sub>3</sub>)  $\delta$ = 16.00, 20.16, 25.35, 29.27, 34.99, 36.25, 52.74, 80.88, 163.61, 200.66.

***Methyl 2-((1S,2R)-2-ethyl-1-hydroxycyclohexyl)-2-oxoacetate and Methyl 2-((1R,2S)-2-ethyl-1-hydroxycyclohexyl)-2-oxoacetate***

The corresponding  $\alpha$ -ketoester of **11b** (160 mg, 69%) was obtained from **10b** (250 mg) as an oily liquid and was further hydrolyzed without further purification.

TLC (Hexane: EtOAc 9:1): R<sub>f</sub> = 0.64

***Methyl 2-((1S,2S)-1-hydroxy-2-((methoxymethoxy)methyl)cyclohexyl)-2-oxoacetate***

The corresponding  $\alpha$ -ketoester of **11c** (170 mg, 60%) was obtained from **10c** (300 mg) as an oily liquid.

TLC (Hexane: EtOAc 9:1): R<sub>f</sub> = 0.60

<sup>1</sup>H NMR (300 MHz, CDCl<sub>3</sub>)  $\delta$ = 1.44-2.40 (m, 8H), 2.59-2.70 (m, 1H), 3.27 (s, 3H), 3.38- 3.42 (m, 2H), 3.87 (s, 3H), 4.42 (dd, 2H, J = 6.6, 18.6 Hz).

<sup>13</sup>C NMR (75 MHz, CDCl<sub>3</sub>)  $\delta$ = 20.74, 23.65, 24.81, 35.62, 42.23, 52.54, 55.50, 68.34, 78.81, 96.24, 161.37, 197.77.

MS (ESI) m/z 282.73 [M + Na]<sup>+</sup>, calculated 282.71 [M + Na]<sup>+</sup>.

***Methyl 2-((1R,2R)-1-hydroxy-2-methylcyclohexyl)-2-oxoacetate and Methyl 2-((1S,2S)-1-hydroxy-2-methylcyclohexyl)-2-oxoacetate***

The corresponding  $\alpha$ -ketoester of **11d** (85 mg, 47%) was obtained from **10d** (235 mg) as an oily liquid.

TLC (Hexane: EtOAc 9:1): Rf = 0.58

$^1\text{H}$  NMR (300 MHz,  $\text{CDCl}_3$ )  $\delta$ = 0.76 (d, 3H, J = 3.6 Hz), 1.29-1.83 (m, 8H), 1.99- 2.11 (m, 1H), 3.86 (s, 3H).

$^{13}\text{C}$  NMR (75 MHz,  $\text{CDCl}_3$ )  $\delta$ = 15.96, 20.11, 25.31, 29.22, 34.95, 36.21, 52.68, 80.84, 163.62, 200.69.

***Methyl 2-((1R,2R)-2-ethyl-1-hydroxycyclohexyl)-2-oxoacetate and Methyl 2-((1S,2S)-2-ethyl-1-hydroxycyclohexyl)-2-oxoacetate***

The corresponding  $\alpha$ -ketoester of **11e** (127 mg, 55%) was obtained from **10e** (250 mg) as an oily liquid and was further hydrolyzed without further purification.

TLC (Hexane: EtOAc 9:1): Rf = 0.61

**General procedure for the synthesis of 2-(1-hydroxy-2-alkylcyclohexyl)-2-oxoacetic acid (**11a-e**)**

To the above synthesized  $\alpha$ -ketoesters was added 1M LiOH in MeOH:  $\text{H}_2\text{O}$  (1:1) and the reaction stirred for 6h at room temperature. The reaction was acidified to pH=2 by addition of 1M HCl. The aqueous layer was extracted with ethyl acetate (3x 20ml). The combined organic phases were washed with brine (30ml) and dried over  $\text{MgSO}_4$ . The solution was concentrated under reduced pressure to furnish the free acid **11a-e** as an oily liquid.

***2-((1S,2R)-1-Hydroxy-2-methylcyclohexyl)-2-oxoacetic acid and 2-((1R,2S)-1-Hydroxy-2-methylcyclohexyl)-2-oxoacetic acid **11a*****

Compound **11a** (105 mg, overall yield for 2 steps 52%) was obtained from **10a** (235 mg) as a oily liquid.

TLC (Hexane: EtOAc: TFA 9:1:0.1): Rf = 0.28

$^1\text{H}$  NMR (400 MHz,  $\text{CDCl}_3$ )  $\delta$ = 0.78 (d, 3H, J = 6.8 Hz), 1.33-1.95 (m, 8H), 2.15 - 2.24 (m, 1H).

$^{13}\text{C}$  NMR (100 MHz,  $\text{CDCl}_3$ )  $\delta$ = 16.32, 20.32, 25.46, 29.41, 35.12, 36.57, 81.55, 162.81, 200.53.

***2-((1S,2R)-2-Ethyl-1-hydroxycyclohexyl)-2-oxoacetic acid and 2-((1R,2S)-2-Ethyl-1-hydroxycyclohexyl)-2-oxoacetic acid **11b*****

Compound **11b** (141 mg, overall yield for 2 steps 65%) was obtained from **10b** (250 mg) as a oily liquid.

TLC (Hexane: EtOAc: TFA 9:1:0.1): R<sub>f</sub> = 0.26

<sup>1</sup>H NMR (400 MHz, CDCl<sub>3</sub>) δ= 0.83 (t, 3H, J= 7.6Hz), 1.13-1.36 (m, 4H), 1.57-1.62 (m, 2H), 1.73-1.96 (m, 5H).

<sup>13</sup>C NMR (100 MHz, CDCl<sub>3</sub>) δ= 11.82, 20.39, 23.95, 25.08, 25.46, 35.32, 43.14, 82.20, 164.12, 201.23.

***2-((1S,2S)-1-Hydroxy-2-((methoxymethoxy)methyl)cyclohexyl)-2-oxoacetic acid 11c***

Compound **11c** (170 mg, overall yield for 2 steps 59%) was obtained from **10c** (300 mg) as an oily liquid.

TLC (Hexane: EtOAc: TFA 9:1:0.1): R<sub>f</sub> = 0.26

<sup>1</sup>H NMR (300 MHz, CDCl<sub>3</sub>) δ= 1.44-1.67 (m, 7H), 2.70-2.80 (m, 1H), 3.26-3.41 (m, 6H), 4.41-4.47 (m, 2H).

<sup>13</sup>C NMR (75 MHz, CDCl<sub>3</sub>) δ= 20.59, 23.34, 24.53, 35.27, 42.79, 55.74, 68.03, 78.38, 96.12, 160.39, 196.63.

***2-((1R,2R)-1-Hydroxy-2-methylcyclohexyl)-2-oxoacetic acid and 2-((1S,2S)-1-Hydroxy-2-methylcyclohexyl)-2-oxoacetic acid 11d***

Compound **11d** (68 mg, overall yield for 2 steps 34%) was obtained from **10d** (235 mg) as an oily liquid.

TLC (Hexane: EtOAc: TFA 9:1:0.1): R<sub>f</sub> = 0.24

<sup>1</sup>H NMR (300 MHz, CDCl<sub>3</sub>) δ= 0.76 (d, 3H, J = 6.6 Hz ), 1.29-1.51 (m, 3H), 1.55-1.62 (m, 2H), 1.67-1.72 (m, 2H), 1.83-1.93 (m, 1H), 2.06-2.18 (m, 1H).

<sup>13</sup>C NMR (75 MHz, CDCl<sub>3</sub>) δ= 16.00, 20.22, 25.37, 29.31, 34.88, 36.21, 80.82, 164.55, 201.85

***2-((1R,2R)-2-Ethyl-1-hydroxycyclohexyl)-2-oxoacetic acid and 2-((1S,2S)-2-Ethyl-1-hydroxycyclohexyl)-2-oxoacetic acid 11e***

Compound **11e** (101 mg, overall yield for 2 steps 51%) was obtained from **10e** (250 mg) as an oily liquid.

TLC (Hexane: EtOAc: TFA 9:1:0.1): R<sub>f</sub> = 0.23

<sup>1</sup>H NMR (300 MHz, CDCl<sub>3</sub>) δ= 0.83 (t, 3H, J= 4.2Hz), 1.12-1.33 (m, 4H), 1.56-1.63 (m, 2H), 1.72-1.97 (m, 5H).

$^{13}\text{C}$  NMR (75 MHz,  $\text{CDCl}_3$ )  $\delta$ = 11.79, 20.38, 23.94, 25.08, 25.47, 35.31, 43.15, 82.21, 164.10, 201.14

***Synthesis of tert-butyl 2-(3-(3-(3,4-dimethoxyphenyl)propanoyl)phenoxy)acetate 13a***

A solution of corresponding phenol<sup>15</sup> (5g, 15.46 mmol) and  $\text{K}_2\text{CO}_3$  (4.8g, 34.9mmol) in acetone (30mL) was treated with tert-butyl bromoacetate (3.7g, 19.21mmol) and stirred at room temperature for 20h. After this time the reaction mixture was filtered, concentrated and flash chromatographed to afford compound 5 (6.6g, 16.5mmol, 94%).

TLC (Hexane:EtOAc 8:2): RF = 0.50.

$^1\text{H}$  NMR (400 MHz,  $\text{CDCl}_3$ )  $\delta$ = 1.45 (s, 9H), 2.97 (t, 2H,  $J$  = 8 Hz), 3.22 (t, 2H,  $J$  = 8 Hz), 3.82 (s, 3H), 3.83 (s, 3H), 4.52 (s, 2H), 6.73-6.78 (m, 3H), 7.09 (dd, 1H,  $J$  = 0.8, 2.4 Hz), 7.33 (t, 1H,  $J$  = 8 Hz), 7.43 (m, 1H), 7.53 (dd, 1H,  $J$  = 1.2, 7.6).

$^{13}\text{C}$  NMR (100 MHz,  $\text{CDCl}_3$ )  $\delta$ = 27.99, 29.77, 40.70, 55.80, 65.63, 82.55, 111.35, 111.81, 113.06, 119.99, 120.12, 121.39, 129.66, 133.77, 138.22, 147.38, 148.88, 158.12, 167.57, 198.77. MS (ESI)  $m/z$  439.13  $[\text{M} + \text{K}]^+$ , calculated 439.15  $[\text{M} + \text{K}]^+$ .

***Synthesis of 3-(3,4-Dimethoxyphenyl)-1-(3-(2-morpholinoethoxy)phenyl)propan-1-one 13b***

A solution of the corresponding phenol (15.6 g, 59.5 mmol) in dry DMF (300 ml) under an atmosphere of nitrogen was treated with  $\text{K}_2\text{CO}_3$  (33.2 g, 240 mmol) and 4-(2-chloroethyl)morpholine hydrochloride (11.1 g, 59.6 mmol). The mixture was heated with stirring at 90°C for 2 hours until TLC indicated complete conversion. The mixture was cooled to room temperature and poured into ice-cold water (3.2 l). The precipitate of the title compound was collected by filtration, washed with water (3 x 200 ml) and dried *in vacuo* to yield 13b (17.7 g, 44.3 mmol, 74%) The product was used for the next step without further purification.

$^1\text{H}$  NMR (300 MHz,  $\text{CDCl}_3$ )  $\delta$ = 2.49-2.54 (m, 4H), 2.75 (t,  $J$  = 5.7 Hz, 2H), 2.94 (t,  $J$  = 7.7 Hz, 2H), 3.20 (t,  $J$  = 7.7 Hz, 2H), 3.65-3.69 (m, 4H), 3.79 (s, 3H), 3.81 (s, 3H), 4.08 (t,  $J$  = 5.6 Hz, 2H), 6.69-6.74 (m, 3H), 7.04 (dd,  $J$  = 0.8 Hz,  $J$  = 2.6 Hz, 1H), 7.29 (t,  $J$  = 7.9 Hz, 1H), 7.41-7.49, (m, 2H).

***Synthesis of (R)-tert-butyl 2-(3-(3-(3,4-dimethoxyphenyl)-1-hydroxypropyl)phenoxy)acetate 5a***

A solution of the ketone 13a (6.5g, 16.48mmol) in isopropanol (50 ml) was charged into the hydrogenation reactor (High-pressure laboratory autoclave Model IV from Roth) along with

$K_2CO_3$  (2.3g, 16.48mmol). The reactor was flushed twice with argon. Afterwards Noyuri catalyst (ABCR AB131600) was added. The reactor was flushed with argon, sealed and hydrogen gas was flushed into the reactor twice. The reaction was then stirred at room temperature with hydrogen gas at 15 bar pressure for 6 days. Afterwards the reaction was filtered through celite pad and washed continuously with diethyl ether. The organic solvent was dried under vacuum to yield compound **6** (6.2g, 15.42mmol, 94%, 99% ee using chiracel OD-H column Hexane: isopropanol isocratic gradient).

TLC (Hexane:EtOAc 8:2):  $R_f = 0.3$

$^1H$  NMR (300 MHz,  $CDCl_3$ )  $\delta = 1.47$  (s, 9H), 2.03 (m, 2H), 2.642 (m, 2H), 3.83 (s, 3H), 3.84 (s, 3H), 4.49 (s, 2H), 4.66-4.61 (m, 1H), 6.70-6.80 (m, 4H), 6.95-6.91 (m, 2H), 7.24(t, 1H,  $J = 7.8$  Hz).

$^{13}C$  NMR (75 MHz,  $CDCl_3$ )  $\delta = 28.01, 31.56, 40.62, 55.79, 55.90, 65.62, 73.55, 82.32, 111.31, 111.80, 112.18, 113.53, 119.08, 120.19, 129.48, 134.40, 146.56, 147.16, 148.82, 158.07, 168.01$ .

MS (ESI)  $m/z$  425.20  $[M + Na]^+$ , 441.17  $[M + K]^+$ , calculated 425.19  $[M + Na]^+$ , 441.17  $[M + K]^+$ .

***Synthesis of (R)-3-(3,4-Dimethoxyphenyl)-1-(3-(2-morpholinoethoxy)phenyl)propan-1-ol 5b***

Dry THF (35 ml) was added under an atmosphere of nitrogen to the **13b** (25 g, 62.6 mmol). The mixture was cooled to  $-20^\circ C$  and a 1.8 M solution of (+)-B-chlorodiisopinocampheylborane [(+)-DIP chloride] in hexane (53 ml, 95.4 mmol) which had been diluted with dry THF (70 ml) was slowly added dropwise. The temperature was kept below  $-10^\circ C$  and the mixture stirred for 3 hours. It was placed in a refrigerator overnight and another 0.2 equivalents of (+)-DIP chloride was added. After another day at  $-20^\circ C$  the solvent was removed under reduced pressure, the residue treated with ether (170 ml) and the mixture cooled to  $0^\circ C$ . Diethanolamine (60 ml) was added and it was stirred for a while. The formed precipitate was removed by filtration and washed with ether. The combined filtrates were concentrated under reduced pressure, and the title compound was obtained from the residue by column chromatography as oil (silica gel;  $CH_2Cl_2$  / MeOH gradient 100:0 to 94:6) to give **5b** (17.2 g, mmol, 68 %).

$^1H$  NMR (300MHz,  $CDCl_3$ )  $\delta = 1.84$ -2.08 (m, 2H), 2.27 (bs, 1H), 2.45-2.52 (m, 4H), 2.52-2.67 (m, 2H), 2.70 (t,  $J = 5.8$  Hz, 2H), 3.61-3.67 (m, 4H), 3.78 (2s, 6H), 4.02 (t,  $J = 5.8$  Hz, 2H), 4.54-4.60 (m, 1H), 6.62-6.76 (m, 4H), 6.82-6.87 (m, 2H), 7.14-7.21 (m, 1H).

MS (ESI)  $m/z$  402  $[M + H]^+$  and 424  $[M + Na]^+$ , calculated 402  $[M + H]^+$ , 424  $[M + Na]^+$ .

***Synthesis of (S)-1-(((9H-fluoren-9-yl)methoxy)carbonyl)piperidine-2-carboxylic acid 28***

A solution of the L-pipecolic acid 27 (3.6g, 38.7 mmol) in 40ml of 10% sodium carbonate was dissolved in a round bottom flask and stirred for 5 min at room temperature. To this solution was added Fmoc oxy-succinimide (8.5g, 34.8 mmol) dissolved in 35 ml dioxane and the reaction was stirred overnight. After 24h water was added and the aqueous layer was extracted with ethyl acetate. The aqueous layer was acidified (pH=2) by addition of concentrated HCl. The acidic layer was extracted with ethyl acetate (3x 40ml). The organic phase was washed with 1N HCl followed by brine, dried over MgSO<sub>4</sub> and concentrated under reduced pressure to yield an oily colorless liquid. The oily liquid was dissolved in ether and cooled to yield a fluffy white solid which was washed with hexane and dried to yield compound 7 (8.2g, 38.7mmol, 83%).

TLC (Hexane: EtOAc: TFA 1:1: 0.2): RF = 0.60

HPLC (Gradient A) retention time= 24.6-24.8 min

<sup>1</sup>H NMR (300 MHz, CDCl<sub>3</sub>) δ=1.28-1.53 (m, 2H), 1.69-1.82 (m, 3H), 2.19-2.37 (m, 1H), 3.15 (t, 1H, J= 13.2Hz), 4.05-4.33 (m, 2H), 4.37-4.49 (m, 2H), 4.76-5.05(m, 1H), 7.28-7.41 (m, 4H), 7.55-7.62 (m, 2H), 1.77 (s, 2H).

<sup>13</sup>C NMR (75 MHz, CDCl<sub>3</sub>) δ= 20.72, 24.70, 26.55, 41.94, 47.25, 54.19, 67.86, 119.97, 125.08, 127.07, 127.68, 141.33, 143.89, 156.65, 177.36

MS (ESI) m/z 352.66 [M + H]<sup>+</sup>, calculated 352.40 [M + H]<sup>+</sup>.

***Synthesis of (S)-1-tert-butyl 2-(3,4-dimethoxyphenethyl) piperidine-1,2-dicarboxylate (precursor of 12a)***

To a solution of 7c (385 mg, 1.57 mmol) in acetone (10ml) was added (S)-1Boc-piperidine-2-carboxylic acid (300mg, 1.30 mmol), K<sub>2</sub>CO<sub>3</sub> (217 mg, 1.57 mmol), and KI (catalytic amount). The reaction mixture was stirred at 60°C for 12h. The mixture was filtered and the solid residue washed with ethyl acetate (3 X 30 ml). The combined organic phases were washed with brine (30ml) and dried over MgSO<sub>4</sub>. The solution was concentrated and then the residue was purified by chromatography using Hexane: EtOAc 8:2 to afford **precursor of 12a** (440mg, 1.12 mmol, 85%).

TLC (Hexane:EtOAc 8:2): RF = 0.46

<sup>1</sup>H NMR (300 MHz, CDCl<sub>3</sub>) δ= 1.46 (s,1H), 1.58-1.59 (m, 3H), 2.17 (d, 1H, j= 13.2 Hz), 2.91 (t, 2H, j= 6.9 Hz), 3.87 (s, 3H), 3.89 (s, 3H), 3.91-4.17 (m, 2H), 4.35 (t, 2H, J= 6.9 Hz), 4.71-4.88(m, 1H), 6.75-6.83(m, 3H).

$^{13}\text{C}$  NMR (75 MHz,  $\text{CDCl}_3$ )  $\delta$ = 28.36, 34.75, 55.80, 55.94, 65.53, 79.89, 111.35, 112.11, 120.90, 147.78, 148.95.

HRMS  $m/z$  294.1694  $[\text{M} - \text{Boc} + \text{H}]^+$ , 394.2277  $[\text{M} + \text{H}]^+$ , 416.2083  $[\text{M} + \text{Na}]^+$ , calculated 294.1716  $[\text{M} - \text{Boc} + \text{H}]^+$ , 394.2151  $[\text{M} + \text{H}]^+$ , 416.2044  $[\text{M} + \text{Na}]^+$ .

#### ***Synthesis of 4-(2-bromoethoxy)-1,2-dimethoxybenzene (7b)***

A solution of 3,4-dimethoxyphenol (500mg, 3.24 mmol) in acetone (5ml) was added to  $\text{K}_2\text{CO}_3$  (538 mg, 3.89 mmol) and the reaction was stirred for 10min. Dibromoethane (2.4g, 12.97 mmol) was added to the reaction mixture before being heated to reflux for 12h. Afterwards the mixture was cooled to room temperature and 1M NaOH solution was added. The organic phase was separated and the aqueous phase was extracted with ethyl acetate (3x 30ml). The combined organic phases were washed with brine (30ml), dried over  $\text{MgSO}_4$  and the residual product was purified by chromatography using Hexane: EtOAc 7:3 to afford 7b (510mg, 1.95 mmol, 60%).

TLC (Hexane: EtOAc 7:3): RF = 0.41

$^1\text{H}$  NMR (300 MHz,  $\text{CDCl}_3$ )  $\delta$ = 3.64 (t, 2H,  $J$ = 6.3 Hz), 3.85 (s,3H), 3.87 (s,3H), 4.26 (t, 2H,  $J$ = 6.3 Hz), 6.42 (dd, 1H,  $J$ = 2.7, 8.7 Hz), 6.57 (d, 1H,  $J$ = 2.7Hz), 6.79 (d, 1H,  $J$ = 8.7Hz).

$^{13}\text{C}$  NMR (75 MHz,  $\text{CDCl}_3$ )  $\delta$ = 20.30, 55.89, 56.42, 65.59, 101.37, 104.27, 111.75, 144.09, 149.97, 152.05

MS (ESI)  $m/z$  261.18  $[\text{M} + \text{H}]^+$ , calculated 261.26  $[\text{M} + \text{H}]^+$ .

#### ***Synthesis of (S)-1-tert-butyl-2-(2-(3,4-dimethoxyphenoxy)ethyl)piperidine-1,2-dicarboxylate (precursor of 12b)***

To a solution of 7b (200mg, 0.76 mmol) in acetone (10ml) was added (S)-1Boc-piperidine-2-carboxylic acid (150 mg, 0.65 mmol),  $\text{K}_2\text{CO}_3$  (108 mg, 0.78 mmol), and KI (catalytic amount). The reaction mixture was stirred at 60°C for 12h. The mixture was filtered and the solid residue was washed with ethyl acetate (3 X 30 ml). The combined organic phases were washed with brine (30ml) and dried over  $\text{MgSO}_4$ . The solution was concentrated and then the residual crude product was purified by chromatography using Hexane: EtOAc 7:3 to afford precursor of 12b (200mg, 0.50 mmol, 77%).

TLC (Hexane:EtOAc 7:3): RF = 0.39

$^1\text{H}$  NMR (600 MHz,  $\text{CDCl}_3$ )  $\delta$ = 1.42 (d, 9H,  $J$ = 19.2 Hz), 1.57-1.65 (m, 4H), 2.17-2.23 (m, 1H), 2.86- 3.01 (m, 1H), 3.82 (s,3H), 3.83 (s,3H), 3.88-4.02 (m, 1H), 4.11 (t, 2H,  $J$ = 4.8 Hz), 4.45 (t, 2H,  $J$ = 4.8 Hz), 4.75 (s, 0.5H), 4.91 (s, 0.5H), 6.37 (dd, 1H,  $J$ = 3, 9 Hz), 6.51 (d, 1H,  $J$ = 1.2 Hz), 6.76 (d, 1H,  $J$ = 8.4 Hz).

$^{13}\text{C}$  NMR (150 MHz,  $\text{CDCl}_3$ )  $\delta$ = 26.79, 28.37, 41.03, 42.08, 53.79, 54.86, 55.81, 56.39, 63.17, 66.49, 101.08, 103.94, 111.68, 143.82, 149.84, 153.02, 171.89.

MS (ESI)  $m/z$  432.20 $[\text{M} + \text{Na}]^+$ , 448.20 $[\text{M} + \text{K}]^+$ , calculated 432.20  $[\text{M} + \text{Na}]^+$ , 448.17 $[\text{M} + \text{K}]^+$ .

***Synthesis of (S)-1-(9H-fluoren-9-yl)methyl 2-((R)-1-(3-(2-tert-butoxy-2-oxoethoxy)phenyl)-3-(3,4-dimethoxyphenyl)propyl) piperidine-1,2-dicarboxylate: (precursor of 12c)***

A solution of alcohol **5a** (2g, 4.97 mmol), carboxylic acid **28** (1.9g, 5.47 mmol), and DMAP (0.06 g, 0.54mmol) in 30mL DCM at room temperature was treated with DCC (1.1g, 5.47 mmol). The mixture was stirred for 12h. Afterwards the organic solvent was dried and the solid was dissolved in diethyl ether (50mL) and filtered through a plug of celite. The filtrate was concentrated and then flash chromatographed using Hexane: EtOAc 2:1 to afford **precursor of 12c** (3.5g, 4.78 mmol, 96%).

TLC (Hexane :EtOAc 2:1):  $R_f$  = 0.4.

$^1\text{H}$  NMR (600 MHz,  $\text{CDCl}_3$ )  $\delta$ = 1.46 (s, 10H), 1.68-1.76 (m, 3H), 1.98-2.04 (m, 1H), 2.14-2.22 (m, 1H), 2.29-2.33 (m, 1H), 2.41-2.58 (m, 2H), 2.96-3.15 (m, 1H), 3.81 (s, 3H), 3.83 (s, 3H), 4.07-4.15 (m, 2H), 4.26-4.49 (m, 5H), 5.02 (d, 1H,  $J$ = 5.4 Hz), 5.73-5.77 (m, 1H), 6.57-6.63 (m, 2H), 6.72-6.81 (m, 2H), 6.88 (s, 1H), 6.93-6.95 (m, 1H), 7.16-7.24 (m, 2H), 7.28-7.48 (m, 2H), 7.57-7.80 (m, 1H), 7.69-7.71 (m, 1H), 7.75-7.77 (m, 1H).

$^{13}\text{C}$  NMR (150 MHz,  $\text{CDCl}_3$ )  $\delta$ = 15.35, 17.89, 20.80, 24.76, 26.81, 28.00, 31.10, 38.03, 42.02, 47.20, 55.77, 55.89, 63.75, 65.72, 67.77, 76.18, 82.35, 104.18, 111.26, 111.56, 111.65, 113.23, 113.90, 119.64, 119.88, 119.89, 119.93, 125.06, 127.02, 127.62, 127.66, 129.65, 133.46, 141.26, 141.67, 143.85, 144.08, 147.25, 148.81, 156.38, 158.01, 167.88, 170.86.

MS (ESI)  $m/z$  758.60 $[\text{M} + \text{Na}]^+$ , 774.53 $[\text{M} + \text{K}]^+$ , calculated 758.33 $[\text{M} + \text{Na}]^+$ , 774.30  $[\text{M} + \text{K}]^+$ .

***Synthesis of (S)-1-(9H-fluoren-9-yl)methyl 2-((R)-3-(3,4-dimethoxyphenyl)-1-(3-(2-morpholinoethoxy)phenyl)propyl) piperidine-1,2-dicarboxylate (precursor of 12d)***

A solution of alcohol **5b** (171 mg, 0.427mmol), carboxylic acid **28** (150mg, 0.427 mmol), and DMAP (5.7 mg, 0.047mmol) in 10mL DCM at room temperature was treated with DCC (113 mg, 0.51 mmol). The mixture was stirred for 12h after which the organic solvent was dried. The solid was dissolved in diethyl ether (50mL) and filtered through a plug of celite. The filtrate was concentrated and then flash chromatographed using DCM: MeOH 9.7:0.3 to afford **precursor of 12d** (280 mg, 0.38 mmol, 89%).

TLC (EtOAc: 1): Rf = 0.56.

$^1\text{H}$  NMR (300 MHz,  $\text{CDCl}_3$ )  $\delta$ = 1.31-1.51 (s, 2H), 1.67-1.82 (m, 3H), 1.89-1.99 (m, 1H), 2.14-2.39 (m, 2H), 2.47-2.64 (m, 6H), 2.70-2.83 (m, 2H), 2.96-3.21 (m, 1H), 3.74 (s, 4H), 3.83 (s, 3H), 3.85 (s, 3H), 4.00-4.04 (m, 1H), 4.09-4.17 (m, 4H), 4.26-4.49 (m, 3H), 5.74-5.80 (m, 1H), 6.60-6.67 (m, 2H), 6.74-6.94 (m, 4H).

$^{13}\text{C}$  NMR (75 MHz,  $\text{CDCl}_3$ )  $\delta$ = 21.04, 24.95, 25.63, 31.22, 38.09, 41.98, 47.22, 54.00, 55.81, 55.92, 57.59, 60.38, 65.57, 66.75, 67.78, 76.28, 111.33, 111.73, 113.04, 113.93, 118.95, 119.95, 120.10, 125.06, 127.06, 127.67, 129.64, 133.51, 141.27, 141.52, 141.71, 143.87, 144.08, 147.33, 148.87, 156.38, 158.77, 170.94.

MS (ESI) m/z 735.57  $[\text{M} + \text{H}]^+$ , calculated 735.40  $[\text{M} + \text{H}]^+$ .

### ***Synthesis of (S)-3,4-dimethoxyphenethyl piperidine-2-carboxylate 12a***

Precursor of **12a** (390 mg, 0.991 mmol) was treated with 20% TFA in DCM at room temperature. The mixture was stirred for 2h. TFA and DCM were evaporated under reduced pressure to yield **12a** (280mg, 0.95mmol, 96.2%).

TLC (Hexane: EtOAc: TEA 7:2.8: 0.2): Rf = 0.24.

$^1\text{H}$  NMR (300 MHz,  $\text{CDCl}_3$ )  $\delta$ = 1.57 (s, 1H), 1.84 (s, 4H), 2.18 (d, 1H, J= 12.9 Hz), 3.54 (s, 1H), 3.86 (s, 3H), 3.87 (s, 3H), 3.89-3.96 (m, 1H), 4.37 (d, 3H, J= 7.8 Hz), 6.73 (d, 2H, J= 6.9 Hz), 6.81 (d, 1H, J= 9.3 Hz).

$^{13}\text{C}$  NMR (75 MHz,  $\text{CDCl}_3$ )  $\delta$ = 21.48, 21.71, 25.52, 34.18, 44.15, 55.83, 55.89, 56.84, 66.97, 111.42, 112.06, 120.81, 129.18, 147.94, 149.00.

MS (ESI) m/z 294.17  $[\text{M} + \text{H}]^+$ , calculated 294.41  $[\text{M} + \text{H}]^+$ .

### ***Synthesis of (S)-2-(3,4-dimethoxyphenoxy)ethyl piperidine-2-carboxylate 12b***

Precursor of **12b** (200 mg, 0.488 mmol) was treated with 20% TFA in DCM at room temperature. The mixture was stirred for 2h. TFA and DCM were evaporated under reduced pressure to yield **12b** (150mg, 0.48mmol, 99%).

TLC (Hexane: EtOAc: TEA 7:2.8: 0.2): Rf = 0.16.

$^1\text{H}$  NMR (600 MHz,  $\text{CDCl}_3$ )  $\delta$ = 1.54-1.61 (m, 1H), 1.82-1.97 (m, 4H), 2.24-2.28 (m, 1H), 2.99-3.04 (m, 1H), 3.55 (d, 1H, J= 12.6 Hz), 3.82 (s, 3H), 3.83 (s, 3H), 3.92 (dd, 1H, J= 3.6, 11.4 Hz), 4.11 (t, 2H, J= 4.2 Hz), 4.45-4.54(m, 2H), 6.35 (dd, 1H, J= 3, 9 Hz), 6.50 (d, 1H, J= 3 Hz), 6.76 (d, 1H, J= 9 Hz).

$^{13}\text{C}$  NMR (150 MHz,  $\text{CDCl}_3$ )  $\delta$ = 21.50, 21.74, 25.60, 44.14, 55.81, 56.39, 56.83, 64.71, 65.85, 100.97, 103.94, 111.74, 143.98, 149.91, 152.71, 168.48.

MS (ESI)  $m/z$  310.36  $[M + H]^+$ , calculated 310.26  $[M + H]^+$ .

***Synthesis of (S)-((R)-1-(3-(2-tert-butoxy-2-oxoethoxy)phenyl)-3-(3,4-dimethoxyphenyl)propyl) piperidine-2-carboxylate 12c***

Precursor of 12c (3.5 g, 4.8 mmol) was treated with 20% 4-methylpiperidine in DCM at room temperature. The mixture was stirred for 4h. 4-methylpiperidine and DCM were evaporated under reduced pressure. Saturated  $NH_4Cl$  solution was added to the filtrate and the solution was stirred for 10 min. The organic phase was separated and the aqueous phase was extracted with ethyl acetate (3x 100ml). The combined organic phases were washed with brine (30ml), dried over  $MgSO_4$  and the residual solid was purified by chromatography using Hexane: EtOAc : TEA 7:2.8: 0.2 to yield **12c** (2.2g, 4.3mmol, 91%).

TLC (Hexane: EtOAc: TEA 7:2.8: 0.2):  $R_f$  = 0.33.

$^1H$  NMR (600 MHz,  $CDCl_3$ )  $\delta$ = 1.42 (s, 9H), 1.43-1.50 (m, 2H), 1.52-1.57 (m, 1H), 1.61-1.68 (m, 1H), 1.69-1.74 (m, 1H), 1.99-2.04 (m, 2H), 2.15-2.21 (m, 1H), 2.44-2.55 (m, 2H), 2.62-2.66 (m, 1H), 3.05-3.08 (m, 1H), 3.42 (dd, 1H,  $J$ = 3, 10.2 Hz), 3.78 (s, 3H), 3.79 (s, 3H), 4.45 (s, 2H), 5.65-5.71 (m, 1H), 6.58-6.62 (m, 2H), 6.70-6.74 (m, 2H), 6.81-6.89 (m, 2H), 7.18 (t, 1H,  $J$ = 8.4Hz).

$^{13}C$  NMR (150 MHz,  $CDCl_3$ )  $\delta$ = 23.53, 24.78, 27.97, 28.41, 31.19, 37.83, 45.08, 55.80, 55.85, 58.08, 65.63, 75.83, 82.29, 112.27, 111.63, 113.07, 113.79, 119.72, 120.09, 129.56, 133.44, 141.60, 146.26, 148.81, 157.97, 167.84, 171.63.

MS (ESI)  $m/z$  514.53 $[M + H]^+$ , calculated 514.27  $[M + H]^+$ .

***Synthesis of (S)-((R)-3-(3,4-dimethoxyphenyl)-1-(3-(2-morpholinoethoxy)phenyl)propyl) piperidine-2-carboxylate 12d***

Precursor of 12d (250 mg, 0.34 mmol) was treated with 20% 4-methylpiperidine in DCM at room temperature. The mixture was stirred for 4h. 4-methylpiperidine and DCM were evaporated under reduced pressure. Saturated  $NH_4Cl$  solution was added to the filtrate and the solution was stirred for 10 min. The organic phase was separated and the aqueous phase was extracted with ethyl acetate (3x 100ml). The combined organic phases were washed with brine (30ml), dried over  $MgSO_4$  and the residual solid was purified by chromatography using Hexane: EtOAc: TEA 2: 7.8: 0.2 to yield **12d** (160 mg, 0.31mmol, 84%).

TLC (Hexane: EtOAc: TEA 7:2.8: 0.2):  $R_f$  = 0.3.

$^1H$  NMR (300 MHz,  $CDCl_3$ )  $\delta$ = 1.48-1.60 (m, 1H), 1.67-1.89 (m, 2H), 1.89-2.10 (m, 3H), 2.17-2.31 (m, 2H), 2.44-2.62 (m, 1H), 2.85 (s, 2H), 3.06 (s, 3H), 3.08 (s, 3H), 3.27-3.42 (m, 1H),

3.77-3.85 (m, 5H), 4.18-4.35 (m, 2H), 5.70 (t, 1H, J= 7.2 Hz), 6.62-6.66 (m, 2H), 6.72-6.80 (m, 2H), 6.86 (d, 1H, J= 7.8Hz), 6.95 (s, 1H), 7.19 (t, 1H, J= 8.1 Hz).

$^{13}\text{C}$  NMR (75 MHz,  $\text{CDCl}_3$ )  $\delta$ = 21.59, 22.00, 26.01, 31.15, 37.82, 44.12, 45.89, 55.91, 55.95, 56.67, 57.17, 64.55, 65.60, 77.65, 111.35, 111.83, 112.36, 111.72, 119.27, 120.18, 129.57, 133.31, 140.98, 147.29, 148.84, 158.45, 167.88.

MS (ESI)  $m/z$  513.29  $[\text{M} + \text{H}]^+$ , calculated 513.32  $[\text{M} + \text{H}]^+$ .

### ***General procedure for coupling of 12a-d with 11a-e to yield 3a-3j***

To a stirred solution of the free amines (12a-d) in acetonitrile under argon was added sequentially *N,N*-Diisopropyl-ethylamine (DIPEA), HATU and the di-ketoacids (11a-e). The reaction mixture was stirred for 16h at room temperature. Saturated  $\text{NH}_4\text{Cl}$  solution was added to the reaction and the solution was stirred for 10 min. The organic phase was separated and the aqueous phase was extracted with ethyl acetate (3x 100ml). The combined organic phases were washed with brine (10ml), dried over  $\text{MgSO}_4$  and the residual solid was purified by column chromatography.

### ***Synthesis of 2-(3-((*R*)-3-(3,4-dimethoxyphenyl)-1-((*S*)-1-(2-((*1S,2R*)-1-hydroxy-2-methylcyclohexyl)-2-oxoacetyl)piperidine-2-carboxyloxy)propyl)phenoxy)acetic acid (3a\*)***

To 12c (211mg, 0.412 mmol) was added DIPEA (160 mg, 1.24 mmol), HATU (234 mg, 0.618 mmol), 11a (92 mg, 0.494 mmol) and the reaction was treated as described above. The residual solid obtained was purified by column chromatography using Hexane: EtOAc 6:4 to yield 3a\* **ester** (46mg, 0.067 mmol, 20%).

TLC (Hexane: EtOAc 6:4):  $R_f$  = 0.41.

HPLC (Gradient A) retention time= 32.1-32.6 min

$^1\text{H}$  NMR (600 MHz,  $\text{CDCl}_3$ )  $\delta$ = 0.84 (t, 3H, J= 5.4 Hz), 1.30-1.41 (m, 6H), 1.47 (m, 9H), 1.61-1.85(m, 7H), 2.00-2.13 (m, 2H), 2.20-2.28(m, 1H), 2.36 (d, 1H, J= 13.8Hz), 2.47-2.61 (m, 2H), 3.10-3.17 (m, 1H), 3.49 (d, 1H, J= 13.2 HZ), 3.85 (s, 6H), 4.53 (s, 2H), 5.29 (s, 1H), 5.74-5.79 (m, 1H), 6.66-6.67 (m, 2H), 6.76-6.78 (m, 1H), 6.81-6.84 (m, 1H), 6.88-6.93 (m, 1H), 6.95-7.00 (m, 1H), 7.25-7.28 (m, 1H).

$^{13}\text{C}$  NMR (150 MHz,  $\text{CDCl}_3$ )  $\delta$ = 16.14, 20.33, 20.92, 25.33, 26.24, 28.02, 29.97, 36.89, 38.05, 44.31, 51.53, 55.80, 65.70, 76.69, 81.21, 82.35, 111.27, 111.68, 113.18, 114.25, 119.85, 120.13, 129.73, 133.47, 141.38, 147.34, 148.83, 158.07, 166.55, 167.87, 169.27, 205.06.

MS (ESI)  $m/z$  682.07  $[\text{M} + \text{H}]^+$ , calculated 682.85  $[\text{M} + \text{H}]^+$ .

**3a\*** ester (46 mg, 0.067 mmol) was treated with 20% TFA in DCM at room temperature. The mixture was allowed to stir for 6h. TFA and DCM was evaporated under reduced pressure to yield the free acid **3a\*** (32mg, 0.051mmol, 77%).

TLC (Hexane: EtOAc: TFA 6:3.9: 0.1): R<sub>f</sub> = 0.33.

HPLC (Gradient A) retention time= 24.6-25.1 min

<sup>1</sup>H NMR (600 MHz, CDCl<sub>3</sub>) δ= 0.82-0.88 (m, 3H), 1.36-1.92 (m, 13H), 2.03-2.13 (m, 2H), 2.23-2.38 (m, 2H), 2.50-2.67 (m, 2H), 3.24-3.31 (m, 1H), 3.48-3.55 (m, 1H), 3.85 (s, 3H), 3.86 (s, 3H), 4.67 (s, 2H), 5.25-5.27 (m, 2H), 5.74-5.77 (m, 1H), 6.56-6.70 (m, 2H), 6.77-6.80 (m, 1H), 6.82-6.87 (m, 1H), 6.89-6.96 (m, 2H), 7.26-7.29 (m, 1H).

<sup>13</sup>C NMR (150 MHz, CDCl<sub>3</sub>) δ= 16.3, 20.16, 20.87, 24.79, 25.29, 26.55, 29.30, 31.35, 35.59, 37.60, 39.45, 44.28, 51.92, 55.87, 55.92, 65.07, 76.86, 82.24, 111.37, 111.70, 115.71, 116.21, 119.71, 120.20, 129.90, 133.21, 141.51, 147.41, 148.89, 157.74, 167.39, 169.20, 171.63, 205.23.

MS (ESI) m/z: found Rt 13.88 min. (Method LCMS), 648.45 [M + Na]<sup>+</sup>,

HRMS 626.2902 [M + H]<sup>+</sup>, calculated 626.2887 [M + H]<sup>+</sup>.

The diastomeric mixture was further separated using preparative HPLC Gradient 62-77% B for 35min to yield diastereomer 3a-1 (6mg) and 3a-2 (9mg).

### **3a-1**

HPLC (Gradient A) retention time= 24.6-24.8min

<sup>1</sup>H NMR (600 MHz, CDCl<sub>3</sub>) δ= 0.82 (d, 3H, J= 5.4 Hz), 1.38-1.43 (m, 2H), 1.44-1.48 (m, 2H), 1.53-1.58 (m, 2H), 1.64-1.70 (m, 3H), 1.74-1.81 (m, 2H), 2.04-2.12 (m, 2H), 2.22-2.28 (m, 1H), 2.52-2.67 (m, 2H), 2.98 (d, 1h, J= 5.4 Hz), 3.08 (s, 1H), 3.12 (s, 1H), 3.25 (dt, 1H, J= 2.4, 13.2 Hz), 3.53 (d, 1H, J=13.2 Hz), 3.64-3.67 (m, 1H), 3.72 (s, 1H), 3.85 (s, 3H), 3.86 (s, 3H), 4.63 (s, 2H), 5.24 (d, 1H, J= 4.8Hz), 5.74-5.80 (m, 1H), 6.66-6.69 (m, 2H), 6.77-6.79 (m, 1H), 6.83-6.94 (m, 3H), 7.26-7.28 (m, 1H).

<sup>13</sup>C NMR (150 MHz, CDCl<sub>3</sub>) δ= 16.15, 20.18, 21.06, 24.79, 25.27, 26.52, 29.68, 31.41, 35.57, 36.61, 37.64, 44.18, 51.88, 55.86, 55.92, 63.81, 81.38, 111.35, 111.68, 115.65, 115.66, 119.54, 120.16, 129.85, 133.19, 141.53, 147.45, 148.93, 157.92, 167.57, 169.26, 169.26, 205.46.

MS (ESI) m/z: found Rt 13.87 min. (Method LCMS), 648.40 [M + Na]<sup>+</sup>, calculated 648.45 [M + Na]<sup>+</sup>.

### **3a-2**

HPLC (Gradient A) retention time= 24.9-25.1min

$^1\text{H}$  NMR (600 MHz,  $\text{CDCl}_3$ )  $\delta$ = 0.84 (d, 3H, J= 6.6Hz), 1.38-1.85 (m, 10H), 2.06 (s, 2H), 2.20-2.31 (m, 1H), 2.49-2.65 (m, 2H), 2.97 (d, 1H, J= 6.6 Hz), 3.05 (s, 1H), 3.12 (s, 1H), 3.25 (t, 1H, J= 12.6Hz), 3.48 (d, 1H, J= 10.8 Hz), 3.65 (s, 1H), 3.72 (s, 2H), 3.84 (s, 3H), 3.85 (s, 3H), 4.81 (s, 2H), 5.26 (s, 1H), 5.74 (s, 1H), 6.66-6.68 (m, 2H), 6.77-6.94 (m, 4H), 7.21-7.24 (m, 1H).

$^{13}\text{C}$  NMR (150 MHz,  $\text{CDCl}_3$ )  $\delta$ = 16.15, 20.21, 20.94, 24.82, 25.31, 26.40, 29.68, 31.35, 35.31, 36.72, 37.15, 42.16, 43.25, 44.25, 44.54, 46.53, 48.81, 51.75, 55.86, 55.92, 56.79, 63.84, 81.66, 111.34, 111.70, 115.51, 119.59, 120.17, 129.82, 133.32, 141.58, 147.41, 148.91, 157.91, 167.37, 169.34, 205.95.

MS (ESI) m/z: found Rt 13.91 min. (Method LCMS), 648.31  $[\text{M} + \text{Na}]^+$ , calculated 648.45  $[\text{M} + \text{Na}]^+$ .

***Synthesis of 3,4-dimethoxyphenethyl 1-(2-((1S,2R)-1-hydroxy-2-methylcyclohexyl)-2-oxoacetyl)piperidine-2-carboxylate (3b\*)***

To **12a** (33mg, 0.112 mmol) was added DIPEA (43.4 mg, 0.336 mmol), HATU (40.5mg, 0.168 mmol) and **11a** (25 mg, 0.134 mmol). The reaction was treated as described above. The residual solid obtained was purified by column chromatography using Hexane: EtOAc 6:4 to yield **3b\*** (25mg, 0.054 mmol, 49%).

TLC (Hexane: EtOAc 6:4): Rf = 0.57.

HPLC (Gradient A) retention time= 25.8-26.2 min

$^1\text{H}$  NMR (600 MHz,  $\text{CDCl}_3$ )  $\delta$ = 0.83 (m, 3H), 1.39-1.77 (m, 14H), 2.07-2.12 (m, 2H), 2.26 (d, 1H, J= 14.4 Hz), 2.89-2.94 (m, 2H), 3.09-3.17 (m, 1H), 3.46 (t, 1H, J= 11.4 Hz), 3.86 (s, 3H), 3.87 (s, 3H), 4.31-4.43 (m, 2H), 5.24 (s, 1H), 6.72-6.81 (m, 3H).

$^{13}\text{C}$  NMR (150 MHz,  $\text{CDCl}_3$ )  $\delta$ = 16.12, 20.35, 20.80, 24.95, 25.37, 26.30, 29.50, 34.56, 35.67, 36.81, 44.04, 51.46, 55.86, 55.91, 65.99, 81.23, 111.29, 111.99, 120.93, 129.85, 147.78, 148.95, 166.83, 169.99, 204.98.

MS (ESI) m/z: found Rt 14.16 min. (Method LCMS), 462.70  $[\text{M} + \text{H}]^+$ , 484.44  $[\text{M} + \text{Na}]^+$ ,

HRMS 462.2944  $[\text{M} + \text{H}]^+$ , calculated 462.2914  $[\text{M} + \text{H}]^+$ .

***Synthesis of 2-(3,4-dimethoxyphenoxy)ethyl 1-(2-((1S,2R)-1-hydroxy-2-methylcyclohexyl)-2-oxoacetyl)piperidine-2-carboxylate (3c\*)***

To **12b** (34.6 mg, 0.112 mmol) was added DIPEA (43.4 mg, 0.336 mmol), HATU (40.5mg, 0.168 mmol) and **11a** (25 mg, 0.134 mmol). The reaction was treated as described above. The residual solid obtained was purified by column chromatography using Hexane : EtOAc 1:1 to yield **3c\*** (33mg, 0.069 mmol, 62%).

TLC (Hexane: EtOAc 1:1): Rf = 0.28.

HPLC (Gradient A) retention time= 25.8-26.2 min

<sup>1</sup>H NMR (600 MHz, CDCl<sub>3</sub>) δ= 0.821 (dd, 3H, J= 6.6Hz), 1.41-1.79 (m, 13H), 2.04-2.13 (m, 1H), 2.35 (d, 1H, J= 13.8 Hz), 3.22- 3.34 (m, 1H), 3.51 (t, 1H, J= 12Hz), 3.83 (s, 3H), 3.85 (s, 3H), 4.13-4.15 (m, 2H), 4.43- 4.56 (m, 2H), 5.30 (d, 1H, J= 5.4Hz), 6.37-6.40 (m, 1H), 6.52 (t, 1H, J= 3Hz), 6.76 (d, 1H, J= 9Hz).

<sup>13</sup>C NMR (150 MHz, CDCl<sub>3</sub>) δ= 16.13, 20.33, 21.06, 24.84, 26.40, 29.47, 34.60, 35.64, 36.82, 44.09, 51.49, 55.85, 56.40, 63.77, 66.35, 81.18, 101.09, 104.07, 111.71, 143.92, 149.88, 152.83, 166.98, 170.03, 205.03.

MS (ESI) m/z: found Rt 13.91 min. (Method LCMS), 478.35 [M + 1]<sup>+</sup>, 500.40 [M + Na]<sup>+</sup>,

HRMS 478.2405 [M + H]<sup>+</sup>, calculated 478.2403 [M + H]<sup>+</sup>.

***2-(3,4-dimethoxyphenoxy)ethyl 1-(2-((1S,2R)-2-ethyl-1-hydroxycyclohexyl)-2-oxoacetyl)piperidine-2-carboxylate (3d\*)***

To **12b** ( 64.4 mg, 0.208 mmol) was added DIPEA (81 mg, 0.624 mmol), HATU (75 mg, 0.312 mmol) and **11b** (50 mg, 0.250 mmol). The reaction was treated as described above. The residual solid obtained was purified by column chromatography using Hexane : EtOAc 1:1 to yield **3d\*** (25 mg, 0.051 mmol, 25%).

TLC (Hexane: EtOAc 6:4): Rf = 0.50.

HPLC (Gradient A) retention time= 25.5-25.9 min

<sup>1</sup>H NMR (600 MHz, CDCl<sub>3</sub>) δ= 0.85-0.88 (m, 3H), 1.41-1.88 (m, 18H), 2.35 (d, 1H, J= 12Hz), 3.22-3.29 (m, 1H), 3.49-3.53 (m, 1H), 3.83 (s, 3H), 3.85 (s, 3H), 4.13-4.16 (m, 2H), 4.35-4.57 (m, 2H), 5.31 (s, 1H), 6.37-6.40 (m, 1H), 6.51-6.53 (m, 1H), 6.77 (d, 1H, J= 9Hz).

<sup>13</sup>C NMR (150 MHz, CDCl<sub>3</sub>) δ= 11.78, 20.66, 20.90, 23.67, 24.94, 25.46, 26.42, 35.91, 43.72, 44.06, 55.85, 56.40, 63.70, 66.36, 82.34, 101.10, 104.08, 111.72, 143.97, 149.88, 152.85, 152.90, 166.82, 170.01, 205.09.

MS (ESI) m/z: found Rt 13.69min. (Method LCMS), 492.21 [M + H]<sup>+</sup>, calculated 492.24 [M + H]<sup>+</sup>.

***Synthesis of (S)-((R)-3-(3,4-dimethoxyphenyl)-1-(3-(2-morpholinoethoxy)phenyl)propyl) 1-(2-((1S,2R)-1-hydroxy-2-methylcyclohexyl)-2-oxoacetyl)piperidine-2-carboxylate (3e\*)***

To **12d** (60mg, 0.117 mmol) was added DIPEA (60 mg, 0.468 mmol), HATU (66mg, 0.175mmol) and **11a** (26 mg, 0.14 mmol) and the reaction was treated as described above. The

residual solid obtained was purified by column chromatography using Hexane : EtOAc 1:1 to yield **3e\*** (41mg, 0.060mmol, 52%).

TLC (DCM: MeOH 9.3:0.7): Rf = 0.50.

HPLC (Gradient A) retention time= 21.1-21.7 min

<sup>1</sup>H NMR (400 MHz, CDCl<sub>3</sub>) δ= 0.79-0.86 (m, 3H), 1.40-1.74 (m, 13H), 1.98-2.38 (m, 7H), 2.48-2.61 (m, 2H), 2.83-2.87 (m, 1H), 2.96-3.05 (m, 2H), 3.09-3.18 (m, 1H), 3.47-3.51 (m, 1H), 3.77-3.85 (m, 11H), 4.17-4.24 (m, 2H), 5.29 (t, 1H, J= 4.4 Hz), 5.74-5.77 (m, 1H), 6.65-6.68 (m, 2H), 6.75-6.78 (m, 2H), 6.81-6.84 (m, 1H), 6.86-6.96 (m, 2H), 7.22-7.27 (m, 1H).

<sup>13</sup>C NMR (100 MHz, CDCl<sub>3</sub>) δ= 16.12, 16.14, 20.25, 20.29, 20.90, 21.11, 24.88, 24.92, 25.32, 25.35, 26.23, 26.32, 29.34, 29.41, 31.17, 31.25, 34.85, 35.31, 36.89, 36.90, 38.01, 38.24, 44.24, 44.29, 51.49, 51.64, 53.67, 53.74, 55.81, 55.90, 57.31, 57.36, 64.82, 64.82, 65.83, 66.03, 77.22, 81.16, 81.23, 111.23, 111.26, 111.65, 111.69, 112.73, 113.06, 114.08, 114.38, 119.23, 119.40, 120.11, 120.13, 129.73, 129.78, 133.30, 133.46, 141.41, 141.59, 147.33, 148.82, 148.85, 158.36, 158.42, 166.59, 166.73, 169.31, 169.40, 205.13, 205.47.

MS (ESI) m/z: found Rt 11.32min. (Method LCMS), 681.38 [M + H]<sup>+</sup>,

HRMS 681.4418 [M + Na]<sup>+</sup>, calculated 681.4373.

**Synthesis of 2-(3-((R)-3-(3,4-dimethoxyphenyl)-1-((S)-1-(2-((1S,2R)-2-ethyl-1-hydroxycyclohexyl)-2-oxoacetyl)piperidine-2-carboxyloxy)propyl)phenoxy)acetic acid (**3f\***)**

To **12c** ( 214mg, 0.416 mmol) was added DIPEA (161 mg, 1.25 mmol), HATU (236 mg, 0.624 mmol) and **11b** (100 mg, 0.499 mmol) and the reaction was treated as described above. The residual solid obtained was purified by column chromatography using Hexane : EtOAc 6:4 to yield **3f\* ester** (62mg, 0.089 mmol, 21%).

TLC (Hexane: EtOAc 6:4): Rf = 0.71.

HPLC (Gradient A) retention time= 32.6-32.9 min

<sup>1</sup>H NMR (600 MHz, CDCl<sub>3</sub>) δ= 0.87 (t, 3H, J= 7.2Hz), 1.28-1.37 (m, 4H), 1.48 (s, 9H), 1.65-1.88 (m, 11H), 2.00-2.09 (m, 1H), 2.20-2.27 (m, 1H), 2.37 (d, 1H, J =13.8Hz), 2.47-2.62 (m, 2H), 3.05-3.20 (m, 1H), 3.49-3.53 (m, 1H), 3.85 (s, 3H), 3.86 (s, 3H), 4.52 (d, 2H, J=4.8 Hz), 5.31 (d, 1H, J= 5.4 Hz), 5.75-5.79 (m, 1H), 6.65-6.67 (m, 2H), 6.76-6.78 (m, 1H), 6.81-6.83 (m, 1H), 6.87-7.00 (m, 2H), 7.25-7.28 (m, 1H).

<sup>13</sup>C NMR (150 MHz, CDCl<sub>3</sub>) δ= 11.78, 20.65, 23.65, 23.66, 24.92, 25.27, 26.26, 28.02, 29.66, 31.17, 35.27, 38.04, 44.28, 51.65, 55.80, 55.90, 65.70, 76.69, 81.99, 82.36, 111.27, 111.68, 113.44, 114.22, 119.87, 120.13, 129.72, 133.48, 141.37, 147.27, 148.83, 156.05, 158.06, 166.58, 167.83, 169.26, 205.17.

MS (ESI) m/z 696.84 [M + H]<sup>+</sup>, calculated 696.72 [M + H]<sup>+</sup>.

**3f\* ester** (62 mg, 0.089 mmol) was treated with 20% TFA in DCM at room temperature. The mixture was allowed to stir for 6h. TFA and DCM was evaporated under reduced pressure to yield the free acid **3f\*** (40mg, 0.062mmol, 80%).

TLC (Hexane: EtOAc: TFA 1:1: 0.2): Rf = 0.45.

HPLC (Gradient A) retention time= 25.3-25.9 min

MS (ESI) m/z: found Rt 15.93 min. (Method LCMS), 662.63 [M + Na]<sup>+</sup>.

HRMS 640.3739[M + H]<sup>+</sup>, calculated 640.3043 [M + H]<sup>+</sup>.

The diastomeric mixture was further separated using preparative HPLC Gradient 65-70% B for 15min to yield diastomer 3f-1 (5mg) and 3f-2 (7mg).

### **3f-1**

HPLC (Gradient A) retention time= 25.3-25.5min

HRMS 640.3773[M + H]<sup>+</sup>, calculated 640.3043 [M + H]<sup>+</sup>.

### **3f-2**

HPLC (Gradient A) retention time= 25.7-25.9min

HRMS 640.3764[M + H]<sup>+</sup>, calculated 640.3043 [M + H]<sup>+</sup>.

### ***Synthesis of (S)-((R)-3-(3,4-dimethoxyphenyl)-1-(3-(2-morpholinoethoxy)phenyl)propyl)-1-(2-((1S,2R)-2-ethyl-1-hydroxycyclohexyl)-2-oxoacetyl)piperidine-2-carboxylate (3g\*)***

To **12d** (60 mg, 0.117 mmol) was added DIPEA (55 mg, 0.425 mmol), HATU (60mg, 0.158 mmol) and **11b** (28 mg, 0.139 mmol) and the reaction was treated as described above. The residual solid obtained was purified by column chromatography using Hexane: EtOAc 1:1 to yield **3g\*** (20mg, 0.028 mmol, 25%).

TLC (DCM: MeOH 9.7: 0.3): Rf = 0.48.

HPLC (Gradient A) retention time= 21.7-22.3 min

<sup>1</sup>H NMR (300 MHz, CDCl<sub>3</sub>) δ= 0.77-0.86 (m, 3H), 1.41-1.74 (m, 15H), 1.96-2.36 (m, 7H), 2.45-2.61 (m, 2H), 2.87-2.89 (m, 1H), 3.00-3.10 (m, 2H), 3.12-3.19 (m, 1H), 3.47-3.51 (m, 1H), 3.77-3.86 (m, 11H), 4.19-4.25 (m, 2H), 5.29 (t, 1H, J= 4.8 Hz), 5.74-5.77 (m, 1H), 6.65-6.69 (m, 2H), 6.76-6.78 (m, 2H), 6.81-6.84 (m, 1H), 6.84-6.98 (m, 2H), 7.23-7.28 (m, 1H).

$^{13}\text{C}$  NMR (75 MHz,  $\text{CDCl}_3$ )  $\delta$ =11.83, 12.40, 20.51, 20.63, 21.55, 22.68, 23.63, 24.93, 25.25, 25.45, 29.36, 30.57, 31.19, 31.29, 31.92, 34.27, 35.56, 38.61, 43.69, 43.77, 44.31, 51.50, 51.62, 53.65, 55.87, 55.95, 57.31, 61.77, 65.56, 70.36, 70.61, 77.22, 82.04, 111.38, 111.78, 113.11, 114.10, 114.42, 120.20, 129.83, 130.91, 133.39, 133.53, 141.61, 147.42, 148.94, 158.32, 158.45, 166.65, 166.69, 169.34, 169.43, 205.13, 205.41.

MS (ESI)  $m/z$ : found Rt 8.95 min. (Method LCMS), 695.45  $[\text{M} + \text{H}]^+$ ,

HRMS 695.4492  $[\text{M} + \text{H}]^+$ , calculated 695.4429  $[\text{M} + \text{H}]^+$ .

***Synthesis of 2-(3-((R)-3-(3,4-dimethoxyphenyl)-1-((S)-1-(2-((1S,2S)-1-hydroxy-2-(hydroxymethyl)cyclohexyl)-2-oxoacetyl)piperidine-2-carbonyloxy)propyl)phenoxy)acetic acid (3h)***

To **12c** (208mg, 0.404 mmol) was added DIPEA (158 mg, 1.22 mmol), HATU (230 mg, 0.608 mmol) and **11c** (120 mg, 0.487 mmol) and the reaction was treated as described above. The residual solid obtained was purified by column chromatography using Hexane: EtOAc 1:1 to yield **3h ester** (60mg, 0.080 mmol, 20%).

TLC (Hexane: EtOAc 1:1): Rf = 0.48.

$^1\text{H}$  NMR (600 MHz,  $\text{CDCl}_3$ )  $\delta$ = 1.26-1.37 (m, 4H), 1.46 (s, 9H), 1.51-1.63 (m, 3H), 1.64-1.79 (m, 5H), 1.96- 2.08 (m, 1H), 2.15-2.26 (m, 2H), 2.33 (d, 1H, J= 14.4 Hz), 2.45-2.62 (m, 2H), 3.13-3.21 (m, 1H), 3.25 (s, 1H), 3.27-3.29 (m, 1H), 3.30 (s, 1H), 3.48-3.53 (m, 1H), 3.55-3.58 (m, 1H), 3.64-3.67 (m, 1H), 3.83-2.84 (m, 6H), 4.44-4.48 (m, 1H), 4.50 (s, 2H), 4.51-4.59 (m, 1H), 5.28 (t, 1H, J= 5.4 Hz), 5.72-5.78 (m, 1H), 6.64-6.67 (m, 2H), 6.75-6.77 (m, 1H), 6.79-6.82 (m, 1H), 6.88-7.00 (m, 2H), 7.23-7.26 (m, 1H).

$^{13}\text{C}$  NMR (150 MHz,  $\text{CDCl}_3$ )  $\delta$ = 14.09, 20.38, 20.40, 22.67, 24.67, 24.72, 24.97, 24.99, 25.12, 25.17, 26.32, 26.46, 29.35, 29.67, 29.69, 31.13, 31.91, 31.92, 35.50, 36.16, 37.98, 38.03, 41.50, 41.64, 44.13, 44.20, 51.60, 51.67, 55.29, 55.35, 55.80, 55.89, 65.69, 69.84, 69.89, 76.56, 76.58, 81.26, 81.28, 82.36, 82.38, 96.39, 96.49, 111.26, 111.67, 113.27, 114.06, 114.13, 119.77, 119.89, 120.13, 129.62, 129.69, 133.40, 133.48, 141.35, 141.54, 147.26, 147.29, 148.82, 148.83, 159.01, 158.04, 165.87, 166.07, 166.81, 167.09, 167.89, 167.90, 169.47, 169.50, 205.48, 206.00

MS (ESI)  $m/z$  764.51  $[\text{M} + \text{Na}]^+$ , calculated 764.36  $[\text{M} + \text{Na}]^+$ .

**3h ester** (60 mg, 0.080 mmol) was treated with 20% TFA in DCM at room temperature. The mixture was allowed to stir for 6h. TFA and DCM was evaporated under reduced pressure to yield the free acid **3h** (16mg, 0.024mmol, 31%).

TLC (Hexane: EtOAc: TFA 6: 4: 0.1): Rf = 0.41.

HPLC (Gradient A) retention time= 25.7-26.1 min

$^1\text{H}$  NMR (600 MHz,  $\text{CDCl}_3$ )  $\delta$ = 1.32-1.88 (m, 13H), 2.02-2.10 (m, 1H), 2.16-2.28 (m, 2H), 2.37-2.40 (m, 1H), 2.51-2.65 (m, 2H), 3.20-3.26 (m, 1H), 3.51-3.59 (m, 1H), 3.60-3.67 (m, 1H), 3.73-3.80 (m, 1H), 3.85 (s, 6H), 4.63-4.70 (m, 2H), 5.32 (d, 1H,  $J$ = 5.4 Hz), 5.73-5.79 (m, 1H), 6.66-6.70 (m, 2H), 6.77-6.80 (m, 1H), 6.84-6.89 (m, 2H), 6.92-6.96 (m, 1H), 7.25-7.29 (m, 1H).

$^{13}\text{C}$  NMR (150 MHz,  $\text{CDCl}_3$ )  $\delta$ = 20.67, 20.80, 21.19, 23.60, 24.92, 25.47, 26.60, 29.68, 31.29, 34.48, 44.50, 44.56, 51.92, 55.91, 65.06, 69.07, 76.67, 81.87, 111.35, 111.72, 115.07, 115.16, 119.99, 120.18, 129.84, 133.26, 141.63, 147.40, 148.85, 157.77, 166.31, 169.38, 169.47, 204.17.

MS (ESI)  $m/z$ : found Rt 13.12 min. (Method LCMS), 642.90  $[\text{M} + \text{H}]^+$ .

HRMS 642.3570  $[\text{M} + \text{H}]^+$ , calculated 642.3536  $[\text{M} + \text{H}]^+$ .

***Synthesis of 2-(3-((R)-3-(3,4-dimethoxyphenyl)-1-((S)-1-(2-((1R,2R)-1-hydroxy-2-methylcyclohexyl)-2-oxoacetyl)piperidine-2-carboxyloxy)propyl)phenoxy)acetic acid (3i\*)***

To **12c** (210mg, 0.412 mmol) was added DIPEA (160 mg, 1.24 mmol), HATU (234 mg, 0.618 mmol) and **11d** (92 mg, 0.494 mmol) and the reaction was treated as described above. The residual solid obtained was purified by column chromatography using Hexane: EtOAc 6:4 to yield **3i\* ester** (38mg, 0.055 mmol, 14%).

**3i\* ester** (38 mg, 0.055 mmol) was treated with 20% TFA in DCM at room temperature. The mixture was allowed to stir for 6h. TFA and DCM was evaporated under reduced pressure to yield the free acid **\*3i** (27mg, 0.043mmol, 77%).

HPLC (Gradient A) retention time=27.3-27.7min

MS (ESI)  $m/z$ : found Rt 15.56 min. (Method LCMS), 648.55  $[\text{M} + \text{Na}]^+$ , calculated 648.45  $[\text{M} + \text{Na}]^+$ .

The diastomeric mixture was further separated using preparative HPLC Gradient 61-71% B for 20min to yield diastomer 3i-1 (5mg) and 3i-2 (8mg).

**3i-1**

HPLC (Gradient A) retention time= 27.2-27.4min.

$^1\text{H}$  NMR (600 MHz,  $\text{CDCl}_3$ )  $\delta$ = 0.82 (d, 3H,  $J$ = 6.6 Hz), 1.36-1.51 (m, 3H), 1.54-1.59 (m, 2H), 1.65-1.72 (m, 3H), 1.77-1.82 (m, 1H), 1.92 (d, 1H,  $J$ = 12.6 Hz), 2.03-2.13 (m, 2H), 2.23-2.30 (m, 1H), 2.37 (d, 1H,  $J$ = 14.4 Hz), 2.52-2.68 (m, 2H), 3.54 (d, 1H,  $J$ = 12.6Hz), 3.64-3.65 (m,

1H), 3.72 (s, 3H), 3.85 (s, 3H), 3.86 (s, 3H), 4.67 (s, 2H), 5.25 (d, 1H, J= 5.4 Hz), 5.75-5.77(m, 1H), 6.67-6.70 (m, 2H), 6.77-6.80 (m, 1H), 6.83 (s, 1H), 6.89-6.94 (m, 2H), 7.27-7.29 (m, 1H). MS (ESI) m/z: found Rt 15.51 min. (Method LCMS), 648.59 [M + Na]<sup>+</sup>, calculated 648.45 [M + Na]<sup>+</sup>.

### **3i-2**

HPLC (Gradient A) retention time= 27.3-27.6min.

<sup>1</sup>H NMR (600 MHz, CDCl<sub>3</sub>) δ= 0.85 (d, 3H, J= 6.6Hz), 1.37-1.86 (m, 12H), 2.02-2.14 (m, 2H), 2.23-2.29 (m, 1H), 2.36 (d, 1H, J= 14.2 Hz), 2.52-2.66 (m, 2H), 3.65 (d, 1H, J= 5.4 Hz), 3.73 (s, 3H), 3.85 (s, 3H), 3.86 (s, 3H), 4.68 (s, 2H), 5.27 (d, 1H, J= 5.4 Hz), 5.74 -5.79 (m, 1H), 6.65-6.70 (m, 2H), 6.79 (d, 1H, J= 7.8 Hz), 6.81-6.95 (m, 3H), 7.24-7.29 (m, 1H).

MS (ESI) m/z: found Rt 15.67 min. (Method LCMS), 648.51 [M + Na]<sup>+</sup>, calculated 648.45 [M + Na]<sup>+</sup>.

### *Synthesis of 2-(3-((R)-3-(3,4-dimethoxyphenyl)-1-((S)-1-(2-((1R,2R)-2-ethyl-1-hydroxycyclohexyl)-2-oxoacetyl)piperidine-2-carbonyloxy)propyl)phenoxy)acetic acid (3j\*)*

To **12c** (21.4mg, 0.041mmol) was added DIPEA (15.1 mg, 0.117 mmol), HATU (23.7 mg, 0.063 mmol) and **11e** (10.0 mg, 0.05 mmol) and the reaction was treated as described above. The residual solid obtained was purified by column chromatography using Hexane: EtOAc 6:4 to yield **3j\* ester** (6.6 mg, 0.009 mmol, 22%).

TLC (Hexane: EtOAc 6: 4): R<sub>f</sub> = 0.46.

HPLC (Gradient A) retention time= 31.5-31.9 min

MS (ESI) m/z 662.55 [M – tBu + Na]<sup>+</sup>, calculated 662.54 [M – tBu + Na]<sup>+</sup>.

**3j\* ester** (6.6 mg, 0.009 mmol) was treated with 20% TFA in DCM at room temperature. The mixture was allowed to stir for 6h. TFA and DCM was evaporated under reduced pressure to yield the free acid **3j\*** (5.7 mg, 0.007 mmol, 91%).

TLC (Hexane: EtOAc: TFA 1:1: 0.1): R<sub>f</sub> = 0.35.

HPLC (Gradient A) retention time= 25.6-26.1 min

MS (ESI) m/z: found Rt 14.29min. (Method LCMS), 662.55 [M + Na]<sup>+</sup>,

HRMS 640.3063 [M + H]<sup>+</sup>, calculated 640.3043 [M + H]<sup>+</sup>.

**Supporting Information.** Reaction schemes of intermediates. This material is available free of charge via the Internet at <http://pubs.acs.org>.

### Crystallography

Crystals and Co-crystals of the FKBP51 Fk1 domain construct comprising residues 16-140 and containing mutation A19T were obtained as previously described<sup>18</sup>. Diffraction data were collected at the European Synchrotron Radiation Facility (ESRF) in Grenoble, France. The data were processed with MOSFLM<sup>40</sup> and XDS<sup>41</sup>, SCALA<sup>42</sup> and TRUNCATE<sup>43</sup>. The crystal structures were solved by molecular replacement employing the program MOLREP<sup>44</sup>. The dictionaries for the ligand compounds were generated with the PRODRG server<sup>45</sup>. The structures were refined with REFMAC<sup>46</sup>. Manual model building was performed with COOT<sup>47</sup>. Molecular-graphics figures were generated using PyMOL (<http://www.pymol.org>).

### Acknowledgement:

We thank Dr. Gerd Rüter and the Lead Discovery Center (Dortmund) for providing building block **5b** and **5c** and Drs. B. Gold and E.R. Sanchez for providing a sample of Timcodar. We are indebted to Claudia Dubler (LMU, Munich, Germany) and Elisabeth Weyher (MPI of Biochemistry, Martinsried, Germany) for NMR spectroscopy and HRMS measurements respectively. We thank Prof. Florian Holsboer for continuous and generous financial support. Support by the Joint Structural Biology Group at the ESRF beamlines is gratefully acknowledged.

### Reference:

- (1) Gaali, S.; Gopalakrishnan, R.; Wang, Y.; Kozany, C.; Hausch, F. The Chemical Biology of Immunophilin Ligands. *Curr. Med. Chem.* 2011, *18*, 5355-5379.
- (2) Huse, M.; Chen, Y.-G.; Massague, J.; Kuriyan, J. Crystal Structure of the Cytoplasmic Domain of the Type I TGF [beta] Receptor in Complex with FKBP12. *Cell* 1999, *96*, 425-436.
- (3) Riggs, D. L.; Roberts, P. J.; Chirillo, S. C.; Cheung-Flynn, J.; Prapapanich, V. et al. The Hsp90-binding peptidylprolyl isomerase FKBP52 potentiates glucocorticoid signaling in vivo. *Embo J* 2003, *22*, 1158-1167.
- (4) Wochnik, G. M.; Ruegg, J.; Abel, G. A.; Schmidt, U.; Holsboer, F. et al. FK506-binding Proteins 51 and 52 Differentially Regulate Dynein Interaction and Nuclear Translocation of the Glucocorticoid Receptor in Mammalian Cells. *J. Biol. Chem.* 2005, *280*, 4609-4616.

- (5) Davies, T. H.; Ning, Y.-M.; Sanchez, E. R. Differential control of glucocorticoid receptor hormone-binding function by tetratricopeptide repeat (TPR) proteins and the immunosuppressive ligand FK506. *Biochemistry* 2005, *44*, 2030-2038.
- (6) Periyasamy, S.; Hinds, T., Jr.; Shemshedini, L.; Shou, W.; Sanchez, E. R. FKBP51 and Cyp40 are positive regulators of androgen-dependent prostate cancer cell growth and the targets of FK506 and cyclosporin A. *Oncogene* 2010, *29*, 1691-1701.
- (7) Ni, L.; Yang, C. S.; Gioeli, D.; Frierson, H.; Toft, D. O. et al. FKBP51 promotes assembly of the Hsp90 chaperone complex and regulates androgen receptor signaling in prostate cancer cells. *Mol Cell Biol* 2010, *30*, 1243-1253.
- (8) Binder, E. B. The role of FKBP5, a co-chaperone of the glucocorticoid receptor in the pathogenesis and therapy of affective and anxiety disorders. *Psychoneuroendocrinology* 2009, *34*, S186-S195.
- (9) Attwood, B. K.; Bourgognon, J. M.; Patel, S.; Mucha, M.; Schiavon, E. et al. Neuropsin cleaves EphB2 in the amygdala to control anxiety. *Nature* 2011, *473*, 372-375.
- (10) Hartmann, J.; Wagner, K. V.; Liebl, C.; Scharf, S. H.; Wang, X. D. et al. The involvement of FK506-binding protein 51 (FKBP5) in the behavioral and neuroendocrine effects of chronic social defeat stress. *Neuropharmacology* 2011.
- (11) Touma, C.; Gassen, N. C.; Herrmann, L.; Cheung-Flynn, J.; Bull, D. R. et al. FK506 Binding Protein 5 Shapes Stress Responsiveness: Modulation of Neuroendocrine Reactivity and Coping Behavior. *Biol Psychiatry* 2011.
- (12) O'Leary, J. C., 3rd; Dharia, S.; Blair, L. J.; Brady, S.; Johnson, A. G. et al. A New Anti-Depressive Strategy for the Elderly: Ablation of FKBP5/FKBP51. *PLoS One* 2011, *6*, e24840.
- (13) Babine, R. E.; Villafranca, J. E.; Gold, B. G. FKBP immunophilin patents for neurological disorders. *Expert Opin Ther. Patents* 2005, *15*, 555-573.
- (14) Wang, X. J.; Etzkorn, F. A. Peptidyl-prolyl isomerase inhibitors. *Biopolymers* 2006, *84*, 125-146.
- (15) Keenan, T.; Yaeger, D. R.; Courage, N. L.; Rollins, C. T.; Pavone, M. E. et al. Synthesis and activity of bivalent FKBP12 ligands for the regulated dimerization of proteins. *Bioorg Med Chem* 1998, *6*, 1309-1335.
- (16) Holt, D. A.; Luengo, J. I.; Yamashita, D. S.; Oh, H. J.; Konilian, A. L. et al. Design, synthesis, and kinetic evaluation of high-affinity FKBP ligands and the X-ray crystal structures of their complexes with FKBP 12. *J Am Chem Soc* 1993, *115*, 9925-9938.

- (17) Kozany, C.; Marz, A.; Kress, C.; Hausch, F. Fluorescent probes to characterise FK506-binding proteins. *Chembiochem* 2009, *10*, 1402-1410.
- (18) Bracher, A.; Kozany, C.; Thost, A. K.; Hausch, F. Structural characterization of the PPIase domain of FKBP51, a cochaperone of human Hsp90. *Acta Crystallogr D Biol Crystallogr* 2011, *67*, 549-559.
- (19) Paulini, R.; Muller, K.; Diederich, F. Orthogonal multipolar interactions in structural chemistry and biology. *Angew Chem Int Ed Engl* 2005, *44*, 1788-1805.
- (20) Birge, R. B.; Wadsworth, S.; Akakura, R.; Abeysinghe, H.; Kanojia, R. et al. A role for schwann cells in the neuroregenerative effects of a non-immunosuppressive fk506 derivative, jnj460. *Neuroscience* 2004, *124*, 351-366.
- (21) Bull, D. J.; Maguire, R. J.; Palmer, M. J.; Wythes, M. J. Heterocyclic compounds as inhibitors of rotamase enzymes. *WO/1999/045006* 1999.
- (22) Varray, S.; Gauzy, C.; Lamaty, F.; Lazaro, R.; Martinez, J. Synthesis of cyclic amino acid derivatives via ring closing metathesis on a poly(ethylene glycol) supported substrate. *J Org Chem* 2000, *65*, 6787-6790.
- (23) Stivanello, M.; Leoni, L.; Bortolaso, R. Synthesis of 1,5-bis(triphenylphosphonium)pentan-3-ol dichloride and its application to the preparation of 1,7-di(pyridin-3-yl)heptan-4-ol. *Organic Process Research & Development* 2002, *6*, 807-810.
- (24) Steiner, J. P.; Hamilton, G. S.; Ross, D. T.; Valentine, H. L.; Guo, H. et al. Neurotrophic immunophilin ligands stimulate structural and functional recovery in neurodegenerative animal models. *Proc Natl Acad Sci U S A* 1997, *94*, 2019-2024.
- (25) Riggs, D. L.; Cox, M. B.; Tardif, H. L.; Hessling, M.; Buchner, J. et al. Noncatalytic role of the FKBP52 peptidyl-prolyl isomerase domain in the regulation of steroid hormone signaling. *Mol Cell Biol* 2007, *27*, 8658-8669.
- (26) Wilson, K. P.; Yamashita, M. M.; Sintchak, M. D.; Rotstein, S. H.; Murcko, M. A. et al. Comparative X-ray structures of the major binding protein for the immunosuppressant FK506 (tacrolimus) in unliganded form and in complex with FK506 and rapamycin. *Acta Crystallogr D Biol Crystallogr* 1995, *51*, 511-521.
- (27) Teague, S. J.; Stocks, M. J. The Affinity of the Excised Binding Domain of Fk-506 for the Immunophilin Fkbp12. *Bioorganic & Medicinal Chemistry Letters* 1993, *3*, 1947-1950.

- (28) Birkenshaw, T. N.; Caffrey, M. V.; Cladingboel, D. E.; Cooper, M. E.; Donald, D. K. et al. Synthetic Fkbp12 Ligands - Design and Synthesis of Pyranose Replacements. *Bioorganic & Medicinal Chemistry Letters* 1994, 4, 2501-2506.
- (29) Caffrey, M. V.; Cladingboel, D. E.; Cooper, M. E.; Donald, D. K.; Furber, M. et al. Synthesis and Evaluation of Dual Domain Macrocyclic Fkbp12 Ligands. *Bioorganic & Medicinal Chemistry Letters* 1994, 4, 2507-2510.
- (30) Mase, N.; Inoue, A.; Nishio, M.; Takabe, K. Organocatalytic alpha-hydroxymethylation of cyclopentanone with aqueous formaldehyde: easy access to chiral delta-lactones. *Bioorganic & Medicinal Chemistry Letters* 2009, 19, 3955-3958.
- (31) Chen, A. Q.; Xu, J.; Chiang, W.; Chai, C. L. L. L-Threonine-catalysed asymmetric alpha-hydroxymethylation of cyclohexanone: application to the synthesis of pharmaceutical compounds and natural products. *Tetrahedron* 2010, 66, 1489-1495.
- (32) Kim do, H.; Kim, K.; Chung, Y. K. A facile synthesis of the basic steroidal skeleton using a Pauson-Khand reaction as a key step. *J Org Chem* 2006, 71, 8264-8267.
- (33) Crabbe, P.; Dollat, J.-M.; Gallina, J.; Luche, J.-L.; Velarde, E. et al. Steric course of cross coupling of organocopper reagents with allylic acetates. *Journal of the Chemical Society, Perkin Transactions 1* 1978, 730-734.
- (34) Leibrock, B.; Vostrowsky, O.; Hirsch, A. Synthesis of new cyclic homoconjugated oligodiacylenes. *European Journal of Organic Chemistry* 2001, 4401-4409.
- (35) Tatlock, J. H.; Kalish, V. J.; Parge, H. E.; Knighton, D. R.; Showalter, R. E. et al. High-affinity FKBP-12 ligands derived from (R)-(-)-carvone. Synthesis and evaluation of FK506 pyranose ring replacements. *Bioorganic & Medicinal Chemistry Letters* 1995, 5, 2489-2494.
- (36) Wu, Y. L.; Li, L. S. An efficient method for synthesis of alpha-keto acid esters from terminal alkynes. *Tetrahedron Letters* 2002, 43, 2427-2430.
- (37) Liu, K. G.; Yan, S.; Wu, Y. L.; Yao, Z. J. A new synthesis of Neu5Ac from D-glucono-delta-lactone. *J Org Chem* 2002, 67, 6758-6763.
- (38) Tatlock, J. H. Oxidation of Alkynyl Ethers with Potassium-Permanganate - a New Acyl Anion Equivalent for the Preparation of Alpha-Keto Esters. *Journal of Organic Chemistry* 1995, 60, 6221-6223.
- (39) Armistead, M. D.; Harding, W. M.; Boger, S. J. Biologically active acylated amino acid derivatives. *US6187784* 1998.
- (40) Leslie, A. G. W. Recent changes to the MOSFLM package for processing film and image plate data. *Jnt CCP4/ESF-EACMB Newsl. Protein Crystallogr.* 1992, 26.

- (41) Kabsch, W. Xds. *Acta Crystallographica Section D-Biological Crystallography* 2010, 66, 125-132.
- (42) Evans, P. R. SCALA. *Jnt CCP4/ESF-EACMB Newsl. Protein Crystallogr.* 1997, 33, 22-24.
- (43) French, S.; Wilson, K. Treatment of Negative Intensity Observations. *Acta Crystallographica Section A* 1978, 34, 517-525.
- (44) Vagin, A.; Teplyakov, A. Molecular replacement with MOLREP. *Acta Crystallographica Section D-Biological Crystallography* 2010, 66, 22-25.
- (45) Schuttelkopf, A. W.; van Aalten, D. M. F. PRODRG: a tool for high-throughput crystallography of protein-ligand complexes. *Acta Crystallographica Section D-Biological Crystallography* 2004, 60, 1355-1363.
- (46) Murshudov, G. N.; Skubak, P.; Lebedev, A. A.; Pannu, N. S.; Steiner, R. A. et al. REFMAC5 for the refinement of macromolecular crystal structures. *Acta Crystallographica Section D-Biological Crystallography* 2011, 67, 355-367.
- (47) Emsley, P.; Lohkamp, B.; Scott, W. G.; Cowtan, K. Features and development of Coot. *Acta Crystallographica Section D-Biological Crystallography* 2010, 66, 486-501.

## Supporting Information

### Evaluation of Synthetic FK506 Analogs as Ligands for FKBP51 and FKBP52

Ranganath Gopalakrishnan<sup>1</sup>, Christian Kozany<sup>1</sup>, Steffen Gaali<sup>1</sup>, Christoph Kress<sup>1</sup>, Bastiaan Hoogeland<sup>1</sup>, Andreas Bracher<sup>2</sup>, Felix Hausch<sup>1\*</sup>.

#### Supporting Information Table of Contents:

**Scheme S1** Enantioselective synthesis of Compound **5a** and **5b**

**Scheme S2** Synthesis of pipercolic acid analogs.

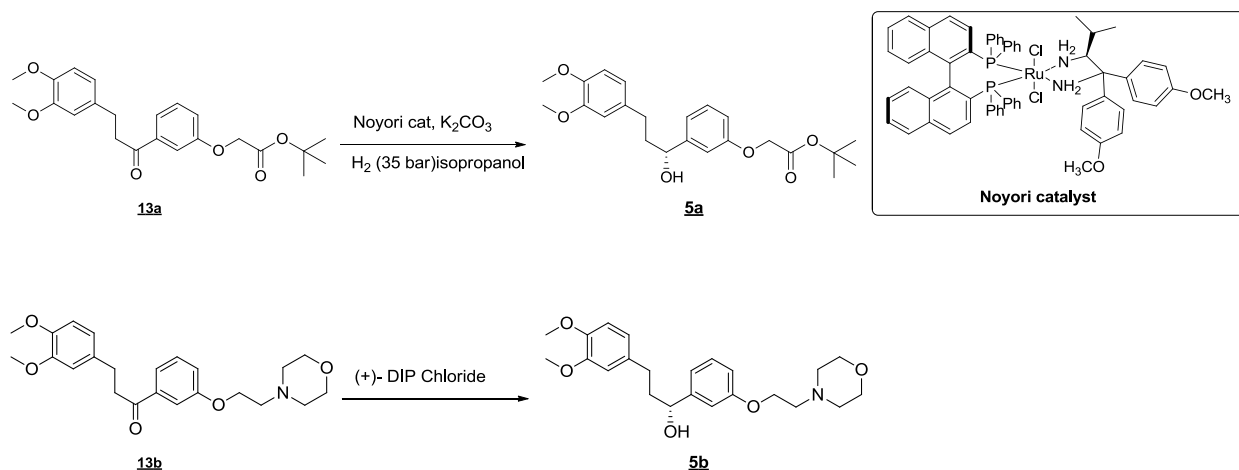
**Scheme S3**

**Scheme S4** Synthesis scheme of compound **6d**

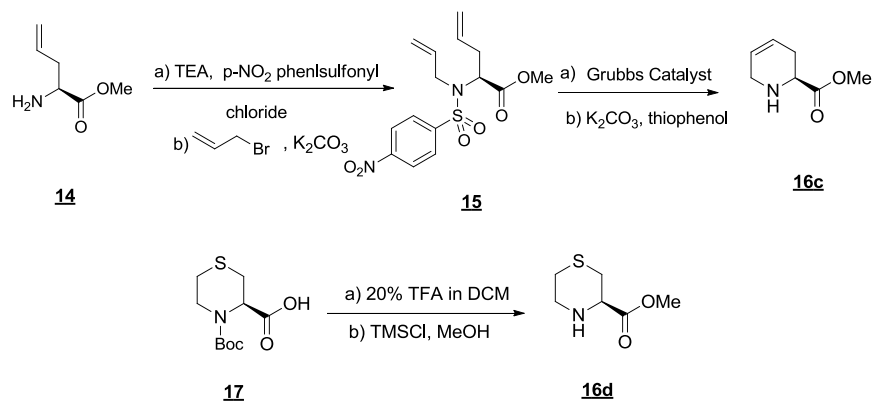
**Scheme S5**

**Scheme S6** Synthesis scheme of compound **6h**

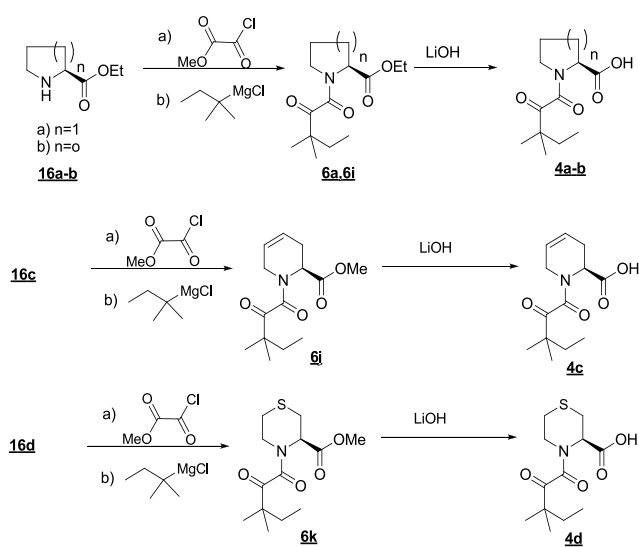
**Table-S1** Data collection and Refinement Statistics (crystallographic data)

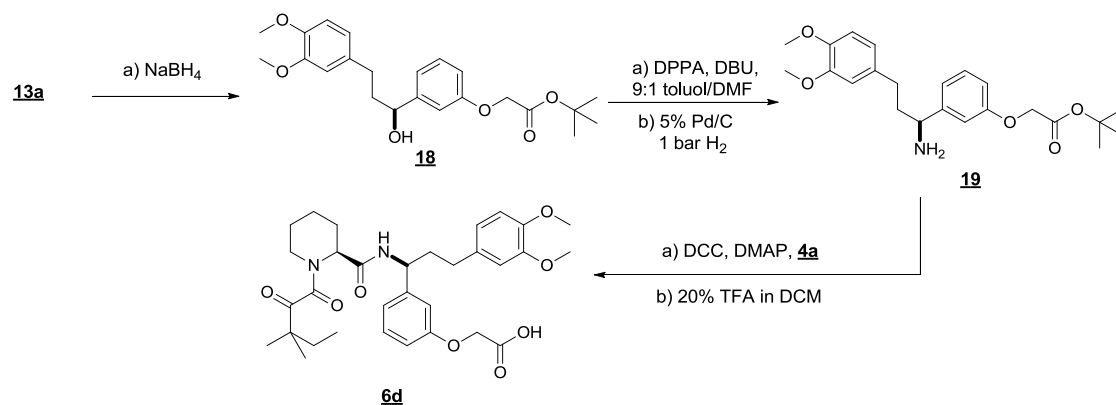
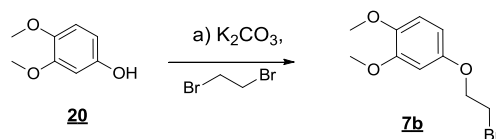
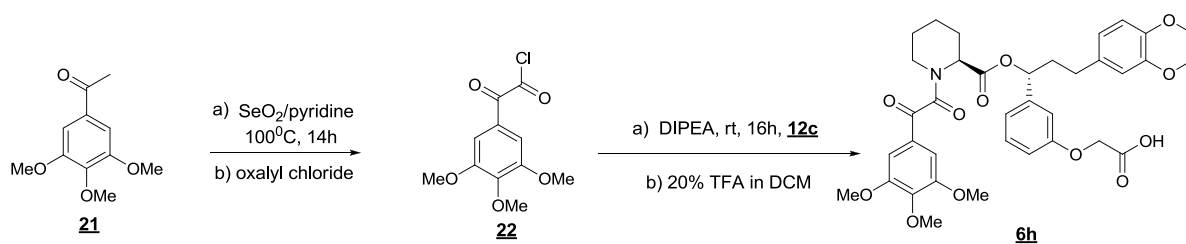
Scheme S1 Enantioselective synthesis of Compound **5a** and **5b**

## Scheme S2 Synthesis of pipercolic acid analogs



## Scheme S3



**Scheme S4** Synthesis scheme of compound **6d****Scheme S5****Scheme S6** Synthesis scheme of compound **6h**

**Table-S1 Data collection and Refinement Statistics**

Dataset	PDB code4DRK	PDB code4DRM	PDB code4DRN	PDB code4DRO	PDB code4DRP
Ligand	2a	3f-1 soak	3f-1 cocryst	3f-2 soak	3f-2 cocryst
Beamline	ESRF, ID23-1	ESRF, ID14-1	ESRF, ID23-1	ESRF, ID14-1	ESRF, ID23-1
wavelength (Å)	0.9757	0.933	0.900	0.933	0.900
space group	<i>P2<sub>1</sub>2<sub>1</sub>2<sub>1</sub></i>	<i>P2<sub>1</sub>2<sub>1</sub>2<sub>1</sub></i>	<i>P2<sub>1</sub>2<sub>1</sub>2<sub>1</sub></i>	<i>P2<sub>1</sub>2<sub>1</sub>2<sub>1</sub></i>	<i>P2<sub>1</sub>2<sub>1</sub>2<sub>1</sub></i>
cell dimensions, a, b, c (Å);	56.16, 62.29, 69.68;	42.16, 55.27, 56.82;	49.27, 52.54, 57.02;	42.19, 54.79, 56.74;	49.91, 56.56, 57.59;
$\alpha, \beta, \gamma$ (°)	90, 90, 90	90, 90, 90	90, 90, 90	90, 90, 90	90, 90, 90
resolution limits (Å)*	30.40 – 1.5 (1.58 – 1.5)	42.15 - 1.48 (1.56 - 1.48)	25.06 - 1.07 (1.13 – 1.07)	33.43 - 1.1 (1.16 - 1.1)	25.38 - 1.79 (1.89 - 1.79)
Rmerge ***	0.085 (0.381)	0.066 (0.477)	0.045 (0.576)	0.067 (0.353)	0.062 (0.190)
I/sigma ***	14.8 (4.2)	11.3 (2.4)	13.2 (1.8)	10.3 (3.1)	12.4 (3.5)
multiplicity *	6.5 (6.2)	3.5 (3.4)	3.7 (3.7)	2.4 (2.4)	3.3 (2.3)
completeness (%) *	99.7 (98.7)	99.5 (97.1)	95.2 (91.4)	99.7 (98.7)	97.5 (84.0)
Wilson B-factor (Å <sup>2</sup> )	11.13	13.31	8.05	6.06	20.88
<b>Refinement</b>					
resolution range	20 – 1.5	20 - 1.48	20 – 1.07	20 - 1.1	20 - 1.8
reflections (test set)	37697 (1995)	21603 (1135)	59549 (3141)	51373 (2699)	14559 (769)
Rcryst	0.1658	0.1760	0.1548	0.1477	0.2200
Rfree	0.1995	0.2082	0.1724	0.1725	0.2609
number of atoms	2610	1299	1364	1357	1205
r.m.s.d. bonds (Å)	0.014	0.015	0.011	0.013	0.013
r.m.s.d. angles (°)	1.579	1.604	1.600	1.613	1.472
Ramachandran plot					
% most favored region***	98.94	98.71	97.3	98.9	99.21
% additionally allowed***	0	0.92	1.8	0	0

\* Values in parenthesis for outer shell.

\*\* As defined in Scala.

\*\*\* As defined in Coot.

### 1.2.2.1.1 Discussion (Manuscript-2)

In this study an extensive SAR analysis of  $\alpha$ -ketoamide containing pipercolates as binders for FKBP51 and FKBP52 was carried out. This class of compounds has been extensively studied and validated for their binding to FKBP12. Here a direct comparison of the binding affinities of these compounds between FKBP12 and larger FKBP5s has been studied.

Starting from the X-ray crystal structure of the lead compound (**2a**), a structure-based design approach was followed to study the contributions of each substructure on the binding affinity for FKBP51 and FKBP52. Firstly, the pipercolate core which is present in **2a** and the natural product was substituted with other core structures (**2b**, **2c** and **2d**). The pipercolate core was found to be essential for binding to the larger FKBP5s. Next the effect of top group modifications on the binding affinity was studied. Larger top group substituents (**2a**, **6e**) were found to have better binding affinity as compared to the smaller top groups (**6a**, **6b** and **6c**). The morpholine top group was found to have the best binding affinity as compared to all other substituents. To further optimize the ligand for their binding affinity, the pipercolic core and the larger top groups were kept constant for the rest of the studies.

Next the interaction with the 80s loop was investigated in detail for gaining affinity and selectivity as both the proteins have a structural divergence in this loop. The tert-pentyl group in the lead compound (**2a**) was proposed to be substituted with a substituent that closely mimics the pyranose group in the natural products FK506 and Rapamycin. The cyclohexyl group was chosen as the pyranose oxygen in FK506 and Rapamycin is dispensable and has been shown to have no interaction with the protein surface<sup>102</sup>. This substitution resulted in compound **3a\*** having 2-5 fold better affinity to the larger FKBP5s as compared to **2a**. Next an extensive SAR around the cyclohexyl group was carried out to systematically understand the importance of the C<sup>10</sup>-and C<sup>11</sup>-substituents. First the role of C<sup>11</sup>-substituent on the cyclohexyl moiety was investigated. A series of cyclohexyl containing compounds were synthesized with varying chain length at the C<sup>11</sup>-methyl substituent (**3a\***, **3f\***, **3h\***). The binding affinity of this series of compounds was similar for the larger FKBP5s thereby concluding that chain length or substitution of carbon with oxygen doesn't affect the binding affinity.

Finally, analogs were designed to investigate the effect of stereochemistry at the C<sup>11</sup>-methyl and C<sup>10</sup>-OH on the binding affinities. This series comprised of the diastereomeric mixture **3a\***, **3f\***, **3i\*** and **3j\***. All these compounds surprisingly had equivalent binding affinities. This observation was unexpected. The natural diastereomers **3a\***, **3f\*** (stereochemistry at C<sup>10</sup> and C<sup>11</sup>

similar to FK506 and Rapamycin) were expected to bind to the protein with a similar binding mode as the natural compound. The unnatural diastereomers **3i\*** and **3j\*** on the other hand were hypothesized to bind weakly as hydrogen bond between OH<sup>10</sup>-Asp<sup>68</sup> and the hydrophobic 80s loop contacts of the C<sup>11</sup>-methyl/ethyl substituents was not possible simultaneously. To further dissect the above observations with respect to the pure diastereomers, the individual diastereomers **3a-1**, **3a-2**, **3i-1**, **3i-2**, **3f-1** and **3f-2** of the diastereomer mixture **3a\***, **3i\*** and **3f\*** were separated. All these compounds were found to have equivalent binding to the FKBP5s. From the above set of compounds we could thus conclude that the stereochemistry at the C<sup>10</sup> and C<sup>11</sup> was not important. This observations concluded from the binding studies were further supported by X-ray co-crystal structures (**3f-1**, **3f-2**).

The X-ray co-crystal structure showed that the binding mode of both the compounds in the active site of FKBP51 was similar. In case with **3f-1** all three hydrogen bonds observed in the co-crystal structure of FK506 are conserved. In **3f-2** the cyclohexyl ring is flipped and the hydrogen bond between HO<sup>10</sup>-**3f-1** and O-Asp<sup>68</sup> is not present. But the retention of the binding affinity can be argued owing to the fact there is presence of an additional water mediated hydrogen bond with Tyr<sup>113</sup> and Ser<sup>118</sup> of FKBP51 and C<sup>10</sup>-OH of **3f-2**.

This elaborate study thus helps us to conclude that the stereochemistry at the hydroxyl and the methyl substituent on the pyranose ring of FK506 and Rapamycin are not important to gain affinity towards the protein subtypes. Overlay of different FKBP51 FK1 domain co-crystal has shown the 80s loop to be flexible. We thus infer that it is this loop flexibility that might make the FKBP5s tolerant towards subtle changes in the stereochemistry around the cyclohexyl group. The rationale for binding of all the diastereomers with multiple binding modes and conserved 80s loop interaction can thus be explained.

### 1.2.2.2 Exploration of Pipecolate Sulfonamides as Binders of the FK506-Binding Proteins 51 and 52 (Manuscript 3)

The electrophilicity of the  $\alpha$ -keto amide moiety present in most of the non-immunosuppressive FK506 analogs (as well as in the compounds of manuscript 2) is an undesired reactive liability that could result in metabolic instability or potential toxicity. In the second approach a bioisosteric replacement of the  $\alpha$ -keto amide moiety of Rapamycin and FK506 with a sulfonamide was envisaged with the retention of the conserved hydrogen bonds. For a rapid and efficient derivatization of a focused sulfonamide library we envisaged a solid phase synthesis strategy which led to ligands with submicromolar affinity for FKBP51 or with 4-fold selectivity versus FKBP52. The molecular binding mode for one sulfonamide analog was confirmed by X-ray crystallography.

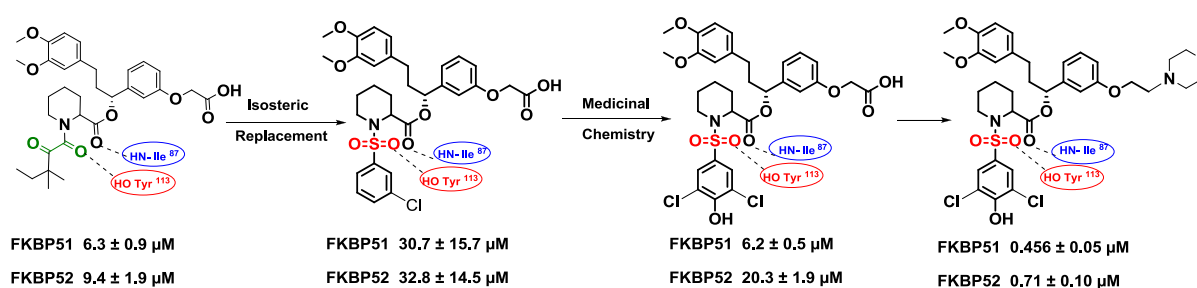


**Figure 14:** Prototypic sulfonamide containing analogs.

#### Own Contributions:

In the attached manuscript my personal contributions have been the following:

1. Establishment of the solid support synthesis protocol (Scheme-1) and the solution phase protocol (Scheme-2). Synthesis, purification and structural characterization of all compounds except compound 38 and 39.
2. Characterization of the final compounds in the fluorescence polarization assay, supported by B. Hoogeland and C. Kozany. Data analysis of the tested compounds.

## Exploration of Pipecolate Sulfonamides as Binders of the FK506-Binding Proteins 51 and 52

**Ranganath Gopalakrishnan**<sup>1</sup>, Christian Kozany<sup>1</sup>, Yansong Wang<sup>1</sup>, Sabine Schneider<sup>3</sup>, Bastiaan Hoogeland<sup>1</sup>, Andreas Bracher<sup>2</sup>, Felix Hausch<sup>1\*</sup>

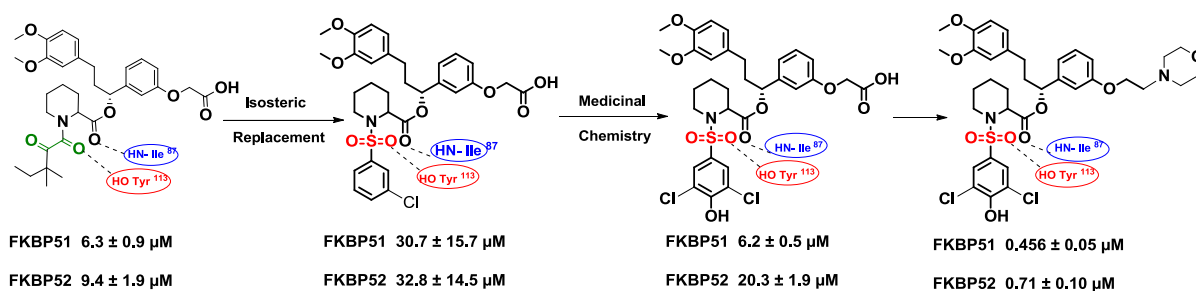
<sup>1</sup>Max Planck Institute of Psychiatry, Kraepelinstr. 2, 80804 Munich, Germany,

<sup>2</sup>Max Planck Institute of Biochemistry, Am Klopferspitz 18, 82152 Martinsried, Germany

<sup>3</sup>Technical University Munich, Department Chemie, Lichtenbergstr. 4, 85747 Garching, Germany

Correspondence: Email: [hausch@mpipsykl.mpg.de](mailto:hausch@mpipsykl.mpg.de), phone: +49(89)30622640, fax: +49(89)30622610

**Abstract:** FK506-binding proteins (FKBP) 51 and 52 are co-chaperones that modulate the signal transduction of steroid hormone receptors. Single nucleotide polymorphisms in the gene encoding FKBP51 have been associated with a variety of psychiatric disorders. Rapamycin and FK506 are two macrocyclic natural products, which tightly bind to all these proteins. A bio-isosteric replacement of the  $\alpha$ -ketoamide moiety of rapamycin and FK506 with a sulfonamide was envisaged with the retention of the conserved hydrogen bonds. A focused solid support-based synthesis protocol was developed, which led to ligands with submicromolar affinity for FKBP51 and FKBP52. The molecular binding mode for one sulfonamide analog was confirmed by X-ray crystallography.



## Introduction:

Members of the FKBP (FK506-binding protein) family display peptidyl prolyl isomerase (PPIase) activity and bind to the immunosuppressive natural products FK506 and rapamycin. The prototypical FKBP12 is the most widely studied member of this family. In complex with FKBP12, FK506 and rapamycin also interact with and inhibit calcineurin (CaN) and mTOR, respectively, thereby mediating their immunosuppressive action. Prior studies led to analogs devoid of immunosuppressive activity<sup>1-3</sup>, as exemplified by compound **2** (Fig. 1)<sup>4</sup>. The high molecular weight multi-domain homologs of FKBP12, FKBP51, and FKBP52 act as co-chaperones for the heat shock protein 90 (Hsp90) and modulate the signal transduction of the glucocorticoid receptor in a mutually antagonistic direction<sup>5-7</sup>. Human genetic studies have shown single nucleotide polymorphisms in the gene encoding FKBP51 to be associated with various stress-related psychiatric disorders<sup>8</sup>. Recent characterization of FKBP51 knockout mice has further validated these findings<sup>9-12</sup>. To further dissect the role of larger FKBP51 and to better understand the underlying biology, selective inhibitors targeting FKBP51 are required. Neither FK506 nor rapamycin can be used as tools as they have nearly equipotent affinities for all FKBP51s.

Extensive medicinal chemistry campaigns on analogs of FK506 and rapamycin have shown that the two conserved hydrogen bonds shown in Fig. 1 are required for binding to FKBP51. The electrophilicity of the  $\alpha$ -ketoamide moiety present in most of the non-immunosuppressive FK506 analogs is an undesired reactive liability that could result in metabolic instability or potential toxicity. For FKBP12 it has been shown that the  $\alpha$ -ketoamide can be bioisosterically replaced by a sulfonamide moiety to yield compounds that retain binding to FKBP12<sup>2,13-15</sup>.

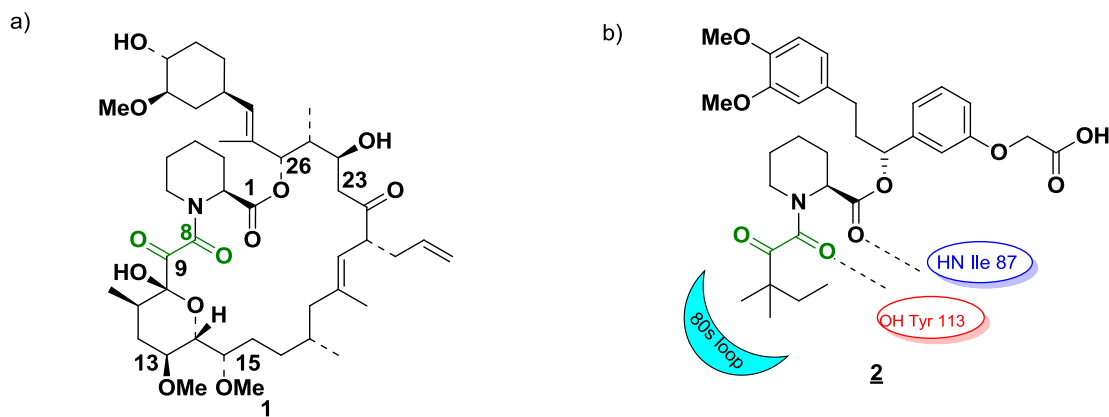


Fig. 1 Natural and synthetic ligands that bind to large FKBP. (a) Structure of FK506 (**1**). (b) The prototypic synthetic ligand **2**, which is devoid of immunosuppressive activity. Key hydrogen bonds with FKBP51 are indicated by dotted lines; the position of the 80s loop interacting with the tert-pentyl moiety is indicated in cyan.

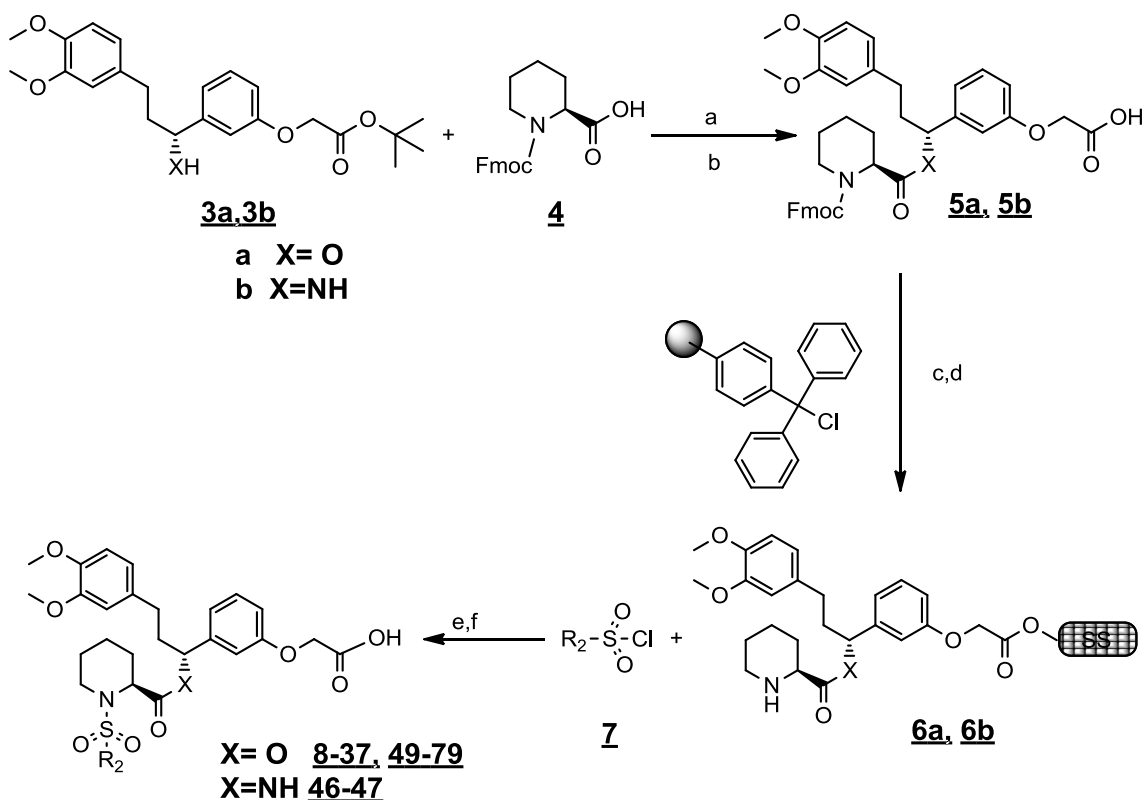
However, these compounds have not been tested for their binding profile with the larger FKBP. Until very recently, compound **2** has been the only synthetic ligand tested for its binding affinity for FKBP51. In quest for finding improved inhibitors of FKBP51 or FKBP52 we envisaged a solid phase synthesis methodology for the synthesis of pipercolate sulfonamide compounds to gain insight into the structure activity relationship (SAR) of this series for the larger FKBP isoforms.

## Results and Discussion:

### Chemistry:

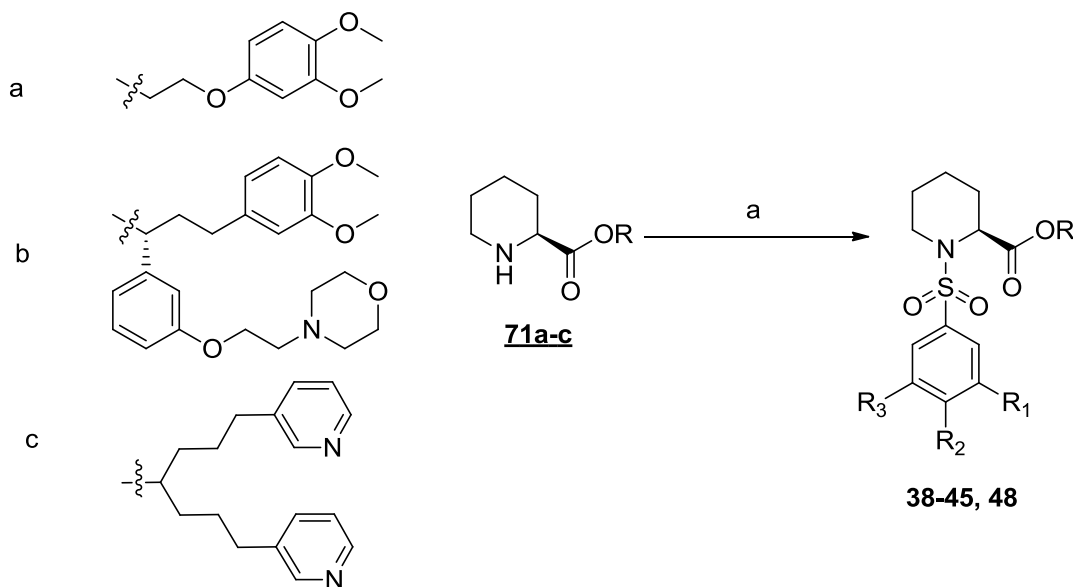
**Strategy:** A three-dimensional alignment of the FK506-binding domains of FKBP51(3O5E)<sup>16</sup>, FKBP52 (to be published) and FKBP12 (2PPN)<sup>17</sup> revealed the largest structural divergences close to the binding pocket at the 80s loop (Ser<sup>118</sup>-Ile<sup>122</sup> of FKBP51/52). The 80s loop of FKBP51 contains Leu<sup>119</sup> which is replaced by Pro<sup>119</sup> in FKBP52 possibly contributing for the structural difference in this region. Importantly, the residue at position 119 was shown to be a major functional determinant for the effect on steroid hormone receptor<sup>18</sup>. Hence an optimization of interactions with this part of the protein has a higher probability of achieving selectivity and functional relevance within the FKBP family. The X-ray structures of FK506 with the FK1 domain of FKBP51 (3O5R) and FKBP52 (unpublished) confirmed that the pyranose group in FK506 (**1**) contacts the 80s loop. Sulfonamide substituents as replacements of the pyranose group have been shown to have contact with the 80s loop in FKBP12<sup>2,13,14,19</sup>. Compound **2**, until very recently the only known synthetic FKBP51 ligand, was chosen as a starting point for the synthesis of sulfonamide analogs. For a rapid derivatization of compounds targeting the 80s loop we envisaged a solid phase strategy for synthesis of a focused sulfonamide library.

**Solid phase synthesis of a focused sulfonamide library:** The precursor **3** was synthesized as described<sup>20</sup>. This was further coupled with the pipercolic acid **4** followed by liberation of the acid to give the building block **5**. The latter was anchored on a 2-chloro trityl resin.

Scheme-1<sup>a</sup>. Synthesis of the pipecolate framework

<sup>a</sup> Reagents and conditions : (a) DCC, DMAP, 0 °C to r.t., 20h (for 3a); HATU, DIPEA, r.t., 2h (for 3b)  
 (b) 20% TFA in CH<sub>2</sub>Cl<sub>2</sub>, r.t., 6h. (c) DIPEA, CH<sub>2</sub>Cl<sub>2</sub>, r.t., 16h; and DIPEA, methanol, r.t., 4h. (d) 20%  
 4-methyl-piperidine, CH<sub>2</sub>Cl<sub>2</sub>, r.t., 1h. (e) DIPEA, CH<sub>2</sub>Cl<sub>2</sub>, r.t., 16h. (f) 1% TFA in CH<sub>2</sub>Cl<sub>2</sub>, r.t., 1h.

The immobilized building block was deprotected to give **6** and was further reacted with a library of commercial sulfonyl chlorides **7**. Cleavage from the solid support under mild acidic conditions yielded compounds **8-37**, **49-79** and **46, 47**. This solid support protocol was used for the synthesis of a small focused library followed by primary screening as well as for the resynthesis of hits for further characterization. The best sulfonamide analogs of this series were further attached to pipecolate core where the free acid moiety in **8-37**, **49-79** was exchanged by a morpholine group in **40-45** (scheme 2).

**Scheme-2<sup>a</sup>. Synthesis of the various top groups containing sulfonamide**

<sup>a</sup> Reagent and conditions : (a) DIPEA, RSO<sub>2</sub>Cl, CH<sub>2</sub>Cl<sub>2</sub>, r.t., 16h.

**Biology:**

The sulfonyl chloride building blocks were designed to initially probe a variety of aliphatic and aromatic sulfonyl moieties as well as substituents around the aromatic rings. Out of 36 compounds in the medium-throughput screening, 28 compounds inhibited tracer binding to FKBP12 by more than 15% while 8 compounds displayed inhibition of more than 85% at 5  $\mu$ M (supplementary information and Table-1). 7 compounds inhibited the tracer binding to the FK1 domain of FKBP52 by more than 15% at 5  $\mu$ M, whereas 5 hits were identified for the FK1 domain of FKBP51. The initial screening assay results indicated that sulfonamides can be surrogates of the  $\alpha$ -ketoamides in the context of this scaffold, but that efficient binding critically depended on the nature of the sulfonamide substituent, at least for the larger FKBP. In general, the inhibitory activity was much higher for FKBP12 than for the larger FKBP. This could be related to the core structure **6** which was designed and optimized for FKBP12 as well as to the more concave 80s loop of FKBP12.

The most promising compounds **8-12** from the primary screening were selected, resynthesized in larger scale and characterized in more detail. The binding affinities of all sulfonamide hits were weaker for all tested FKBP compared to the reference compound **2**. However, in general, the affinity for FKBP12 was compromised in a stronger way than those for the larger FKBP.

Compounds **9** and **10** turned out to have the highest binding affinity for FKBP51 and 52 and were further evaluated in two series (Table-2).

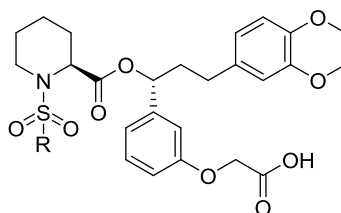


Table-1 Binding affinities for the primary hits towards FKBP paralogs.

Compd. No.	R	Purity %	FKBP12			FKBP51FK1			FKBP52FK1		
			IC <sub>50</sub> ( $\mu$ M)								
<b>2</b>		>99	0.114 $\pm$ 0.015	6.3 $\pm$ 0.9	9.37 $\pm$ 1.9						
<b>8</b>		>99	1.8 $\pm$ 0.1	62.8 $\pm$ 10.7	>100						
<b>9</b>		>98	1.2 $\pm$ 0.2	30.7 $\pm$ 15.7	32.8 $\pm$ 14.5						
<b>10</b>		>99	1.1 $\pm$ 0.1	11.6 $\pm$ 1.1	32.5 $\pm$ 3.5						
<b>11</b>		>96	10.1 $\pm$ 1.0	>100	>100						
<b>12</b>		>99	4.6 $\pm$ 0.15	67.1 $\pm$ 12.1	>100						

Binding affinity to FKBP12, FKBP51 (FK1 domain) and FKBP52 (FK1 domain) determined by a fluorescence polarization assay<sup>21</sup>.

**Exploration of the SAR:** The first series of derivatives probed the influence of the substituent at the meta position. The compounds in this series included m-CN **13**, m-NO<sub>2</sub> **14**, m-NH<sub>2</sub> **15**, m-(2-methylpyrimidin-4-yl) **16**, m-(pyrimidin-4-yl) **17**, m-F **18**, and m-Br **19** aromatic sulfonamides. All these compounds had binding affinity between 0.3-10  $\mu$ M for FKBP12. The meta-substituted halogen derivatives had better binding affinity to the larger FKBP, among these **19** being the best. Compound **15** was synthesized by reduction of the nitro group in **14**.

The m-CN **13**, m-NO<sub>2</sub> **14** and m-NH<sub>2</sub> **15** analogs had slightly reduced binding affinities to the FKBP5s compared to the m-Cl aromatic sulfonamide **9**, while compound **16** and **17** were inactive for the larger FKBP5s.

We next set out to explore multi-substituted aromatic sulfonamide groups. The di-chloro substituted aromatic sulfonamide **20** had slightly better binding affinity than the mono meta-chloro substituted aromatic sulfonamide **9** (Table-2). In contrast, an additional chloro-substituent in the para-position **21** was found to substantially reduce binding to the FKBP5s. A similar result was found for the meta, para-dimethoxy substituted sulfonamide **22** but, interestingly, compound **23** having an m-Cl, p-OMe substitution had better binding affinity. This series of compounds indicated the following SAR m-di-Cl > m-Cl > m,p-di-Cl >> p-Cl >> o-Cl for the aryl sulfonamide substituents.

To further explore the acceptable nature of the groups at the meta positions the derivatives m-difluoro **24**, 3,5-bis(trifluoromethyl) **25**, 3-bromo-5-(trifluoromethyl) **26**, and 3,5-bis(carboxymethyl) **27** were synthesized. Compound **24** had reduced affinity compared to the mono-fluoro substituted analog **18**, while the three other compounds were inactive for FKBP51 or FKBP52. This series led us to conclude that a halogen is a preferred substituent at the meta-position for the larger FKBP5s (Table-2).

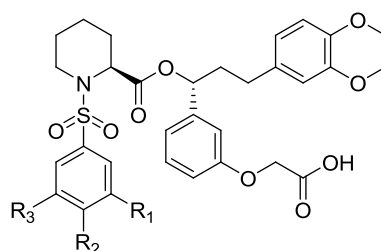


**Table-2** Meta substituted analogs synthesized for SAR extrapolation.

Compd. No	R1	R2	R3	Purity %	FKBP12	FKBP51FK1		FKBP52FK1	
						IC <sub>50</sub> (μM)			
<b>13</b>	CN	H	H	>98	3.8 ± 0.3	28.5 ± 9.6	69.9 ± 65.4		
<b>14</b>	NO <sub>2</sub>	H	H	>98	1.9 ± 0.13	47.2 ± 7.1	>100		
<b>15</b>	NH <sub>2</sub>	H	H	>99	1.9 ± 0.2	45.4 ± 13.1	>100		

<u>16</u>		H	H	>99	$8.1 \pm 1.2$	>100	>100
<u>17</u>		H	H	>99	$9.1 \pm 0.7$	>100	>100
<u>18</u>	F	H	H	>99	$1.09 \pm 0.07$	$54.05 \pm 7.0$	$84.5 \pm 51.00$
<u>19</u>	Br	H	H	>99	$0.32 \pm 0.03$	$15.78 \pm 1.25$	$15.69 \pm 6.84$
<u>20</u>	Cl	H	Cl	>99	$0.80 \pm 0.08$	$22.6 \pm 8.2$	$14.3 \pm 1.8$
<u>21</u>	Cl	Cl	H	>99	$6.1 \pm 5.7$	>100	>100
<u>22</u>	OMe	OMe	H	>96	$7.6 \pm 1.9$	>100	>100
<u>23</u>	Cl	OMe	H	>99	$0.60 \pm 0.07$	$29.6 \pm 1.9$	$40.3 \pm 5.1$
<u>24</u>	F	H	F	>98	$1.00 \pm 0.06$	$88.2 \pm 11.6$	Not measured
<u>25</u>	CF <sub>3</sub>	H	CF <sub>3</sub>	>99	$5.1 \pm 0.4$	>100	>100
<u>26</u>	CF <sub>3</sub>	H	Br	>99	$2.4 \pm 0.2$	>100	>100
<u>27</u>	COO Me	H	COOMe	>98	$4.5 \pm 0.5$	>100	>100
<u>28</u>	Cl	OH	Cl	>99	$0.67 \pm 0.04$	$6.2 \pm 0.5$	$20.3 \pm 1.9$
<u>29</u>	Cl	OMe	Cl	>99	$0.23 \pm 0.02$	$16.4 \pm 1.7$	$17.7 \pm 1.6$
<u>30</u>	Cl	N-Ac	Cl	>98	$1.18 \pm 0.04$	$16.1 \pm 0.96$	$20.5 \pm 2.7$
<u>31</u>	OMe	OMe	COOH	>98	No binding	No binding	No binding
<u>32</u>	NO <sub>2</sub>			>98	$1.5 \pm 0.14$	$27.2 \pm 3.1$	$43.9 \pm 10.1$
<u>33</u>	NH <sub>2</sub>			>98	$2.57 \pm 0.55$	>100	>100
<u>34</u>	H			>98	$1.2 \pm 0.09$	$18.4 \pm 1.4$	$26.5 \pm 4.9$

<u>35</u>	H		>99	0.021 ± 0.02	14.7 ± 1.1	66.5 ± 27.1
<u>36</u>	H		>99	0.66 ± 0.05	>100	>100
<u>37</u>	H		>98	0.75 ± 0.04	>100	>100

The purity of the compounds was confirmed using HPLC. The binding affinity of the compounds to FKBP12, FKBP51 (FK1 domain) and FKBP52 (FK1 domain) was determined by a fluorescence polarization assay<sup>21</sup>.

The second series of sulfonamide derivatives was designed to probe the substitution pattern at the fused thiazole ring of compound **10**. A substitution by methyl at C-2 resulted in compound **34** which had equivalent binding to **10**. Conversion to the corresponding benzothiazol-2(3H)-one **35** resulted in nanomolar affinity for FKBP12, low micromolar binding for FKBP51 and high micromolar affinity to FKBP52. The reasons for this striking selective preference for FKBP12 are currently unknown. However, the sulfur in the meta-position seems to be extremely important since substitution by a methylene as in **36** or oxygen **37** resulted in a dramatic loss of affinity for all FKBP (Table-2).

**X-Ray Crystal Structure.** The X-ray crystal structure of the FK506-binding domain of FKBP51 complexed with ligand **20** was solved to 1.0 Å resolution. In this complex, FKBP51 adopts the same folding topology as found in FKBP51 complexed with **1** and **2**. Compared to the latter structures Asp<sup>68</sup> moves into the binding pocket, while Tyr<sup>113</sup> and Ser<sup>118</sup> move out. The ligand adopts a similar binding mode compared to that of **1** or **2** with the common pipecolate ring being nearly superimposable (Fig. **2b**). The pipecolyl ring of each ligand sits atop the indole of Trp<sup>90</sup>, which forms the floor of the FKBP binding pocket. Similar to FK506 the C<sup>1</sup>-carbonyl of the pipecolate forms a hydrogen bond with the backbone amide of Ile<sup>87</sup>. One oxygen of the sulfonamide (S=O<sub>A</sub>) engages the ε-hydrogen of Phe<sup>130</sup> and the hydroxyl group of Tyr<sup>113</sup>. This latter contact is substantially longer (3.37Å) compared to the corresponding hydrogen bonds formed between Tyr<sup>113</sup> and the C<sup>8</sup>-carbonyl groups of α-ketoamides like FK506, **2** or analogs thereof. The p-oxygen of Tyr<sup>113</sup> engages in a rather short dipolar contact with the C<sup>1</sup>-carbonyl of **20** (3.06Å). Similar although less intense dipolar interactions have also been observed in FKBP51-complexes with FK506 and **2**. FKBP51 and **20** engage in a number of aromatic CH ⋯ O-acceptor interactions, e.g., the oxygen of the sulfonamide (S=O<sub>B</sub>) and the

$\epsilon$ -hydrogens of Tyr<sup>57</sup>, Phe<sup>67</sup> and Phe<sup>130</sup>. These interactions correspond to the contacts formed by the C<sup>9</sup>-keto group of FK506 with the same residues of FKBP51 thereby confirming that the sulfonamide is a bioisosteric mimic of the  $\alpha$ -ketoamide moiety. As expected, the dichloro aryl ring sits below the 80s loop and packs on Ile<sup>122</sup>. The two ortho-hydrogens of the sulfonylphenyl ring form close contacts (2.95Å) with the p-oxygen of Tyr<sup>113</sup> and with carboxylate of Asp<sup>68</sup>, respectively. One of the aromatic chlorines might form a van-der-Waals contact with Lys<sup>121</sup>, while the other chlorine engages Ser<sup>118</sup>. For the latter, two conformations seem possible, one compatible with a hydrogen bond to the aromatic chlorine, the other with a linear C-Cl $\cdots$ O geometry consistent with a halogen bond<sup>22,23</sup>. The dimethoxyphenyl and acetoxyphenyl rings were poorly resolved in the electron density map indicating strong disorder. In the most populated conformer the top group is rotated by 120° compared to compound **2**, most likely stabilized by  $\pi$ - $\pi$  stacking interactions between the acetoxyphenyl ring B and the dichloro aryl substituent of the sulfonamide. The dimethoxyphenyl ring A stacks on the edge of Phe<sup>77</sup> and points into a solvent channel. Its ortho-hydrogen forms an aromatic hydrogen bond (d=2.97Å) to the backbone carbonyl of Gln<sup>85</sup>.

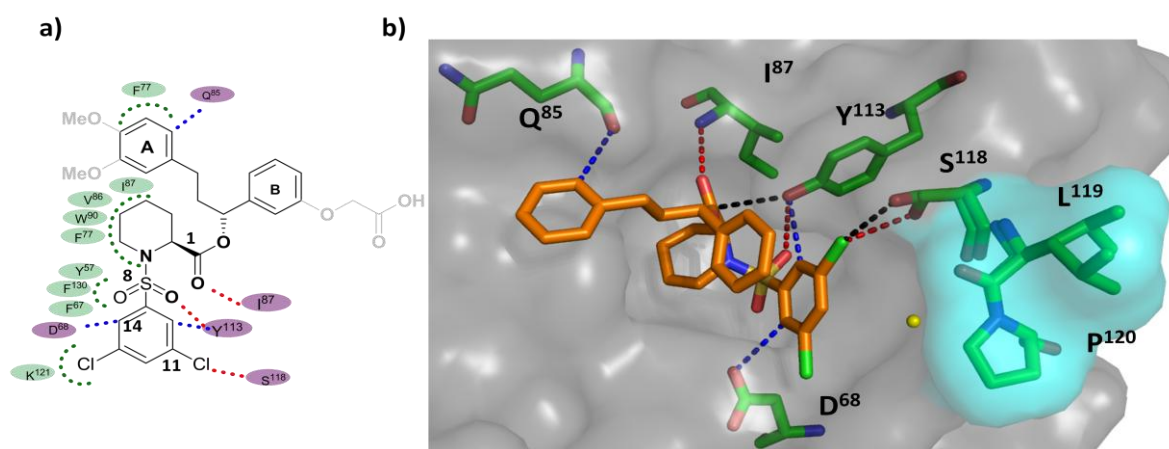


**Fig. 2** X-ray crystal structure of **20** in complex with the FK1 domain of FKBP51. (a) Chemical structure of **20**. Hydrophobic contacts with FKBP51 are indicated in green, hydrogen bonds are shown as dotted lines in pink, aromatic hydrogen bonds are indicated in blue and the unresolved groups are in grey. (b) **20** bound to the FK1 domain of FKBP51. The three hydrogen bonds between O<sup>1</sup>-**20** and HN-Ile<sup>87</sup>, between O<sup>8</sup>-**20** and HO-Tyr<sup>113</sup>, and between Cl<sup>11</sup> and O-S<sup>118</sup> are shown as dotted red lines. The dipolar interaction between the C<sup>1</sup>-carbonyl and HO-Tyr<sup>113</sup> and the halogen bond between Cl<sup>11</sup> and O-S<sup>118</sup> are shown in black. Aromatic hydrogen bonds between ring A and Gln<sup>85</sup>, C<sup>10</sup>-H and OH-Tyr<sup>113</sup>, C<sup>14</sup>-H and OH-Asp<sup>68</sup> are shown in blue. Leu<sup>119</sup> and Pro<sup>120</sup> at the top of the 80s loop are colored in cyan and the conserved water below the 80s loop is shown in yellow.

## SAR extension

The X-ray co-crystal structure of the sulfonamide **20** revealed a water molecule engaged in a hydrogen bond with the amide of Lys<sup>121</sup> that is situated close to the para-position of the sulfonamide aromatic ring (Fig. 2b). Water molecules below Pro<sup>120</sup> of the 80s loop have been observed in several FKBP51 crystal structures<sup>16</sup> (unpublished observations). We therefore explored whether this conserved water molecule could be engaged by substituents in the para-position of the sulfonamide aromatic ring. Introduction of a p-OH substituent in compound **28** did not affect the affinity for FKBP51 while improving the selectivity vs. FKBP52 three-fold (Table-2). A similar trend was observed for the p-NHAc substituted analog **30**, but not in the p-OMe substituted analog **29**. The tri-substituted analog **33** had similar affinities compared to the corresponding mono-substituted derivative **15**, whereas for **32** the affinities were slightly increased compared to **14**. The tri-substituted analog **31** was inactive, similar to the disubstituted analog **22**.

## Modification of the top group

The charged carboxylic acid attached to ring B in the above series is likely to reduce the cell permeability of these compounds. To remove this undesired property the free acid moiety was replaced by various groups as shown in Scheme 2 to yield compounds **38-48**. Simplified substituents at C-1 as in compounds **38** and **39** resulted in complete loss of activity for the large FKBP5s. The next series of compounds included the substitution of the free acid moiety with a morpholine group. Surprisingly, in the morpholine-series phenyl sulfonamides substituted with meta-dichloro **40**, with meta-dichloro, p-OMe **41** and the benzothiazole analog **42** were inactive for all FKBP5s including FKBP12 (Table-3). This could be attributed in part to a detection limit imposed by the lower solubility of these compounds. In striking contrast, the meta-dichloro, para-hydroxy substituted analog **42** displayed submicromolar affinities for all tested FKBP5s. This potency and the almost equal affinity for the large FKBP5s vs. FKBP12 is remarkable, especially when compared to the very close analogs **22** (carboxyl group instead of morpholine), **40**, **43** (para-hydrogen or para-methoxy instead of para-hydroxy) and **45** (para NH-acetyl). A similar unexpected activity was observed for the morpholine-containing benzothiazol-2(3H)-one analog **44** which was much more active than thiazole-containing analog **41** or the carboxyl-derivative **35**. The affinity of **44** rivaled those of the natural product

FK506 (Table-2). The molecular underpinnings for the extraordinary activities of 42 and 44 remain to be established.

Last but not the least we replaced the pipercolate C<sup>1</sup> ester by an amide (46, 47), which completely abolished the binding to larger FKBP. Compound 47 retained substantial binding to FKBP12 in line with the preference of this substituent for FKBP12 observed with 44. The loss of binding affinity of 46 and 47 can be attributed to the additional hydrogen bond donor that would point in the direction of the aromatic ring when bound in a homologous binding mode as 20. Finally, in 48 the top group was replaced by a symmetric top group as present in Biricodar<sup>3</sup> which resulted in equivalent affinity as 28.

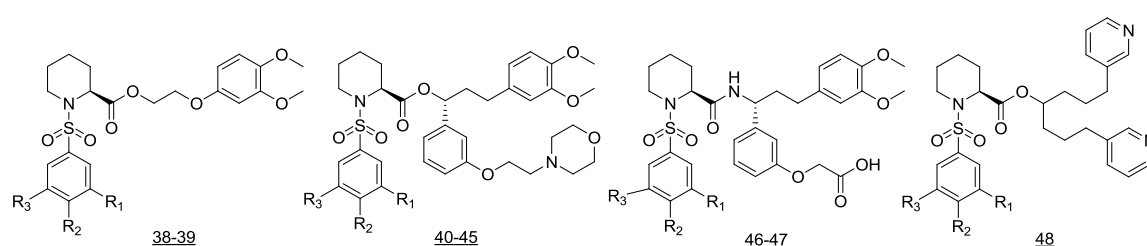


Table-3. FKBP binding affinity of sulfonamides with different pipercolate ester substituents

Compd. No.	R1	R2	R3	Purity %	FKBP12	FKBP51FK1	FKBP52FK1
						IC <sub>50</sub> ( $\mu$ M)	
<u>38</u>	Cl	H	Cl	>98	>100	>100	>100
<u>39</u>	H			>99	0.20 $\pm$ 0.10	66.27 $\pm$ 37.9	>100
<u>40</u>	Cl	H	Cl	>99	>50 $\mu$ M <sup>a</sup>	>50 $\mu$ M <sup>a</sup>	>50 $\mu$ M <sup>a</sup>
<u>41</u>	H			>98	>50 $\mu$ M <sup>a</sup>	>50 $\mu$ M <sup>a</sup>	>50 $\mu$ M <sup>a</sup>
<u>42</u>	Cl	OH	Cl	>99	0.115 $\pm$ 0.014	0.456 $\pm$ 0.05	0.71 $\pm$ 0.10
<u>43</u>	Cl	OMe	Cl	>99	>50 $\mu$ M <sup>a</sup>	>50 $\mu$ M <sup>a</sup>	>50 $\mu$ M <sup>a</sup>
<u>44</u>	H			>99	0.003 $\pm$ 0.0005	2.03 $\pm$ 0.09	3.41 $\pm$ 0.42
<u>45</u>	Cl	N-Ac	Cl	>99	0.45 $\pm$ 0.03	12.3 $\pm$ 18.9	8.3 $\pm$ 6.8

<u>46</u>	Cl	OH	Cl	>99	>100	>100	>100
<u>47</u>	H			>99	1.4 ± 0.21	>100	>100
<u>48</u>	Cl	OH	Cl	>99	0.87 ± 0.07	9.69 ± 0.76	15.13 ± 0.23

<sup>a</sup> Low solubility impaired binding measurements.

**Conclusion:** Using a bioisosteric replacement strategy we converted the  $\alpha$ -ketoamide motif derived from FK506 and rapamycin into a sulfonamide motif with conservation of the hydrogen bond pattern as confirmed by the co-crystal structure of 20. By using a solid phase synthesis protocol we were able to generate, screen and optimize a focused library of these compounds. This led to the identification of aromatic sulfonamides with soft substituents in the meta-position as preferred binders of the larger FKBP51 and FKBP52 compared to the starting compound 2. The most advanced compound 42 is the best synthetic ligand known for the large FKBP51 and FKBP52. Compound 44 has exceptionally high affinity for FKBP12 rivaling those of the natural products FK506 and rapamycin.

### Experimental section:

**Chemistry:** All solvents were purchased from Roth, reagents were bought from Aldrich-Fluka and the sulfonyl chlorides were obtained from Maybridge, Sigma Aldrich, ABCR or AKos, unless otherwise stated.

Chromatographic separations were performed either by manual flash chromatography or by automated flash chromatography using an Interchim-Puriflash 430 with a UV detector. Extracts were dried over MgSO<sub>4</sub> and the solvents were removed under reduced pressure. Merck F-254 commercial plates were used for analytical TLC to follow the course of reaction and visualized by UV light at either 254 or 365 nm. Silica gel 60 (Merck 70-230 mesh) was used for column chromatography. NMR spectra of all compounds were obtained from the Department of Chemistry and Pharmacy, LMU, on a Bruker AC 300, a Bruker XL 400, or a Bruker AMX 600 at room temperature in deuterio-CDCl<sub>3</sub> with tetramethylsilane (TMS) as internal standard, unless otherwise stated. Mass spectra (m/z) were recorded on a Thermo Finnigan LCQ DECA XP Plus mass spectrometer at the Max Planck Institute of Psychiatry, while the high resolution mass spectrometry was carried out at the MPI for Biochemistry (Microchemistry Core Facility) on a Varian Mat711 mass spectrometer.

HPLC analysis was carried out using a Jupiter 4  $\mu\text{m}$  Proteo column (250 x 4.6 mm, 5 $\mu\text{m}$  particle size), **Wavelength:** 224nm, 280nm; **Flow rate:** 1ml/min; **Buffer A:** 0.1% TFA in 5% MeCN/water; **Buffer B:** 0.1% TFA in 95% MeCN/water; **Gradient A:** After 1min elution with 100% buffer A, linear gradient of 0-100% buffer B for 30 min.

**Method LCMS:** YMC Pro C-8 (100 x 4.6 mm, 3 $\mu\text{m}$  particle size) column, **Wavelength:** 224nm, 280nm; **Flow rate:** 1ml/min; **Buffer A:** 0.1% HCOOH in 5% MeCN/water; **Buffer B:** 0.1% HCOOH in 95% MeCN/water; **Gradient B:** 1min 100% buffer A, then linear gradient of 0-100% buffer B for 11 min.

Final compounds were purified using a preparative HPLC Jupiter 10 $\mu\text{m}$  Proteo (250 x 21.7 mm, 10 $\mu\text{m}$  particle size) column. Compounds were dissolved in 40% buffer B and the purification was carried out with an injection loop volume of 2ml. **Wavelength:** 224nm; **Flow rate:** 25ml/min; **Buffer A:** 0.1% TFA in 5% MeOH/Water; **Buffer B:** 0.1% TFA in 95% MeOH/water; **Gradient C:** 40% B, then a linear gradient of 60-70% B for 15 min.

*Synthesis of 2-(3-((1R)-1-(1-(((9H-fluoren-9-yl)methoxy)carbonyl)piperidine-2-carbonyloxy)-3-(3,4-dimethoxyphenyl)propyl)phenoxy)acetic acid **5a**.*

The reaction was performed as previously described<sup>20</sup> to yield the pipercolic ester 1.

To the **pipercolic ester 1** (3g, 4mmol) a solution of 20% TFA in DCM (20mL) was added at 0°C. The mixture was allowed to warm to room temperature and stirred for 6h after which time it was diluted with DCM and evaporated under reduced pressure to remove solvents and TFA. The crude material was then subjected to column chromatography using hexane: EtOAc: TFA 7.2:2.8: 0.2 to afford product **5a** (2.7g, 4mmol, 100%).

TLC (Hexane: EtOAc: TFA 7:2.8:0.2): Rf = 0.38.

HPLC (Gradient A) retention time= 32.21-32.62 min

<sup>1</sup>H NMR (600 MHz, CDCl<sub>3</sub>)  $\delta$ = 1.39-1.49 (m, 2H), 1.74 (dd, 3H, J= 11.7, 45.6 Hz), 2.02-2.11 (m, 1H), 2.15-2.31 (m, 2H), 2.53-2.70 (m, 2H), 2.75-2.83 (m, 1H), 3.19 (t, 1H, J= 12.1 Hz), 3.85 (s, 6H), 3.99-4.12 (m, 1H), 4.22 (t, 1H, J= 6.8Hz), 4.33-4.45 (m, 1H), 4.65 (dd, 1H, J= 16.6 35.3 Hz), 4.83 (s, 0.5H), 4.99 (d, 0.5H, J= 4 Hz), 5.67 (dd, 1H, J= 4.8, 8.3 Hz), 6.54-6.71 (m, 2H), 6.72-6.82 (m, 2H), 6.82-6.97 (m, 2H), 7.16-7.31 (m, 4H), 7.31-7.41 (m, 2H), 7.51-7.55 (m, 1H), 7.67-7.77 (m, 2H).

<sup>13</sup>C NMR (150 MHz, CDCl<sub>3</sub>)  $\delta$ = 21.07, 25.02, 27.27, 31.80, 38.43, 42.24, 47.39, 54.95, 56.23, 56.30, 65.56, 68.68, 76.94, 110.38, 111.76, 112.07, 115.98, 120.07, 120.33, 120.60, 125.32, 127.45, 128.11, 130.17, 133.71, 141.60, 142.52, 143.91, 144.09, 147.70, 149.21, 157.22, 158.17, 170.94, 172.24.

**Synthesis of 2-(3-((1R)-1-(1-(((9H-fluoren-9-yl)methoxy)carbonyl)piperidine-2-carbonyloxy)-3-(3,4-dimethoxyphenyl)propyl)phenoxy)acetic acid 5b.**

The reaction was done as previously described<sup>20</sup> to yield the pipecolic ester 2.

To the **pipecolic ester 2** (0.52 g, 0.71 mmol) a solution of 20% TFA in DCM (20mL) was added at 0°C. The mixture was allowed to warm to room temperature and stirred for 2.5 h after which time it was diluted with DCM and evaporated under reduced pressure to remove solvents and TFA. The crude material was then subjected to column chromatography using Hexane: EtOAc: TFA 6:4: 0.1 to yield product **5b** (410g, 0.60 mmol, 84%).

TLC (Hexane: EtOAc: TFA 6:4:0.1): R<sub>f</sub> = 0.38.

MS (ESI) m/z: found Rt 14.72 min. (Method LCMS), 679.77 [M + H]<sup>+</sup>, 701.53 [M + Na]<sup>+</sup>, calculated 679.35 [M + H]<sup>+</sup>, 701.28 [M + Na]<sup>+</sup>.

**Coupling of free acid 5a to the trityl resin.**

2-Chloro tritylresin (6.1g, 7.9mmol, Novabiochem) resin was swollen in DCM for 1h and added to a mixture of 2-(3-((1R)-1-(1-(((9H-fluoren-9-yl)methoxy)carbonyl) piperidine-2-carbonyloxy)-3-(3,4-dimethoxyphenyl)propyl)phenoxy) acetic acid **5a** (2.7 g, 3.97mmol ) and *i*-Pr<sub>2</sub>EtN (2g, 15.89mmol) in 20 ml dry DCM. The reaction was monitored by removing aliquots of the reactant mixture (10 μL) over a period of 1- 24h which were filtered and dried. The analytes were then re-dissolved in buffer A subjected to HPLC analysis and checked for the disappearance of compound **5a**. The slurry was agitated for 16h and then filtered. The resin was washed with DCM (3 x 50ml); DCM: MeOH: *i*-Pr<sub>2</sub>EtN 17:2:1 (3 x 50ml); DCM (3 x 20ml); DMF (3 x 25ml); MeOH (3 x 50ml); CHCl<sub>3</sub> (3 x 50ml) and diethyl ether (3 x 50ml). The resin was dried under high vacuum overnight to yield a free flowing resin immobilized with compound **5a**. The loading of the free acid was calculated using Fmoc deprotection and measurement of the Fmoc absorbance.

**Coupling of free acid 5b to the trityl resin.**

Loading reaction was carried out as described previously.

**Final Library Synthetic route:**

Fmoc-protected immobilized pipecolate **5a** was pre-weighed (approximately 50 mg, 0.019 mmol) and transferred to each of 36 wells of a 96-well parallel synthesis reactor platform obtained from FlexChem® peptide synthesis system. The resin was swollen for 1h in 1mL

DCM followed by addition of 2mL of 20% 4-methyl piperdiene in DCM and the reactor was stirred for 1h for the Fmoc deprotection to give **6a**. The wells were washed with DCM (1X 3mL) by vacuum assisted filtration. The resins were dried and the sulfonyl chlorides (0.095 mmol) obtained commercially from Maybridge were weighed (15- 40mg) and added to the wells as a solution in DIPEA (30 mg, 0.237 mmol) in 0.25mL DCM for the first coupling and 15 mg (0.119 mmol) in 0.25mL DCM for the second coupling with 0.057 mmol (5- 12mg) sulfonyl chloride. The reaction time was 4h for first coupling and 20h for the second coupling. The wells were subsequently washed with DCM and ethanol to completely remove excess of unreacted sulfonyl chlorides. The compounds were finally cleaved in presence of 1mL of 1% TFA solution in DCM for 20 min. Each of the solutions were collected by vacuum filtration and dried by air blowing to give approximately 12mg of the crude products. The purity of the above crude products was analyzed by HPLC using gradient A and 36 of these compounds were further purified by preparative HPLC using the gradient B. The remaining compound 50 was purified using ion exchange column chromatography to get rid of the traces of unreacted educt. The purified compounds were characterized using mass spectroscopy and dried under high vacuum to yield approximately 1-3 mg of the final desired sulfonamides.

### **Medium Scale synthesis:**

#### ***Deprotection of Fmoc resin 6a:***

The coupled resin **5a** was weighed (210 mg, 0.08mmol) and added to syringes, swollen in DCM (4 mL) for 1h, and the Fmoc protecting group was removed using 20% 4-methyl piperidine/DCM (4ml) for 1h. After filtration, the resin was washed with DCM (3 x 5ml) and used for the next coupling step.

#### ***Synthesis of sulfonamides:***

To the above resin *i*-Pr<sub>2</sub>EtN (40mg, 0.317mmol) in dry DCM (3 mL) was added and stirred for 20min. To this solution the sulfonyl chloride (0.237mmol) in 500 µL of DCM was added and the reaction was stirred for 4h at room temperature. After the first coupling step the resins were filtered, washed with DCM (3 x 10ml) and then subjected to second coupling with *i*-Pr<sub>2</sub>EtN (30mg, 0.237mmol), sulfonyl chloride (0.158 mmol) in DCM (3 mL) and stirred for 16h at room temperature. The resins were washed with DCM (3 x 5ml) and dried to give the derivatized resins. These were re-swollen in DCM reacted with 1% TFA/DCM (3ml) for 1h and then washed with 1% TFA/DCM (3 x 3ml) and further washed with DCM (3 x 5ml). The combined filtrates were concentrated *in vacuo* to yield the compounds **8-37**. (crude weight ~

50mg). The crude compounds were further purified by preparative HPLC using Gradient C. The purified peaks were further dried by lyophilization.

***Synthesis of 2-(3-((R)-3-(3,4-dimethoxyphenyl)-1-((S)-1-(4-(pyrimidin-2-yl)phenylsulfonyl)piperidine-2-carboxyloxy) propyl)phenoxy)acetic acid 8***

TLC (Hexane: EtOAc: TFA 6:3.8:0.2): R<sub>f</sub> = 0.18, yield= 13.5mg (30%).

HPLC (Gradient A) retention time= 25.1-25.3 min

<sup>1</sup>H NMR (600 MHz, CDCl<sub>3</sub>) δ= 1.29 (t, 1H, *J* = 7.2 Hz), 1.55 (dd, 1H, *J* = 3.6, 9 Hz), 1.67 (d, 1H, *J* = 12.6), 1.72 (d, 1H, *J* = 13.8 Hz), 1.85-1.91 (m, 1H), 1.93-1.99 (m, 1H), 2.13- 2.19 (m, 1H), 2.24 (d, 1H, *J* = 13.2 Hz), 2.45- 2.50 (m, 2H), 2.55- 2.59 (m, 1H), 3.11-3.16 (m, 2H), 3.75 (d, 1H, *J* = 9.6 Hz), 3.82 (s, 3H), 3.83 (s, 3H), 4.91 (d, 1H, *J* = 4.8 Hz), 5.53 (q, 1H, *J* = 3, 4.8 Hz), 6.61 (s, 1H), 6.63 (d, 1H, *J* = 7.8 Hz), 6.74 (d, 1H, *J* = 7.8 Hz), 6.80 (s, 1H), 6.92 (d, 1H, *J* = 7.2 Hz), 7.01(d, 1H, *J* = 7.8 Hz), 7.32- 7.35 (m, 2H), 7.59 (d, 2H, *J* = 8.4 Hz), 8.25 (d, 2H, *J* = 8.4 Hz), 8.91 (d, 2H, *J* = 4.8 Hz).

<sup>13</sup>C NMR (150 MHz, CDCl<sub>3</sub>) δ= 20.02, 24.74, 28.17, 31.42, 38.30, 42.45, 45.66, 55.33, 55.82, 65.24, 76.43, 111.28, 111.60, 112.94, 114.37, 118.85, 120.02, 120.09, 127.61, 128.51, 130.01, 133.25, 140.05, 141.31, 142.19, 147.34, 148.85, 157.41, 157.77, 162.90, 169.73

MS (ESI) m/z: found Rt 11.74 min. (Method LCMS), 676.12 [M + H]<sup>+</sup>, 698.16 [M + Na]<sup>+</sup>, HRMS 676.2305 [M + H]<sup>+</sup>, calculated 676.2251 [M + H]<sup>+</sup>.

***Synthesis of 2-(3-((R)-1-((S)-1-(3-chlorophenylsulfonyl)piperidine-2-carboxyloxy)-3-(3,4-dimethoxy phenyl) propyl- phenoxy)acetic acid 9***

TLC (Hexane: EtOAc: TFA 6:3.8:0.2): R<sub>f</sub> = 0.50, yield= 25.4 mg (57%).

HPLC (Gradient A) retention time= 26.1-26.5 min

<sup>1</sup>H NMR (400 MHz, DMSO) δ= 1.12-1.18 (m, 4H), 1.59 (t, 2H, *J* = 13.6 Hz), 1.98-2.13 (m, 2H), 2.40 (t, 2H, *J* = 6.8 Hz), 3.07 (t, 1H, *J* = 12 Hz), 3.61 (d, 1H, *J* = 12 Hz), 3.69 (s, 3H), 3.70 (s, 3H), 4.55 (s, 2H), 4.68 (d, 1H, *J* = 4Hz), 5.50 (t, 1H, *J* = 4.8Hz), 6.56 (d, 1H, *J* = 7.6 Hz), 6.60 (s, 1H), 6.72 (d, 1H, *J* = 8 Hz), 6.76-6.80 (m, 3H), 7.19- 7.26 (m, 2H), 7.46 (d, 2H, *J* = 7.2 Hz), 7.61 (s, 1H).

<sup>13</sup>C NMR (100 MHz, DMSO) δ= 20.05, 24.51, 27.74, 31.05, 37.92, 42.79, 55.32, 55.76, 64.99, 76.13, 111.95, 112.23, 112.85, 114.11, 119.22, 120.33, 125.36, 126.62, 129.77, 130.88, 132.66, 133.48, 134.48, 141.75, 141.95, 147.34, 148.92, 158.18, 169.61, 172.41.

MS (ESI) m/z: found Rt 12.34 min. (Method LCMS), 654.17, 656.16 [M + Na]<sup>+</sup>.

HRMS 632.2212, 634.2205[M + H]<sup>+</sup>, calculated 632.2143 [M + H]<sup>+</sup>.

***Synthesis of 2-(3-((R)-1-((S)-1-(benzo[d]thiazol-5-ylsulfonyl)piperidine-2-carboxyloxy)-3-(3,4-dimethoxyphenyl)propyl)phenoxy)acetic acid 10***

TLC (Hexane: EtOAc: TFA 6:3.8:0.2): R<sub>f</sub> = 0.20, yield= 25.4mg (59%).

HPLC (Gradient A) retention time= 24.6-25.0 min

<sup>1</sup>H NMR (600 MHz, CDCl<sub>3</sub>) δ= 1.08-1.15 (m,1H), 1.38-1.45 (m,1H), 1.60 (t, 2H, *J* = 12 Hz), 1.70-1.76 (m,1H), 1.94-2.00 (m,1H), 2.11- 2.18 (m,1H), 2.43- 2.54 (m,1H), 3.23 (dt, 1H, *J* = 3, 6 Hz), 3.76-3.78 (m,1H), 3.85(s, 6H), 4.65 (s, 2H), 4.84 (d, 1H, *J* = 4.2 Hz), 5.55 (t, 1H, *J* = 7.2 Hz), 6.63 (s, 1H), 6.64 (d, 1H, *J* = 1.8 Hz), 6.78 (d, 2H, *J* = 5.4 Hz), 6.81 (dd, 1H, *J* = 2.4, 6 Hz), 6.85 (d, 2H, *J* = 8.5 Hz), 7.22 (t, 1H, *J* = 7.8 Hz), 7.8 (dd, 1H, *J* = 1.8, 8.4 Hz), 8.13 (d, 1H, *J* = 8.4 Hz), 8.46 (d, 1H, *J* = 1.8 Hz), 9.18 (s, 1H).

<sup>13</sup>C NMR (150 MHz, CDCl<sub>3</sub>) δ= 19.91, 24.61, 27.69, 31.22, 37.87, 42.81, 55.27, 55.91, 55.92, 65.00, 76.54, 111.34, 111.73, 112.91, 114.16, 119.88, 120.14, 121.92, 123.95, 124.83, 129.78, 133.20, 133.83, 137.56, 141.50, 147.39, 148.87, 154.92, 157.56, 158.03, 169.95, 171.84

MS (ESI) m/z: found Rt 11.34 min. (Method LCMS), 655.06 [M + H]<sup>+</sup>, 677.16 [M + Na]<sup>+</sup>.

HRMS 655.2286 [M + H]<sup>+</sup>, calculated 655.2206 [M + H]<sup>+</sup>.

***Synthesis of 2-(3-((R)-3-(3,4-dimethoxyphenyl)-1-((S)-1-(furan-3-ylsulfonyl)piperidine-2-carboxyloxy)propyl)phenoxy)acetic acid 11***

TLC (Hexane: EtOAc: TFA 6:3.8:0.2): R<sub>f</sub> = 0.37, yield= 25mg (56%).

HPLC (Gradient A) retention time= 24.4-24.8 min

<sup>1</sup>H NMR (300 MHz, CDCl<sub>3</sub>) δ= 1.10-1.18 (m,1H), 1.43-1.52 (m,1H), 1.61-1.81(m,2H), 2.00-2.12(m,1H), 2.19-2.30 (m, 2H), 2.37 (s,2H), 2.52-2.65 (m,2H), 3.14-3.28 (m,2H), 3.87(s,3H), 3.88 (s,3H), 4.68 (s, 2H), 4.82 (d, 1H, *J* = 4.5 Hz), 5.70 (dd, 1H, *J* = 2.1,5.7 Hz), 6.58 (q,1H, *J* = 0.9, 1.2Hz), 6.70 (dd, 2H, *J* = 2.1, 4.5 Hz), 6.79-6.87 (m,2H), 6.91-6.96 (m, 2H), 7.25 (d, 1H, *J* = 2.1 Hz), 7.44 (t, 1H, *J* = 2.4 Hz), 7.91 (q, 1H, *J* = 0.9 Hz).

<sup>13</sup>C NMR (75 MHz, CDCl<sub>3</sub>) δ= 21.45, 24.62, 27.72, 31.25, 37.92, 42.57, 55.18, 55.93, 55.94, 64.92, 76.40, 108.52, 111.40, 111.80, 112.88, 114.30, 119.97, 120.20, 127.37, 128.21, 133.29, 141.86, 144.42, 145.50, 147.42, 148.92, 157.66, 170.10

MS (ESI) m/z: found Rt 11.29 min. (Method LCMS), 610.16 [M + Na]<sup>+</sup>.

HRMS 588.2354 [M + H]<sup>+</sup>, calculated 588.2325 [M + H]<sup>+</sup>.

***Synthesis of 2-(3-((R)-1-((S)-1-(benzo[b]thiophen-2-ylsulfonyl)piperidine-2-carboxyloxy)-3-(3,4-dimethoxyphenyl)propyl)phenoxy)acetic acid 12***

TLC (Hexane: EtOAc: TFA 6:3.8:0.2): R<sub>f</sub> = 0.62, yield= 23.8 mg (55%).

HPLC (Gradient A) retention time= 21.8-22.2 min

<sup>1</sup>H NMR (300 MHz, CDCl<sub>3</sub>) δ= 1.12- 1.21 (m, 1H), 1.44-1.52(m, 1H), 1.60-1.64 (m, 2H), 1.70-1.81 (m, 1H), 1.96-2.07 (m, 1H), 2.14-2.26(m, 2H). 2.47-2.65(m, 2H), 3.36 (dt, 1H, J = 3 Hz), 3.86 (s, 3H), 3.87 (s, 3H), 4.66 (s, 2H), 4.87 (d, 1H, J = 4.2 Hz), 5.65 (dd, 1H, J = 2.4, 6.6 Hz), 6.66-6.69 (m, 2H), 6.77-6.85 (m, 2H), 6.91(d, 2H, J = 7.2), 7.24 (t, 1H, J = 8.1 Hz), 7.40-7.49(m, 2H), 7.79-7.84 (m, 3H).

<sup>13</sup>C NMR (75 MHz, CDCl<sub>3</sub>) δ= 19.87, 24.47, 27.45, 31.28, 37.98, 43.04, 55.47, 55.93, 55.94, 64.90, 76.44, 111.39, 111.84, 112.73, 114.36, 119.95, 120.22, 122.66, 125.36, 125.58, 127.08, 128.91, 129.76, 133.36, 137.63, 141.35, 141.61, 141.82, 147.39, 148.90, 157.59, 169.84.

MS (ESI) m/z: found Rt 12.28 min. (Method LCMS), 676.95 [M + Na]<sup>+</sup>.

HRMS 732.2501 [M + DMSO]<sup>+</sup>, calculated 732.2592[M + DMSO]<sup>+</sup>.

***Synthesis of 2-(3-((R)-1-((S)-1-(3-cyanophenylsulfonyl)piperidine-2-carbonyloxy)-3-(3,4-dimethoxyphenyl)propyl)phenoxy)acetic acid 13***

TLC (Hexane: EtOAc: TFA 6:3.8:0.2): R<sub>f</sub> = 0.58, yield= 29.5mg (61%).

<sup>1</sup>H NMR (600 MHz, CDCl<sub>3</sub>) δ= 1.02- 1.10 (m, 1H), 1.40-1.47 (m, 1H), 1.60-1.64 (m, 2H), 1.72-1.78 (m, 1H), 1.99-2.06 (m, 1H), 2.16-2.22 (m, 2H), 2.49-2.59 (m, 2H), 3.15(dt, 1H, J = 3 Hz, 13.2 Hz), 3.7 (d, 1H, J = 9.6 Hz), 3.86 (s, 3H), 3.87 (s, 3H), 4.67 (s, 2H), 4.81 (d, 1H, J = 4.8 Hz), 5.60 (dd, 1H, J = 6 Hz), 6.67-6.69 (m, 2H), 6.81 (d, 1H, J = 7.8 Hz), 6.83-6.84 (m, 1H), 6.90 (d, 1H, J = 7.8 Hz), 7.26 (dd, 1H, J = 7.8 Hz), 7.56 (t, 1H, J = 7.8 Hz), 7.78 (td, 1H, J = 1.2 Hz, 7.8 Hz), 7.99-7.99 (m, 1H), 8.07 (t, 1H, J = 1.8 Hz).

<sup>13</sup>C NMR (150 MHz, CDCl<sub>3</sub>) δ= 19.83, 24.63, 27.80, 31.25, 37.82, 42.88, 55.39, 55.93, 55.97, 64.78, 76.70, 111.37, 111.82, 112.95, 113.38, 114.23, 117.30, 120.00, 120.16, 129.87, 130.70, 131.05, 133.16, 135.56, 141.58, 141.77, 147.43, 148.88, 157.53, 169.67, 171.85.

MS (ESI) m/z: found Rt 13.12min. (Method LCMS), 645.40 [M + Na]<sup>+</sup>.

HRMS 701.2628 [M + DMSO]<sup>+</sup>, calculated 701.2624 [M + DMSO]<sup>+</sup>.

***Synthesis of 2-(3-((R)-3-(3,4-dimethoxyphenyl)-1-((S)-1-(3-nitrophenylsulfonyl)piperidine - 2-carbonylo xy propyl)phenoxy)acetic acid 14***

TLC (Hexane: EtOAc: TFA 5.5:4.5:0.2): R<sub>f</sub> = 0.44, yield= 24.0 mg (48%).

HPLC (Gradient A) retention time= 24.4-24.8 min

<sup>1</sup>H NMR (600 MHz, CDCl<sub>3</sub>) δ= 1.00- 1.01 (m, 1H), 1.43-1.49 (m, 1H), 1.60-1.63 (m, 2H), 1.74-1.80 (m, 1H), 1.98-2.04 (m, 1H), 2.15-2.23 (m, 2H), 2.46-2.57 (m, 2H), 3.15 (dt, 1H, J = 2.4 Hz,

12.6 Hz), 3.74 (td, 1H,  $J = 2.4, 9.6$  Hz), 3.85 (s, 3H), 3.86 (s, 3H), 4.65 (s, 2H), 4.85 (d, 1H,  $J = 4.2$  Hz), 5.57 (dd, 1H,  $J = 6.6$  Hz), 6.65-6.67 (m, 2H), 6.79-6.82 (m, 3H), 6.87 (d, 1H,  $J = 7.8$  Hz), 7.24 (dd, 1H,  $J = 7.8$  Hz), 7.62 (t, 1H,  $J = 7.8$  Hz), 8.06-8.08 (m, 1H), 8.34-8.36 (m, 1H), 8.59 (t, 1H,  $J = 1.8$  Hz).

$^{13}\text{C}$  NMR (150 MHz,  $\text{CDCl}_3$ )  $\delta = 19.81, 24.65, 27.86, 31.21, 37.76, 42.88, 55.47, 55.92, 55.93, 64.76, 76.73, 111.35, 111.77, 112.98, 114.14, 120.12, 122.34, 126.91, 129.85, 130.13, 132.62, 133.17, 141.53, 142.09, 147.40, 148.07, 148.87, 157.55, 169.65, 172.65$

MS (ESI)  $m/z$ : found RT 13.40 min. (Method LCMS), 665.25  $[\text{M} + \text{Na}]^+$ .

HRMS 721.2027  $[\text{M} + \text{DMSO}]^+$ , calculated 721.2022  $[\text{M} + \text{DMSO}]^+$ .

### **Synthesis of 2-(3-((R)-1-((S)-1-(3-aminophenylsulfonyl)piperidine-2-carboxyloxy)-3-(3,4-dimethoxyphenyl)propyl)phenoxy)acetic acid 15**

TLC (Hexane: EtOAc: TFA 6:3.8:0.2):  $R_f = 0.28$ , yield= 35 mg (66%).

HPLC (Gradient A) retention time= 21.32-21.52 min

$^1\text{H}$ NMR (600 MHz,  $\text{CDCl}_3$ )  $\delta = 1.21-1.29$  (m, 1H), 1.46-1.52 (m, 1H), 1.60-1.66 (m, 1H), 1.69-1.74 (m, 1H), 1.79- 1.86 (m, 1H), 1.89-1.96 (m, 1H), 2.07-2.13 (m, 1H), 2.42-2.56 (m, 2H), 3.10-3.25 (m, 1H), 3.74-3.79 (m, 1H), 3.84 (s, 6H), 4.66 (s, 2H), 4.70-4.74 (m, 1H), 5.53 (s, 1H), 6.60-6.68 (m, 3H), 6.74-6.80 (m, 2H), 6.82-6.86 (m, 2H), 7.13-7.20 (m, 2H), 7.36-7.54 (m, 2H).

$^{13}\text{C}$  NMR (150 MHz,  $\text{CDCl}_3$ )  $\delta = 20.06, 24.80, 28.03, 31.36, 37.99, 42.76, 55.20, 55.89, 55.92, 65.02, 76.38, 111.33, 111.68, 112.54, 114.44, 118.69, 119.84, 120.12, 123.19, 124.25, 129.94, 130.21, 133.19, 139.69, 140.92, 141.93, 147.39, 148.87, 157.64, 169.72, 172.07$

MS (ESI)  $m/z$ : found RT 10.87 min. (Method LCMS), 613.12  $[\text{M} + \text{H}]^+$ , 635.17  $[\text{M} + \text{Na}]^+$ ,

HRMS 613.2704  $[\text{M} + \text{H}]^+$ , calculated 613.2682  $[\text{M} + \text{H}]^+$ .

### **Synthesis of 2-(3-((R)-3-(3,4-dimethoxyphenyl)-1-((S)-1-(3-(2-methylpyrimidin-4-yl)phenylsulfonyl)piperidine-2-carboxyloxy)propyl)phenoxy)acetic acid 16**

TLC (Hexane: EtOAc: TFA 6:3.8:0.2):  $R_f = 0.22$ , yield= 48.3 mg (90%).

HPLC (Gradient A) retention time= 23.1-23.5 min

$^1\text{H}$ NMR (600 MHz,  $\text{CDCl}_3$ )  $\delta = 1.14- 1.21$  (m, 1H), 1.51-1.58 (m, 1H), 1.61-1.63 (m, 1H), 1.71-1.75 (m, 1H), 1.83-1.90 (m, 1H), 1.96-2.02 (m, 1H), 2.12-2.18 (m, 1H), 2.32 (d, 1H,  $J = 13.8$  Hz), 2.45- 2.49 (m, 1H), 2.52-2.57 (m, 1H), 3.66 (d, 1H,  $J = 12$  Hz), 3.79 (s, 3H), 3.80 (s, 3H), 4.59 (d, 1H,  $J = 16.8$  Hz), 4.67 (d, 2H,  $J = 16.8$  Hz), 4.98 (d, 1H,  $J = 5.4$  Hz), 5.51 (dd, 1H,  $J = 5.4$  Hz), 6.66-6.64 (m, 2H), 6.75 (m, 2H,  $J = 8.4$  Hz), 6.81-6.86 (m, 2H), 7.26 (m, 1H), 7.66 (t, 1H,  $J$

= 7.8 Hz), 8.01(d, 1H,  $J = 6$  Hz), 8.01- 8.08 (m, 1H), 8.41-8.43(m,1H), 8.73 (t, 1H,  $J = 1.8$  Hz), 9.07 (d, 1H,  $J = 6.6$  Hz).

$^{13}\text{C}$  NMR (150 MHz,  $\text{CDCl}_3$ )  $\delta = 20.19, 22.94, 24.75, 28.08, 31.23, 37.79, 43.03, 55.21, 55.87, 55.88, 65.36, 77.06, 111.41, 111.61, 112.78, 115.21, 115.33, 118.94, 120.22, 127.02, 129.86, 130.19, 131.83, 132.08, 133.02, 134.97, 141.62, 141.84, 147.39, 148.85, 151.43, 157.99, 164.28, 167.69, 170.58, 171.54$

MS (ESI)  $m/z$ : found Rt 12.59 min. (Method LCMS), 690.37  $[\text{M} + \text{H}]^+$ , 712.17  $[\text{M} + \text{Na}]^+$ , HRMS 690.2936  $[\text{M} + \text{H}]^+$ , calculated 690.2907  $[\text{M} + \text{H}]^+$ .

**Synthesis of 2-(3-((R)-3-(3,4-dimethoxyphenyl)-1-((S)-1-(3-(pyrimidin-4-yl)phenylsulfonyl)piperidine-2-carboxyloxy)propyl)phenoxy)acetic acid 17**

TLC (Hexane: EtOAc: TFA 5:4.8:0.2):  $R_f = 0.43$ , yield= 41.9 mg (80%).

HPLC (Gradient A) retention time= 24.2-24.6 min

$^1\text{H}$ NMR (600 MHz,  $\text{CDCl}_3$ )  $\delta = 1.10- 1.17$  (m,1H), 1.37-1.44 (m,1H), 1.58-1.61 (m,2H), 1.66-1.72 (m,1H), 1.94-2.00 (m,1H), 2.13-2.19 (m,2H), 2.42-2.47 (m,1H), 2.50- 2.55 (m,1H), 3.25(dt,1H,  $J = 3$  Hz, 12.6 Hz), 3.83 (d, 1H,  $J = 6$  Hz), 3.85 (s,3H), 3.85 (s, 3H), 4.67 (d, 2H,  $J = 6$  Hz), 4.83 (d, 1H,  $J = 4.2$  Hz), 5.60 (dd, 1H,  $J = 5.4$  Hz), 6.62-6.64 (m,2H), 6.77 (d, 1H,  $J = 8.4$  Hz), 6.80-6.82 (m, 1H), 6.86-6.88 (m,2H), 7.22 (t, 1H,  $J = 8.4$  Hz), 7.28 (t, 1H,  $J = 4.8$  Hz), 7.59 (t, 1H,  $J = 7.8$  Hz), 7.92-7.94 (m, 1H), 8.55 (dd, 1H,  $J = 1.2$  Hz, 7.8Hz), 8.85 (d, 3H,  $J = 4.8$  Hz).

$^{13}\text{C}$  NMR (150 MHz,  $\text{CDCl}_3$ )  $\delta = 19.99, 24.53, 27.41, 31.28, 38.02, 42.93, 55.35, 55.88, 55.92, 64.85, 111.31, 111.74, 112.30, 114.60, 119.88, 119.95, 120.17, 127.01, 129.17, 129.45, 129.71, 132.08, 133.42, 137.71, 141.12, 141.77, 147.27, 148.79, 157.41, 157.63, 162.78, 170.08, 172.04$ .

MS (ESI)  $m/z$ : found Rt 13.30 min. (Method LCMS), 676.20  $[\text{M} + \text{H}]^+$ , 698.33  $[\text{M} + \text{Na}]^+$ , HRMS 676.2783  $[\text{M} + \text{H}]^+$ , calculated 676.2811  $[\text{M} + \text{H}]^+$ .

**Synthesis of 2-(3-((R)-3-(3,4-dimethoxyphenyl)-1-((S)-1-(3-fluorophenylsulfonyl)piperidine-2-carboxyloxy)propyl)phenoxy)acetic acid 18**

TLC (Hexane: EtOAc: TFA 5.5:4.5:0.2):  $R_f = 0.44$ , yield= 23.5 mg (49%).

HPLC (Gradient A) retention time= 24.70-24.85 min

$^1\text{H}$ NMR (300 MHz,  $\text{CDCl}_3$ )  $\delta = 1.24-1.33$  (m,1H), 1.41-1.53(m,1H), 1.63-1.85 (m, 3H), 1.94-2.06 (m,1H), 2.12-2.27 (m, 2H), 2.45-2.61 (m, 2H), 3.18 (t, 1H,  $J = 12.7$  Hz), 3.74 (d, 1H,  $J =$

12.6 Hz), 3.85 (s, 6H), 4.71 (s, 2H), 4.80 (d, 1H,  $J = 4.8$  Hz), 5.63 (t, 1H,  $J = 7.8$  Hz), 6.65-6.67 (m, 2H), 6.75 (d, 1H,  $J = 8.7$  Hz), 6.89- 6.93 (m, 3H), 7.13- 7.34 (m, 3H), 7.39-7.41 (m, 2H).

$^{13}\text{C}$  NMR (75 MHz,  $\text{CDCl}_3$ )  $\delta = 20.05, 24.62, 27.89, 31.24, 37.95, 42.77, 55.37, 55.88, 55.93, 65.32, 76.34, 111.38, 111.78, 112.56, 114.18, 114.50, 119.43, 119.71, 120.18, 122.83, 129.86, 130.49, 133.29, 141.77, 147.39, 148.89, 157.75, 160.53, 163.86, 165.31, 169.73$ .

MS (ESI)  $m/z$ : found Rt 13.19 min. (Method LCMS), 638.19  $[\text{M} + \text{Na}]^+$ .

HRMS 616.2488  $[\text{M} + \text{H}]^+$  calculated 616.2468  $[\text{M} + \text{H}]^+$ .

### Synthesis of 2-(3-((R)-1-((S)-1-(3-bromophenylsulfonyl)piperidine-2-carboxyloxy)-3-(3,4-dimethoxyphenyl)propyl)phenoxy)acetic acid 19

TLC (Hexane: EtOAc: TFA 5.5:4.5:0.2):  $R_f = 0.36$ , yield= 29.87mg (57%).

HPLC (Gradient A) retention time= 25.89-26.02 min

$^1\text{H}$ NMR (300 MHz,  $\text{CDCl}_3$ )  $\delta = 1.24-1.32$  (m, 1H), 1.39-1.52 (m, 1H), 1.62-1.85 (m, 3H), 1.94-2.05 (m, 1H), 2.11-2.27 (m, 2H), 2.44-2.62 (m, 2H), 3.16 (dt, 1H,  $J = 2.7; 12.6$  Hz), 3.71 (d, 1H,  $J = 9.9$  Hz), 4.70 (s, 2H), 4.80 (d, 1H,  $J = 4.5$  Hz), 5.65 (t, 1H,  $J = 8.1$  Hz), 6.65-6.68 (m, 2H), 6.79 (d, 1H,  $J = 8.7$  Hz), 6.88-6.93 (m, 3H), 7.11 (t, 1H,  $J = 8.1$  Hz), 7.31 (t, 1H,  $J = 8.25$  Hz), 7.52 (dd, 1H,  $J = 0.9; 7.8$  Hz), 7.59 (dd, 1H,  $J = 0.9, 7.9$  Hz), 7.87 (t, 1H,  $J = 1.8$  Hz).

$^{13}\text{C}$  NMR (75 MHz,  $\text{CDCl}_3$ )  $\delta = 20.06, 24.59, 27.87, 31.23, 37.96, 42.79, 55.48, 55.89, 55.94, 64.86, 76.43, 111.41, 111.80, 112.60, 114.53, 120.09, 120.21, 122.73, 125.64, 129.89, 130.33, 133.32, 135.46, 141.60, 141.75, 147.37, 148.86, 157.75, 169.81, 172.68$ .

MS (ESI)  $m/z$ : found Rt 13.33 min. (Method LCMS), 698.31, 700.12  $[\text{M} + \text{Na}]^+$ .

HRMS 676.1716, 678.1715  $[\text{M} + \text{H}]^+$ , calculated 676.1718  $[\text{M} + \text{H}]^+$ .

### Synthesis of 2-(3-((R)-1-((S)-1-(3,5-dichlorophenylsulfonyl)piperidine-2-carboxyloxy)-3-(3,4-dimethoxyphenyl)propyl)phenoxy)acetic acid 20

TLC (Hexane: EtOAc: TFA 5.5:4.5:0.2):  $R_f = 0.58$ , yield= 22.6mg (44%).

HPLC (Gradient A) retention time= 26.8-27.3 min

$^1\text{H}$ NMR (600 MHz,  $\text{CDCl}_3$ )  $\delta = 1.03- 1.10$  (m, 1H), 1.40-1.47 (m, 1H), 1.60-1.63 (m, 2H), 1.71-1.77 (m, 1H), 1.99-2.06 (m, 1H), 2.16-2.23 (m, 2H), 2.49-2.59 (m, 2H), 3.20 (dt, 1H,  $J = 2.4$  Hz, 12.6 Hz), 3.71 (td, 1H,  $J = 1.2, 12.6$  Hz), 3.85 (s, 3H), 3.86 (s, 3H), 4.66 (s, 2H), 4.78 (d, 1H,  $J = 4.8$  Hz), 5.63 (dd, 1H,  $J = 6$  Hz), 6.66-6.68 (m, 2H), 6.79 (d, 1H,  $J = 7.8$  Hz), 6.83-6.84 (m, 1H), 6.85 (t, 1H,  $J = 2.4$  Hz), 6.90 (d, 1H,  $J = 7.8$  Hz), 7.26 (dd, 1H,  $J = 7.8$  Hz), 7.49 (t, 1H,  $J = 1.8$  Hz), 7.66 (d, 1H,  $J = 1.8$  Hz).

$^{13}\text{C}$  NMR (150 MHz,  $\text{CDCl}_3$ )  $\delta$ = 19.74, 24.61, 27.74, 31.28, 37.84, 42.89, 55.32, 55.92, 64.78, 76.65, 111.33, 111.75, 112.95, 114.17, 120.00, 120.17, 125.45, 129.87, 132.42, 133.21, 135.73, 141.63, 142.89, 147.40, 148.86, 157.53, 169.57, 172.53.

MS (ESI) m/z: found Rt 14.33 min. (Method LCMS), 688.19, 690.19  $[\text{M} + \text{Na}]^+$ .

HRMS 666.1753, 668.1713  $[\text{M} + \text{H}]^+$ , calculated 666.1753  $[\text{M} + \text{H}]^+$ .

***Synthesis of 2-(3-((R)-1-((S)-1-(2,3-dichlorophenylsulfonyl)piperidine-2-carbonyloxy)-3-(3,4-dimethoxyphenyl)propyl)phenoxy)acetic acid 21***

TLC (Hexane: EtOAc: TFA 6:3.8:0.2): Rf = 0.50, yield= 18.7 mg (43%)

HPLC (Gradient A) retention time= 27.1-27.5 min

$^1\text{H}$ NMR (600 MHz,  $\text{CDCl}_3$ )  $\delta$ = 1.02- 1.08 (m,1H), 1.41-1.46 (m,1H), 1.60-1.64 (m,2H), 1.70-1.76 (m,1H), 2.00-2.06 (m,1H), 2.15-2.24 (m,2H), 2.50-2.60 (m,2H), 3.21 (dt,1H,  $J$  = 2.4 Hz, 12.6 Hz), 3.70 (td, 1H,  $J$  = 1.2, 12.6 Hz), 3.85 (s,3H), 3.86 (s, 3H), 4.65 (s,2H), 4.77 (d, 1H,  $J$  = 4.8 Hz), 5.63 (dd, 1H,  $J$  = 6 Hz), 6.65-6.67(m,2H), 6.73 (d, 1H,  $J$  = 7.8 Hz), 6.80-6.82 (m, 1H), 6.85 (t,1H,  $J$  = 2.4 Hz), 6.92 (s,1H), 7.25 (dd, 1H,  $J$  = 7.8 Hz), 7.49 (t, 1H,  $J$  = 1.8 Hz), 7.67 (d, 1H,  $J$  = 1.8 Hz).

MS (ESI) m/z: found Rt 12.79 min. (Method LCMS), 688.14, 690.11  $[\text{M} + \text{Na}]^+$ .

HRMS 688.1090 , 690.1061  $[\text{M} + \text{Na}]^+$ , calculated 688.1086, 690.1092  $[\text{M} + \text{Na}]^+$ .

***Synthesis of 2-(3-((R)-3-(3,4-dimethoxyphenyl)-1-((S)-1-(3,4-dimethoxyphenylsulfonyl)piperidine-2-carbonyloxy)propyl)phenoxy)acetic acid 22***

TLC (Hexane: EtOAc: TFA 6:3.8:0.2): Rf = 0.38, yield- 32.89 mg (62%).

HPLC (Gradient A) retention time= 23.1-23.5 min

$^1\text{H}$ NMR (600 MHz,  $\text{CDCl}_3$ )  $\delta$ = 1.08- 1.15 (m,1H), 1.32-1.39(m,1H), 1.53-1.60(m,2H), 1.64-1.70(m,1H), 1.99-2.06 (m,1H), 2.14-2.23(m,2H). 2.48-2.59(m,2H), 3.19 (dt, 1H,  $J$  = 3, 10.2 Hz), 3.63 (d,1H,  $J$  = 11.4Hz), 3.83 (s,3H), 3.84 (s,3H), 3.87 (s,3H), 3.87 (s, 3H), 4.65 (s,2H), 4.78 (d, 1H,  $J$  = 4.8 Hz), 5.64 (dd, 1H,  $J$  = 1.2, 6.0 Hz), 6.66 (d,2H,  $J$  = 7.2 Hz), 6.73 (s, 1H,  $J$  = 8.4Hz), 6.81- 6.83(m, 2H), 6.88-6.91 (m, 2Hz), 7.22-7.24(m,2H), 7.41 (dd,1H,  $J$  = 0.6, 8.4Hz).

$^{13}\text{C}$  NMR (150 MHz,  $\text{CDCl}_3$ )  $\delta$ = 20.04, 24.43, 27.53, 31.25, 37.98,42.63, 55.16, 55.88,55.89, 56.06, 56.17, 64.89, 76.48, 109.76, 110.41, 111.32, 111.74, 112.74, 114.40, 119.85, 120.16, 121.03, 129.75, 131.88, 133.30, 141.79, 147.34, 148.84, 148.93, 152.41, 157.58

MS (ESI) m/z: found Rt 12.83 min. (Method LCMS), 680.21  $[\text{M} + \text{Na}]^+$ .

HRMS 680.2753  $[\text{M} + \text{Na}]^+$ , calculated 658.2744.

**Synthesis of 2-(3-((R)-1-((S)-1-(3-chloro-4-methoxyphenylsulfonyl)piperidine-2-carbonyloxy)-3-(3,4-dimethoxyphenyl)propyl)phenoxy)acetic acid 23**

TLC (Hexane: EtOAc: TFA 6:3.8:0.2): R<sub>f</sub> = 0.45, yield- 11.7mg (25%).

HPLC (Gradient A) retention time= 24.98-25.12 min

<sup>1</sup>H NMR (300 MHz, CDCl<sub>3</sub>) δ= 1.25-1.34 (m, 1H), 1.41-1.54 (m, 1H), 1.63-1.85 (m, 3H), 1.95-2.06 (m, 1H), 2.13-2.27 (m, 2H), 2.46-2.64 (m, 2H), 3.15 (dt, 1H, J= 2.7, 12.6 Hz), 3.69 (d, 1H, J= 12.1 Hz), 3.86 (s, 6H), 3.89 (s, 3H), 4.72 (s, 2H), 4.81 (d, 1H, J= 4.5 Hz), 5.66 (t, 1H, J= 6.6 Hz), 6.65-6.72 (m, 3H), 6.78 (d, 1H, J= 8.7 Hz), 6.91- 6.96 (m, 3H), 7.32 (t, 1H, J= 8.3 Hz), 7.47 (dd, 1H, J= 2.4, 9.3 Hz), 7.72 (d, 1H, J= 2.4 Hz)

<sup>13</sup>C NMR (75 MHz, CDCl<sub>3</sub>) δ= 20.09, 24.60, 27.93, 31.25, 38.11, 42.63, 55.31, 55.90, 55.94, 56.37, 64.87, 76.21, 111.33, 111.38, 111.79, 112.22, 114.68, 120.14, 120.19, 122.95, 127.55, 129.16, 129.85, 132.20, 133.30, 142.00, 147.40, 148.89, 157.74, 158.07, 169.87, 172.04.

MS (ESI) m/z: found Rt 13.48 min. (Method LCMS), 684.27 [M + Na]<sup>+</sup>.

HRMS 662.2304, 664.2288 [M + H]<sup>+</sup>, calculated 662.2308 [M + H]<sup>+</sup>.

**Synthesis of 2-(3-((R)-1-((S)-1-(3,5-difluorophenylsulfonyl)piperidine-2-carbonyloxy)-3-(3,4-dimethoxyphenyl)propyl)phenoxy)acetic acid 24**

TLC (Hexane: EtOAc: TFA 6:3.8:0.2): R<sub>f</sub> = 0.38, yield= 23.5mg (57%).

HPLC (Gradient A) retention time= 25.22-25.39 min

<sup>1</sup>H NMR (300 MHz, CDCl<sub>3</sub>) δ= 1.21-1.35 (m, 1H), 1.42-1.55 (m, 1H), 1.65-1.84 (m, 3H), 1.96-2.08 (m, 1H), 2.14-2.30 (m, 2H), 2.45-2.63 (m, 2H), 3.17 (t, 1H, J= 12 Hz), 3.73 (d, 1H, J= 11.9 Hz), 3.85 (s, 6H), 4.78 (s, 2H), 4.72 (s, 1H), 5.66 (t, 1H, J= 6 Hz), 6.65-6.68 (m, 2H), 6.79 (d, 1H, J= 4.4 Hz), 6.87-6.93 (m, 4H), 7.20 (d, 2H, J= 1.8 Hz), 7.31 (t, 1H, J= 7.5 Hz).

<sup>13</sup>C NMR (75 MHz, CDCl<sub>3</sub>) δ= 20.09, 24.66, 27.88, 31.23, 37.83, 42.99, 53.42, 55.59, 55.87, 55.93, 77.23, 107.66, 107.98, 110.43, 110.79, 111.39, 111.76, 112.74, 114.49, 120.09, 120.18, 129.93, 133.26, 141.51, 143.17, 147.40, 148.88, 157.69, 160.92, 164.13, 169.63.

MS (ESI) m/z: found Rt 13.46min. (Method LCMS), 656.19 [M + Na]<sup>+</sup>.

HRMS 634.7102 [M + H]<sup>+</sup>, calculated 634.7099 [M + H]<sup>+</sup>.

**Synthesis of 2-(3-((R)-1-((S)-1-(3,5-bis(trifluoromethyl)phenylsulfonyl)piperidine-2-carbonyloxy)-3-(3,4-dimethoxyphenyl)propyl)phenoxy)acetic acid 25**

TLC (Hexane: EtOAc: TFA 6:3.8:0.2): R<sub>f</sub> = 0.47, yield= 30.1mg (51%).

HPLC (Gradient A) retention time= 27.5-27.8 min

$^1\text{H}$ NMR (600 MHz,  $\text{CDCl}_3$ )  $\delta$ = 0.99- 1.01 (m,1H), 1.40-1.47(m,1H), 1.59-1.61(m,2H), 1.73-1.79 (m,1H), 1.99-2.05 (m,1H), 2.14-2.23(m,2H). 2.46-2.56(m,2H), 3.09 (dt, 1H,  $J$  = 2.4 Hz),3.69 (dd, 1H,  $J$  = 1.8 Hz), 3.84 (s,3H), 3.85 (s, 3H), 4.64 (s,2H), 4.83 (d, 1H,  $J$  = 4.2 Hz), 5.56 (t, 1H,  $J$  = 6.6 Hz), 6.63-6.66 (m,2H), 6.78(d,1H,  $J$  = 7.8 Hz), 6.80-6.82 (m,2H), 6.88(d, 2H,  $J$ = 7.8), 7.24 (t, 1H,  $J$  =7. 8 Hz), 8.031(s, 1H), 8.20(s, 1H).

$^{13}\text{C}$  NMR (150 MHz,  $\text{CDCl}_3$ )  $\delta$ = 19.74, 24.58, 27.88, 31.21, 37.71, 42.83, 55.59, 55.87, 55.88, 64.73, 76.92, 111.31, 111.71, 113.02, 114.13, 119.98, 120.09, 121.62, 123.44, 125.27, 127.29, 127.51, 129.87, 133.12, 141.57, 142.63, 147.39, 148.83, 157.48, 169.47, 172.22

MS (ESI) m/z: found Rt 14.65 min. (Method LCMS), 756.20  $[\text{M} + \text{Na}]^+$ .

HRMS 812.2680  $[\text{M} + \text{DMSO}]^+$ , calculated 812.2619  $[\text{M} + \text{DMSO}]^+$ .

***Synthesis of 2-(3-((R)-1-((S)-1-(3-bromo-5-(trifluoromethyl)phenylsulfonyl)piperidine-2-carbonyloxy)-3-(3,4-dimethoxyphenyl)propyl)phenoxy)acetic acid 26***

TLC (Hexane: EtOAc: TFA 6:3.8:0.2): Rf = 0.50, yield= 28.5mg (47%).

HPLC (Gradient A) retention time= 27.5-27.8 min

$^1\text{H}$ NMR (600 MHz,  $\text{CDCl}_3$ )  $\delta$ = 0.97-1.04 (m,1H), 1.40-1.46(m,1H), 1.59-1.62(m,2H), 1.71-1.77(m,1H), 1.99-2.05(m,1H), 2.15-2.22(m,2H). 2.47-2.57(m,2H), 3.15 (dt, 1H,  $J$  2.4, 12.6 Hz), 3.68 (dd, 1H,  $J$  = 2.6Hz), 3.84 (s,3H), 3.85 (s, 3H), 4.65 (s,2H), 4.80 (d, 1H,  $J$  = 4.8 Hz), 5.59 (t, 1H,  $J$  = 7.2 Hz), 6.64-6.67 (m,2H), 6.78 (d, 1H,  $J$  = 8.4Hz), 6.81-6.84(m, 2H), 6.89(d,1H,  $J$  = 7.2Hz), 7.25 (t, 1H,  $J$  = 7.8Hz), 7.90(s, 1H), 7.95 (s,1H), 8.08(s,1H)

$^{13}\text{C}$  NMR (150 MHz,  $\text{CDCl}_3$ )  $\delta$ = 19.74, 24.59, 27.80, 31.24, 37.77, 42.86, 55.45, 55.90, 64.75, 76.77, 111.32, 111.74, 112.98, 114.15, 119.99, 120.14, 122.80, 123.32, 129.87, 132.12, 132.15, 133.17, 133.25, 141.60, 142.89, 147.39, 148.84, 157.49, 169.49, 172.39.

MS (ESI) m/z: found Rt 14.60 min. (Method LCMS), 766.16, 768.08  $[\text{M} + \text{Na}]^+$ .

HRMS 766.1568, 768.1556  $[\text{M} + \text{Na}]^+$ , calculated 744.1511.

***Synthesis of 2-(3-((R)-1-((S)-1-(3,5-bis(methoxycarbonyl)phenylsulfonyl)piperidine-2-carbonyloxy)-3-(3,4-dimethoxyphenyl)propyl)phenoxy)acetic acid 27***

TLC (Hexane: EtOAc: TFA 6:3.8:0.2): Rf = 0.52, yield= 22mg (41%).

HPLC (Gradient A) retention time= 24.82-25.02 min

$^1\text{H}$ NMR (400 MHz,  $\text{CDCl}_3$ )  $\delta$ = 1.21-1.31 (m, 1H), 1.37-1.47 (m, 1H), 1.61-1.80 (m, 3H), 1.91-2.00 (m, 1H), 2.08-2.17 (m, 1H), 2.28 (d, 1H,  $J$ = 6.8 Hz), 2.40-2.55 (m, 2H), 3.15 (dt, 1H,  $J$ = 2.8, 12.8 Hz), 3.78 (d, 1H,  $J$ = 12.6 Hz), 3.82 (s, 3H), 3.83 (s, 3H), 3.93 (s, 6H), 4.70 (s, 2H),

4.81 (s, 1H, J= 2.4 Hz), 5.63 (t, 1H, J= 6.8 Hz), 6.61-6.63 (m, 2H), 6.75 (d, 1H, J= 4.2 Hz), 6.84-6.88 (m, 3H), 7.23-7.27 (m, 1H), 8.54 (s, 1H), 8.55 (s, 1H), 8.76 (t, 1H, J= 1.6 Hz).

$^{13}\text{C}$  NMR (100 MHz,  $\text{CDCl}_3$ )  $\delta$ = 20.21, 24.65, 27.77, 31.13, 37.76, 43.04, 52.85, 55.61, 55.84, 55.89, 64.91, 76.47, 111.27, 111.68, 112.70, 114.57, 120.08, 120.10, 129.79, 131.53, 131.95, 133.25, 134.01, 141.30, 141.73, 147.31, 148.80, 157.58, 164.86, 169.61, 172.02.

MS (ESI) m/z: found Rt 11.80 min. (Method LCMS), 736.16  $[\text{M} + \text{Na}]^+$ .

HRMS 714.2720  $[\text{M} + \text{H}]^+$ , calculated 714.2642  $[\text{M} + \text{H}]^+$ .

***Synthesis of 2-(3-((R)-1-((S)-1-(3,5-dichloro-4-hydroxyphenylsulfonyl)piperidine-2-carbonyl-oxy)-3-(3,4-dimethoxyphenyl)propyl)phenoxy)acetic acid 28***

TLC (Hexane: EtOAc: TFA 4.8 :5:0.2): Rf = 0.50, yield= 12.3mg (23%).

HPLC (Gradient A) retention time= 26.8-27.1 min

$^1\text{H}$ NMR (300 MHz,  $\text{CDCl}_3$ )  $\delta$ = 1.00-1.10 (m, 1H), 1.38-1.53 (m, 1H), 1.60-1.68 (m, 2H), 1.74-1.87 (m, 1H), 2.01-2.12 (m, 1H), 2.16-2.26 (m, 2H), 2.53-2.62 (m, 2H), 3.21 (t, 1H, J= 12Hz), 3.72 (d, 1H, J= 12Hz), 3.87 (s, 6H), 4.65 (s, 2H), 4.77 (d, J= 2.7Hz), 5.63 (t, J= 6Hz), 6.69-6.71(m, 2H), 6.80-6.93(m, 4H), 7.28 (s, 1H), 7.78 (s, 1H), 7.99 (s, 1H).

$^{13}\text{C}$  NMR (75 MHz,  $\text{CDCl}_3$ )  $\delta$ = 19.66, 24.66, 27.85, 31.34, 37.88, 43.01, 55.4, 55.95, 64.82, 77.21, 111.44, 111.83, 113.02, 114.23, 119.84, 120.21, 122.20, 127.86, 128.97, 129.89, 139.94, 141.75, 145.83, 147.22, 148.89, 153.52, 157.56, 169.51, 172.35.

MS (ESI) m/z: found Rt 13.66 min. (Method LCMS), 704.68  $[\text{M} + \text{Na}]^+$ .

HRMS 682.1962, 684.1949  $[\text{M} + \text{H}]^+$ , calculated 682.1902  $[\text{M} + \text{H}]^+$ .

***Synthesis of 2-(3-((R)-1-((S)-1-(3,5-dichloro-4-methoxyphenylsulfonyl)piperidine-2-carbonyl-oxy)-3-(3,4-dimethoxyphenyl)propyl)phenoxy)acetic acid 29***

TLC (Hexane: EtOAc: TFA 6:3.8:0.2): Rf = 0.41, yield= 18.3mg (39%).

HPLC (Gradient A) retention time= 27.25-27.47 min.

$^1\text{H}$ NMR (600 MHz,  $\text{CDCl}_3$ )  $\delta$ = 1.02-1.09 (m,1H), 1.39-1.46(m,1H), 1.59-1.62(m,2H), 1.70-1.76(m,1H), 1.99-2.05(m,1H), 2.15-2.23(m,2H). 2.49-2.59(m,2H), 3.18 (dt, 1H, J 2.4, 12.6 Hz, ), 3.68 (dd, 1H, J = 3, 12.6 Hz), 3.84 (s,3H), 3.85 (s, 3H), 3.92 (s, 3H), 4.66 (s,2H), 4.76 (d, 1H, J = 4.8 Hz), 5.61 (t, 1H, J = 6.6 Hz), 6.64-6.67 (m,2H), 6.78 (d, 1H, J = 8.4Hz), 6.81-6.84(m, 2H), 6.89(d,1H, J = 7.8Hz), 7.25 (t, 1H, J = 7.8Hz), 7.71(s, 2H).

$^{13}\text{C}$  NMR (150 MHz,  $\text{CDCl}_3$ )  $\delta$ = 19.78, 24.58, 27.70, 31.28, 37.83, 42.84, 55.31, 55.90, 60.95, 64.85, 76.64, 111.34, 111.76, 112.90, 114.23, 120.01, 120.17, 127.73, 129.85, 130.06, 133.19, 136.95, 141.66, 147.37, 148.84, 155.65, 157.48, 169.67.

MS (ESI) m/z: found RT 11.84 min. (Method LCMS), 718.37, 720.26 [M + Na]<sup>+</sup>.

HRMS 696.1423, 698.2819 [M + H]<sup>+</sup>, calculated 696.1418, 698.2807 [M + H]<sup>+</sup>.

***Synthesis of 2-(3-((R)-1-((S)-1-(4-acetamido-3,5-dichlorophenylsulfonyl)piperidine-2-carboxonyloxy)-3-(3,4-dimethoxyphenyl)propyl)phenoxy)acetic acid 30***

TLC (Hexane: EtOAc: TFA 6:3.8:0.2): R<sub>f</sub> = 0.48, yield= 10.98 mg (21%).

HPLC (Gradient B) retention time= 22.45-22.67min

<sup>1</sup>HNMR (300 MHz, CDCl<sub>3</sub>) δ= 1.27 (s, 3H), 1.63-1.81 (m, 1H), 1.95-2.05 (m, 2H), 2.12-2.33 (m, 5H), 2.51 (t, 2H, J= 6.9 Hz), 3.06 (t, 1H, J= 10.8 Hz), 3.74 (d, 1H, J= 10.2 Hz), 3.85 (s, 3H), 3.86 (s, 3H), 4.67 (s, 3H), 4.80 (d, 1H, J= 4.8 Hz), 5.63 (t, 1H, J= 6 Hz), 6.65-6.68 (m, 2H), 6.74(s, 1H), 6.80 (d, 1H, J= 8.4 Hz), 6.85-6.92 (m, 2H), 7.29 (t, 1H, J= 7.9Hz), 7.68 (s, 2H).

<sup>13</sup>C NMR (75 MHz, CDCl<sub>3</sub>) δ= 20.14, 24.80, 28.02, 29.69, 31.24, 37.65, 43.11, 55.61, 55.86, 55.96, 64.97, 76.72, 111.41, 111.77, 112.99, 114.45, 120.25, 120.30, 127.00, 130.00, 133.20, 134.24, 135.52, 140.49, 141.28, 147.38, 148.84, 157.66, 169.49, 169.60, 171.46.

MS (ESI) m/z: found Rt 12.25 min. (Method LCMS), 723.02, 725.02 [M + 1]<sup>+</sup>.

HRMS 723.2017, 725.2081 [M + H]<sup>+</sup>, calculated 723.2022, 725.2040 [M + H]<sup>+</sup>.

***Synthesis of 5-((S)-2-(((R)-1-(3-(carboxymethoxy)phenyl)-3-(3,4-dimethoxyphenyl)-propoxy)carbonyl)piperidine-1-ylsulfonyl)-2,3-dimethoxybenzoic acid 31***

TLC (DCM: MeOH 9.7:0.3): R<sub>f</sub> = 0.38, yield= 7.23mg (45%).

HPLC (Gradient A) retention time- 22.79-22.95 min

<sup>1</sup>HNMR (400 MHz, DMSO) δ= 1.58-1.73 (m, 3H), 1.94-2.05 (m, 2H), 2.15-2.30 (m, 4H), 2.71-2.97 (m, 3H), 3.67-3.71 (m, 9H), 3.80 (s, 3H), 4.22 (t, 1H, J= 7.6 Hz), 4.58 (s, 2H), 5.35 (s, 1H), 6.68-6.72 (m, 1H), 6.75 (s, 1H), 6.81-6.89 (m, 4H), 6.95-6.99 (m, 1H), 7.06-7.11 (m, 1H), 7.16-7.20 (m, 1H).

<sup>13</sup>C NMR (100 MHz, DMSO) δ= 21.20, 25.10, 31.08, 31.61, 36.50, 51.04, 52.19, 55.33, 55.92, 56.03, 56.06, 61.24, 64.84, 108.62, 111.06, 112.33, 112.40, 112.62, 114.33, 120.46, 120.71, 129.88, 133.63, 135.79, 137.97, 145.07, 147.45, 147.74, 148.33, 148.59, 149.09, 151.85, 158.28, 170.61.

MS (ESI) m/z: found Rt 10.48 min. (Method LCMS), 702.10 [M + H]<sup>+</sup>.

HRMS 702.2761 [M + H]<sup>+</sup>, calculated 702.2142 [M + H]<sup>+</sup>.

***Synthesis of 2-(3-((R)-3-(3,4-dimethoxyphenyl)-1-((S)-1-(7-nitro-2,3-dihydrobenzofuran-5-ylsulfonyl)piperidine-2-carbonyloxy)propyl)phenoxy)acetic acid 32***

TLC (DCM: MeOH 9.7:0.3): R<sub>f</sub> = 0.43, yield= 22mg (42%).

HPLC (Gradient A) retention time= 24.08-24.24 min

<sup>1</sup>H NMR (400 MHz, CDCl<sub>3</sub>) δ= 1.24-1.32 (m, 1H), 1.47-1.50 (m, 1H), 1.67-1.77 (m, 2H), 1.82-1.91 (m, 1H), 1.92-2.01 (m, 1H), 2.09-2.19 (m, 1H), 2.28 (d, 1H, J= 12.4Hz), 2.41-2.60 (m, 2H), 2.92-3.04 (m, 1H), 3.11-3.20 (m, 2H), 3.74 (d, 1H, J= 12Hz), 3.83 (s, 3H), 3.84 (s, 3H), 4.70 (s, 2H), 4.78-4.87 (m, 3H), 4.78-4.87 (m, 3H), 5.55-5.59 (m, 1H), 6.61-6.64 (m, 2H), 6.76 (d, 1H, J= 8Hz), 6.80-6.88 (m, 3H), 7.27 (t, 1H, J= 8Hz), 7.52 (d, 1H, J= 2Hz), 8.24 (d, 1H, J= 2Hz).

<sup>13</sup>C NMR (100 MHz, CDCl<sub>3</sub>) δ= 20.17, 24.75, 28.16, 28.29, 31.28, 38.25, 42.17, 55.52, 55.85, 55.90, 64.78, 74.88, 76.31, 111.30, 111.62, 111.97, 114.46, 119.62, 120.12, 124.34, 128.80, 129.83, 131.69, 132.14, 133.13, 133.79, 141.85, 147.37, 148.85, 157.74, 157.90, 169.71, 171.79

MS (ESI) m/z: found Rt 11.54 min. (Method LCMS), 707.14 [M + Na]<sup>+</sup>.

HRMS 685.2601[M + H]<sup>+</sup>, calculated 685.2589 [M + H]<sup>+</sup>.

***Synthesis of 2-(3-((R)-1-((S)-1-(7-amino-2,3-dihydrobenzofuran-5-ylsulfonyl)piperidine-2-carbonyloxy)-3-(3,4-dimethoxyphenyl)propyl)phenoxy)acetic acid 33***

TLC (DCM: MeOH 9.7:0.3): R<sub>f</sub> = 0.35, yield= 6.7mg (14%).

HPLC (Gradient A) retention time= 21.68-21.89 min

<sup>1</sup>H NMR (600 MHz, CDCl<sub>3</sub>) δ = 1.24-1.32 (m, 1H), 1.47-1.50 (m, 1H), 1.67-1.77 (m, 2H), 1.82-1.91 (m, 1H), 1.92-2.01 (m, 1H), 2.09-2.19 (m, 1H), 2.28 (d, 1H, J= 12.4Hz), 2.41-2.60 (m, 2H), 2.92-3.04 (m, 1H), 3.11-3.20 (m, 2H), 3.74 (d, 1H, J= 12Hz), 3.83 (s, 3H), 3.84 (s, 3H), 4.70 (s, 2H), 4.78-4.87 (m, 3H), 4.78-4.87 (m, 3H), 5.55-5.59 (m, 1H), 6.61-6.64 (m, 2H), 6.76 (d, 1H, J= 8Hz), 6.84 (s, 1H), 6.90-6.98 (m, 3H), 7.27 (t, 1H, J= 8Hz), 8.24 (d, 1H, J= 2Hz).

<sup>13</sup>C NMR (150 MHz, CDCl<sub>3</sub>) δ = 20.17, 24.75, 28.16, 28.29, 31.28, 38.25, 42.17, 55.52, 55.85, 55.90, 64.78, 74.88, 76.31, 111.30, 111.62, 111.97, 114.46, 119.62, 120.12, 124.34, 128.80, 129.83, 131.69, 132.14, 133.13, 137.16, 141.85, 147.37, 148.85, 157.74, 157.90, 169.71, 171.79

MS (ESI) m/z: found Rt 12.22 min. (Method LCMS), 655.08 [M + H]<sup>+</sup>, 677.25 [M + Na]<sup>+</sup>,

HRMS 655.2291 [M + H]<sup>+</sup>, calculated 655.2247 [M + H]<sup>+</sup>.

**Synthesis of 2-(3-((R)-3-(3,4-dimethoxyphenyl)-1-((S)-1-(2-methylbenzo[d]thiazol-6-ylsulfonyl)piperidine-2-carbonyloxy)propyl)phenoxy)acetic acid 34**

TLC (DCM: MeOH 9.7:0.3): R<sub>f</sub> = 0.26, yield= 22mg (43%).

HPLC (Gradient A) retention time= 24.22-24.38 min

<sup>1</sup>H NMR (400 MHz, CDCl<sub>3</sub>) δ= 1.24-1.32 (m, 1H), 1.50-1.61 (m, 1H), 1.65-1.73 (m, 2H), 1.85-1.95 (m, 2H), 2.03-2.13 (m, 1H), 2.18 (d, 1H, J=13.6 Hz), 2.38-2.54 (d, 2H), 2.89 (s, 3H), 3.17-3.25 (m, 1H), 3.81 (s, 3H), 3.82 (s, 3H), 4.72 (d, 1H, J= 8.4 Hz), 4.82 (d, 1H, J= 4.4 Hz), 5.44-5.47 (m, 1H), 6.58-6.61 (m, 2H), 6.68 (s, 1H), 6.74 (d, 1H, J= 8 Hz), 6.98-7.02 (m, 1H).

<sup>13</sup>C NMR (100 MHz, CDCl<sub>3</sub>) δ= 19.76, 19.96, 24.74, 28.21, 31.33, 38.54, 42.44, 55.07, 55.82, 55.88, 65.29, 75.86, 111.25, 111.55, 112.34, 114.90, 119.22, 120.06, 120.93, 121.81, 125.10, 130.15, 133.14, 134.98, 135.77, 142.02, 147.34, 148.83, 154.03, 157.70, 169.43, 171.12, 172.52.

MS (ESI) m/z: found Rt 11.66 min. (Method LCMS), 668.16 [M + H]<sup>+</sup>, 691.11 [M + Na]<sup>+</sup>, HRMS 669.2459 [M + H]<sup>+</sup>, calculated 669.2462 [M + H]<sup>+</sup>.

**Synthesis of 2-(3-((R)-3-(3,4-dimethoxyphenyl)-1-((S)-1-(2-oxo-2,3-dihydrobenzo[d]thiazol-6-ylsulfonyl)piperidine-2-carbonyloxy)propyl)phenoxy)acetic acid 35**

TLC (DCM: MeOH 9.7:0.3): R<sub>f</sub> = 0.37, yield= 24.20mg (46.8%).

HPLC (Gradient A) retention time= 22.74-22.94 min

<sup>1</sup>H NMR (600 MHz, CDCl<sub>3</sub>) δ= 1.38-1.45 (m, 1H), 1.59-1.66 (m, 1H), 1.73-1.75 (m, 2H), 1.89-1.99 (m, 2H), 2.09-2.16 (m, 2H), 2.41-2.46 (m, 1H), 2.52-2.57 (m, 1H), 3.23 (t, 1H, J= 10.2 Hz), 3.78 (d, 1H, J= 7.8Hz), 3.82 (s, 3H), 3.83 (s, 3H), 4.72-4.82 (m, 3H), 5.41-5.43 (m, 1H), 6.18 (d, 1H, J= 8.4Hz), 6.58-6.65 (m, 3H), 6.76 (d, 1H, j= 8.4 Hz), 6.92 (d, 1H, J= 6.6Hz), 7.01 (d, 1H, J= 8.4Hz), 7.09 (d, 1H, J= 8.4Hz), 7.41 (t, 1H, J= 7.8Hz), 7.66 (d, 1H, J= 1.8Hz).

<sup>13</sup>C NMR (150 MHz, CDCl<sub>3</sub>) δ= 19.52, 24.83, 28.47, 31.44, 38.63, 42.16, 54.77, 55.85, 55.92, 64.28, 75.54, 111.34, 111.60, 111.69, 113.56, 118.85, 120.12, 121.10, 124.32, 125.93, 130.27, 133.04, 133.23, 138.48, 142.51, 147.43, 148.89, 157.44, 169.46, 172.87, 173.00.

MS (ESI) m/z: found Rt 11.08 min. (Method LCMS), 693.26 [M + Na]<sup>+</sup>.

HRMS 671.2268 [M + H]<sup>+</sup>, calculated 671.2255 [M + H]<sup>+</sup>.

**Synthesis of 2-(3-((R)-3-(3,4-dimethoxyphenyl)-1-((S)-1-(2-oxoindolin-5-ylsulfonyl)piperidine-2-carbonyloxy)propyl)phenoxy)acetic acid 36**

TLC (Hexane: EtOAc: TFA 6:4:0.1): R<sub>f</sub> = 0.25, yield= 6.0mg (12.5%).

HPLC (Gradient A) retention time= 21.21-21.40min

$^1\text{H}$ NMR (600 MHz,  $\text{CDCl}_3$ )  $\delta$ = 1.55-1.64 (m, 1H), 1.69-1.76 (m, 2H), 1.91-2.00 (m, 2H), 2.10-2.16 (m, 2H), 2.43-2.48 (m, 1H), 2.53-2.58 (m, 1H), 3.16-3.21 (m, 1H), 3.39 (d, 1H,  $J$ = 22.8 Hz), 3.52 (d, 1H,  $J$ = 22.8 Hz), 3.73 (s, 1H), 3.82 (s, 3H), 3.83 (s, 3H), 3.87 (s, 1H), 4.71-4.81 (m, 3H), 5.43-5.45 (m, 1H), 6.25 (d, 1H,  $J$ = 8.4 Hz), 6.60-6.62 (m, 2H), 6.72-6.77 (m, 2H), 6.84-6.89 (m, 1H), 7.04-7.10 (m, 2H), 7.38 (t, 1H,  $J$ = 8.4 Hz), 7.45 (s, 1H).

$^{13}\text{C}$  NMR (150 MHz,  $\text{CDCl}_3$ )  $\delta$ = 19.63, 24.79, 28.43, 31.39, 36.16, 38.61, 42.13, 54.81, 55.83, 55.90, 63.93, 75.75, 110.47, 111.35, 111.61, 113.16, 113.50, 118.85, 120.14, 123.25, 125.28, 128.33, 130.10, 133.09, 142.60, 145.55, 147.37, 148.85, 157.49, 169.65, 171.81, 179.46.

MS (ESI)  $m/z$ : found Rt 11.03 min. (Method LCMS), 675.18  $[\text{M} + \text{Na}]^+$

HRMS 653.2603  $[\text{M} + \text{H}]^+$ , calculated 653.2591  $[\text{M} + \text{H}]^+$ .

**Synthesis of 2-(3-((*R*)-3-(3,4-dimethoxyphenyl)-1-((*S*)-1-(2-oxo-2,3-dihydrobenzo[*d*]oxazol-6-yl-sulfonyl)piperidine-2-carboxyloxy)propyl)phenoxy)acetic acid 37**

TLC (Hexane: EtOAc: TFA 6:4:0.1):  $R_f$  = 0.42, yield= 6.4mg (24.6%).

HPLC (Gradient A) retention time= 21.68-21.85min

$^1\text{H}$ NMR (600 MHz,  $\text{CDCl}_3$ )  $\delta$ = 1.57-1.64 (m, 1H), 1.701.75 (m, 2H), 1.91-1.99 (m, 2H), 2.10-2.16 (m, 2H), 2.43-2.48 (m, 1H), 2.53-2.59 (m, 1H), 3.19-3.24 (m, 1H), 3.36 (d, 1H,  $J$ = 22.2 Hz), 3.48 (d, 1H,  $J$ = 22.2 Hz), 3.74 (s, 2H), 3.83 (s, 3H), 3.84 (s, 3H), 4.75 (d, 2H,  $J$ = 19.0 Hz), 4.80-4.81 (m, 1H), 5.44-5.46 (m, 1H), 6.20 (d, 1H,  $J$ = 8.4 Hz), 6.59-6.63 (m, 2H), 6.72-6.78 (m, 2H), 6.89 (d, 1H,  $J$ = 8.4 Hz), 7.05 (d, 1H,  $J$ = 7.8Hz), 7.10 (d, 1H,  $J$ = 7.8 Hz), 7.39 (t, 1H,  $J$ = 8.4 Hz), 7.44 (s, 1H).

MS (ESI)  $m/z$ : found Rt 14.66 min. (Method LCMS), 677.66  $[\text{M} + \text{Na}]^+$ , calculated 677.54  $[\text{M} + \text{Na}]^+$ .

**Synthesis of 2-(3,4-dimethoxyphenoxy)ethyl 1-(3,5-dichlorophenylsulfonyl)piperidine-2-carboxylate 38**

To 71a ((50mg, 0.162mmol) in DCM DIPEA (62.7mg, 0.485mmol) and 3,5-dichlorobenzene sulfonyl chloride (39.7mg,0.162mmol) were added. The reaction was stirred at room temperature overnight and was purified by flash chromatography using cyclohexane : EtOAc 3:1 to yield 38.

TLC (Cyclohexane: EtOAc 3:1):  $R_f$  = 0.57, yield= 17mg (20%).

HPLC (Gradient A) retention time= 22.74-22.94 min

$^1\text{H}$ NMR (600 MHz,  $\text{CDCl}_3$ )  $\delta$ = 1.47-1.63 (m, 2H), 1.65-1.71 (m, 2H), 1.73-1.85 (m, 1H), 2.16-2.21 (m, 1H), 3.16-3.24 (m, 1H), 3.72-3.77 (m, 1H), 3.84(s, 3H), 3.85 (s, 3H), 3.97-4.03 (m,

1H), 4.03-4.08 (m, 1H), 4.25-4.30 (m, 1H), 4.35-4.40 (m, 1H), 4.75-4.80 (m, 1H), 6.34 (dd, 1H, J= 2.83, 8.73 Hz), 6.48 (d, 1H, J= 2.8Hz), 6.76 (d, 1H, J= 8.7Hz), 7.49 (t, 1H, J= 1.86, 1.86 Hz), 7.64(d, 2H, J= 1.85 Hz).

<sup>13</sup>C NMR (150 MHz, CDCl<sub>3</sub>) δ= 19.88, 24.73, 27.92, 42.88, 55.31, 55.85, 56.41, 63.48, 66.13, 101.06, 103.99, 111.76, 125.55, 132.29, 135.64, 142.67, 143.99, 149.92, 152.82, 170.23

MS (ESI) m/z: found Rt 13.97 min. (Method LCMS), 518.55, 520.57 [M + H]<sup>+</sup>, 540.45, 542.23 [M + Na]<sup>+</sup>.

HRMS 518.1343, 520.1326 [M + H]<sup>+</sup>, calculated 518.1289. 520.1312 [M + H]<sup>+</sup>.

### ***Synthesis of 2-(3,4-dimethoxyphenoxy)ethyl 1-(benzo[d]thiazol-6-ylsulfonyl)piperidine-2-carboxylate 39***

To **71a** (50mg, 0.162mmol) in DCM DIPEA (62.7mg,0.485mmol) and benzo[d]thiazole-6-sulfonyl chloride(76mg, 0.323mmol) were added. The reaction was stirred at room temperature overnight and was purified by flash chromatography using cyclohexane: EtOAc 1:1 to yield **39** TLC (Cyclohexane: EtOAc 1:1): R<sub>f</sub> = 0.3, yield= 39mg (48%).

HPLC (Gradient A) retention time= 22.74-22.94 min

<sup>1</sup>H NMR (300 MHz, CDCl<sub>3</sub>) δ= 1.3-1.62 (m, 2H), 1.62-1.74(m,2H), 1.74-1.88 (m, 1H), 2.15-2.25 (m, 1H), 3.21-3.34 (m, 1H), 3.74-3.83 (m, 1H), 3.85 (s, 3H), 3.86 (s, 3H), 3.89-4.05(m,2H), 4.09-4.38(m, 2H), 4.85-4.91 (m, 1H), 6.31-6.37(m, 1H), 6.47-6.51(m, 1H), 6.75-6.81(m, 1H), 7.90-7.96 (m, 1H), 8.19-8.24(m, 1H), 8.47-8.51(m, 1H), 9.18-9.22(m,1H).

<sup>13</sup>C NMR (75 MHz, CDCl<sub>3</sub>) δ= 19.98, 24.75, 27.94, 42.80, 55.21, 55.89, 56.44, 63.47, 66.16, 101.09, 104.07, 111.80, 122.00, 123.98, 124.98, 133.95, 137.34, 144.01, 149.04, 152.84, 155.20, 157.63, 170.56.

MS (ESI) m/z: found Rt 12.15 min. (Method LCMS), 507.56 [M + H]<sup>+</sup>, 529.38 [M + Na]<sup>+</sup>.

HRMS 507.1779[M + H]<sup>+</sup>, calculated 507.1681 [M + H]<sup>+</sup>.

### **General Procedure for the synthesis of Compound 40-45.**

To **71b** (19mg, 0.037 mmol) DIPEA (9.2 mg, 0.055 mmol) and the corresponding sulfonyl chloride (0.055 mmol) were added The reaction was stirred at room temperature overnight and was purified by prep HPLC using gradient C to yield compound **40-45**.

### ***Synthesis of (S)-((R)-3-(3,4-dimethoxyphenyl)-1-(3-(2-morpholinoethoxy)phenyl)propyl)-1-(3,5-dichlorophenylsulfonyl)piperidine-2-carboxylate 40***

TLC (DCM: MeOH 9.7:0.3): R<sub>f</sub> = 0.48, yield= 16.42 mg (62%).

HPLC (Gradient A) retention time= 20.8-21.2 min

<sup>1</sup>H NMR (600 MHz, CDCl<sub>3</sub>) δ= 1.28-1.31 (m, 1H), 1.38-1.47 (m, 1H), 1.64-1.79 (m, 1H), 1.98-2.04 (m, 1H), 2.15-2.21 (m, 1H), 2.27 (d, 1H, J= 13.8 Hz), 2.48-2.53 (m, 1H), 2.56-2.60 (m, 1H), 3.09-3.18 (m, 3H), 3.56 (t, 2H, J= 4.8 Hz), 3.66 (dd, 1H, J= 2.4, 13.2Hz), 3.76 (d, 2H, J= 12Hz), 3.84 (s, 3H), 3.85 (s, 3H), 3.95 (t, 2H, J= 12.6 Hz), 4.02 (d, 1H, J= 2.4Hz), 4.04 (d, 1H, J= 2.4 Hz), 4.39 (t, 2H, J= 4.6 Hz), 4.79 (d, 1H, J= 4.8Hz), 6.65-6.67 (m, 2H), 6.77 (d, 1H, J= 7.8 Hz), 6.80-6.82 (m, 1H), 6.85-6.86 (m, 1H), 6.91 (d, 1H, J= 7.8 Hz), 7.29 (t, 1H, J=8.1 Hz), 7.46 (t, 1H, J=1.8Hz), 7.55 (s, 1H), 7.55 (s, 1H).

<sup>13</sup>C NMR (150 MHz, CDCl<sub>3</sub>) δ= 20.15, 24.71, 27.93, 31.28, 37.86, 43.01, 53.93, 55.64, 55.86, 55.95, 57.55, 65.55, 66.45, 77.21, 111.34, 111.73, 112.87, 114.24, 119.07, 120.13, 125.53, 129.82, 132.35, 133.33, 135.64, 141.19, 142.98, 147.42, 148.92, 158.7, 169.61

MS (ESI) m/z: found Rt 8.76 min. (Method LCMS), 721.65, 723.37 [M + H]<sup>+</sup>.

HRMS 721.2797, 723.2766 [M + H]<sup>+</sup>, calculated 721.2739, 723.2745 [M + H]<sup>+</sup>.

***Synthesis of (S)-((R)-3-(3,4-dimethoxyphenyl)-1-(3-(2-morpholinoethoxy)phenyl)propyl ) 1-(benzo[d]thiazol-6-ylsulfonyl)piperidine-2-carboxylate 41***

TLC (DCM: MeOH 9.7:0.3): R<sub>f</sub> = 0.27, yield= 31.72mg (91%).

HPLC (Gradient A) retention time= 20.78-20.98 min

<sup>1</sup>H NMR (300 MHz, CDCl<sub>3</sub>) δ= 1.61-1.74 (m, 3H), 1.77-1.87 (m, 3H), 1.94-2.06 (m, 1H), 2.13-2.31 (m, 1H), 2.47-2.66 (m, 2H), 3.05-3.23 (m, 3H), 3.55-3.57 (m, 2H), 3.66-3.81 (m, 3H), 3.85 (s, 6H), 4.00 (s, 4H), 4.46 (s, 2H), 2.90 (d, 1H, J= 4.5 Hz), 5.58-5.63 (m, 1H), 6.65-6.68 (m, 2H), 6.88-6.96 (m, 3H), 7.24-7.29 (m, 1H), 7.32-7.37 (m, 1H), 7.64-7.68 (m, 1H), 7.89-7.96 (m, 1H), 8.35 (s, 1H), 9.20 (s, 1H).

<sup>13</sup>C NMR (75 MHz, CDCl<sub>3</sub>) δ= 24.56, 27.80, 31.30, 33.33, 42.74, 46.50, 52.74, 55.42, 55.85, 55.93, 56.47, 62.47, 63.91, 76.23, 111.37, 111.73, 112.28, 114.31, 119.97, 120.16, 121.93, 123.74, 124.85, 129.02, 130.08, 133.25, 137.21, 142.29, 147.42, 148.93, 155.00, 157.39, 157.99, 169.98.

MS (ESI) m/z: found Rt 8.45 min. (Method LCMS), 710.51 [M + H]<sup>+</sup>.

HRMS 710.2517 [M + H]<sup>+</sup>, calculated 710.2492 [M + H]<sup>+</sup>.

***Synthesis of (S)-((R)-3-(3,4-dimethoxyphenyl)-1-(3-(2-morpholinoethoxy)phenyl)propyl)1-(3,5-dichloro-4-hydroxyphenylsulfonyl)piperidine-2-carboxylate 42***

TLC (DCM: MeOH 9.7:0.3): R<sub>f</sub> = 0.45, yield= 15.96mg (58%).

HPLC (Gradient A) retention time= 19.28-19.61 min

<sup>1</sup>H NMR (300 MHz, CDCl<sub>3</sub>) δ= 1.54-2.06 (m, 6H), 2.14-2.30 (m, 2H), 2.44-2.64 (m, 2H), 2.99-3.27 (m, 3H), 3.51 (s, 2H), 3.74-3.80 (m, 3H), 3.86 (s, 3H), 3.87 (s, 3H), 4.06 (s, 4H), 4.43 (s, 2H), 4.72 (d, 1H, J= 4.2Hz), 5.53-5.59 (m, 1H), 6.65-6.69 (m, 3H), 6.78-6.85 (m, 2H), 6.92 (d, 1H, J=7.8 Hz), 7.29-7.33 (m, 1H), 7.49 (s, 2H).

<sup>13</sup>C NMR (75 MHz, CDCl<sub>3</sub>) δ= 20.15, 24.94, 28.07, 31.45, 37.87, 42.86, 53.05, 55.25, 55.87, 55.95, 56.81, 62.50, 63.96, 76.25, 111.39, 111.71, 112.71, 114.02, 119.57, 120.15, 121.53, 127.30, 130.22, 132.31, 133.18, 141.75, 147.47, 148.95, 151.71, 157.01, 169.52.

MS (ESI) m/z: found RT 8.76 min. (Method LCMS), 737.04, 739.13 [M + H]<sup>+</sup>.

HRMS 737.2532, 739.2506 [M + H]<sup>+</sup>, calculated 737.2501, 739.2542 [M + H]<sup>+</sup>.

**Synthesis of (S)-((R)-3-(3,4-dimethoxyphenyl)-1-(3-(2-morpholinoethoxy)phenyl)propyl)-1-(3,5-dichloro-4-methoxyphenylsulfonyl)piperidine-2-carboxylate 43**

TLC (DCM: MeOH 9.7:0.3): R<sub>f</sub> = 0.42, yield= 21mg (75%).

HPLC (Gradient A) retention time= 23.31-23.63min

<sup>1</sup>H NMR (600 MHz, CDCl<sub>3</sub>) δ= 1.27-1.31 (m, 1H), 1.41-1.46 (m, 1H), 1.65 (d, 1H, J= 13.8Hz), 1.71-1.80 (m, 2H), 1.99-2.05 (m, 1H), 2.17-2.23 (m, 1H), 2.28 (d, 1H, J= 14.4 Hz), 2.49-2.54 (m, 1H), 2.56-2.61 (m, 1H), 3.09 (t, 2H, J= 11.4Hz), 3.15(dt, 1H, J= 3, 12.6Hz), 3.54 (t, 2H, J= 5.2Hz), 3.66 (d, 1H, J= 10.8Hz), 3.71-3.74 (m, 2H), 3.84 (s, 6H), 3.91 (s, 3H), 3.96-4.03 (m, 4H), 4.40 (d, 2H, J =5.0Hz), 4.79 (d, 1H, J= 4.8Hz), 5.68 (q, 1H, J=3, 5.4 Hz), 6.65-6.67 (m, 2H), 6.77 (d, 1H, J= 7.8Hz), 6.81-6.83 (m, 1H), 6.85(t, 1H, J= 1.8Hz), 6.90(d, 1H, J= 7.2Hz), 7.29 (t, 1H, J= 7.8 Hz), 7.61 (s, 2H).

<sup>13</sup>C NMR (150 MHz, CDCl<sub>3</sub>) δ= 20.05, 24.56, 27.73, 31.26, 37.95, 42.93, 52.87, 55.57, 55.82, 55.91, 56.58, 60.94, 62.32, 63.90, 76.44, 111.32, 111.70, 112.33, 141.12, 120.03, 120.15, 127.73, 129.98, 130.07, 133.24, 137.01, 141.83, 147.38, 148.88, 155.61, 157.27, 169.80.

MS (ESI) m/z: found RT 9.08 min. (Method LCMS), 751.53, 753.32 [M + H]<sup>+</sup>.

HRMS 751.2705, 753.2674 [M + H]<sup>+</sup>, calculated 751.2675, 753.2682 [M + H]<sup>+</sup>.

**Synthesis of (S)-((R)-3-(3,4-dimethoxyphenyl)-1-(3-(2-morpholinoethoxy)phenyl)propyl)-1-(2-oxo-2,3-dihydrobenzo[d]thiazol-6-ylsulfonyl)piperidine-2-carboxylate 44**

TLC (DCM: MeOH 9.7:0.3): R<sub>f</sub> = 0.39, yield= 6.4mg (24.6%).

HPLC (Gradient A) retention time= 18.92-19.16min

<sup>1</sup>H NMR (300 MHz, CDCl<sub>3</sub>) δ= 1.71-1.81 (m, 2H), 1.84-2.01 (m, 2H), 2.06-2.22 (m, 2H), 2.39-2.62 (m, 2H), 3.01-3.12 (m, 2H), 3.26-3.37 (m, 2H), 3.54 (s, 2H), 3.80-3.91 (m, 12H), 4.06 (s, 4H), 4.26-4.50 (m, 2H), 4.74 (d, 1H, J= 4.8Hz), 5.36-5.41 (m, 1H), 6.55-6.64 (m, 4H), 6.77 (d,

1H, J= 7.5Hz), 6.89 (d, 1H, J= 6.9 Hz), 6.99 (d, 1H, J= 7.5 Hz), 7.19 (d, 1H, J= 8.4 Hz), 7.38 (t, 1H, J= 7.6 Hz), 7.62 (d, 1H, J= 1.8Hz).

<sup>13</sup>C NMR (75 MHz, CDCl<sub>3</sub>) δ= 24.98, 28.29, 31.43, 38.45, 42.48, 53.47, 54.79, 55.87, 55.94, 57.28, 62.02, 63.93, 75.83, 111.03, 111.37, 111.69, 112.73, 113.79, 119.18, 120.17, 121.54, 124.28, 125.73, 130.46, 133.10, 133.39, 138.88, 142.22, 147.47, 148.93, 156.99, 169.62.

MS (ESI) m/z: found Rt 9.47 min. (Method LCMS), 726.29 [M + H]<sup>+</sup>.

HRMS 726.3111 [M + H]<sup>+</sup>, calculated 726.3091 [M + H]<sup>+</sup>.

### Synthesis of (S)-((R)-3-(3,4-dimethoxyphenyl)-1-(3-(2-morpholinoethoxy)phenyl)propyl)1-(4-acetamido-3,5-dichlorophenylsulfonyl)piperidine-2-carboxylate **45**

TLC (DCM: MeOH 9.7:0.3): R<sub>f</sub> = 0.12, yield= 15.4mg (70.8%).

HPLC (Gradient A) retention time= 19.64-19.81min

<sup>1</sup>H NMR (600 MHz, CDCl<sub>3</sub>) δ= 1.27-1.29 (m, 1 H), 1.49-1.51 (m, 1H), 1.67 (d, 1H, J=12.6 Hz), 1.73 (d, 1H, J= 13.2 Hz), 1.78-1.84 (m, 1H), 1.95-2.00 (m, 1H), 2.13-2.19 (m, 1H), 2.26 (s, 4H), 2.48-2.55 (m, 2H), 3.08-3.14 (m, 3H), 3.54 (s, 2H), 3.65-3.74 (m, 3H), 3.81 (s, 3H), 3.84 (s, 3H), 3.92-3.98 (m, 2H), 4.00-4.04 (m, 2H), 4.36 (m, 2H), 4.78 (d, 1H, J= 4.8Hz), 5.58 (t, 1H, J= 7.2 Hz), 6.62-6.64 (m, 2H), 6.76-6.81 (m, 3H), 6.90 (d, 1H, J= 7.8 Hz), 7.28 (t, 1H, J= 7.8 Hz), 7.61 (s, 2H).

<sup>13</sup>C NMR (150 MHz, CDCl<sub>3</sub>) δ= 19.95, 24.60, 27.88, 29.66, 31.16, 37.54, 42.98, 53.07, 55.76, 55.93, 56.80, 61.99, 63.80, 63.82, 76.65, 111.38, 111.68, 114.17, 116.07, 120.06, 120.30, 126.96, 126.97, 130.13, 133.21, 135.30, 141.68, 147.29, 148.76, 157.19, 159.79, 160.05, 160.32, 160.58, 169.76

MS (ESI) m/z: found Rt 10.30 min. (Method LCMS), 778.25, 780.31 [M + H]<sup>+</sup>, 800.23, 802.20 [M + Na]<sup>+</sup>

HRMS 778.3114, 780.3122 [M + H]<sup>+</sup>, calculated 778.3154, 780.3162 [M + H]<sup>+</sup>.

### Deprotection of Fmoc (resin **6b**)

The coupled resin **5b** was weighed (190 mg, 0.05mmol) and added to syringes, swollen in DCM (4 mL) for 1h, and the Fmoc protecting group was removed using 20% 4-methyl piperidine/DCM (4ml) for 1h. After filtration, the resin was washed with DCM (3 x 5ml) and used for the next coupling step.

**Synthesis of sulfonamides**

To the above resin *i*-Pr<sub>2</sub>EtN (25mg, 0.20mmol) in dry DCM (3 mL) was added and stirred for 20min. To this solution the sulfonyl chloride (0.15mmol) in 500 μL of DCM was added and the reaction was stirred for 4h at room temperature. After the first coupling step the resins were filtered, washed with DCM (3 x 10ml) and then subjected to second coupling with *i*-Pr<sub>2</sub>EtN (30mg, 0.237mmol), sulfonyl chloride (0.158 mmol) in DCM (3 mL) and stirred for 16h at room temperature. The resins were washed with DCM (3 x 5ml) and dried to give the derivatized resins. These were re-swollen in DCM reacted with 1% TFA/DCM (3ml) for 1h and then washed with 1% TFA/DCM (3 x 3ml) and further washed with DCM (3 x 5ml). The combined filtrates were concentrated *in vacuo* to yield the compounds **46-47**. (crude weight ~ 50mg). The crude compounds were further purified by preparative HPLC using Gradient C. The purified peaks were further dried by lyophilization.

**Synthesis of 2-(3-((R)-1-((S)-1-(3,5-dichloro-4-hydroxyphenylsulfonyl)piperidine-2-carboxamido)-3-(3,4-dimethoxyphenyl)propyl)phenoxy)acetic acid **46****

TLC (Hexane: EtOAc: TFA 6:3.8:0.2): R<sub>f</sub> = 0.31, yield= 8 mg (17.4 %).

HPLC (Gradient A) retention time= 22.6-22.9 min

<sup>1</sup>HNMR (600 MHz, CDCl<sub>3</sub>) δ= 1.30-1.36 (m, 1H), 1.46 (d, 1H, J= 13.2 Hz), 1.51-1.55 (m, 1H), 2.01-2.14 (m, 3H), 2.26 (d, 1H, J= 13.2 Hz), 2.49-2.63 (m, 2H), 2.85-2.94 (m, 1H), 3.79-3.83 (m, 2H), 3.85 (s, 3H), 3.86 (s, 3H), 4.49 (d, 1H, J= 4.8 Hz), 4.67 (s, 2H), 4.92-4.97 (m, 1H), 6.68-6.70 (m, 2H), 6.77- 6.80 (m, 2H), 6.82-6.84 (m, 1H), 6.92 (d, 1H, J= 7.8 Hz), 7.28 (t, 1H, J= 7.8 Hz), 7.75 (s, 2H).

MS (ESI) m/z: found Rt 13.45 min. (Method LCMS), 681.67, 683.48 [M + H]<sup>+</sup>, 703.85, 705.57 [M + Na]<sup>+</sup>, Calculated 681.58, 683.50 [M + H]<sup>+</sup>, 703.13, 705.24 [M + Na]<sup>+</sup>.

**Synthesis of 2-(3-((R)-3-(3,4-dimethoxyphenyl)-1-((S)-1-(2-oxo-2,3-dihydrobenzo[d]thiazol-6-ylsulfonyl)piperidine-2-carboxamido)propyl)phenoxy)acetic acid **47****

TLC (Hexane: EtOAc: TFA 6:3.8:0.2): R<sub>f</sub> = 0.32, yield= 8.2 mg (17.5 %).

HPLC (Gradient A) retention time= 21.14-21.35min

<sup>1</sup>HNMR (600 MHz, CDCl<sub>3</sub>) δ= 1.38-1.42 (m, 1H), 1.57-1.66 (m, 5H), 1.93-2.17 (m, 3H), 2.44-2.56 (m, 2H), 3.71-3.76 (m, 1H), 3.83-3.84 (m, 6H), 4.55-4.60 (m, 1H), 4.72-4.73 (m, 2H), 4.77-4.84 (m, 1H), 6.46 (t, 1H, J= 8.4 Hz), 6.64- 6.73 (m, 3H), 6.77 (d, 1H, J= 7.8 Hz), 6.81-6.83 (m, 1H), 6.93-6.96 (m, 1H), 7.29-7.36 (m, 2H), 7.78-7.79 (m, 1H).

MS (ESI) m/z: found Rt 13.27 min. (Method LCMS), 670.50 [M + H]<sup>+</sup>, 692.49 [M + Na]<sup>+</sup>,  
Calculated 670.23 [M + H]<sup>+</sup>, 692.17 [M + Na]<sup>+</sup>.

**Synthesis of (S)-1,7-di(pyridine-3-yl)heptane-4-yl 1-(3,5-dichloro-4-hydroxyphenyl-sulfonyl)piperidine-2-carboxylate 48**

TLC (DCM: MeOH 9.5:0.5): R<sub>f</sub> = 0.49, yield= 10.2 mg (47.7%).

HPLC (Gradient A) retention time= 28.9-29.2min

MS (ESI) m/z: found Rt 7.01 min. (Method LCMS), 606.18, 608.20 [M + H]<sup>+</sup>

Calculated 606.18, 608.22 [M + H]<sup>+</sup>.

**X-ray crystallography**

Crystals and co-crystals of the FKBP51 Fk1 domain construct comprising residues 16-140 and containing mutation A19T were obtained as previously described<sup>16</sup>. Diffraction data were collected at beamline X06DA of the Swiss Light Source (SLS) synchrotron in Villigen, Switzerland. The data were processed with MOSFLM<sup>24</sup> and XDS<sup>25</sup>, SCALA<sup>26</sup> and TRUNCATE<sup>27</sup>. The crystal structure was isomorphous with the apo structure (PDB code 3O5R). The dictionaries for the ligand compounds were generated with the PRODRG server<sup>28</sup>. The structures were refined with REFMAC<sup>29</sup>. Manual model building was performed with COOT<sup>30</sup>. Molecular graphic figures were generated using PyMOL (<http://www.pymol.org>).

**Supporting Information.** Purity and activity data for compounds 47-77 from the high throughput synthesis and assay. This material is available free of charge via the Internet at <http://pubs.acs.org>.

**Acknowledgments**

We thank Dr. Gerd Rühter and the Lead Discovery Center (Dortmund) for providing the precursor for the synthesis of morpholine analogs and compound 46. We thank Prof. Florian Holsboer and the CIPSM for financial support. We are indebted to Mrs. E. Weyher and Dr. S. Uebel (MPI of Biochemistry) and to Mrs. C. Dubler (Ludwig-Maximilians-Universität Munich) for HRMS and NMR measurements. This research project has been supported by the European Commission under the 7th Framework Program: Research Infrastructures. Grant Agreement Number 226716.

## References

- (1) Holt, D. A.; Luengo, J. I.; Yamashita, D. S.; Oh, H. J.; Konilian, A. L. et al. Design, synthesis, and kinetic evaluation of high-affinity FKBP ligands and the X-ray crystal structures of their complexes with FKBP 12. *J Am Chem Soc* 1993, *115*, 9925-9938.
- (2) Hudack, R. A. Design, Synthesis, and Biological Activity of Novel Polycyclic Aza-Amide FKBP12 Ligands *Journal of Medicinal Chemistry* 2006, *49*, 1202-1206.
- (3) Gaali, S.; Gopalakrishnan, R.; Wang, Y.; Kozany, C.; Hausch, F. The chemical biology of immunophilin ligands. *Curr Med Chem* 2011, *18*, 5355-5379.
- (4) Keenan, T.; Yaeger, D. R.; Courage, N. L.; Rollins, C. T.; Pavone, M. E. et al. Synthesis and activity of bivalent FKBP12 ligands for the regulated dimerization of proteins. *Bioorg Med Chem* 1998, *6*, 1309-1335.
- (5) Riggs, D. L.; Roberts, P. J.; Chirillo, S. C.; Cheung-Flynn, J.; Prapapanich, V. et al. The Hsp90-binding peptidylprolyl isomerase FKBP52 potentiates glucocorticoid signaling in vivo. *Embo J* 2003, *22*, 1158-1167.
- (6) Wochnik, G. M.; Ruegg, J.; Abel, G. A.; Schmidt, U.; Holsboer, F. et al. FK506-binding Proteins 51 and 52 Differentially Regulate Dynein Interaction and Nuclear Translocation of the Glucocorticoid Receptor in Mammalian Cells. *J. Biol. Chem.* 2005, *280*, 4609-4616.
- (7) Davies, T. H.; Ning, Y.-M.; Sanchez, E. R. Differential control of glucocorticoid receptor hormone-binding function by tetratricopeptide repeat (TPR) proteins and the immunosuppressive ligand FK506. *Biochemistry* 2005, *44*, 2030-2038.
- (8) Binder, E. B. The role of FKBP5, a co-chaperone of the glucocorticoid receptor in the pathogenesis and therapy of affective and anxiety disorders. *Psychoneuroendocrinology* 2009, *34*, S186-S195.
- (9) Touma, C.; Gassen, N. C.; Herrmann, L.; Cheung-Flynn, J.; Bull, D. R. et al. FK506 Binding Protein 5 Shapes Stress Responsiveness: Modulation of Neuroendocrine Reactivity and Coping Behavior. *Biol Psychiatry* 2011.
- (10) Hartmann, J.; Wagner, K. V.; Liebl, C.; Scharf, S. H.; Wang, X. D. et al. The involvement of FK506-binding protein 51 (FKBP5) in the behavioral and neuroendocrine effects of chronic social defeat stress. *Neuropharmacology* 2011.
- (11) Attwood, B. K.; Bourgoignon, J. M.; Patel, S.; Mucha, M.; Schiavon, E. et al. Neuropsin cleaves EphB2 in the amygdala to control anxiety. *Nature* 2011, *473*, 372-375.

- (12) O'Leary, J. C., 3rd; Dharia, S.; Blair, L. J.; Brady, S.; Johnson, A. G. et al. A New Anti-Depressive Strategy for the Elderly: Ablation of FKBP5/FKBP51. *PLoS One* 2011, 6, e24840.
- (13) Choi, C.; Li, J. H.; Vaal, M.; Thomas, C.; Limburg, D. et al. Use of parallel-synthesis combinatorial libraries for rapid identification of potent FKBP12 inhibitors. *Bioorganic & Medicinal Chemistry Letters* 2002, 12, 1421-1428.
- (14) Wei, L.; Wu, Y. Q.; Wilkinson, D. E.; Chen, Y.; Soni, R. et al. Solid-phase synthesis of FKBP12 inhibitors: N-sulfonyl and N-carbamoylprolyl/pipecolyl amides. *Bioorganic & Medicinal Chemistry Letters* 2002, 12, 1429-1433.
- (15) Juli, C.; Sippel, M.; Jager, J.; Thiele, A.; Weiwad, M. et al. Pipecolic Acid Derivatives As Small-Molecule Inhibitors of the Legionella MIP Protein. *Journal of Medicinal Chemistry* 2011, 54, 277-283.
- (16) Bracher, A.; Kozany, C.; Thost, A. K.; Hausch, F. Structural characterization of the PPIase domain of FKBP51, a cochaperone of human Hsp90. *Acta Crystallogr D Biol Crystallogr* 2011, 67, 549-559.
- (17) Szep, S.; Park, S.; Boder, E. T.; Van Duyne, G. D.; Saven, J. G. Structural coupling between FKBP12 and buried water. *Proteins-Structure Function and Bioinformatics* 2009, 74, 603-611.
- (18) Riggs, D. L.; Cox, M. B.; Tardif, H. L.; Hessling, M.; Buchner, J. et al. Noncatalytic role of the FKBP52 peptidyl-prolyl isomerase domain in the regulation of steroid hormone signaling. *Mol Cell Biol* 2007, 27, 8658-8669.
- (19) Sun, F.; Li, P. Y.; Ding, Y.; Wang, L. W.; Bartlam, M. et al. Design and structure-based study of new potential FKBP12 inhibitors. *Biophysical Journal* 2003, 85, 3194-3201.
- (20) Gopalakrishnan, R.; Hausch, F. Evaluation of Synthetic FK506 Analogs as Ligands for FKBP51 and FKBP52. *To be Submitted*.
- (21) Kozany, C.; Marz, A.; Kress, C.; Hausch, F. Fluorescent probes to characterise FK506-binding proteins. *Chembiochem* 2009, 10, 1402-1410.
- (22) Bissantz, C.; Kuhn, B.; Stahl, M. A medicinal chemist's guide to molecular interactions. *J Med Chem* 2010, 53, 5061-5084.
- (23) Hardegger, L. A.; Kuhn, B.; Spinnler, B.; Anselm, L.; Ecabert, R. et al. Systematic investigation of halogen bonding in protein-ligand interactions. *Angew Chem Int Ed Engl* 2011, 50, 314-318.
- (24) Leslie, A. G. W. Recent changes to the MOSFLM package for processing film and image plate data. *Jnt CCP4/ESF-EACMB Newsl. Protein Crystallogr.* 1992, 26.

- (25) Kabsch, W. Xds. *Acta Crystallographica Section D-Biological Crystallography* 2010, 66, 125-132.
- (26) Evans, P. R. SCALA. *Jnt CCP4/ESF-EACMB Newsl. Protein Crystallogr.* 1997, 33, 22-24.
- (27) French, S.; Wilson, K. Treatment of Negative Intensity Observations. *Acta Crystallographica Section A* 1978, 34, 517-525.
- (28) Schuttelkopf, A. W.; van Aalten, D. M. F. PRODRG: a tool for high-throughput crystallography of protein-ligand complexes. *Acta Crystallographica Section D-Biological Crystallography* 2004, 60, 1355-1363.
- (29) Murshudov, G. N.; Skubak, P.; Lebedev, A. A.; Pannu, N. S.; Steiner, R. A. et al. REFMAC5 for the refinement of macromolecular crystal structures. *Acta Crystallographica Section D-Biological Crystallography* 2011, 67, 355-367.
- (30) Emsley, P.; Lohkamp, B.; Scott, W. G.; Cowtan, K. Features and development of Coot. *Acta Crystallographica Section D-Biological Crystallography* 2010, 66, 486-501.

## Supporting Information

### **Exploration of Pipecolate Sulfonamides as Binders of the FK506-Binding Proteins 51 and 52**

**Ranganath Gopalakrishnan**<sup>1</sup>, Christian Kozany<sup>1</sup>, Yansong Wang<sup>1</sup>, Sabine Schneider<sup>3</sup>, Bastiaan Hoogeland<sup>1</sup>, Andreas Bracher<sup>2</sup>, Felix Hausch<sup>1\*</sup>

<sup>1</sup>Max Planck Institute of Psychiatry, Kraepelinstr. 2, 80804 Munich, Germany,

<sup>2</sup>Max Planck Institute of Biochemistry, Am Klopferspitz 18, 82152 Martinsried, Germany

<sup>3</sup>Technical University Munich, Lichtenbergstr. 4, 85747 Garching, Germany

### **Supporting Information Table of Contents:**

- 1. Medium throughput small scale synthesis**
- 2. Library Testing**
- 3. Table-S1** Summary of the sulfonamide library synthesized by the solid support protocol for screening along with the mass, % purity and % inhibition.
- 4. Table-S2** Data collection and Refinement Statistics (crystallographic data)

### 1. Medium throughput small scale synthesis:

Pre-weighed samples of Fmoc protected immobilized pipecolate solid support were distributed to each of 36 wells of a 96 well parallel synthesis reactor platform obtained from FlexChem® peptide synthesis system. The Fmoc deprotection was carried out individually in each of the wells followed by coupling with sulfonyl chlorides obtained commercially from Maybridge. The unreacted excess sulfonyl chlorides were washed followed by the cleavage of the pipecolate sulfonamides from the resin under mild acidic condition.

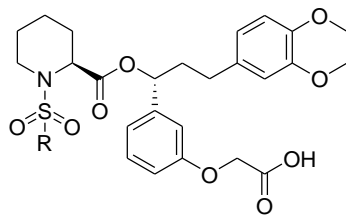
Out of the 36 compounds 35 compounds were purified by preparative HPLC. Analytical HPLC showed the compounds had at least > 90 % purity with most compounds were > 95% pure (except 50, 65 and 73). The correct identity was confirmed by mass spectroscopy, as summarized in Table-S1. Compound 50 was purified using ion exchange chromatography to only 81 % purity.

### 2. Library Testing:

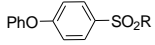
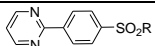
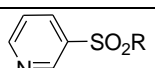
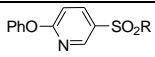
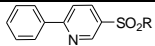
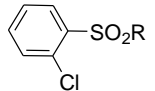
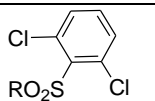
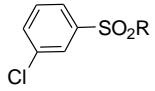
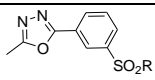
The 36 purified and chemically validated compounds were tested for their binding to FKBP12 and to the FK1 domains of FKBP51 and FKBP52 in a fluorescence polarization assay<sup>1</sup>. The binding of the compounds to the proteins was analyzed by calculating the % inhibition at a concentration of 5  $\mu$ M (Table 1).

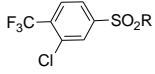
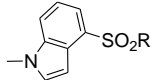
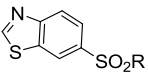
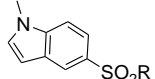
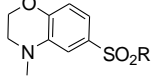
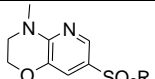
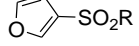
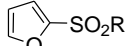
Compounds having better than 15 % inhibition were considered as hits. This threshold yielded 5 compounds (**8-12**) having activity for all the three proteins.

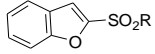
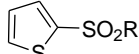
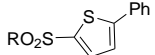
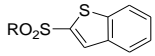
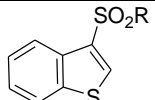
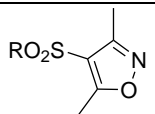
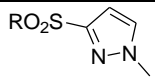
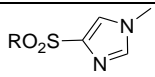
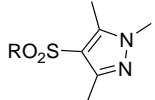
## 3. Table-S1:



Compound No. (a)	Substituent Structure	Mol Wt Calc	Mol Wt found	% purity HPLC	FKBP 51 FK1 % inhibition	FKBP52 FK1 % inhibition	FKBP 12 % inhibition
49		549.20	550.40 [M + H] <sup>+</sup>	96	6.1	3.8	9.6
50		563.22	585.42 [M + Na] <sup>+</sup> , 601.42 [M + K] <sup>+</sup>	81	6.1	8.5	5.8
51		631.16	654.13 [M + Na] <sup>+</sup>	98	11.7	15.2	96.1
52		645.19	663.34 [M + NH <sub>4</sub> ] <sup>+</sup>	96	4.3	0	2.0
53		615.19	633.00 [M + NH <sub>4</sub> ] <sup>+</sup> , 638.33 [M + Na] <sup>+</sup>	96	4.3	6.6	93.6
54		653.27	652.27 [M - H] (a)	98	8.3	14.2	85.3
55		665.19	688.13 [M + Na] <sup>+</sup> , 702.13 [M	99	8.9	12.3	85.3

			+ K] <sup>+</sup>				
<b>56</b>		689.2 3	712.33 [M + Na] <sup>+</sup> , 726.27 [M + K] <sup>+</sup>	97	7.2	15.2	72.6
<b>8</b>		675.2 3	676.13 [M + H] <sup>+</sup> , 698.27 [M + Na] <sup>+</sup>	99	16.3	15.2	77.0
<b>57</b>		598.2 0	599.33 [M + H] <sup>+</sup> , 621.20 [M + Na] <sup>+</sup>	97	6.6	9.5	70.1
<b>58</b>		690.2 2	689.27 [M - 1] (a)	99	3.7	11.4	71.3
<b>59</b>		674.2 3	675.33 [M + H] <sup>+</sup>	99	2.6	8.5	56.7
<b>60</b>		631.1 6	654.20 [M + Na] <sup>+</sup> , 668.27 [M + K] <sup>+</sup>	99	1.4	9.5	10.9
<b>61</b>		665.1 3	688.27 [M + Na] <sup>+</sup> , 706.20 [M + K] <sup>+</sup>	99	3.2	9.5	23.0
<b>9</b>		631.1 6	649.27 [M + NH <sub>4</sub> ] <sup>+</sup> , 654.27 [M + Na] <sup>+</sup> , 670.27 [M + K] <sup>+</sup>	99	17.5	18.0	101.9
<b>62</b>		679.2 2	679.93 [M + H] <sup>+</sup> , 702.33 [M + Na] <sup>+</sup> , 716.33	95	4.9	3.8	69.4

			[M + K] <sup>+</sup>				
<b>63</b>		699.1 5	716.93 [M + NH <sub>4</sub> ] <sup>+</sup> , 722.20 [M + Na] <sup>+</sup> , 736.27 [M + K] <sup>+</sup>	91	-0.2	11.4	70.1
<b>64</b>		650.2 3	673.20 [M + Na] <sup>+</sup> , 689.27 [M + K] <sup>+</sup>	95	-0.8	6.6	19.8
<b>10</b>		654.1 7	655.07 [M + H] <sup>+</sup> , 677.20 [M + Na] <sup>+</sup>	93	25.5	16.1	82.1
<b>65</b>		650.2 3	668.20 [M + NH <sub>4</sub> ] <sup>+</sup> , 673.13 [M + Na] <sup>+</sup> , 689.20 [M + K] <sup>+</sup>	86 (b)	10.0	10.4	87.2
<b>66</b>		668.2 4	669.40 [M + H] <sup>+</sup>	93	9.5	6.6	94.9
<b>67</b>		669.2 4	670.27 [M + H] <sup>+</sup> , 692.20 [M + Na] <sup>+</sup> , 708.33 [M + K] <sup>+</sup>	99	3.2	1.9	74.5
<b>11</b>		587.1 8	610.24 [M + Na] <sup>+</sup> , 626.18 [M + K] <sup>+</sup>	97	15.2	16.2	96.1
<b>68</b>		587.1 8	610.27 [M + Na] <sup>+</sup> , 624.20 [M + K] <sup>+</sup>	97	2.0	5.7	55.4

<b>69</b>		637.2 0	660.13 [M + Na] <sup>+</sup> , 674.33 [M + K] <sup>+</sup> .	99	5.5	6.6	66.9
<b>70</b>		603.1 6	626.27 [M + Na] <sup>+</sup> , 642.13 [M + K] <sup>+</sup> .	95	3.2	8.5	76.4
<b>71</b>		679.1 9	702.27 [M + Na] <sup>+</sup> .	99	3.2	9.5	- 0.5
<b>12</b>		653.1 8	676.27 [M + Na] <sup>+</sup> , 691.93 [M + K] <sup>+</sup> .	98	12.4	15.2	84.0
<b>72</b>		653.1 8	676.07 [M + Na] <sup>+</sup> .	99	3.2	4.7	36.3
<b>73</b>		616.2 1	639.20 [M + Na] <sup>+</sup> , 655.27 [M + K] <sup>+</sup> .	89	-3.0	3.8	- 0.5
<b>74</b>		601.2 1	602.27 [M + H] <sup>+</sup> , 624.20 [M + Na] <sup>+</sup> , 640.13 [M + K] <sup>+</sup> .	97	2.1	4.7	42.7
<b>75</b>		601.2 1	602.20 [M + H] <sup>+</sup> , 617.07 [M + NH <sub>4</sub> ] <sup>+</sup> , 624.40 [M + Na] <sup>+</sup> , 638.40 [M + K] <sup>+</sup> .	96	-2.5	3.8	32.5
<b>76</b>		629.2 4	630.27 [M + H] <sup>+</sup> , 652.27 [M + Na] <sup>+</sup> , 668.20	97	5.5	1.9	0

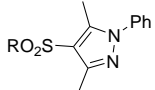
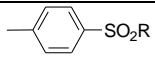
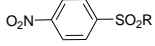
			$[M + K]^+$				
<b>77</b>		691.2 6	692.33 $[M + H]^+$ , 714.20 $[M + Na]^+$ , 728.47 $[M + K]^+$	94	0.9	4.7	-1.1
<b>78</b>		611.2 2	634.27 $[M + Na]^+$	95	3.2	3.8	79.0
<b>79</b>		642.1 9	665.07 $[M + Na]^+$	95	0.3	0	63.1

Table S1: Summary of the sulfonamide library synthesized by the solid support protocol for screening along with the mass, % purity and % inhibition. (a) Negative mode; (b) two peaks in HPLC spectrum. The major peak (86 %) while the other is a minor peak corresponding to 12% of the AUC.

**4. Table-S2 Data collection and Refinement Statistics**

<b>Dataset</b>	<b>PDB code 4DRQ</b>
Ligand	Cmpd 20
beamline	SLS, X06DA
wavelength (Å)	0.9116
space group	<i>P2<sub>1</sub>2<sub>1</sub>2<sub>1</sub></i>
cell dimensions, a, b, c (Å);	41.966, 54.641, 56.596;
$\alpha$ , $\beta$ , $\gamma$ (°)	90, 90, 90
resolution limits (Å)*	41.97 – 1.0 (1.06 – 1.0)
Rmerge ***	0.033 (0.285)
I/sigma ***	18.4 (3.6)
multiplicity *	3.8 (3.6)
completeness (%) *	99.5 (99.0)
<b>Refinement</b>	
resolution range	20 – 1.0
reflections (test set)	66559 (3503)
Rcryst	0.1375
Rfree	0.1508
number of atoms	1332
r.m.s.d. bonds (Å)	0.012
r.m.s.d. angles (°)	1.724
Ramachandran plot	
% most favored region***	97.67
% additionally allowed***	1.16

\* Values in parenthesis for outer shell.

\*\* As defined in Scala.

\*\*\* As defined in Coot.

**S.Reference.**

- (1) Kozany, C.; Marz, A.; Kress, C.; Hausch, F. Fluorescent probes to characterise FK506-binding proteins. *Chembiochem* **2009**, *10*, 1402-1410.

### 1.2.2.2.1 Discussion (Manuscript 3)

Bioisosteric replacement of equivalent moieties is an established approach to design analogues to eradicate the metabolic instability or potential toxicity there by helping to improve stability and optimize activity.

In this strategy the  $\alpha$ -ketoamide was substituted with sulfonamides to generate new scaffolds with a conserved hydrogen bond pattern. A solid phase synthesis strategy was established to generate a focused library of sulfonamide analogs. Firstly, a focused library was designed taking into consideration various substitution patterns. This library consisted of 36 compounds which were synthesized and further tested in the medium throughput screening platform (fluorescence polarization assay) at a single dose concentration. The best hits (**8-12**) identified were resynthesized and screened for their binding to FKBP51. This pilot study led to the primary identification of two active aromatic sulfonamides series (**9, 10**).

These lead structures were further optimized and a detailed systemic SAR analysis was carried out. In the first series various substituents at the meta-positions were incorporated to study their effect on the binding to the larger FKBP51 (**13-33**). Halogen substitution at the meta position (**18-21**) was found to be favorable as compared to larger substituents (**13-17, 24-27, 31-33**). The Di-meta Cl substituted analog (**20**) was used as a representative compound of this series, and the postulated binding mode was confirmed by solving the co-crystal structure with the FK1 domain of FKBP51. Compound **20** bound to FKBP51 with retention of the conserved hydrogen bonds present in the crystal structure of  $\alpha$ -ketoamides. Additional dipolar interactions and aromatic hydrogen bonds were also present. This co-crystal structure was used as a template to gain insights for further modifications to gain selectivity and affinity (**28-30**). Compound **28** having a p-OH substituent in addition to the Di-m-Cl substituent was found to have three folds selectivity for FKBP51 while, substitution with p-OMe rescued the affinity of **29** for FKBP52.

The second series consisted of fused ring substituents (**34-37**). Compound **35** was found to have an unexpected high binding affinity for FKBP12. Substitution of sulfur in the fused ring by carbon or oxygen (**36, 37**) resulted in complete loss of activity for the larger FKBP51. This gives an indication that sulfur at this position is important to retain binding to the FKBP51.

The best hit analogs from the two series were further combined with various top group substituents. The larger top group modifications were found to have better binding affinity (**40-45, 46**) as compared to small modifications (**38, 39**). Reference sulfonamide compounds having a similar scaffold which have been identified and published to have high binding affinities for FKBP12/ MIP were also resynthesized to evaluate their effect on larger

FKBPs<sup>55,63</sup>. Surprisingly these compounds were not active for FKBP12 in the fluorescence polarization assay as claimed in the literature. The compounds did not show any measurable binding to the larger FKBP51 and FKBP52 (Table- 3) in line with the SAR established before. The synthesis of these compounds have been incorporated in patent No. **EP-11195970.6**).

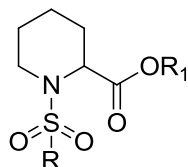


**Table: 3** Purity of the re-synthesized reference compounds and their binding affinity determined in a fluorescence polarization assay.

Compd. No.	R <sub>1</sub>	R	Reference	FKBP12	FKBP51FK1	FKBP52FK1
					IC <sub>50</sub> (μM)	
<u>A</u>	Et			63.5 ± 14.4	>100	>100
<u>B</u>	Et		<u>63</u>	54.7 ± 12.7	>100	>100
<u>C</u>			<u>55</u>	9.8 ± 7.4	>100	>100
<u>D</u>			<u>63</u>	9.2 ± 3.7	>100	>100

The best hit analogs (compound **42** and **44**) resulted in 15-60 fold enhancement of binding affinity for the FKBP51 and FKBP52 as compared to the lead compound **2**. The molecular underpinning of the unexpected high binding affinity of compound **42** and **44** is yet to be investigated. This study proved the hypothesis that sulfonamides adopt a similar binding mode as the  $\alpha$ -ketoamides in the binding site of FKBP and can be used as efficient surrogates for  $\alpha$ -ketoamides. Further, this campaign resulted in identifying and dissecting specific substituents that are important for gaining binding affinity for the FKBP51 and FKBP52. This study has resulted in finding two potent binders, (1) compound **42** is so far the best synthetic ligand known for the larger FKBP51 and FKBP52, (2) compound **44** is one of the most potent ligand known with equivalent potency for FKBP12 compared to the natural products FK506 and Rapamycin.

The identified sulfonamide lower parts have further being investigated and adapted in rigid bicyclic and polycyclic scaffolds. Combination of the sulfonamide substituents discovered in this work together with bicyclic scaffold has given substantial increase in the potency of this series of ligands. (Wang, Y manuscript *in prep.*). The polycyclic series of compound is discussed in detail in the next section.

### 1.2.3 Design of Ligand Efficiency by Conformation Control (Manuscript 4)

Yansong Wang<sup>1</sup>, Christian Kozany<sup>1</sup>, **Ranganath Gopalakrishnan<sup>1</sup>**, Christoph Kress<sup>1</sup>, Bastiaan Hoogeland<sup>1</sup>, Andreas Bracher<sup>2</sup>, Felix Hausch<sup>1\*</sup>.

FK506 and Rapamycin have high binding affinity to the FKBP. This might be in part due to the rigid backbone that is present in these macrocyclic compounds. The synthetic compounds analyzed in manuscript 2 and 3 have high conformational flexibility. From the co-crystal structure elucidated above we postulated the incorporation of an axial substituent at the C<sup>6</sup>-position of the pipercolate ring which could be further cyclized with the C<sup>1</sup>-carbonyl to limit the flexibility and to yield polycyclic aza-amide compounds.

One of the polycycle compounds known for FKBP12 was resynthesized and the postulated binding mode was further confirmed by solving the co-crystal structure of this polycyclic compound with FKBP51.

The most promising lower substructures identified in manuscript 2 and 3 were attached to this rigid polycycle core. This series of compounds contained four additional compounds.

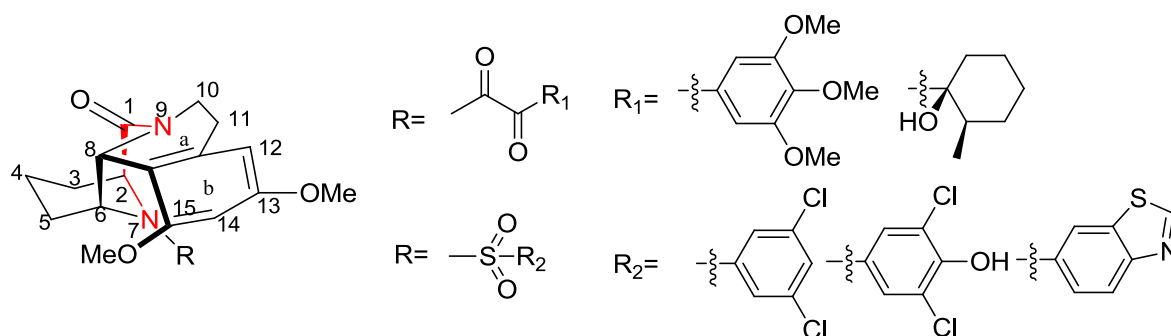


**Figure 15:** Prototypic compounds of the proposed series.

This work will be part of the manuscript submitted to The Journal of American Chemical Society.

This work comprises a small part of the above manuscript and hence the complete manuscript will not be attached and only my contribution will be discussed in the following pages.

### 1.2.3.1.1 Background

The diketoamides and the sulfonamides ligands that have been described above have a high degree of conformational flexibility due to presence of rotatable bonds as compared to the natural products FK506 and Rapamycin. This might be a reason for the weak binding affinities of these analogs compared to the natural products. In order to identify more efficient scaffolds we adopted the polycyclic aza amide core which has been previously described for FKBP12<sup>106,107</sup>. To further understand if this concept can be extended to the larger FKBP51 compound **29** was resynthesized and was found to bind to FKBP51 and 52 with equal potency compared to the lead compound (compound **2a** ketoamide manuscript).

The postulated binding mode of **29** was further confirmed by solving the co-crystal structure with the FK1 domain of FKBP51 to 1.05Å. Compound **29** bound to FKBP51 similar to compounds that were described in the above two manuscripts 2 and 3. Apart from these conserved interactions ring B and ring C stack atop each other via [pi] - [pi] interactions (**Fig. 16**). The preorganization of ring B might lock ring C into a conformation which is favourable for binding. The stacking of these two rings represents a productive ligand hydrophobic collapse<sup>108</sup>.

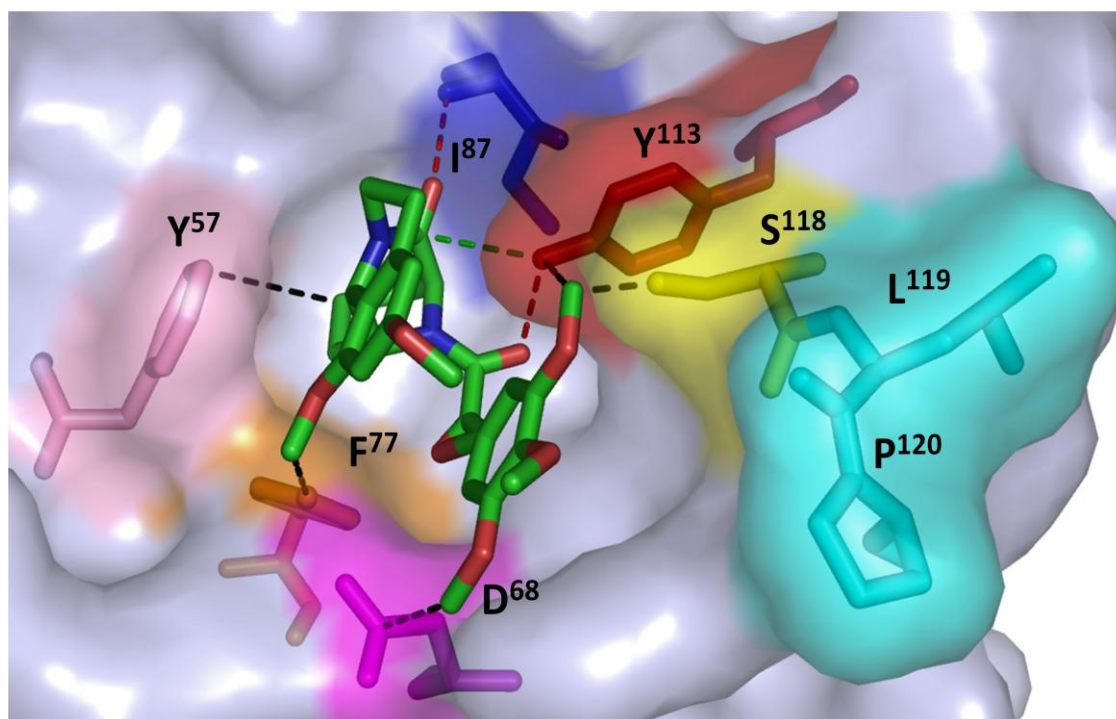
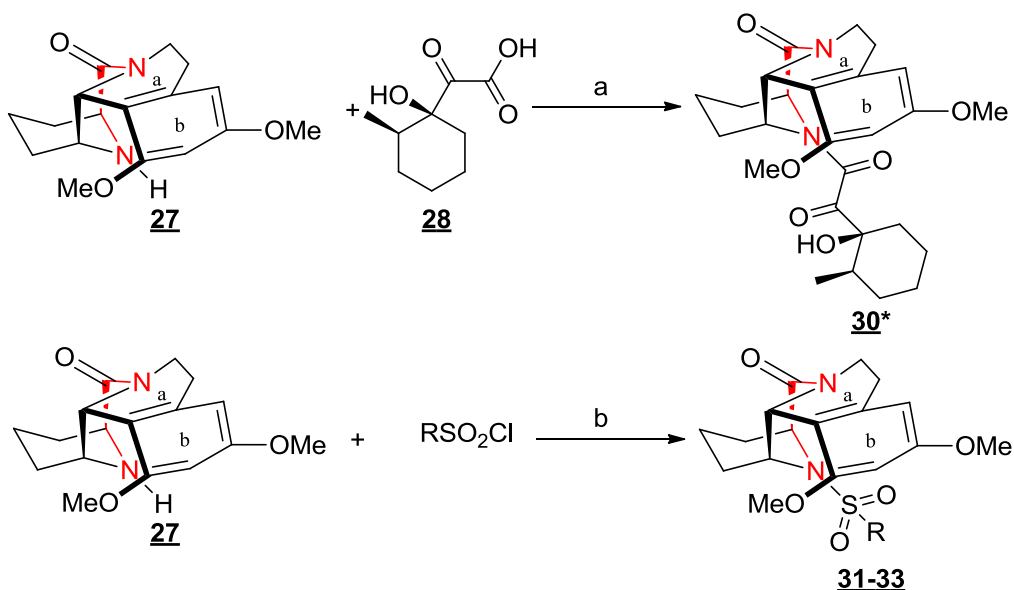


**Figure 16:** X-ray crystal structure of **29** in complex with the FK1 domain of FKBP51. The two hydrogen bonds between O<sup>1</sup>-**29** and HN-Ile<sup>87</sup>, and between O<sup>16</sup>-**29** and HO-Tyr<sup>113</sup>, are shown as dotted red lines. The dipolar interaction between the C<sup>1</sup>-carbonyl and HO-Tyr<sup>113</sup> is shown in green. Van-der-Waals interactions of the ligand with Y<sup>57</sup>, D<sup>68</sup>, F<sup>77</sup>, Y<sup>113</sup> and S<sup>118</sup> are shown in black. Leu<sup>119</sup> and Pro<sup>120</sup> at the top of the 80s loop are colored in cyan.

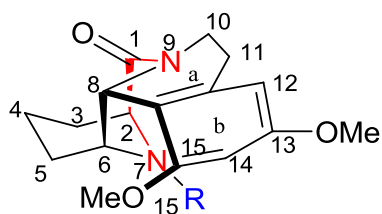
### 1.2.3.1.2 Result and Discussion

Taking these observations as an initial lead we further synthesized this polycycle with the cyclohexyl ring **30\*** (Scheme-1) that mimic the pyranose of FK506 or Rapamycin and which we had identified previously as preferred substructures compared to the trimethoxyphenyl moieties in a monocyclic scaffold [manuscript 2]. In contrast, in the polycyclic context a dramatic decrease of the binding affinity was observed when ring C was changed to cyclohexyl  $\alpha$ -keto amide **30\***. The lower affinity of **30\*** might be due to the loss of favourable [pi] - [pi] interactions leading to a loss of the preorganized conformation. Next, the best substituents from the sulfonamide series were attached to the polycyclic rigid core (Scheme-1). Compound **31** and **32** had low to no binding affinity for the larger FKBP's though the binding to FKBP12 was still conserved to some extent. Compound **33** was the only compound in this series that had detectable affinity for the larger FKBP's.

Scheme-1



<sup>a</sup> Reagents and conditions : **(a)** HATU, DIPEA, rt, 16h, **(b)** DIPEA, CH<sub>2</sub>Cl<sub>2</sub>, r.t., 1.5h. \*Mixture of Diastereomers.



Compd. No.	R	FKBP12	FKBP51FK1	FKBP52FK1
±29			5.21 ± 3.39	6.92 ± 5.12
±30*		2.8 ± 4.5	inactive	inactive
±31		0.87 ± 2.5	inactive	inactive
±32		2.09 ± 0.27	>100	>200
±33		0.70 ± 0.92	13.9 ± 9.7	22.7 ± 19.6

**Table 4:** Binding affinity to FKBP12, FKBP51 (FK1 domain) and FKBP52 (FK1 domain) determined by a fluorescence polarization assay<sup>105</sup>. \* Diastereomeric mixture.

### 1.2.3.1.3 Experimental section

**Chemistry:** All solvents were purchased from Roth, reagents were bought from Aldrich-Fluka and the sulfonyl chlorides were obtained from Maybridge, Sigma Aldrich, or ABCR unless otherwise stated.

Chromatographic separations were performed either by manual flash chromatography or by automated flash chromatography using an Interchim-Puriflash 430 with an UV detector. Extracts were dried over MgSO<sub>4</sub> and the solvents were removed under reduced pressure. Merck F-254 commercial plates were used for analytical TLC to follow the course of reaction and visualized by UV light at either 254 or 365 nm. Silica gel 60 (Merck 70-230 mesh) was used for column chromatography. NMR spectra of all compounds were obtained from the Department of Chemistry and Pharmacy, LMU, on a Bruker AC 300, a Bruker XL 400, or a Bruker AMX 600 at room temperature in deuterio-CDCl<sub>3</sub> with tetramethylsilane (TMS) as internal standard, unless otherwise stated. Mass spectra (m/z) were recorded on a Thermo Finnigan LCQ DECA XP Plus mass spectrometer at the Max Planck Institute of Psychiatry.

HPLC analysis was carried out using a Jupiter 4 μm Proteo column (250 x 4.6 mm, 5 μm particle size), **Wavelength:** 224nm, 280nm; **Flow rate:** 1ml/min; **Buffer A:** 0.1% TFA in 5% MeCN/water; **Buffer B:** 0.1% TFA in 95% MeCN/water; **Gradient A:** After 1min elution with 100% buffer A, linear gradient of 0-100% buffer B for 30 min.

**Method LCMS:** YMC Pro C-8 (100 x 4.6 mm, 3 μm particle size) column, **Wavelength:** 224nm, 280nm; **Flow rate:** 1ml/min; **Buffer A:** 0.1% HCOOH in 5% MeCN/water; **Buffer B:** 0.1% HCOOH in 95% MeCN/water; **Gradient B:** 1min 100% buffer A, then linear gradient of 0-100% buffer B for 11 min.

#### **Synthesis of Polycycle core (27).**

The polycycle core (27) was synthesized either by Christoph Kress in the group of Dr. Felix Hausch or by the Lead Discovery Center (Taros) as previously described<sup>106</sup>.

#### **Synthesis of compound 30\***.

To 7 (108mg, 0.358 mmol) DIPEA (139 mg, 1.07 mmol), HATU (129 mg, 0.537 mmol), 28 (80 mg, 0.430 mmol) were added. The reaction was stirred at room temperature for 16 h and the product was purified by column chromatography (Hexane: EtOAc 2:8) to yield compound 30\*

TLC (EtOAc: TEA 9.9:0.1): R<sub>f</sub> = 0.66, Yield= 25mg (16%).

HPLC (Gradient A) retention time = 19.2-19.6 min.

$^1\text{H}$ NMR (600 MHz,  $\text{CDCl}_3$ )  $\delta$ = 0.71-0.74 (m, 3H); 1.12-1.42 (m, 7H); 1.58-1.64 (m, 3H); 1.80-1.91 (m, 4H); 2.01-2.16 (m, 2H); 3.76-3.88 (m, 6H); 4.57-4.68 (m, 1.5H); 4.84-4.94 (m, 1H); 5.07 (s, 0.5H); 6.23-6.26 (m, 1H); 6.32 (s, 0.5H); 6.36-6.38 (m, 0.5H).

$^{13}\text{C}$  NMR (150 MHz,  $\text{CDCl}_3$ )  $\delta$ = 15.63, 16.02, 18.03, 18.06, 20.25, 20.46, 25.34, 27.22, 29.27, 29.30, 30.08, 31.79, 36.74, 36.82, 40.55, 46.86, 51.01, 52.79, 55.30, 55.47, 58.67, 58.83, 80.75, 81.24, 97.25, 97.40, 104.99, 105.25, 115.79, 116.55, 138.29, 139.04, 157.20, 157.31, 159.80, 159.93, 163.09, 163.99, 168.66, 168.92, 204.10, 204.75.

MS (ESI):  $m/z$ = 471.33  $[\text{M} + \text{H}]^+$ , calculated: 471.56 $[\text{M} + \text{H}]^+$ .

### Synthesis of compound **31**.

To **7** (75mg, 0.247 mmol) DIPEA (45 mg, 0.346 mmol) and 3,5-dichloro-4-hydroxybenzene-1-sulfonyl chloride (81mg, 0.346 mmol) were added. The reaction was stirred at room temperature for 1.5 h and the product was purified by column chromatography (Hexane: EtOAc 1:1) to yield compound **4** as white solid.

TLC (Hexane: EtOAc 3:7):  $R_f$  = 0.51, Yield- 100mg (77%).

HPLC (Gradient A) retention time = 27.2-27.5 min.

$^1\text{H}$ NMR (300 MHz,  $\text{CDCl}_3$ )  $\delta$ = 1.80-2.37 (m, 8H), 2.56 (dt, 1H,  $J$  = 3.3, 12.6 Hz, ), 3.84 (s, 3H), 3.80 (s, 3H), 4.48 (s, 1H), 4.55 (t, 1H,  $J$  = 2.1 Hz), 4.76-4.82 (m, 1H), 4.89-4.91 (m, 1H), 6.06 (d, 1H, ,  $J$  = 2.4 Hz ), 6.31 (d, 1H,  $J$  = 2.4 Hz), 7.24 (s, 1H), 7.25 (s, 1H), 7.31 (t, 1H,  $J$  = 1.8Hz).

$^{13}\text{C}$  NMR (75 MHz,  $\text{CDCl}_3$ )  $\delta$ = 17.56, 28.02, 29.50, 31.53, 40.44, 51.66, 54.84, 55.17, 55.50, 59.05, 97.08, 105.60, 116.06, 125.07, 132.23, 135.60, 138.15, 143.56, 157.05, 159.45, 168.06.

MS (ESI):  $m/z$ = 511.87, 513.47  $[\text{M} + \text{H}]^+$ , calculated: 511.48, 513.13 $[\text{M} + \text{H}]^+$ .

### Synthesis of compound **32**.

To **7** (50mg, 0.165 mmol) DIPEA (29.9 mg, 0.232 mmol) and 3,5-dichloro-4-hydroxybenzene-1-sulfonyl chloride (60.5mg, 0.232 mmol) were added. The reaction was stirred at room temperature for 2 h and the product was purified by crystallization from methanol to yield **5** as white solid.

TLC (DCM: MeOH 9.6: 0.4):  $R_f$  = 0.44, Yield= 19.28mg (23%).

HPLC (Gradient A) retention time = 23.3-23.6 min

$^1\text{H}$ NMR (400 MHz,  $\text{CDCl}_3$  :  $\text{CD}_3\text{OD}$  8 : 2)  $\delta$ = 1.91-2.07 (m,6H), 2.27-2.31 (m,2H), 2.50-2.57 (m, 1H), 3.76 (s,3H), 3.79 (s, 3H), 4.44 (s, 1H), 4.51-4.53 (m,1H), 4.72-4.78 (m, 1H), 4.78-4.81 (m, 1H), 6.02 (d, 1H, ,  $J$  = 2.4 Hz ), 6.25 (d, 1H,  $J$  = 2.4 Hz), 7.24 (s, 1H), 7.25 (s,1H).

$^{13}\text{C}$  NMR (100 MHz,  $\text{CDCl}_3$ :  $\text{CD}_3\text{OD}$  8:2)  $\delta$ = 17.55, 27.90, 29.47, 31.34, 40.52, , 51.21, 54.53, 55.10, 55.44, 59.10, 97.93, 105.19, 116.00, 121.73, 127.00, 132.60, 137.97, 151.88, 156.95, 159.33, 168.57.

MS (ESI):  $m/z$ = 527.71, 529.62  $[\text{M} + \text{H}]^+$ , calculated: 527.46, 529.14  $[\text{M} + \text{H}]^+$ .

### Synthesis of compound **33**.

To **7** (50mg, 0.165 mmol), DIPEA (29.9 mg, 0.232 mmol) and benzo[d]thiazole-6-sulfonyl chloride (60.5mg, 0.232 mmol) were added The reaction was stirred at room temperature for 1.5 h and the product was purified by column chromatography (Hexane: EtOAc 2:8) to yield **6** as white solid.

TLC (Hexane: EtOAc 1:9):  $R_f$  = 0.21, Yield= 79.2mg (95%).

HPLC (Gradient A) retention time = 22.1-22.3 min.

$^1\text{H}$ NMR (300 MHz,  $\text{CDCl}_3$ )  $\delta$ = 1.79-2.15 (m,8H), 2.46 (dt, 1H,  $J$  = 3, 12.6 Hz ), 3.74 (s,3H), 3.84 (s, 3H), 4.46 (s, 1H), 4.60-4.70 (m,2H), 5.00 (d, 1H,  $J$  = 1.8 Hz), 5.70 (d, 1H,  $J$  = 2.4 Hz), 6.27 (d, 1H, ,  $J$  = 2.4 Hz ), 7.51 (dd, 1H,  $J$  = 1.8, 8.7 Hz), 7.95 (m, 2H), 9.15 (s,1H).

$^{13}\text{C}$  NMR (75 MHz,  $\text{CDCl}_3$ )  $\delta$ = 17.62, 28.10, 29.21, 31.87, 40.11, 51.83, 54.71, 55.19, 55.51, 58.86, 96.98, 104.98, 116.52, 121.40, 123.96, 124.33, 133.77, 138.10, 138.17, 155.00, 157.20, 157.40, 159.22, 168.38.

MS (ESI):  $m/z$ = 500.59  $[\text{M} + \text{H}]^+$ , calculated: 500.65 $[\text{M} + \text{H}]^+$ .

## **2. Synthesis of novel photoactivable Tricyclic antidepressant analogs**

## 2.1 Introduction

### 2.1.1 Depression

The most common psychiatric disorders prevalent in the society are major depression and bipolar disorder. The most prominent symptoms of these disorders which effect the everyday life of the patient include long lasting depressive mood, guilt feeling, anxiety, recurrent thoughts of death and suicide and are collectively referred to as “depressive syndrome”<sup>109</sup>. The disease treatment and the associated direct and indirect costs have a huge economic burden on the society. This explains the huge market share the antidepressants have in the CNS drug category, which has continuously increased in the past decades.

Both non-genetic and genetic factors play an equal role in the development of depression. The non-genetic social factors that are the causative reasons include physical and emotional stress, affective trauma, viral infection or neurodevelopmental abnormalities. The genetic contribution for the risk of depression has been estimated to be roughly about 30-40%. However few individual genes that contribute to this risk have been identified<sup>110</sup>, and a single gene abnormality fails to explain the multifaceted symptoms of depression<sup>111</sup>.

The central topic of depression research in the last 60 years that has been driving the pharmaceutical industry to search for cure is the monoamine hypothesis. The mechanism of action of all classes of antidepressants can be accounted for by the monoamine theory. As compared to other disease conditions and disorders the knowledge of the brain and its neural circuits are limited. In addition there is a lack of objective diagnostic test which means that the diagnosis of this disorder is highly variable with no clear demarcation between a normal, mild and highly depressed individual. The antidepressants available in the market are effective in only 50% of the treated patients which gives an indication that apart from the monoamine theory other pathways can also play a role in the etiology of depression. The known animal models for mood disorders also fail to explain the reason why chronic treatment of the antidepressants is required in humans before the clinical effects starts to be seen<sup>112</sup>. Most of these animal models are based on the monoamine theory and hence it is unclear whether new novel antidepressants working by a novel mechanism can be identified using these models.

### 2.1.2 Monoamine Hypothesis

The monoamine hypothesis proposes that disruptions in the serotonergic and the noradrenergic systems can result in depression or depression-like symptoms. The therapeutic strategy is to

restore the monoamine levels in such patients. Those classical classes of drugs are present which elicit their effect in accordance with the monoamine hypothesis. The oldest antidepressants are the monoamine oxidase inhibitors (MAO-I) while the second class of drugs are the tricyclic antidepressants. However, new evidences have suggested that the monoamine hypothesis fails to explain the whole mechanism of action of antidepressants. The cytokine hypothesis of depression<sup>113-117</sup>, the hypothalamic pituitary thyroid hypothesis of depression<sup>118-120</sup>, the role of brain derived neurotrophic factor<sup>121-123</sup> and cAMP response element binding protein<sup>124-126</sup> have been recently shown to partially explain the mechanism of antidepressants.

### 2.1.3 Monoamine transporter inhibitors as antidepressants

The primary mechanism of action of most or all antidepressant drugs available in market is that they are modulators of monoaminergic neurotransmission. As stated above these drugs can be divided into three broad class (i) monoamine oxidase inhibitors (MAOIs), (ii) monoamine transporter inhibitors (iii) monoamine receptor ligands.

MAOIs were the first compounds that were available for therapy in the 1960s. The early MAOIs like iproniazide, tranylcypromine or phenelzine irreversibly inhibit MAO-A which is the main catabolic enzyme for the monoamine transmitter's noradrenaline (NA), serotonin (5-HT), and dopamine (DA) (**Fig.17**). The end result is the generalized increased in monoamine levels throughout the CNS<sup>127,128</sup>. The newer analogs of this class of compounds, e.g., Moclobemide, are reversible MAO inhibitors. However, MAOIs are very powerful drugs, and are the last line of defense as its use is limited due to hepatotoxicity and prominent and lethal adverse effect (“the cheese effect”) which leads to hypertensive crisis due to high tyramine ingestion<sup>128</sup>.

The tricyclic antidepressants (e.g., imipramine) elicited their antidepressant effect by inhibiting the membrane transporters and the reuptake of 5-HT or NE, thereby causing an increase in the synaptic concentrations of monoamines. This class of drugs is very efficient and potent although they are characterized by a wide profile of side effects arising due to a variable degree of antagonism at the muscarinic, adrenergic and histaminergic receptors (**Fig. 17**). The second generation of TCAs was comparatively more selective to NE uptake (desipramine, nortriptyline, maprotiline) with no significant betterment of the side effect. The subsequent development of the selective serotonin reuptake inhibitors (SSRIs) fluoxetine and its introduction in the clinic has provided the clinicians with a safer treatment alternative and a lesser side effect profile.

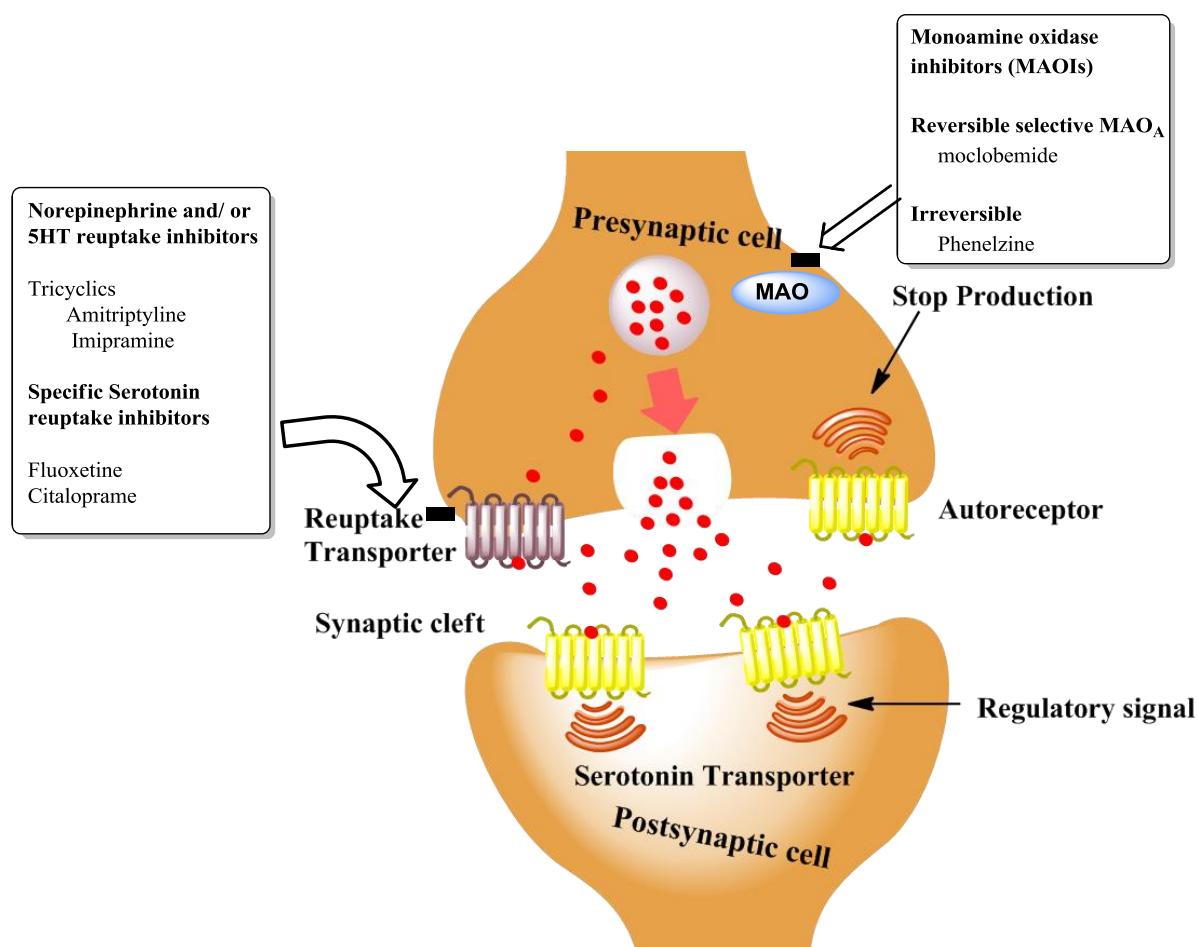


**Figure 17** Mechanism of action of various classes of antidepressants on a prototypic monoamine transporter (serotonin).

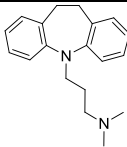
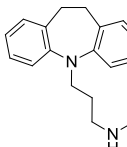
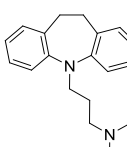
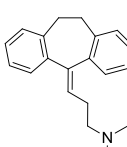
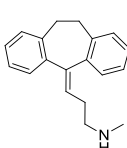
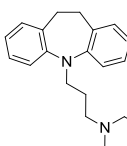
However, the SSRIs have been found to be ineffective in treating certain class of patients which has led to the development of the dual selective drugs SNRIs (venlafaxine and duloxetine)<sup>129</sup>.

#### 2.1.4 SAR studies of TCA class of drugs.

Tricyclic antidepressants or various other classes of antidepressants preferentially bind to the transporters SERT and NET. The binding mode of these compounds to the transporters is not fully clarified as the structural insights of these transporters have been controversial. Structure activity relationships and homology modeling has been able to provide clues about the distinct binding mode and binding site of these classes of drugs. Also, mutagenesis studies have provided information regarding residues that are important and required for inhibitor binding<sup>130-142</sup>. The first tricyclic antidepressant drug, imipramine (**34**), was launched by Geigy in 1951. The core structure of this drug was obtained by modification of the antipsychotic drug

chlorpromazine. Further modification on the TCA ring gave rise to Clomipramine (**36**), Cyanopramine and Amitriptyline (**37**). It has been shown that modifications on the TCA ring at position 3 resulted in analogs with retention of activity<sup>143,144</sup>. These drugs have the same dimethylamino group as in chlorpromazine but have different tricyclic core. Imipramine (**34**), Clomipramine (**36**), and Cyanopramine have a dibenzoazepine core while in Amitriptyline (**37**) the nitrogen is replaced by carbon to give the dibenzocycloheptene core and an ethylidene moiety at position 5.

**Table 4**

No.	Name of the Drug	Structure	Company	Approved	Ki (nM) <sup>a</sup>	
					hSERT	hNET
34	Imipramine		Geigy	1951	1.4	37
35	Desipramine		Geigy	1964	17.6	0.83
36	Clomipramine		Geigy	1970	0.28	38
37	Amitriptyline		Hoffmann-La Roche	1961	4.3	35
38	Nortriptyline		Geigy	1963	18	4.4
39	Lofepramine		LEO AB	1980	70	5.4

<sup>a</sup> Values taken from<sup>144</sup>.

All four compounds have equipotent affinity to SERT and NET which proved that these minor structural changes are not of crucial importance<sup>143</sup>.

The corresponding N-desmethyl metabolites of the above compounds also have been shown to have therapeutic activity. The N-desmethyl metabolites Desipramine (**35**), and nortriptyline (**38**) have a slight preference on NET as compared to their corresponding precursors which have preference for SERT<sup>143</sup>. This gives an indication that the dimethylamino substituent is important for higher SERT affinity while the N-desmethyl version gives higher NET affinity. Lofepramine (**39**)<sup>145</sup>, a close analog of imipramine (**34**) where one of the methyl in the dimethylamino center is replaced with a longer side chain, has 14 times more preference to NET as compared to SERT<sup>146</sup>. The above series of compounds shows that any subtle changes in the dimethylamino group of imipramine gives rise to compounds with varying selectivity towards NET and SERT.

## 2.2 Aim of the work (Manuscript-5)

Tricyclic antidepressants (TCA) tightly bind to a variety of proteins and exert their pharmacological action via a wide mechanism of action. The broad pharmacological background and molecular mechanisms of these drugs is still poorly understood. The unspecific binding of these drugs to wide protein class is thought to be the contributing factor for its clinical efficacy and side effects. Hence a photo-labeling approach was conceptualized to explore and define the TCA-binding proteome which will help in understanding the mechanism of action of antidepressants in detail.

To identify and fish the binding proteome, the first step is the development and functional validation of a chemically modified antidepressant analog with retention of the drug-like properties of the parent drug (Imipramine, in this case). The final tool compound should be amenable to affinity purification and identification of photo-crosslinked antidepressant binding proteins in lysates and endogenous tissue (**Fig. 18**). Ideally, it should also be applicable to integral transmembrane proteins which comprise all currently known antidepressant targets. Such a tool could also enable the structural fine-mapping of the binding sites in these proteins.

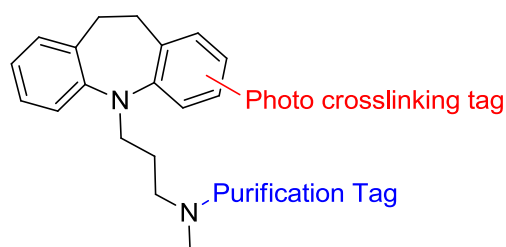


**Figure 18.** Proposed series of photoreactive TCA analogs.

## Photoactivable Tricyclic Antidepressants as Trifunctional Probes for the Serotonin transporter

**Ranganath Gopalakrishnan**, Serena Cuboni, Florian Holsboer, and Felix Hausch\*

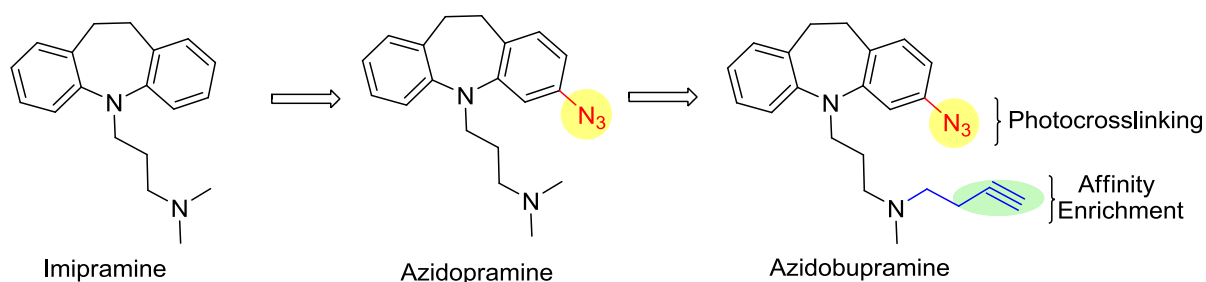
Max Planck Institute of Psychiatry, Kraepelinstr. 2, 80804 Munich, Germany,

Correspondence: Email: [hausch@mpipsykl.mpg.de](mailto:hausch@mpipsykl.mpg.de), phone: +49(89)30622640, fax: +49(89)30622610

---

### Abstract:

Monoamine transporter inhibitors have been the front line therapy for depression for decades. The exact binding mode of these drugs to their canonical target, the serotonin transporter, is matter of debate. Moreover, these antidepressants are characterized by an extremely complex polypharmacology and the role of additional targets for their clinical efficacy is been unclear. Here we present the development of multifunctional analogs of the tricyclic antidepressant imipramine. These tools inhibit monoamine uptake by the serotonin transporter with nanomolar potency, allow for photocrosslinking and contain an acetylene tag for affinity enrichment by click chemistry. These chemical tools will be useful for the fine-mapping of the binding mode of tricyclic antidepressants or for the identification of alternative targets by mass spectroscopy.



Depression is one of the most common disorders and it is expected to be the leading cause of disability in 2030 [WHO: The global burden of disease (2004 update)]. The established targets for most antidepressants are transporters of monoamine neurotransmitters<sup>1</sup>. While there has been substantial progress in the structural biology of this protein class, the exact antidepressant binding site has remained controversial, in part due to the poor biochemical tractability of these integral membrane proteins<sup>2-5</sup>. In addition to the monoamine transporters additional protein targets have been repeatedly been discussed to contribute to the efficacy of the currently available antidepressants and the ultimate mechanism of action of these drugs has remained elusive. A better understanding of antidepressants has been complicated by their extremely broad polypharmacology as well as by a lack of adequate chemical tools<sup>6,7</sup>. In fact, some antidepressants are among the most “dirty” drugs currently in clinical use.

To study the targets of antidepressants in endogenous systems in an unbiased manner, we set out to develop antidepressants analogs that would allow for covalent labelling of antidepressant binding proteins. Towards this end, we started with the prototypic tricyclic antidepressant Imipramine (**1**) as a chemical starting point. Clinically effective analogs like Clomipramine (**3**) and Cyanopramine (**4**)<sup>8-11</sup> suggested that substituents in the 3-position of the tricyclic ring system would not compromise the antidepressant activity of this class of drugs [Fig. 1]. We thus set out to introduce an azido group in the 3-position of Imipramine to graft the known photoreactivity of aromatic azides into the tricyclic ring system.

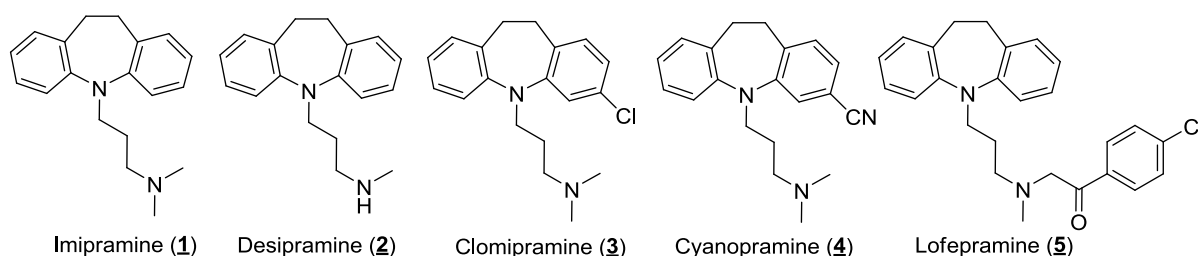
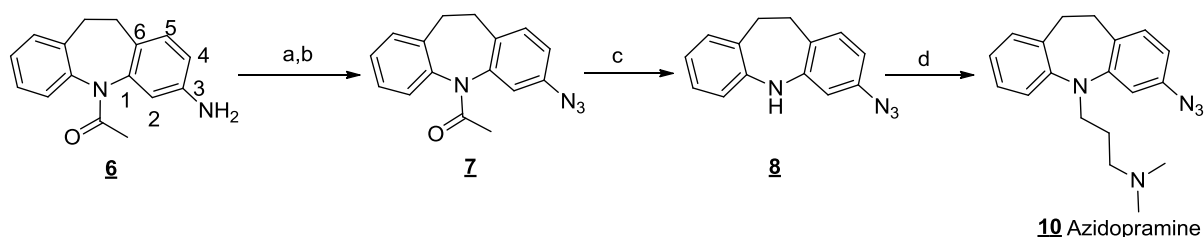


**Figure.1** Tricyclic antidepressants drugs used in the clinic.

The Imipramine analog Azidopramine **9** was synthesized from the commercially available azepine analog 1-(3-amino-10,11-dihydro-5H-dibenzo[b,f]azepin-5-yl)ethanone **6** in four steps. The primary amine of **6** was first converted to the corresponding azide **7**. Basic deprotection of the acetyl group provided the free secondary amine **8** which was alkylated with **9** to yield the tricyclic antidepressant analog Azidopramine (**10**).



**Scheme 1:** Synthesis of Azidopramine (**10**): (a)  $\text{NaNO}_2$ , 10% HCl. (b)  $\text{NaN}_3$ ,  $\text{H}_2\text{O}$ , rt, 1h. (c) KOH, MeOH,  $60^\circ\text{C}$ , 15h. (d) NaH,  $\text{ClCH}_2\text{CH}_2\text{CH}_2\text{N}(\text{CH}_3)_2$  (**9**),  $0$ - $60^\circ\text{C}$ , toluene.

The photoreactivity of the aromatic azide **10** was then tested by subjecting the compound to UV light exposure (254 nm). TLC analysis (**Fig. 2**) showed a time dependent conversion under these conditions. This confirmed that the introduction of the azide group in Azidopramine resulted indeed in a photoreactive AD analog.

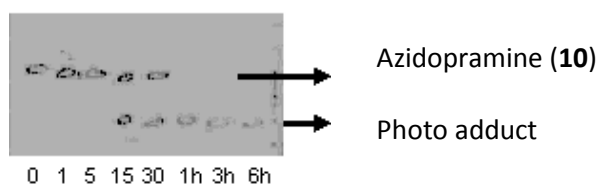


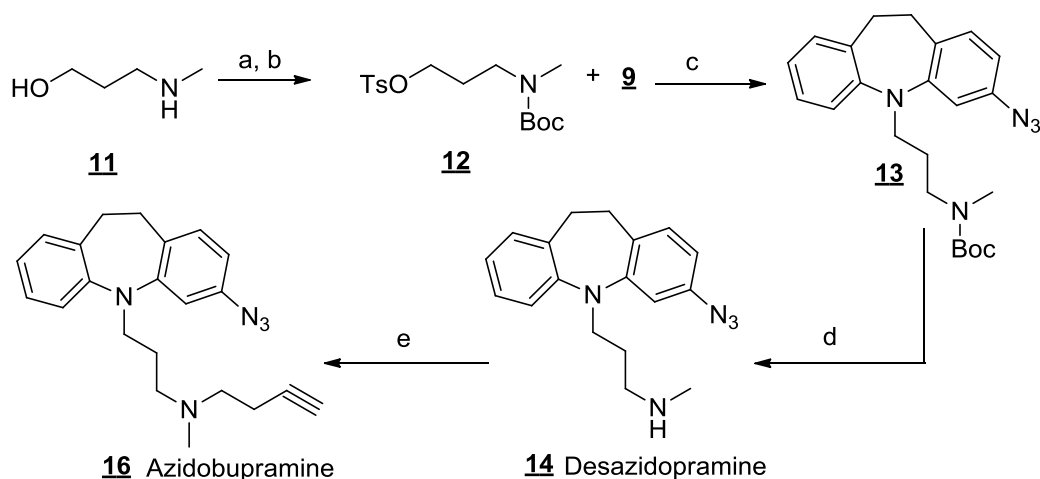
**Figure 2** Photoreactivity of Azidopramine (**10**) when subjected to UV light (254 nm) analyzed by thin layer chromatography (TLC), mobile phase DCM: MeOH 9.2:0.8

To verify that Azidopramine retained its biological activity we then tested it in an uptake assay for its primary target, the serotonin transporter (SERT). Gratifyingly, Azidopramine inhibited the uptake of SERT with an  $\text{IC}_{50}$  of 28nM, i.e., with equal potency compared to the parent compound Imipramine. This shows that addition of the azide group at position 3 was indeed tolerated (**Table-1**).

For Azidopramine (**10**) to be useful as a tool to study the mechanism of action of antidepressants, a convenient way to detect Azidopramine in biological samples would be extremely useful. We thus set out to explore the possibilities to introduce additional chemical tags into Azidopramine (**10**) to make it amenable to sensitive biochemical detection. Two approaches can be envisioned, (i) to convert Azidopramine into a radiotracer, (ii) to introduce additional bioorthogonal reactive chemical tags that allow a specific and sensitive labeling of Azidopramine photocrosslinking adducts.

We first envisaged the synthesis of the demethylated analog Desazidopramine **13**. The coupling of the necessary Boc-protected building block **11** to the azepine **8** turned out to be more demanding than the corresponding 3-chloropropyl-dimethyl amine (**9**) used for the synthesis of

Azidopramine. Stronger activation with a tosyl group and optimization of the reaction conditions eventually furnished compound **13** in 64% yield which was deprotected to the desired Desazidopramine **14** (Scheme 2).



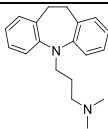
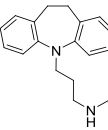
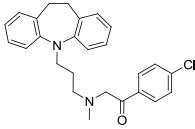
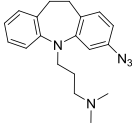
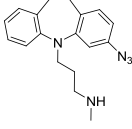
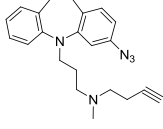
**Scheme 2:** Synthesis protocol of Desazidopramine (**14**) and Azidobupramine (**15**): (a) (Boc)<sub>2</sub>O, DMAP, ACN, rt, 2h. (b) TsCl, Et<sub>3</sub>N, DCM, 0°C. (c) NaHMDS, toluene, -78°C to 70°C, 6h. (d) 20% TFA, DCM, rt, 4h. (e) 1-bromo-3-butyne (**15**), K<sub>2</sub>CO<sub>3</sub>, KI, 60°C, 12h, acetone.

Demethylation in Desazidopramine substantially reduced activity in the uptake assay for the serotonin transporter (SERT) compared to Azidopramine (Table 1). The loss in activity was similar to the clinically used antidepressant Desipramine, in line with the known preference of the serotonin transporter for di-N-methylated TCA analogs<sup>8,9,11</sup>. Desazidopramine can be used, however, as the precursor for the synthesis of tritiated Azidopramine by radioactive methylation.

To allow for a non-radioactive detection of Azidopramine, we alkylated **14** with 1-bromo-3-butyne (**15**) to introduce a “click tag” to generate Azidobupramine **16** (Scheme-2). This second generation antidepressant analog carried an additional terminal alkyne group for selective derivatization with labeled azides by copper-catalyzed cycloaddition. The introduction of propyne group was not envisaged in place of the butyne because the resulting compound will have a structure similar to MAOIs, e.g. pargyline. This could lead to an additional MAO inhibition thereby possibly confounding the interpretation of biological effects<sup>12</sup>.

Azidobupramine (**16**) was further tested in the radioactive uptake assay for SERT. Its SERT-inhibiting activity was found to be weaker than Azidopramine (**10**), but a stronger compared to Des-azidopramine (**14**) and substantially stronger than the clinically used Lofepramine (**5**), one of the few TCA analogs with a longer N-alkyl substituent<sup>13</sup>.

**Table-1** SERT uptake assay: [ $H^3$ ]-5HT Uptake assay for using HEK293 cells stably over expressing human SERT.

Compd. No.	Compd. Name	Structure	IC <sub>50</sub> (nM) hSERT
1	Imipramine		22 ± 6
2	Desipramine		1400 ± 400
5	Lofepramine		2747 ± 1573
10	Azidopramine		28 ± 15
14	Des-Azidopramine		1400 ± 400
16	Azidobupramine		560 ± 25

In conclusion, this study provides functionalized antidepressant analogs as chemical tools for molecular psychiatry. Azidopramine (**10**) allows for the covalent derivatization of membrane-localized antidepressant targets like the serotonin transporters. [ $H^3$ ]-labelled Azidopramine or the tri-functional analog Azidobupramine (**16**) can both be used to fine-map the antidepressants binding site of SERT. Azidobupramine further allows for an affinity enrichment to enable a mass spectrometry analysis of the antidepressant binding proteome. Importantly, Azidobupramine (**16**) can interrogate antidepressant binding sites in their native environment in an unbiased manner. It is small enough that it could even be used in intact animals, e.g., in

animal model of depression. This should be useful to expand our understanding of the mechanism of action of clinically used antidepressants.

### Methods:

**Chemistry.** Chromatographic separations were performed either by manual flash chromatography or by automated flash chromatography using an Interchim- Puriflash 430 with an UV detector. Organic phases were dried over  $\text{MgSO}_4$ , and the solvents were removed under reduced pressure. Merck F-254 (thickness 0.25mm) commercial plates were used for analytical TLC to follow the progress of reactions. Silica gel 60 (Merck 70-230 mesh) was used for manual column chromatography. Unless otherwise specified,  $^1\text{H}$  NMR spectra,  $^{13}\text{C}$  NMR spectra, 2D HSQC, HMBC and COSY of all intermediates were obtained from the Department of Chemistry and Pharmacy, LMU, on a Bruker AC 300, a Bruker XL 400, or a Bruker AMX 600 at room temperature. Chemical shifts for  $^1\text{H}$ ,  $^{13}\text{C}$  are given in ppm ( $\delta$ ) relative to tetramethylsilane (TMS) as internal standard. Mass spectra ( $m/z$ ) were recorded on a Thermo Finnigan LCQ DECA XP Plus mass spectrometer at the Max Planck Institute of Psychiatry, while the high resolution mass spectrometry was carried out at MPI for Biochemistry. (Microchemistry Core facility) on Varian Mat711 mass spectrometer. The purity of the compounds was verified by reversed phase HPLC (Jupiter 4  $\mu\text{m}$  Proteo 90 A, 250\*4.6 mm, Phenomenex, Torrance, USA) using gradient A (acetonitrile:water gradient:0.1% TFA of 0 – 100% in 45 min) unless otherwise specified. Solvents were purchased from Roth, reagents were obtained from Aldrich-Fluka unless otherwise noted.

**HPLC conditions for product analysis; Column:** Jupiter 4  $\mu\text{m}$  Proteo 90 A, 250 x 4.6 mm, Phenomenex, Torrance, USA, **Wavelength:** 224nm, 280nm **Flow rate:** 1ml/min, **Buffer A:** 0.1% TFA in 5% MeCN/Water, **Buffer B:** 0.1% TFA in 95% MeCN/water. **Gradient A** After 1min elution with 100% buffer A, : linear gradient of 0-100% buffer B for 30 min.

### *Synthesis of 1-(3-azido-10,11-dihydro-5H-dibenzo[b,f]azepin-5-yl)ethanone 7*

To a stirred solution of 1-(3-amino-10,11-dihydro-5H-dibenzo [b,f]azepin-5-yl)ethanone **6** ( Wako Chemicals, 100 mg, 0.396 mmol) in 10% aqueous hydrochloric acid (2ml), a solution of sodium nitrite (27.3 mg, 0.396 mmol) in water was added at 0-5°C with vigorous stirring. The mixture was kept below 5°C for 30 min, and then a solution of sodium azide (28.3 mg, 0.436 mmol) in water (5ml) was added dropwise while the reaction was kept at the same temperature. After being stirred for 1h, the mixture was warmed to room temperature and extracted with EtOAc and water. The organic layer was washed with brine, dried with  $\text{MgSO}_4$  and

concentrated under reduced pressure to give 110mg (0.396 mmol, 100%) of compound **7** as yellow oily liquid.

TLC (Hexane: EtOAc 11:9):  $R_f = 0.58$

$^1\text{H}$  NMR (400 MHz,  $\text{CDCl}_3$ )  $\delta = 2.03$  (s, 3H,  $\text{CH}_3$ ), 2.77-2.86 (m, 2H,  $\text{CH}_2\text{CH}_2$ ), 3.28-3.48 (m, 2H,  $\text{CH}_2\text{CH}_2$ ), 6.85 (d, 1H,  $J = 8.4$  Hz), 6.96 (s, 1H), 7.07 (s, 1H), 7.13 (d, 1H,  $J = 8.4$  Hz), 7.29 (m, 4H).

$^{13}\text{C}$  NMR (100.5 MHz,  $\text{CDCl}_3$ )  $\delta = 22.64, 30.01, 30.59, 118.42, 119.19, 127.46, 127.60, 128.75, 129.88, 131.87, 137.41, 138.13, 140.94, 142.24, 143.69, 170.56$ .

MS (ESI):  $m/z = 279.13$   $[\text{M} + \text{H}]^+$ ,  $301.13$   $[\text{M} + \text{Na}]^+$ . Mass Calculated: 278.31.

### ***Synthesis of 3-azido-10,11-dihydro-5H-dibenzo[b,f]azepine **8*****

To 110 mg of compound **7** (0.395 mmol) was added potassium hydroxide (72mg, 1.38 mmol) dissolved in 10ml of methanol and the reaction mixture was refluxed for 6 h under an argon atmosphere. Afterwards, methanol was evaporated and the mixture was extracted with  $\text{CH}_2\text{Cl}_2$ . The oily liquid was dissolved in minimum amount of EtOAc and then recrystallised from hexane in the cold to yield needle shaped crystals of **8** (85 mg, 0.359 mmol, 85%).

TLC (Hexane: EtOAc 9:1):  $R_f = 0.6$ .

$^1\text{H}$  NMR (300 MHz,  $\text{CDCl}_3$ )  $\delta = 3.07$  (s, 4H), 6.39 (d, 1H,  $J = 2.1$  Hz), 6.49 (dd, 1H,  $J = 2.1, 6$  Hz), 6.75 (d, 1H,  $J = 0.9$  Hz), 6.84 (dt, 1H,  $J = 1.2, 7.5$  Hz), 7.03 (d, 1H,  $J = 8.1$ Hz), 7.06-7.15 (m, 2H)

$^{13}\text{C}$  NMR (75 MHz,  $\text{CDCl}_3$ )  $\delta = 34.55, 34.81, 108.06, 109.83, 118.15, 120.12, 125.39, 126.95, 129.02, 130.64, 132.06, 138.55, 141.87, 143.53$ .

MS (ESI):  $m/z = 237.20$   $[\text{M} + \text{H}]^+$ , Mass Calculated: 237.27  $[\text{M} + \text{H}]^+$ .

### ***Synthesis of 3-dimethylamino-1-propylchloride **9*****

Sodium hydroxide and 3-dimethylamino-1-propylchloride hydrochloride (TCI Europe) were dissolved separately in water (10 mL). These two solutions were mixed and the pH was adjusted to ~14. After extraction with dichloromethane (3x30 mL), the extracts were dried over anhydrous sodium sulfate and the solvent was removed to afford 50 mg (53%) of the free base. High vacuum was not used as the amine obtained is volatile.

### ***Synthesis of 3-(3-azido-10,11-dihydro-5H-dibenzo[b,f]azepin-5-yl)-N,N-dimethyl propan-1-amine **10** (Azidopramine)***

A solution of compound **8** (50 mg, 0.212 mmol) was prepared in dry toluene (sure seal, Fluka, 10ml) at 0°C under argon. To the solution was added a suspension of NaH (6.09 mg, 0.254

mmol) in toluene (3ml) and the reaction was stirred for 30min. Freshly prepared solution of 3-dimethylamino-1-propylchloride **9** (33.5mg, 0.275 mmol) (generated from its hydrochloride salt) as described above was added dropwise and the reaction was allowed to warm to room temperature. The reaction was heated to 60°C and stirred overnight. TLC analysis showed complete disappearance of the starting educt **8**. The reaction mixture was poured into water and extracted with EtOAc. The organic layer was washed with brine, dried over MgSO<sub>4</sub> and concentrated by rotary evaporation. Column chromatography in dichloromethane: MeOH 95:05 of the crude reaction mixture was performed to give compound **10** (Azidopramine, 45 mg, 0.14mmol, 66%).

TLC (DCM: MeOH 9:1): R<sub>f</sub> = 0.38.

HPLC (gradient A) Rt: 21.2min, Purity= 99 %.

<sup>1</sup>H NMR (300 MHz, CDCl<sub>3</sub>) δ= 1.70-1.80 (m, 2H), 2.19 (s, 6H), 2.26-2.37 (m, 2H), 3.15 (s, 4H), 3.76 (t, 2H, *J* = 6.9 Hz) 6.61 (dd, 1H *J* = 2.4, 5.7 Hz), 6.73 (d, 1H, *J* = 2.1 Hz), 6.984 (dt, 1H, *J* = 1.5, 5.4, 6.9 Hz), 7.06 (d, 1H, *J* = 8.1Hz), 7.11- 7.20 (m, 3H).

<sup>13</sup>C NMR (75 MHz, CDCl<sub>3</sub>) δ= 25.94, 31.65, 32.22, 45.42, 48.84, 57.49, 110.46, 112.45, 120.56, 123.22, 126.55, 129.43, 129.96, 131.33, 135.17, 137.87, 147.91, 149.20.

MS (ESI) : m/z = 322.27 [M + H]<sup>+</sup>.

HRMS: 322.1861[M + H]<sup>+</sup>, Mass Calculated: 322.1853 [M + H]<sup>+</sup>.

### ***Synthesis of 3-(tert-butoxycarbonyl(methyl)amino)propyl 4-methylbenzenesulfonate **12*****

To 3-(methylamino)propan-1-ol **11** (250 mg, 6.28 mmol) in acetonitrile was added BOC anhydride (680 mg, 12.56 mmol) and a catalytic amount of DMAP. The reaction was stirred for 2 hours until the disappearance of alcohol **11**. The crude mixture was subjected to column chromatography (Hexane: EtOAc 55:45) and dried under reduced pressure to obtain (460 mg, 2.43 mmol, 87%) of the desired product.

TLC (Hexane: EtOAc 1:1): R<sub>f</sub> = 0.46.

<sup>1</sup>H NMR (300 MHz, CDCl<sub>3</sub>) δ= 1.45 (s, 9H), 1.66-1.67 (m, 2H), 2.62 (s, 3H), 3.37 (s, 2H), 3.52 (s, 2H).

<sup>13</sup>C NMR (75 MHz, CDCl<sub>3</sub>) δ= 28.35, 29.63, 34.13, 44.21, 58.08, 79.96, 157.19.

To the above compound (90 mg, 0.475 mmol) in dichloromethane was added p-toluene sulfonylchloride (136 mg, 0.713 mmol) and triethylamine (96 mg, 0.951 mmol) and the mixture was stirred at 0°C for 4 h. The reaction mixture was then quenched with water and extracted using diethyl ether. The ethereal layer was washed with brine and dried over MgSO<sub>4</sub>

to yield the crude product which was further subjected to column chromatography using Hexane: EtOAc 13: 7 to yield 135 mg (0.393 mmol, 84%) of **12** as white oily liquid.

TLC (Hexane: EtOAc 1:1):  $R_f = 0.46$ .

$^1\text{H}$  NMR (300 MHz,  $\text{CDCl}_3$ )  $\delta = 1.41$  (s, 9H), 1.81- 1.90 (m, 2H), 2.44 (s, 3H), 2.78 (s, 3H), 3.23 (t, 2H,  $J = 6.9$  Hz), 4.02 (t, 2H,  $J = 6.3$  Hz), 7.34 (d, 2H,  $J = 7.8$  Hz), 7.77 (d, 2H,  $J = 8.4$  Hz).

$^{13}\text{C}$  NMR (75 MHz,  $\text{CDCl}_3$ )  $\delta = 21.63, 27.53, 28.35, 34.59, 45.28, 68.2, 79.62, 125.94, 127.87, 129.10, 129.88, 132.86, 144.87, 155.60$ .

MS (ESI):  $m/z = 244.13$  [M - Boc] $^+$ , Mass Calculated: 244.08[M - Boc] $^+$ .

***Synthesis of tert-butyl 3-(3-azido-10,11-dihydro-5H-dibenzo[b,f]azepin-5-yl)propyl(methyl) carbamate 13***

To a solution of 3-azido-10,11-dihydro-5H-dibenzo[b,f]azepine **8** (130 mg, 0.550 mmol) in 5ml dry toluene was added 0.660mL of a 1M solution of sodium bis (trimethylsilyl) amide in hexane (0.660 mmol) under an argon atmosphere at  $-78^\circ\text{C}$  and the mixture was stirred for 0.5h. Freshly prepared tosyl analog **12** (227 mg, 0.660 mmol) was added dropwise to the above mixture and the reaction flask was allowed to warm to room temperature. The reaction was further stirred at  $70^\circ\text{C}$  overnight and the completion of the reaction was monitored using thin layer chromatography. The crude product was poured into water and extracted with EtOAc. The organic layer was washed with brine and dried over  $\text{MgSO}_4$  and concentrated to dryness. Column chromatography of the crude reaction mixture was performed in (Hexane: EtOAc 19:1) as eluent to give compound **13** (150 mg, 0.368 mmol, 67%).

TLC (Hexane: EtOAc 19:1):  $R_f = 0.23$

$^1\text{H}$  NMR (400 MHz,  $\text{CDCl}_3$ )  $\delta = 1.39$  (s, 9H), 1.72- 1.79 (m, 2H), 2.44 (s, 3H), 2.72 (s, 3H), 3.09 – 3.16 (m, 4H), 3.23 (t, 2H,  $J = 6.8$  Hz), 3.69 (t, 2H,  $J = 6.8$  Hz), 6.59 (dd, 1H,  $J = 2.4, 5.6$  Hz), 6.68 (d, 1H,  $J = 2$  Hz), 6.96 (dt, 1H,  $J = 1.2, 7.2$  Hz), 7.05 (t, 2H,  $J = 8$  Hz), 7.10-7.16 (m, 2H).

$^{13}\text{C}$  NMR (100 MHz,  $\text{CDCl}_3$ )  $\delta = 26.26, 28.39, 31.58, 32.14, 34.23, 46.71, 48.09, 79.31, 110.27, 112.52, 120.36, 123.33, 126.54, 129.49, 129.91, 131.37, 135.17, 137.89, 147.67, 149.12, 155.69$ .

***Synthesis of 3-(3-azido-10,11-dihydro-5H-dibenzo[b,f]azepin-5-yl)-N-methylpropan-1-amine 14 (Desazidopramine)***

Compound **13** (150mg, 0.368mmol) was deprotected in the presence of 20% trifluoroacetic acid solution in DCM for 3.5h at room temperature to yield **14**. TFA was evaporated under reduced pressure and the crude mixture was subjected to a small wash out silica gel column using hexane: EtOAc: TEA 3.8:6.0:0.2 to give pure Desazidopramine **14** (85mg, 0.276mmol, 75%).

TLC (Hexane: EtOAc: TEA 3.8:6.0:0.2):  $R_f = 0.29$ .

HPLC (gradient A) Rt: 19.2 min, Purity= 98%

$^1\text{H}$  NMR (600 MHz,  $\text{CDCl}_3$ )  $\delta = 1.88-1.93$  (m, 2H), 2.42 (s, 3H), 2.85 (t, 2H,  $J = 7.2$ ), 3.07 – 3.12 (m, 4H), 3.75 (t, 2H,  $J = 6.6$  Hz), 6.62 (dd, 1H,  $J = 2.4, 6$  Hz), 6.64 (d, 1H,  $J = 1.8$  Hz), 6.967(dt, 1H,  $J = 1.2, 6$  Hz), 7.03 (q, 2H,  $J = 4.8, 7.2$  Hz), 7.10-7.15 (m, 2H).

$^{13}\text{C}$  NMR (150 MHz,  $\text{CDCl}_3$ )  $\delta = 24.69, 31.48, 31.96, 33.26, 47.49, 47.62, 110.15, 112.95, 120.12, 123.71, 126.70, 129.68, 129.98, 131.50, 135.06, 138.08, 147.15, 148.68$ .

MS (ESI)  $m/z$  308.12  $[\text{M} + \text{H}]^+$ .

HRMS: 308.1685  $[\text{M} + \text{H}]^+$ , Mass Calculated: 308.1704  $[\text{M} + \text{H}]^+$ .

**Synthesis of *N*-(3-(3-azido-10,11-dihydro-5H-dibenzo[*b,f*]azepin-5-yl)propyl)-*N*-methylbut-3-yn-1-amine **16** (Azidobupramine)**

To a solution of **14** (80 mg, 0.260 mmol) in acetone (10ml) was added potassium carbonate (180mg, 1.30 mmol) and a catalytical amount of potassium iodide. The mixture was stirred for 30 min and then further reacted with the 4-bromobut-1-yne (**15**) (41mg, 0.312 mmol) and refluxed at 60°C overnight. Acetone was evaporated followed by an aqueous work up and extraction with  $\text{CH}_2\text{Cl}_2$ . The crude mixture was subjected to column chromatography in DCM: MeOH mixture to give the desired product **16** (47 mg, 0.130 mmol, 50%).

TLC (DCM: MeOH 9.2:0.8):  $R_f = 0.38$ .

HPLC (gradient A) Rt: 19.8 min, Purity= 85 %

$^1\text{H}$  NMR (300 MHz,  $\text{CDCl}_3$ )  $\delta = 1.69-1.79$  (m, 2H), 1.94-1.96 (t, 1H,  $J = 2.4$  Hz), 2.21 (s, 3H), 2.27-2.33 (m, 2H), 2.45 (t, 2H,  $J = 7.5$  Hz), 2.56 (t, 2H,  $J = 7.2$  Hz), 3.15 (s, 4H), 3.78 (t, 2H,  $J = 6.9$  Hz), 6.62 (dd, 1H,  $J = 2.4$  Hz), 6.74 (d, 1H,  $J = 2.4$  Hz), 6.90-7.20 (m, 5H).

$^{13}\text{C}$  NMR (75 MHz,  $\text{CDCl}_3$ )  $\delta = 15.73, 24.45, 30.55, 31.33, 40.86, 47.62, 53.77, 54.90, 67.86, 81.68, 109.36, 111.29, 119.45, 122.09, 125.41, 128.30, 128.81, 130.21, 134.06, 136.75, 146.80, 148.10$

MS (ESI):  $m/z = 360.16$   $[\text{M} + \text{H}]^+$ .

HRMS: 360.2057  $[\text{M} + \text{H}]^+$ , Mass Calculated: 360.2061  $[\text{M} + \text{H}]^+$ .

### **Radioactive Serotonin uptake assay in HEK293 hSERT**

Serotonin (5-HT) uptake was performed in HEK293 cells over expressing the human serotonin transporter SERT (hSERT). The cell line was kindly provided by the Blakely lab. Cells were cultured in Dulbecco's Modified Eagle Medium (DMEM) containing 10% foetal calf serum (FCS), 100U/ml penicillin, 100 µg/ml Streptomycin and for the selection 250 µg/ml geneticine G418.

For the uptake assay the protocol from Deecher *et al.* with some modifications was followed. 15.000 cells/well were plated in 96 well plates (Corning 3610) containing complete medium. Before the plating of the cells, wells were precoated with poly D-lysine for 2 hours. After 48 hours incubation of the cells in a cell incubator (37°C, 5% CO<sub>2</sub>), the medium was removed and substituted with 150µl of assay buffer (25mM HEPES, 120mM NaCl, 5mM KCl, 2.5mM CaCl<sub>2</sub>, 1.2mM MgSO<sub>4</sub>, 2mg/ml glucose, pH 7.4) added with 1µM pargyline. Cells were incubated with different compound concentrations in presence of 15nM [H<sup>3</sup>]-5HT (Hydroxytryptamine creatinine sulphate, 5-[1,2-<sup>3</sup>H(N)-]serotonin, NET498, PerkinElmer). Compounds were diluted in DMSO with a final concentration of 0.5% in the assay.

After 30 minutes incubation with [H<sup>3</sup>]-5HT the free radioligand was removed with two washing steps using 200µl of assay buffer. Cells were then lysed with 25µl NaOH 0.25N and shaken for 5 min. Finally 75µl of scintillation cocktail was added and plate was incubated and shaken for 30 minutes. Radioactivity was counted using a Wallac Microbeta counter (PerkinElmer). The uptake assays were performed in triplicates in the plate format. The curves were analysed using SigmaPlot11. Data was fitted to a four parameter logistic curve to deduce the IC<sub>50</sub> values.

### **Acknowledgments**

We thank Dr. Blakely for providing the HEK293 cells over expressing the human serotonin transporter SERT (hSERT). We are indebted to Mrs. E. Weyher and Dr. S. Uebel (MPI of Biochemistry) and to Mrs. C. Dubler (Ludwig-Maximilians-Universität Munich) for HRMS and NMR measurements.

### **Author contributions**

R.G and F.H. designed the molecules. R.G. synthesized the molecules. S.C. and R.G. tested compounds. R.G. and F.H. wrote the manuscript.

**References:**

- (1) Daws, L. C. Unfaithful neurotransmitter transporters: focus on serotonin uptake and implications for antidepressant efficacy. *Pharmacol Ther* **2009**, *121*, 89-99.
- (2) Nestler, E. J.; Barrot, M.; DiLeone, R. J.; Eisch, A. J.; Gold, S. J. et al. Neurobiology of depression. *Neuron* **2002**, *34*, 13-25.
- (3) Sarker, S.; Weissensteiner, R.; Steiner, I.; Sitte, H. H.; Ecker, G. F. et al. The high-affinity binding site for tricyclic antidepressants resides in the outer vestibule of the serotonin transporter. *Mol Pharmacol* **2010**, *78*, 1026-1035.
- (4) El-Kasaby, A.; Just, H.; Malle, E.; Stolt-Bergner, P. C.; Sitte, H. H. et al. Mutations in the carboxyl-terminal SEC24 binding motif of the serotonin transporter impair folding of the transporter. *J Biol Chem* **2010**, *285*, 39201-39210.
- (5) Wildling, L.; Rankl, C.; Haselgrubler, T.; Gruber, H. J.; Holy, M. et al. Probing binding pocket of serotonin transporter by single molecular force spectroscopy on living cells. *J Biol Chem* **2012**, *287*, 105-113.
- (6) Lanni, C.; Govoni, S.; Lucchelli, A.; Boselli, C. Depression and antidepressants: molecular and cellular aspects. *Cell Mol Life Sci* **2009**, *66*, 2985-3008.
- (7) Wang, C. I.; Lewis, R. J. Emerging structure-function relationships defining monoamine NSS transporter substrate and ligand affinity. *Biochem Pharmacol* **2010**, *79*, 1083-1091.
- (8) Tatsumi, M.; Groshan, K.; Blakely, R. D.; Richelson, E. Pharmacological profile of antidepressants and related compounds at human monoamine transporters. *Eur J Pharmacol* **1997**, *340*, 249-258.
- (9) Owens, M. J.; Morgan, W. N.; Plott, S. J.; Nemeroff, C. B. Neurotransmitter receptor and transporter binding profile of antidepressants and their metabolites. *J Pharmacol Exp Ther* **1997**, *283*, 1305-1322.
- (10) White, K. J.; Walline, C. C.; Barker, E. L. Serotonin transporters: implications for antidepressant drug development. *AAPS J* **2005**, *7*, E421-433.
- (11) Batra, S.; Biorcklund, A. Binding affinities of four tricyclic antidepressive drugs to muscarinic cholinergic receptors in human parotid gland. *Psychopharmacology (Berl)* **1986**, *90*, 1-4.
- (12) Murphy, D. L.; Karoum, F.; Pickar, D.; Cohen, R. M.; Lipper, S. et al. Differential trace amine alterations in individuals receiving acetylenic inhibitors of MAO-A (clorgyline) or MAO-B (selegiline and pargyline). *J Neural Transm Suppl* **1998**, *52*, 39-48.

- (13) Sanchez, C.; Hyttel, J. Comparison of the effects of antidepressants and their metabolites on reuptake of biogenic amines and on receptor binding. *Cell Mol Neurobiol* **1999**, *19*, 467-489.

## 2.3 Discussion

In this manuscript photoactivable tricyclic antidepressants analogs were developed which can be used as tools to study the targets and mechanism of clinically used antidepressants.

These tool compounds were designed starting from clinically used antidepressants. In this strategy, in the first step the chloride or the cyano group at position 3 of Clomipramine or Cyanopramine was substituted by an azide group to generate Azidopramine (**9**). The corresponding aryl azide moiety was further shown to be activated by UV light, thereby generating a highly photoreactive analog, which can in principle covalently cross-link to binding partners. Azidopramine (**9**) was further tested in the established uptake assay and was shown to retain the high *in vitro* affinity for the hSERT. This indicated that the azido substitution is well tolerated at this position. Subsequently, Azidobupramine (**14**) was generated as a second generation antidepressant analog, by substituting one methyl of the dimethyl amino group with a terminal alkyne to introduce a click handle. The introduction of Boc-protected **11** to azepine **8** required substantial optimization. The purification of product **13** from the educt was difficult and hence a modified synthesis protocol had to be established. Herein, the activated tosyl analog **12** was reacted with building block **8** under various conditions (Table-5).

**TABLE -5**

<b>Educt</b>	<b>Base</b>	<b>Condition</b>	<b>Comment</b>
<b>12</b>	NaH	55-110 °C, toluene	No reaction, <b>8</b> repurified and <b>12</b> degraded.
<b>12</b>	n-BuLi	-78°C, toluene	No reaction, <b>8</b> repurified and <b>12</b> degraded.
<b>12</b>	NaHMDS	70 °C, THF	No reaction, <b>8</b> repurified and <b>12</b> degraded.
<b>12</b>	NaHMDS	-78 to 70 °C, toluene	Product obtained

Azidobupramine (**16**) had moderate binding ability *in vitro* for the hSERT. Nevertheless, the terminal alkyne in **16** provides a handle for clicking the transporter ligand complex with biotin for enrichment and protein identification or with a fluorophore for imaging in cells. In addition this compound can also be used in fine mapping of the binding site of antidepressants in their transporters. Finally, the precursor Des-azidopramine (**14**) can also be used to synthesize [<sup>3</sup>H] Azidopramine which can be used as a photoreactive radiotracer.

### 3. Summary

The present study employs different medicinal chemistry approaches to rationally design compounds that can be used as tools to dissect and understand the functions of specific protein targets implicated in depression.

In the first part of the thesis three different approaches were pursued to identify compounds binding to FKBP51 and FKBP52. The compounds synthesized in all three approaches were designed to target the 80s loop. The 80s loop had been shown to have structural differences resulting in divergent functions. In the first approach the tert-pentyl group of the lead compound was substituted by a cyclohexyl group which mimics the pyranose moiety in natural products FK506 and Rapamycin. Here the effect of the stereochemistry at C<sup>10</sup> and C<sup>11</sup> on binding affinity was studied in detail, followed by X-ray co-crystal analysis. The study revealed that the diverging 80s loop is flexible enough to accommodate various stereochemical motifs with different binding modes. In the second approach a focused library of sulfonamides was synthesized. The sulfonamides were hypothesized to be bio-isosters for the  $\alpha$ -ketoamide motif. Medium throughput library synthesis and screening identified two potential lead compounds. These lead series was further optimized to draw a conclusive SAR. The study led to the identification of two highly potent compounds for FKBP12, FKBP51 and FKBP52. In the third methodology the best lower parts from the above two methodologies was further amalgamated with bicyclic/ polycyclic rigid scaffold. The bicyclic scaffolds turned out to be more efficient than the polycyclic counterparts. This study for the first time has generated and identified putative ligands that bind to FKBP51 and FKBP52 with submicromolar affinity. Our data suggest that further medicinal chemistry and rational optimization of these leads can lead to potent selective ligands for FKBP51 and FKBP52.

In the second part of the thesis we aimed to synthesize compounds which can help to understand the function and mechanism of classical antidepressants. The chemical tools thus synthesized had an azide and an alkyne group. The azide group was incorporated for photo-crosslinking while the alkyne group would be used for affinity purification followed by identification or for imaging. The designed tool compounds were shown to retain the biological property of the clinical antidepressants in an uptake assay. Further these analogs were shown to be photoreactive. The initial data suggested that these compounds can be effectively used as tools for chemo-proteomic approaches as well as for fine mapping of the binding sites in interacting proteins.

## 4. Materials

### 4.1 Solvents, reagents and salts

Compound name	CAS No.	Company	Product code	Purity
n-Hexane	110-54-3	Roth	7339.1	≥98%
Cyclohexane	110-82-7	Roth	6570.4	≥99.5%
Ethylacetate	141-78-6	Roth	CP42.6	≥ 99.5%
Chloroform	67-66-3	Roth	Y015.3	≥ 99%
Dichloromethane	75-09-2	Roth	6053.5	≥ 99.5%
Dichloromethane dry	75-09-2	Roth	6053.1	≥ 99.5%
Tetrahydrofuran	109-99-9	Roth	Ae07.1	≥ 99.9%
2-propanol	67-63-0	Roth	7343.1	≥ 99.9%
Acetone	67-64-1	Roth	5025.4	≥ 99.5 %
Methanol	67-56-1	Roth	8388.4	≥ 99 %
Methanol HPLC	67-56-1	Roth	7342.1	≥ 99.9 %
Acetonitrile HPLC	75-05-8	Roth	8825.2	≥ 99.9%
Toluene	108-88-3	Roth	Ae06.1	≥ 99.5 %
Diethylether	60-29-7	Roth	T900.1	≥ 99.8 %
DMF	68-12-2	Roth	A5291.1	99%
TFA	76-05-1	Roth	P088.2	≥ 99.9 %
Formic acid	64-18-6	Roth	4724.3	≥ 98%
DIPEA	7087-68-5	Fluka	03440-250	≥ 98%
Triethylamine	121-44-8	Merck	8.08352-1000	99%
HCl	7647-01-0	Roth	9277.1	37 %
MgSO <sub>4</sub>	7487-88-9	Roth	0261.3	99 – 101 %
KMnO <sub>4</sub>	7722-64-7	Merck	1.05082.0250	≥97%

Compound name	CAS No.	Company	Product code	Purity
NaCl	7647-14-5	VWR	27810.295	99.8 %
LiOH	1310-65-2	Sigma	545856-100g	≥99 %
n-BuLi 2M in cyclohexane	109-72-8	Aldrich	302120-800 ml	
AgNO <sub>3</sub>	7761-88-8	Riedel-de Haen	61630	≥ 99.8 %
4-Methyl piperidine	626-58-4	Aldrich	M73206-500ml	≥ 96%
NaN <sub>3</sub>	26628-22-8	Aldrich	71290-100g	≥ 99 %
KOH	1310-58-3	Roth	6571.3	≥ 85%
NaH 60% dispersion	7646-69-7	Aldrich	45,291-2	60%
K <sub>2</sub> CO <sub>3</sub>	584-08-7	Roth	X894.2	≥ 99.9 %
NaNO <sub>2</sub>	7632-00-0	Roth	8604.1	≥ 98.7 %
KI	7681-11-0	Roth	8491.1	≥ 99 %
DMAP	1122-58-3	Fluka	29224	≥ 99.0 %
NaHMDS 1M in THF	1070-89-9	Aldrich	24558-5	
L-threonine	72-19-5	Sigma	T8625-25g	≥ 98 %
NaHCO <sub>3</sub>	144-55-8	Roth	8551.1	≥ 99 %
HCHO	50-00-0	Roth	4979.14	37 %
NH <sub>4</sub> Cl	12125-02-9	Merck	1.01145.0500	99.8 %
HATU	148893-10-1	Nova Biochem	8.51013-0025	
NBS	128-08-5	ABCR	AB114308	99%
DCC	538-75-0	Aldrich	D,800-2	99%
Noyori catalyst	212143-24-3	ABCR	AB131601	
MOM-Cl	107-30-2	Aldrich	100331-25g	
CDCl <sub>3</sub>	865-49-6	Roth	Ae54.1	≥ 99.38 %

## 4.2 Chemicals

Compound name	CAS No.	Company	Product code	Purity
3-chlorobenzene-1-sulfonyl chloride		Maybridge	BTB06460	97%
5-methyl-4-isoxaazolesulfonyl chloride		Maybridge	CC00271	95%
3,5-dimethylisoxazole-4-sulfonyl chloride		Maybridge	CC00603	97%
1,3-benzodioxole-5-sulfonyl chloride		Maybridge	CC01603	95%
Furan-2-sulfonyl chloride		Maybridge	CC02003	97%
Furan-3-sulfonyl chloride		Maybridge	CC02103	97%
5-(2-pyridyl)thiophene-2-sulfonyl chloride		Maybridge	CC02203	Tech
1-methyl-1H-imidazole-4-sulfonyl chloride		Maybridge	CC03603	95%
Pyridine-3-sulfonyl chloride hydrochloride		Maybridge	CC04103	95%
2,4-dimethyl-1,3-thiazole-5-sulfonyl chloride		Maybridge	CC05803	97%
1,3-benzothiazole-6-sulfonyl chloride		Maybridge	CC05903	95%
1-benzofuran-2-sulfonyl chloride		Maybridge	CC06603	95%
5-phenyl-2-thiophenesulfonyl chloride		Maybridge	CC10503	95%
1-benzothiophene-2-sulfonyl chloride		Maybridge	CC12203	97%
1-benzothiophene-3-sulfonyl chloride		Maybridge	CC12303	97%
Thiophene-2-sulfonyl chloride		Maybridge	CC13003	97%
1,3,5-trimethyl-1H-pyrazole-4-sulfonyl chloride		Maybridge	CC14703	97%
6-morpholine-4-yl-pyridine-3-sulfonyl chloride		Maybridge	CC17503	97%
6-phenoxy-3-pyridinesulfonyl chloride		Maybridge	CC19603	90%
6-phenyl-3-pyridinesulfonyl chloride		Maybridge	CC21103	97%

Compound name	CAS No.	Company	Product code	Purity
3-(2-methyl-4-pyrimidinyl)benzene-sulfonyl chloride		Maybridge	CC31603	95%
4-methyl-3,4-dihydro-2H-1,4-benzoxazine-6-sulfonyl chloride		Maybridge	CC36103	
1-methyl-1H-indole-5-sulfonyl chloride		Maybridge	CC41403	90%
1-methyl-1H-indole-4-sulfonyl chloride		Maybridge	CC45803	97%
3,5-dimethyl-1-phenyl-1H-pyrazole-4-sulfonyl chloride		Maybridge	CC48003	Tech
1-methyl-1H-pyrazole-3-sulfonyl chloride		Maybridge	CC48303	97%
2-oxoindoline-5-sulfonyl chloride		Maybridge	CC53303	Tech
4-pyrimidine-2-ylbenzenesulfonyl chloride		Maybridge	CC56203	97%
3-pyrimidine-2-ylbenzenesulfonyl chloride		Maybridge	CC56303	95%
4-methyl-3,4-dihydro-2H-pyrido[3,2-b][1,4]oxazine-7-sulfonyl chloride		Maybridge	CC62003	97%
1-methyl-1H-pyrazole-5-sulfonyl chloride		Maybridge	CC62303	97%
1-methyl-1H-indole-7-sulfonyl chloride		Maybridge	CC66903	97%
4-fluorobenzenesulfonyl chloride		Maybridge	DSHS00791	
1-2-dimethyl-1H-imidazole-4-sulfonyl chloride		Maybridge	KM10104	95%
3-(5-methyl-1,3,4-oxadiazol-2-yl)benzenesulfonyl chloride		Maybridge	MO00158	Tech
(4-chlorophenyl)methanesulfonyl chloride		Maybridge	MO00927	90%
4-chloro-3-(trifluoromethyl)benzene sulfonyl chloride		Maybridge	MO07002	97%

Compound name	CAS No.	Company	Product code	Purity
4-phenoxybenzenesulfonyl chloride		Maybridge	MO07030	97%
2-propanesulfonyl chloride		Maybridge	MO08485	
1-ethanesulfonyl chloride		Maybridge	MO08486	
4-chlorobenzene-1-sulfonyl chloride		Maybridge	SB00912	97%
4-(trifluoromethyl)benzene-1-sulfonyl chloride		Maybridge	TL00175	97%
3,4-dichlorobenzene-1-sulfonyl chloride		Maybridge	TL00303	90%
4-(tert-butyl)benzene-1-sulfonyl chloride		Maybridge	TL00417	
4-methoxybenzene-1-sulfonyl chloride		Maybridge	TL00513	97%
3,4 dimethoxybenzosulfonyl chloride		Aldrich	452467-1G	98%
3,4 dimethoxyphenylethyl bromide	40173-90-8	Aldrich	653675-5G	97%
2-Nitrobenzenesulfonyl chloride	1694-92-4	Aldrich	N1,150-7	97%
Ethyl pipercolinate	15862-72-3	Aldrich	198803-5G	98%
3-Nitrobenzenesulfonyl chloride	121-51-7	Aldrich	254665-5G	97%
3,5-Dichlorobenzenesulfonyl chloride	705-21-5	Aldrich	546933-5G	97%
3-Cyanobenzenesulfonyl chloride	56542-67-7	Aldrich	638358-1G	97%
3-(3,4-Dimethoxyphenyl)-1-propanol	3929-47-3	Aldrich	197688-5G	99%
Boc-Pip-OH	26250-84-0	Aldrich	516368-5G	98%
2,2-Dimethylbutyric acid	595-37-9	Aldrich	D15,260-9	96%
Cyclohexanone	108-94-1	Aldrich	398241-500ml	99%
Phenylmethanesulfonyl chloride	1939-99-7	Aldrich	159719-5G	98%

Compound name	CAS No.	Company	Product code	Purity
Benzoic acid A.C.S. reagent	65-85-0	Aldrich	242381-25G	≥99.5%
3-Pyridinepropanol	2859-67-8	Aldrich	P7120-7	98%
3'-Hydroxyacetophenone	121-71-1	Aldrich	328103-25G	≥99%
(S)-(-)-N-Boc carbonyl-2-piperidinecarboxylic acid	26250-84-0	Aldrich	516368-5G	98% ee
Pipecolinic acid	535-75-1	Aldrich	P4,585-0	98%
Cyclohexene	110-83-8	Fluka	29230-100ml	≥99.5%
tert-Butyl bromoacetate	5292-43-3	Fluka	17035-50ml	≥97%
2-Methylcyclohexanone	583-60-8	Fluka	66380	≥98%
(s)-Pyrrolidine-2-carboxylic acid	147-85-3	Fluka	81710-10G	≥99%
L-Pipecolinic acid	3105-95-1	Alfa Aesar	L15373	99%
3-bromo,5 -(trifluoromethyl) benzenesulfonyl chloride	351003-46-8	ABCR	AB180851	97%
2- Ethyl cyclohexanone	4423-94-3	ABCR	AB126350	99%
3-5 Bis(trifluoromethyl) benzenesulfonyl chloride	39234-86-1	ABCR	AB103447	97%
4-Nitrobenzenesulfonyl chloride	98-74-8	ABCR	AB118187	98%
3-Bromobenzenesulfonyl chloride	2905-24-0	ABCR	AB114107	97%
3,5-Dichloro-4-hydroxybenzenesulfonyl chloride	13432-81-0	ABCR	AB181058	97%
3-Chloro-4methoxybenzenesulfonyl chloride	22952-43-8	ABCR	AB267265	95%
3-Fluorobenzene-10sulfonyl chloride	701-27-9	ABCR	AB226807	97%
3,5-Difluorobenzenesulfonyl chloride	210532-25-5	ABCR	AB173895	97%
Trimethylsilyl acetylene	1066-54-2	ABCR	AB102117	98%
3-Dimethylamino-1-propanol	3179-63-3	ABCR	AB116149	99%
3-(Methylamino)-1-propanol		TCI	M1484	>97%

Compound name	CAS No.	Company	Product code	Purity
N-Methyl-3-chloropropylamine Hydrochloride		TCI	M1048	>99%
2-Chlorotriyl chloride resin (100-200 mesh)		Novabiochem	01-64-0114	
5-Acetyl-10,11-dihydro-5H- dibenz[b,f]azepin-3-amine		Wako	326-38523	
4-hydroxy-3,5-diisopropyl- benzenesulfonyl chloride		ChemCollect	SV000244	
4-hydroxy-3-methoxy-benzenesulfonyl chloride		ChemCollect	SV000258	
5-(chlorosulfonyl)-2,3- dimethoxybenzoic acid		AKOS	AKOS000131666	
5-(Chlorosulfonyl)-isophthalic acid dimethyl ester		AKOS	AKOS001074083	
4-Acetamido-3,5-dichlorobenzene-1- sulfonyl chloride		AKOS	AKOS000153961	
2-Methylbenzo[d]thiazole-6-sulfonyl chloride		AKOS	AKOS000301981	
2-Oxo-2,3-dihydrobenzo[d]thiazole-6- sulfonyl chloride		AKOS	AKOS000302227	
7-nitro-2,3-dihydro-1-benzofuran-5- sulfonyl chloride		AKOS	AKOS005072576	
2,6-dimethylmorpholine-4-sulfonyl chloride		AKOS	AKOS000321499	
4-bromo-1-butyne	38771-21-0	Aldrich	675725-5G	98%

## 5. Personal Future Outlook.

Interdisciplinary research is very important and crucial for the advancement of available medical therapies. Medicinal Chemistry and Chemical Biology are two disciplines which exemplify the symbiosis between chemistry and biology which can bring about a better understanding of disease and help in paving new drug therapies for the future. Drug research and development is a resource and money thirsty campaign normally taken by big pharmaceutical companies. Academic involvement in such projects is limited and rare.

During my PhD study, I have been lucky to be involved in an academic oriented drug discovery program either as a main driver or as a collaborator. Close collaboration and interactions with clinicians, researchers, pharmacist and leaders in the field has helped me to troubleshoot the problems and grow in various aspects of drug development during my PhD studies. This experience has helped me to learn and grow in the field of lead identification and optimization and has given me a wide and through experience in medicinal chemistry, high throughput screening and target identification platforms.

Rational drug design, structure based drug design campaigns and chemical biology technologies clearly suggest that chemical probes will be a routine armory on the table of biologists. With parallel improvements in designing chemical probes (synthetic chemistry, molecular modeling) and technology platforms (mass spectrometers, DNA sequencing), I believe that personalized medicine therapies is just around the corner.

Spending 4.5 years in a closely knit interdisciplinary environment (research and clinical setting), I believe my experience at the Max Planck Institute of Psychiatry will help me in my future endeavors. In the near future I look forward to make progress and contributions to tackle unanswered biological questions by designing versatile and potent chemical probes which can be applied in clinical and biological settings.

## 6. Curriculum Vitae

**Ranganath Gopalakrishnan**

### Personal Information

Date of Birth:	5 January 1984
Place of Birth:	Ahmedabad, Gujarat
Gender:	Male
Family status:	Unmarried
Nationality:	Indian

### Academic Qualification

<b>2007-to present</b>	<b>Ph.D. student at Hausch Lab,</b> Max Planck Institute of Psychiatry Munich, Germany
<b>2005-2007</b>	<b>Master of Science (M. S.) Pharm</b> Medicinal Chemistry, National Institute of Pharmaceutical Edu. & Res. (NIPER), India
<b>2001-2005</b>	<b>Bachelor of Pharmacy (B. Pharm),</b> K.B. Institute of Pharmaceutical Edu. & Res. Gujarat Univ. India

### Patents Filed.

1. **Pipicolate-diketoamides for treatment of psychiatric disorders.** (Patent No. **EP-11075275.5**) **Gopalakrishnan. R.** Hausch. F.
2. **Pipicolate-sulfonamides for treatment of psychiatric disorders.** (Patent No. **EP-11195970.6**) **Gopalakrishnan. R.** Hausch. F.

### Talks

1. **Ligands for FKBP51 and FKBP52.** MPI Psychiatry Ringberg symposium 2011.

### Publications and Manuscripts

1. **The Chemical Biology of Immunophilin Ligands,** Current Medicinal Chemistry, 2011, 18, 5355-5379, Gaali. S, **Gopalakrishnan. R.** Wang. Y, Kozany. C, Hausch. F.
2. **Evaluation of Synthetic FK506 Analogs as Ligands for FKBP51 and FKBP52.** J. Medicinal Chemistry, 2012 Mar 29. [Epub ahead of print]. **Ranganath Gopalakrishnan**, Christian Kozany, Steffen Gaali, Christoph Kress, Bastiaan Hoogeland, Andreas Bracher, Felix Hausch.

- 3. Design, Synthesis and Structure-Activity Relationship Exploration of Sulfonamide Analogues as Binders of the FK506-Binding Proteins 51 and 52.** J. Medicinal Chemistry, 2012 Mar 29. [Epub ahead of print]. Ranganath Gopalakrishnan, Christian Kozany, Yansong Wang, Sabine Schneider, Bastiaan Hoogeland, Andreas Bracher, Felix Hausch.
- 4. Design of Ligand efficiency by conformation control,** *In prep.* for JACS. Yansong Wang, Christian Kozany, Ranganath Gopalakrishnan, Christoph Kress, Bastiaan Hoogeland, Andreas Bracher, Felix Hausch.
- 5. Photoreactive Tricyclic Antidepressant analog for chemo proteomics and target identification.** *In prep* Ranganath Gopalakrishnan\*, Thomas Kirmeier\*, Vanessa Ganal, Serena Cuboni, Theo Rein, Felix Hausch.

#### Poster presentations

- 1. Azidopramine: A Photoreactive Tricyclic Antidepressant Analog.** Institute Symposium 2009. Gopalakrishnan R, Kirmeier T, Ganal V, Schmidt M, Muller M, Turck C, Rein T, Hausch F
- 2. Beyond monoamines: A novel strategy to reveal the pathophysiology of depression by elucidating antidepressants' mode of action.** Institute Symposium 2009. Kirmeier T, Ganal V, Gopalakrishnan R, Schmidt M, Maccarrone G, Turck CW, Holsboer F, Müller M, Hausch F, Rein T.
- 3. Are the antidepressants as selective as originally thought?,** Institute Symposium 2011, Kirmeier T, Ganal V, Gopalakrishnan R, Werner AM, Maccarrone G, Schmidt MV, Henes K, Wotjak CT, Müller M, Turck CW, Hausch F, Holsboer F, Rein T.
- 4. Chemical Exploration of the FK506-Binding Proteins 51 and 52.** Keystone Symposia "Chemical Biology and Novel tools in Pharmacology" Santa Fe, 2012 Gopalakrishnan R, Kozany C, Hoogeland B, Bracher A, Hausch F.

## 7. References

- (1) Harding, M. W.; Galat, A.; Uehling, D. E.; Schreiber, S. L. A receptor for the immunosuppressant FK506 is a cis-trans peptidyl-prolyl isomerase. *Nature* **1989**, *341*, 758-760.
- (2) Siekierka, J. J.; Hung, S. H.; Poe, M.; Lin, C. S.; Sigal, N. H. A cytosolic binding protein for the immunosuppressant FK506 has peptidyl-prolyl isomerase activity but is distinct from cyclophilin. *Nature* **1989**, *341*, 755-757.
- (3) Galat, A. Peptidylprolyl cis/trans isomerases (immunophilins): biological diversity--targets--functions. *Curr Top Med Chem* **2003**, *3*, 1315-1347.
- (4) Blackburn, E. A.; Walkinshaw, M. D. Targeting FKBP isoforms with small-molecule ligands. *Curr Opin Pharmacol* **2011**, *11*, 365-371.
- (5) Pemberton, T. J.; Kay, J. E. Identification and comparative analysis of the peptidyl-prolyl cis/trans isomerase repertoires of *H. sapiens*, *D. melanogaster*, *C. elegans*, *S. cerevisiae* and *Sz. pombe*. *Comp Funct Genomics* **2005**, *6*, 277-300.
- (6) Gerard, M.; Deleersnijder, A.; Demeulemeester, J.; Debyser, Z.; Baekelandt, V. Unraveling the role of peptidyl-prolyl isomerases in neurodegeneration. *Mol Neurobiol* **2011**, *44*, 13-27.
- (7) Kay, L. E.; Muhandiram, D. R.; Farrow, N. A.; Aubin, Y.; Forman-Kay, J. D. Correlation between dynamics and high affinity binding in an SH2 domain interaction. *Biochemistry* **1996**, *35*, 361-368.
- (8) Clardy, J. Borrowing to make ends meet. *Proc Natl Acad Sci U S A* **1999**, *96*, 1826-1827.
- (9) Edlich, F.; Weiwad, M.; Erdmann, F.; Fanghanel, J.; Jarczowski, F. et al. Bcl-2 regulator FKBP38 is activated by Ca<sup>2+</sup>/calmodulin. *EMBO J* **2005**, *24*, 2688-2699.
- (10) Edlich, F.; Maestre-Martinez, M.; Jarczowski, F.; Weiwad, M.; Moutty, M. C. et al. A novel calmodulin-Ca<sup>2+</sup> target recognition activates the Bcl-2 regulator FKBP38. *J Biol Chem* **2007**, *282*, 36496-36504.
- (11) Davies, T. H.; Sanchez, E. R. Fkbp52. *Int J Biochem Cell Biol* **2005**, *37*, 42-47.
- (12) Crabtree, G. R.; Schreiber, S. L. SnapShot: Ca<sup>2+</sup>-calcineurin-NFAT signaling. *Cell* **2009**, *138*, 210, 210 e211.
- (13) Xu, X.; Su, B.; Barndt, R. J.; Chen, H.; Xin, H. et al. FKBP12 is the only FK506 binding protein mediating T-cell inhibition by the immunosuppressant FK506. *Transplantation* **2002**, *73*, 1835-1838.
- (14) Weiwad, M.; Edlich, F.; Kilka, S.; Erdmann, F.; Jarczowski, F. et al. Comparative analysis of calcineurin inhibition by complexes of immunosuppressive drugs with human FK506 binding proteins. *Biochemistry* **2006**, *45*, 15776-15784.

- (15) Gaali, S.; Gopalakrishnan, R.; Wang, Y.; Kozany, C.; Hausch, F. The chemical biology of immunophilin ligands. *Curr Med Chem* **2011**, *18*, 5355-5379.
- (16) Soulard, A.; Hall, M. N. SnapShot: mTOR signaling. *Cell* **2007**, *129*, 434.
- (17) Laplante, M.; Sabatini, D. M. An emerging role of mTOR in lipid biosynthesis. *Curr Biol* **2009**, *19*, R1046-1052.
- (18) Zoncu, R.; Efeyan, A.; Sabatini, D. M. mTOR: from growth signal integration to cancer, diabetes and ageing. *Nat Rev Mol Cell Biol* **2011**, *12*, 21-35.
- (19) Hui, K. K.; Liadis, N.; Robertson, J.; Kanungo, A.; Henderson, J. T. Calcineurin inhibition enhances motor neuron survival following injury. *J Cell Mol Med* **2010**, *14*, 671-686.
- (20) Park, K. K.; Liu, K.; Hu, Y.; Smith, P. D.; Wang, C. et al. Promoting axon regeneration in the adult CNS by modulation of the PTEN/mTOR pathway. *Science* **2008**, *322*, 963-966.
- (21) Babine, R. E.; Villafranca, J. E.; Gold, B. G. FKBP immunophilin patents for neurological disorders. *Expert Opin Ther. Patents* **2005**, *15*, 555-573.
- (22) Steiner, J. P.; Connolly, M. A.; Valentine, H. L.; Hamilton, G. S.; Dawson, T. M. et al. Neurotrophic actions of nonimmunosuppressive analogues of immunosuppressive drugs FK506, rapamycin and cyclosporin A. *Nat Med* **1997**, *3*, 421-428.
- (23) Klettner, A.; Herdegen, T. The immunophilin-ligands FK506 and V-10,367 mediate neuroprotection by the heat shock response. *Br J Pharmacol* **2003**, *138*, 1004-1012.
- (24) Yamazaki, S.; Yamaji, T.; Murai, N.; Yamamoto, H.; Price, R. D. et al. FK1706, a novel non-immunosuppressive immunophilin ligand, modifies the course of painful diabetic neuropathy. *Neuropharmacology* **2008**, *55*, 1226-1230.
- (25) Kupina, N. C.; Detloff, M. R.; Dutta, S.; Hall, E. D. Neuroimmunophilin ligand V-10,367 is neuroprotective after 24-hour delayed administration in a mouse model of diffuse traumatic brain injury. *J Cereb Blood Flow Metab* **2002**, *22*, 1212-1221.
- (26) Liu, D.; McIlvain, H. B.; Fennell, M.; Dunlop, J.; Wood, A. et al. Screening of immunophilin ligands by quantitative analysis of neurofilament expression and neurite outgrowth in cultured neurons and cells. *J Neurosci Methods* **2007**, *163*, 310-320.
- (27) Summers, M. Y.; Leighton, M.; Liu, D.; Pong, K.; Graziani, E. I. 3-normeridamycin: a potent non-immunosuppressive immunophilin ligand is neuroprotective in dopaminergic neurons. *J Antibiot (Tokyo)* **2006**, *59*, 184-189.
- (28) Costantini, L. C.; Cole, D.; Chaturvedi, P.; Isacson, O. Immunophilin ligands can prevent progressive dopaminergic degeneration in animal models of Parkinson's disease. *Eur J Neurosci* **2001**, *13*, 1085-1092.
- (29) Ruan, B.; Pong, K.; Jow, F.; Bowlby, M.; Crozier, R. A. et al. Binding of rapamycin analogs to calcium channels and FKBP52 contributes to their neuroprotective activities. *Proc Natl Acad Sci U S A* **2008**, *105*, 33-38.

- (30) Edlich, F.; Weiwad, M.; Wildemann, D.; Jarczowski, F.; Kilka, S. et al. The specific FKBP38 inhibitor N-(N',N'-dimethylcarboxamidomethyl)cycloheximide has potent neuroprotective and neurotrophic properties in brain ischemia. *J Biol Chem* **2006**, *281*, 14961-14970.
- (31) Steiner, J. P.; Hamilton, G. S.; Ross, D. T.; Valentine, H. L.; Guo, H. et al. Neurotrophic immunophilin ligands stimulate structural and functional recovery in neurodegenerative animal models. *Proc Natl Acad Sci U S A* **1997**, *94*, 2019-2024.
- (32) Minematsu, T.; Lee, J.; Zha, J.; Moy, S.; Kowalski, D. et al. Time-dependent inhibitory effects of (1R,9S,12S,13R,14S,17R,18E,21S,23S,24R,25S,27R)-1,14-dihydroxy-12-(E)-2-[(1R,3R,4R)-4-hydroxy-3-methoxycyclohexyl]-1-methylvinyl-23,25-dimethoxy-13, 19,21,27-tetramethyl-17-(2-oxopropyl)-11,28-dioxo-4-azatricyclo[22.3.1.0(4,9)]octacos-18-ene-2,3,10,16-tetrone (FK1706), a novel nonimmunosuppressive immunophilin ligand, on CYP3A4/5 activity in humans in vivo and in vitro. *Drug Metab Dispos* **2010**, *38*, 249-259.
- (33) Gopalakrishnan, R.; Hausch, F. Evaluation of Synthetic FK506 Analogs as Ligands for FKBP51 and FKBP52. *To be Submitted*.
- (34) Harper, S.; Bilsland, J.; Young, L.; Bristow, L.; Boyce, S. et al. Analysis of the neurotrophic effects of GPI-1046 on neuron survival and regeneration in culture and in vivo. *Neuroscience* **1999**, *88*, 257-267.
- (35) Bocquet, A.; Lorent, G.; Fuks, B.; Grimee, R.; Talaga, P. et al. Failure of GPI compounds to display neurotrophic activity in vitro and in vivo. *Eur J Pharmacol* **2001**, *415*, 173-180.
- (36) Zhao, L.; Huang, W.; Liu, H.; Wang, L.; Zhong, W. et al. FK506-binding protein ligands: structure-based design, synthesis, and neurotrophic/neuroprotective properties of substituted 5,5-dimethyl-2-(4-thiazolidine)carboxylates. *J Med Chem* **2006**, *49*, 4059-4071.
- (37) Birge, R. B.; Wadsworth, S.; Akakura, R.; Abeysinghe, H.; Kanojia, R. et al. A role for schwann cells in the neuroregenerative effects of a non-immunosuppressive fk506 derivative, jnj460. *Neuroscience* **2004**, *124*, 351-366.
- (38) Hamilton, G. S.; Norman, M. H.; Wu, Y.-Q. Carboxylic acids and carboxylic acid isosters of N-heterocyclic compounds. *WO00/32588* **2000**.
- (39) Marshall, V. L.; Grosset, D. G. GPI-1485 (Guilford). *Curr Opin Investig Drugs* **2004**, *5*, 107-112.
- (40) Armistead, D. M.; Badia, M. C.; Deininger, D. D.; Duffy, J. P.; Saunders, J. O. et al. Design, synthesis and structure of non-macrocyclic inhibitors of FKBP12, the major binding protein for the immunosuppressant FK506. *Acta Crystallogr D Biol Crystallogr* **1995**, *51*, 522-528.
- (41) Armistead, D., M. Methods and Compositions for Stimulating Neurite Growth. *WO 96/41609* **1996**.
- (42) Germann, U. A.; Shlyakhter, D.; Mason, V. S.; Zelle, R. E.; Duffy, J. P. et al. Cellular and biochemical characterization of VX-710 as a chemosensitizer: reversal of P-glycoprotein-mediated multidrug resistance in vitro. *Anticancer Drugs* **1997**, *8*, 125-140.

- (43) Dey, S. Biricodar. Vertex Pharmaceuticals. *Curr Opin Investig Drugs* **2002**, *3*, 818-823.
- (44) Arceci, R. J.; Stieglitz, K.; Bierer, B. E. Immunosuppressants FK506 and rapamycin function as reversal agents of the multidrug resistance phenotype. *Blood* **1992**, *80*, 1528-1536.
- (45) Norville, I. H.; O'Shea, K.; Sarkar-Tyson, M.; Zheng, S.; Titball, R. W. et al. The structure of a *Burkholderia pseudomallei* immunophilin-inhibitor complex reveals new approaches to antimicrobial development. *Biochem J* **2011**, *437*, 413-422.
- (46) Holt, D. A.; Konialianbeck, A. L.; Oh, H. J.; Yen, H. K.; Rozamus, L. W. et al. Structure-Activity Studies of Synthetic Fkbp Ligands as Peptidyl-Prolyl Isomerase Inhibitors. *Bioorganic & Medicinal Chemistry Letters* **1994**, *4*, 315-320.
- (47) Holt, D. A.; Luengo, J. I.; Yamashita, D. S.; Oh, H. J.; Konilian, A. L. et al. Design, synthesis, and kinetic evaluation of high-affinity FKBP ligands and the X-ray crystal structures of their complexes with FKBP 12. *J Am Chem Soc* **1993**, *115*, 9925-9938.
- (48) Wilson, K. P.; Yamashita, M. M.; Sintchak, M. D.; Rotstein, S. H.; Murcko, M. A. et al. Comparative X-ray structures of the major binding protein for the immunosuppressant FK506 (tacrolimus) in unliganded form and in complex with FK506 and rapamycin. *Acta Crystallogr D Biol Crystallogr* **1995**, *51*, 511-521.
- (49) Guo, C.; Augelli-Szafran, C., E.; Bender, S., L.; Bigge, C., F.; Caprathe, B., W. et al. Heterobicycles FKBP-ligands. *WO02089806* **2002**.
- (50) Caffrey, M. V.; Cladingboel, D. E.; Cooper, M. E.; Donald, D. K.; Furber, M. et al. Synthesis and Evaluation of Dual Domain Macrocyclic Fkbp12 Ligands. *Bioorganic & Medicinal Chemistry Letters* **1994**, *4*, 2507-2510.
- (51) Teague, S. J.; Stocks, M. J. The Affinity of the Excised Binding Domain of Fk-506 for the Immunophilin Fkbp12. *Bioorganic & Medicinal Chemistry Letters* **1993**, *3*, 1947-1950.
- (52) Birkenshaw, T. N.; Caffrey, M. V.; Cladingboel, D. E.; Cooper, M. E.; Donald, D. K. et al. Synthetic Fkbp12 Ligands - Design and Synthesis of Pyranose Replacements. *Bioorganic & Medicinal Chemistry Letters* **1994**, *4*, 2501-2506.
- (53) Tatlock, J. H.; Kalish, V. J.; Parge, H. E.; Knighton, D. R.; Showalter, R. E. et al. High-affinity FKBP-12 ligands derived from (R)-(-)-carvone. Synthesis and evaluation of FK506 pyranose ring replacements. *Bioorganic & Medicinal Chemistry Letters* **1995**, *5*, 2489-2494.
- (54) Dubowchik, G. M.; Vrudhula, V. M.; Dasgupta, B.; Ditta, J.; Chen, T. et al. 2-Aryl-2,2-difluoroacetamide FKBP12 ligands: synthesis and X-ray structural studies. *Org Lett* **2001**, *3*, 3987-3990.
- (55) Choi, C.; Li, J. H.; Vaal, M.; Thomas, C.; Limburg, D. et al. Use of parallel-synthesis combinatorial libraries for rapid identification of potent FKBP12 inhibitors. *Bioorganic & Medicinal Chemistry Letters* **2002**, *12*, 1421-1428.

- (56) Wei, L.; Wu, Y. Q.; Wilkinson, D. E.; Chen, Y.; Soni, R. et al. Solid-phase synthesis of FKBP12 inhibitors: N-sulfonyl and N-carbamoylprolyl/pipecolyl amides. *Bioorganic & Medicinal Chemistry Letters* **2002**, *12*, 1429-1433.
- (57) Holt, D. A.; Konialian, A. L.; Brandt, M.; Levy, M. A.; Bossard, M. J. et al. Structure-Activity Studies of Nonmacrocylic Rapamycin Derivatives. *Bioorganic & Medicinal Chemistry Letters* **1993**, *3*, 1977-1980.
- (58) Bell, A.; Monaghan, P.; Page, A. P. Peptidyl-prolyl cis-trans isomerases (immunophilins) and their roles in parasite biochemistry, host-parasite interaction and antiparasitic drug action. *Int J Parasitol* **2006**, *36*, 261-276.
- (59) Kohler, R.; Fanghanel, J.; Konig, B.; Luneberg, E.; Frosch, M. et al. Biochemical and functional analyses of the Mip protein: influence of the N-terminal half and of peptidylprolyl isomerase activity on the virulence of *Legionella pneumophila*. *Infect Immun* **2003**, *71*, 4389-4397.
- (60) Moro, A.; Ruiz-Cabello, F.; Fernandez-Cano, A.; Stock, R. P.; Gonzalez, A. Secretion by *Trypanosoma cruzi* of a peptidyl-prolyl cis-trans isomerase involved in cell infection. *EMBO J* **1995**, *14*, 2483-2490.
- (61) Oz, H. S.; Hughes, W. T.; Thomas, E. K.; McClain, C. J. Effects of immunomodulators on acute *Trypanosoma Cruzi* infection in mice. *Med Sci Monit* **2002**, *8*, BR208-211.
- (62) Ceymann, A.; Horstmann, M.; Ehses, P.; Schweimer, K.; Paschke, A. K. et al. Solution structure of the *Legionella pneumophila* Mip-rapamycin complex. *BMC Struct Biol* **2008**, *8*, 17.
- (63) Juli, C.; Sippel, M.; Jager, J.; Thiele, A.; Weiwad, M. et al. Pipecolic Acid Derivatives As Small-Molecule Inhibitors of the *Legionella* MIP Protein. *Journal of Medicinal Chemistry* **2011**, *54*, 277-283.
- (64) Echeverria, P. C.; Picard, D. Molecular chaperones, essential partners of steroid hormone receptors for activity and mobility. *Biochim Biophys Acta* **2010**, *1803*, 641-649.
- (65) Chen, S.; Sullivan, W. P.; Toft, D. O.; Smith, D. F. Differential interactions of p23 and the TPR-containing proteins Hop, Cyp40, FKBP52 and FKBP51 with Hsp90 mutants. *Cell Stress Chaperones* **1998**, *3*, 118-129.
- (66) Morishima, Y.; Kanelakis, K. C.; Murphy, P. J.; Lowe, E. R.; Jenkins, G. J. et al. The hsp90 cochaperone p23 is the limiting component of the multiprotein hsp90/hsp70-based chaperone system in vivo where it acts to stabilize the client protein: hsp90 complex. *J Biol Chem* **2003**, *278*, 48754-48763.
- (67) Riggs, D. L.; Roberts, P. J.; Chirillo, S. C.; Cheung-Flynn, J.; Prapapanich, V. et al. The Hsp90-binding peptidylprolyl isomerase FKBP52 potentiates glucocorticoid signaling in vivo. *Embo J* **2003**, *22*, 1158-1167.

- (68) Wochnik, G. M.; Ruegg, J.; Abel, G. A.; Schmidt, U.; Holsboer, F. et al. FK506-binding Proteins 51 and 52 Differentially Regulate Dynein Interaction and Nuclear Translocation of the Glucocorticoid Receptor in Mammalian Cells. *J. Biol. Chem.* **2005**, *280*, 4609-4616.
- (69) Davies, T. H.; Ning, Y.-M.; Sanchez, E. R. Differential control of glucocorticoid receptor hormone-binding function by tetratricopeptide repeat (TPR) proteins and the immunosuppressive ligand FK506. *Biochemistry* **2005**, *44*, 2030-2038.
- (70) Riggs, D. L.; Cox, M. B.; Tardif, H. L.; Hessling, M.; Buchner, J. et al. Noncatalytic role of the FKBP52 peptidyl-prolyl isomerase domain in the regulation of steroid hormone signaling. *Mol Cell Biol* **2007**, *27*, 8658-8669.
- (71) Olefsky, J. M. Nuclear receptor minireview series. *J Biol Chem* **2001**, *276*, 36863-36864.
- (72) Holsboer, F. The corticosteroid receptor hypothesis of depression. *Neuropsychopharmacology* **2000**, *23*, 477-501.
- (73) de Kloet, E. R.; Joels, M.; Holsboer, F. Stress and the brain: from adaptation to disease. *Nat Rev Neurosci* **2005**, *6*, 463-475.
- (74) Binder, E. B.; Salyakina, D.; Lichtner, P.; Wochnik, G. M.; Ising, M. et al. Polymorphisms in FKBP5 are associated with increased recurrence of depressive episodes and rapid response to antidepressant treatment. *Nat Genet* **2004**, *36*, 1319-1325.
- (75) Kirchheiner, J.; Lorch, R.; Lebedeva, E.; Seeringer, A.; Roots, I. et al. Genetic variants in FKBP5 affecting response to antidepressant drug treatment. *Pharmacogenomics* **2008**, *9*, 841-846.
- (76) Lekman, M.; Laje, G.; Charney, D.; Rush, A. J.; Wilson, A. F. et al. The FKBP5-gene in depression and treatment response--an association study in the Sequenced Treatment Alternatives to Relieve Depression (STAR\*D) Cohort. *Biol Psychiatry* **2008**, *63*, 1103-1110.
- (77) Zou, Y. F.; Wang, F.; Feng, X. L.; Li, W. F.; Tao, J. H. et al. Meta-analysis of FKBP5 gene polymorphisms association with treatment response in patients with mood disorders. *Neurosci Lett* **2010**, *484*, 56-61.
- (78) Willour, V. L.; Chen, H.; Toolan, J.; Belmonte, P.; Cutler, D. J. et al. Family-based association of FKBP5 in bipolar disorder. *Mol Psychiatry* **2009**, *14*, 261-268.
- (79) Brent, D.; Melhem, N.; Ferrell, R.; Emslie, G.; Wagner, K. D. et al. Association of FKBP5 polymorphisms with suicidal events in the Treatment of Resistant Depression in Adolescents (TORDIA) study. *Am J Psychiatry* **2010**, *167*, 190-197.
- (80) Roy, A.; Gorodetsky, E.; Yuan, Q.; Goldman, D.; Enoch, M. A. Interaction of FKBP5, a stress-related gene, with childhood trauma increases the risk for attempting suicide. *Neuropsychopharmacology* **2010**, *35*, 1674-1683.
- (81) Supriyanto, I.; Sasada, T.; Fukutake, M.; Asano, M.; Ueno, Y. et al. Association of FKBP5 gene haplotypes with completed suicide in the Japanese population. *Prog Neuropsychopharmacol Biol Psychiatry* **2011**, *35*, 252-256.

- (82) Koenen, K. C.; Saxe, G.; Purcell, S.; Smoller, J. W.; Bartholomew, D. et al. Polymorphisms in FKBP5 are associated with peritraumatic dissociation in medically injured children. *Mol Psychiatry* **2005**, *10*, 1058-1059.
- (83) Ising, M.; Depping, A. M.; Siebertz, A.; Lucae, S.; Unschuld, P. G. et al. Polymorphisms in the FKBP5 gene region modulate recovery from psychosocial stress in healthy controls. *Eur J Neurosci* **2008**, *28*, 389-398.
- (84) Binder, E. B.; Bradley, R. G.; Liu, W.; Epstein, M. P.; Deveau, T. C. et al. Association of FKBP5 polymorphisms and childhood abuse with risk of posttraumatic stress disorder symptoms in adults. *JAMA* **2008**, *299*, 1291-1305.
- (85) Koenen, K. C.; Uddin, M. FKBP5 polymorphisms modify the effects of childhood trauma. *Neuropsychopharmacology* **2010**, *35*, 1623-1624.
- (86) Zimmermann, P.; Bruckl, T.; Nocon, A.; Pfister, H.; Binder, E. B. et al. Interaction of FKBP5 gene variants and adverse life events in predicting depression onset: results from a 10-year prospective community study. *Am J Psychiatry* **2011**, *168*, 1107-1116.
- (87) Attwood, B. K.; Bourgognon, J. M.; Patel, S.; Mucha, M.; Schiavon, E. et al. Neuropsin cleaves EphB2 in the amygdala to control anxiety. *Nature* **2011**, *473*, 372-375.
- (88) Touma, C.; Gassen, N. C.; Herrmann, L.; Cheung-Flynn, J.; Bull, D. R. et al. FK506 Binding Protein 5 Shapes Stress Responsiveness: Modulation of Neuroendocrine Reactivity and Coping Behavior. *Biol Psychiatry* **2011**.
- (89) Hartmann, J.; Wagner, K. V.; Liebl, C.; Scharf, S. H.; Wang, X. D. et al. The involvement of FK506-binding protein 51 (FKBP5) in the behavioral and neuroendocrine effects of chronic social defeat stress. *Neuropharmacology* **2011**.
- (90) O'Leary, J. C., 3rd; Dharia, S.; Blair, L. J.; Brady, S.; Johnson, A. G. et al. A New Anti-Depressive Strategy for the Elderly: Ablation of FKBP5/FKBP51. *PLoS One* **2011**, *6*, e24840.
- (91) Romano, S.; Mallardo, M.; Romano, M. F. FKBP51 and the NF-kappaB regulatory pathway in cancer. *Curr Opin Pharmacol* **2011**, *11*, 288-293.
- (92) Li, L.; Lou, Z.; Wang, L. The role of FKBP5 in cancer aetiology and chemoresistance. *Br J Cancer* **2011**, *104*, 19-23.
- (93) Periyasamy, S.; Warriar, M.; Tillekeratne, M. P.; Shou, W.; Sanchez, E. R. The immunophilin ligands cyclosporin A and FK506 suppress prostate cancer cell growth by androgen receptor-dependent and -independent mechanisms. *Endocrinology* **2007**, *148*, 4716-4726.
- (94) Ni, L.; Yang, C. S.; Gioeli, D.; Frierson, H.; Toft, D. O. et al. FKBP51 promotes assembly of the Hsp90 chaperone complex and regulates androgen receptor signaling in prostate cancer cells. *Mol Cell Biol* **2010**, *30*, 1243-1253.
- (95) Periyasamy, S.; Hinds, T., Jr.; Shemshedini, L.; Shou, W.; Sanchez, E. R. FKBP51 and Cyp40 are positive regulators of androgen-dependent prostate cancer cell growth and the targets of FK506 and cyclosporin A. *Oncogene* **2010**, *29*, 1691-1701.

- (96) Mukaide, H.; Adachi, Y.; Taketani, S.; Iwasaki, M.; Koike-Kiriyama, N. et al. FKBP51 expressed by both normal epithelial cells and adenocarcinoma of colon suppresses proliferation of colorectal adenocarcinoma. *Cancer Invest* **2008**, *26*, 385-390.
- (97) Romano, S.; Di Pace, A.; Sorrentino, A.; Bisogni, R.; Sivero, L. et al. FK506 binding proteins as targets in anticancer therapy. *Anticancer Agents Med Chem* **2010**, *10*, 651-656.
- (98) Pei, H.; Li, L.; Fridley, B. L.; Jenkins, G. D.; Kalari, K. R. et al. FKBP51 affects cancer cell response to chemotherapy by negatively regulating Akt. *Cancer Cell* **2009**, *16*, 259-266.
- (99) Quinta, H. R.; Maschi, D.; Gomez-Sanchez, C.; Piwien-Pilipuk, G.; Galigniana, M. D. Subcellular rearrangement of hsp90-binding immunophilins accompanies neuronal differentiation and neurite outgrowth. *J Neurochem* **2010**, *115*, 716-734.
- (100) Matsushita, R.; Hashimoto, A.; Tomita, T.; Yoshitawa, H.; Tanaka, S. et al. Enhanced expression of mRNA for FK506-binding protein 5 in bone marrow CD34 positive cells in patients with rheumatoid arthritis. *Clin Exp Rheumatol* **2010**, *28*, 87-90.
- (101) Nakamura, N.; Shimaoka, Y.; Tougan, T.; Onda, H.; Okuzaki, D. et al. Isolation and expression profiling of genes upregulated in bone marrow-derived mononuclear cells of rheumatoid arthritis patients. *DNA Res* **2006**, *13*, 169-183.
- (102) Bracher, A.; Kozany, C.; Thost, A. K.; Hausch, F. Structural characterization of the PPIase domain of FKBP51, a cochaperone of human Hsp90. *Acta Crystallogr D Biol Crystallogr* **2011**, *67*, 549-559.
- (103) Wu, B.; Li, P.; Liu, Y.; Lou, Z.; Ding, Y. et al. 3D structure of human FK506-binding protein 52: implications for the assembly of the glucocorticoid receptor/Hsp90/immunophilin heterocomplex. *Proc Natl Acad Sci U S A* **2004**, *101*, 8348-8353.
- (104) Paulini, R.; Muller, K.; Diederich, F. Orthogonal multipolar interactions in structural chemistry and biology. *Angew Chem Int Ed Engl* **2005**, *44*, 1788-1805.
- (105) Kozany, C.; Marz, A.; Kress, C.; Hausch, F. Fluorescent probes to characterise FK506-binding proteins. *Chembiochem* **2009**, *10*, 1402-1410.
- (106) Hudack, R. A. Design, Synthesis, and Biological Activity of Novel Polycyclic Aza-Amide FKBP12 Ligands *Journal of Medicinal Chemistry* **2006**, *49*, 1202-1206.
- (107) Guo, C.; Reich, S.; Shoqalter, R.; Villafrance, E.; Dong, L. A concise synthesis of AG5473/5507 utilizing *N*-acyliminium ion chemistry. *Tetrahedron Letters* **2000**, *41*, 5307-5311.
- (108) Babine, R. E.; Bender, S. L. Molecular Recognition of Protein-Ligand Complexes: Applications to Drug Design. *Chem Rev* **1997**, *97*, 1359-1472.
- (109) Nestler, E. J.; Barrot, M.; DiLeone, R. J.; Eisch, A. J.; Gold, S. J. et al. Neurobiology of depression. *Neuron* **2002**, *34*, 13-25.
- (110) Fava, M.; Kendler, K. S. Major depressive disorder. *Neuron* **2000**, *28*, 335-341.

- (111) Burmeister, M. Basic concepts in the study of diseases with complex genetics. *Biol Psychiatry* **1999**, *45*, 522-532.
- (112) Hyman, S. E.; Nestler, E. J. Initiation and adaptation: a paradigm for understanding psychotropic drug action. *Am J Psychiatry* **1996**, *153*, 151-162.
- (113) Smith, R. S. The macrophage theory of depression. *Med Hypotheses* **1991**, *35*, 298-306.
- (114) Connor, T. J.; Leonard, B. E. Depression, stress and immunological activation: the role of cytokines in depressive disorders. *Life Sci* **1998**, *62*, 583-606.
- (115) Pfennig, A.; Kunzel, H. E.; Kern, N.; Ising, M.; Majer, M. et al. Hypothalamus-pituitary-adrenal system regulation and suicidal behavior in depression. *Biol Psychiatry* **2005**, *57*, 336-342.
- (116) Capuron, L.; Neuraeter, G.; Musselman, D. L.; Lawson, D. H.; Nemeroff, C. B. et al. Interferon-alpha-induced changes in tryptophan metabolism. relationship to depression and paroxetine treatment. *Biol Psychiatry* **2003**, *54*, 906-914.
- (117) Schiepers, O. J.; Wichers, M. C.; Maes, M. Cytokines and major depression. *Prog Neuropsychopharmacol Biol Psychiatry* **2005**, *29*, 201-217.
- (118) Bschor, T.; Baethge, C.; Adli, M.; Lewitzka, U.; Eichmann, U. et al. Hypothalamic-pituitary-thyroid system activity during lithium augmentation therapy in patients with unipolar major depression. *J Psychiatry Neurosci* **2003**, *28*, 210-216.
- (119) Sauvage, M. F.; Marquet, P.; Rousseau, A.; Raby, C.; Buxeraud, J. et al. Relationship between psychotropic drugs and thyroid function: a review. *Toxicol Appl Pharmacol* **1998**, *149*, 127-135.
- (120) Shelton, R. C.; Winn, S.; Ekhatore, N.; Loosen, P. T. The effects of antidepressants on the thyroid axis in depression. *Biol Psychiatry* **1993**, *33*, 120-126.
- (121) Shimizu, E.; Hashimoto, K.; Okamura, N.; Koike, K.; Komatsu, N. et al. Alterations of serum levels of brain-derived neurotrophic factor (BDNF) in depressed patients with or without antidepressants. *Biol Psychiatry* **2003**, *54*, 70-75.
- (122) Duman, R. S. Role of neurotrophic factors in the etiology and treatment of mood disorders. *Neuromolecular Med* **2004**, *5*, 11-25.
- (123) Coppell, A. L.; Pei, Q.; Zetterstrom, T. S. Bi-phasic change in BDNF gene expression following antidepressant drug treatment. *Neuropharmacology* **2003**, *44*, 903-910.
- (124) Donati, R. J.; Rasenick, M. M. G protein signaling and the molecular basis of antidepressant action. *Life Sci* **2003**, *73*, 1-17.
- (125) Nibuya, M.; Nestler, E. J.; Duman, R. S. Chronic antidepressant administration increases the expression of cAMP response element binding protein (CREB) in rat hippocampus. *J Neurosci* **1996**, *16*, 2365-2372.

- (126) Wallace, T. L.; Stellitano, K. E.; Neve, R. L.; Duman, R. S. Effects of cyclic adenosine monophosphate response element binding protein overexpression in the basolateral amygdala on behavioral models of depression and anxiety. *Biol Psychiatry* **2004**, *56*, 151-160.
- (127) Eisenhofer, G.; Kopin, I. J.; Goldstein, D. S. Catecholamine metabolism: a contemporary view with implications for physiology and medicine. *Pharmacol Rev* **2004**, *56*, 331-349.
- (128) Riederer, P.; Lachenmayer, L.; Laux, G. Clinical applications of MAO-inhibitors. *Curr Med Chem* **2004**, *11*, 2033-2043.
- (129) Kent, J. M. SNaRIs, NaSSAs, and NaRIs: new agents for the treatment of depression. *Lancet* **2000**, *355*, 911-918.
- (130) Barker, E. L.; Perlman, M. A.; Adkins, E. M.; Houlihan, W. J.; Pristupa, Z. B. et al. High affinity recognition of serotonin transporter antagonists defined by species-scanning mutagenesis. An aromatic residue in transmembrane domain I dictates species-selective recognition of citalopram and mazindol. *J Biol Chem* **1998**, *273*, 19459-19468.
- (131) Ravna, A. W.; Sylte, I.; Dahl, S. G. Molecular mechanism of citalopram and cocaine interactions with neurotransmitter transporters. *J Pharmacol Exp Ther* **2003**, *307*, 34-41.
- (132) Kitayama, S.; Shimada, S.; Xu, H.; Markham, L.; Donovan, D. M. et al. Dopamine transporter site-directed mutations differentially alter substrate transport and cocaine binding. *Proc Natl Acad Sci U S A* **1992**, *89*, 7782-7785.
- (133) Barker, E. L.; Moore, K. R.; Rakhshan, F.; Blakely, R. D. Transmembrane domain I contributes to the permeation pathway for serotonin and ions in the serotonin transporter. *J Neurosci* **1999**, *19*, 4705-4717.
- (134) Paczkowski, F. A.; Bryan-Lluka, L. J. Tyrosine residue 271 of the norepinephrine transporter is an important determinant of its pharmacology. *Brain Res Mol Brain Res* **2001**, *97*, 32-42.
- (135) Roubert, C.; Cox, P. J.; Bruss, M.; Hamon, M.; Bonisch, H. et al. Determination of residues in the norepinephrine transporter that are critical for tricyclic antidepressant affinity. *J Biol Chem* **2001**, *276*, 8254-8260.
- (136) Paczkowski, F. A.; Bonisch, H.; Bryan-Lluka, L. J. Pharmacological properties of the naturally occurring Ala(457)Pro variant of the human norepinephrine transporter. *Pharmacogenetics* **2002**, *12*, 165-173.
- (137) Roman, D. L.; Walline, C. C.; Rodriguez, G. J.; Barker, E. L. Interactions of antidepressants with the serotonin transporter: a contemporary molecular analysis. *Eur J Pharmacol* **2003**, *479*, 53-63.
- (138) Barker, E. L.; Blakely, R. D. Identification of a single amino acid, phenylalanine 586, that is responsible for high affinity interactions of tricyclic antidepressants with the human serotonin transporter. *Mol Pharmacol* **1996**, *50*, 957-965.

- (139) Thompson, B. J.; Jessen, T.; Henry, L. K.; Field, J. R.; Gamble, K. L. et al. Transgenic elimination of high-affinity antidepressant and cocaine sensitivity in the presynaptic serotonin transporter. *Proc Natl Acad Sci U S A* **2011**, *108*, 3785-3790.
- (140) Sarker, S.; Weissensteiner, R.; Steiner, I.; Sitte, H. H.; Ecker, G. F. et al. The high-affinity binding site for tricyclic antidepressants resides in the outer vestibule of the serotonin transporter. *Mol Pharmacol* **2010**, *78*, 1026-1035.
- (141) El-Kasaby, A.; Just, H.; Malle, E.; Stolt-Bergner, P. C.; Sitte, H. H. et al. Mutations in the carboxyl-terminal SEC24 binding motif of the serotonin transporter impair folding of the transporter. *J Biol Chem* **2010**, *285*, 39201-39210.
- (142) Wildling, L.; Rankl, C.; Haselgrubler, T.; Gruber, H. J.; Holy, M. et al. Probing binding pocket of serotonin transporter by single molecular force spectroscopy on living cells. *J Biol Chem* **2012**, *287*, 105-113.
- (143) Owens, M. J.; Morgan, W. N.; Plott, S. J.; Nemeroff, C. B. Neurotransmitter receptor and transporter binding profile of antidepressants and their metabolites. *J Pharmacol Exp Ther* **1997**, *283*, 1305-1322.
- (144) Tatsumi, M.; Groshan, K.; Blakely, R. D.; Richelson, E. Pharmacological profile of antidepressants and related compounds at human monoamine transporters. *Eur J Pharmacol* **1997**, *340*, 249-258.
- (145) Sanchez, C.; Hyttel, J. Comparison of the effects of antidepressants and their metabolites on reuptake of biogenic amines and on receptor binding. *Cell Mol Neurobiol* **1999**, *19*, 467-489.
- (146) Andersen, J.; Kristensen, A. S.; Bang-Andersen, B.; Stromgaard, K. Recent advances in the understanding of the interaction of antidepressant drugs with serotonin and norepinephrine transporters. *Chem Commun (Camb)* **2009**, 3677-3692.